APPLICATION OF SOLAR ENERGY FOR WATER AND ROOM HEATING

THESIS SUBMITTED FOR THE AWARD
OF DOCTOR OF PHILOSOPHY
IN PHYSICS

By
H. P. GARG, M. Sc.

UNIVERSITY OF ROORKEE
ROORKEE
1972

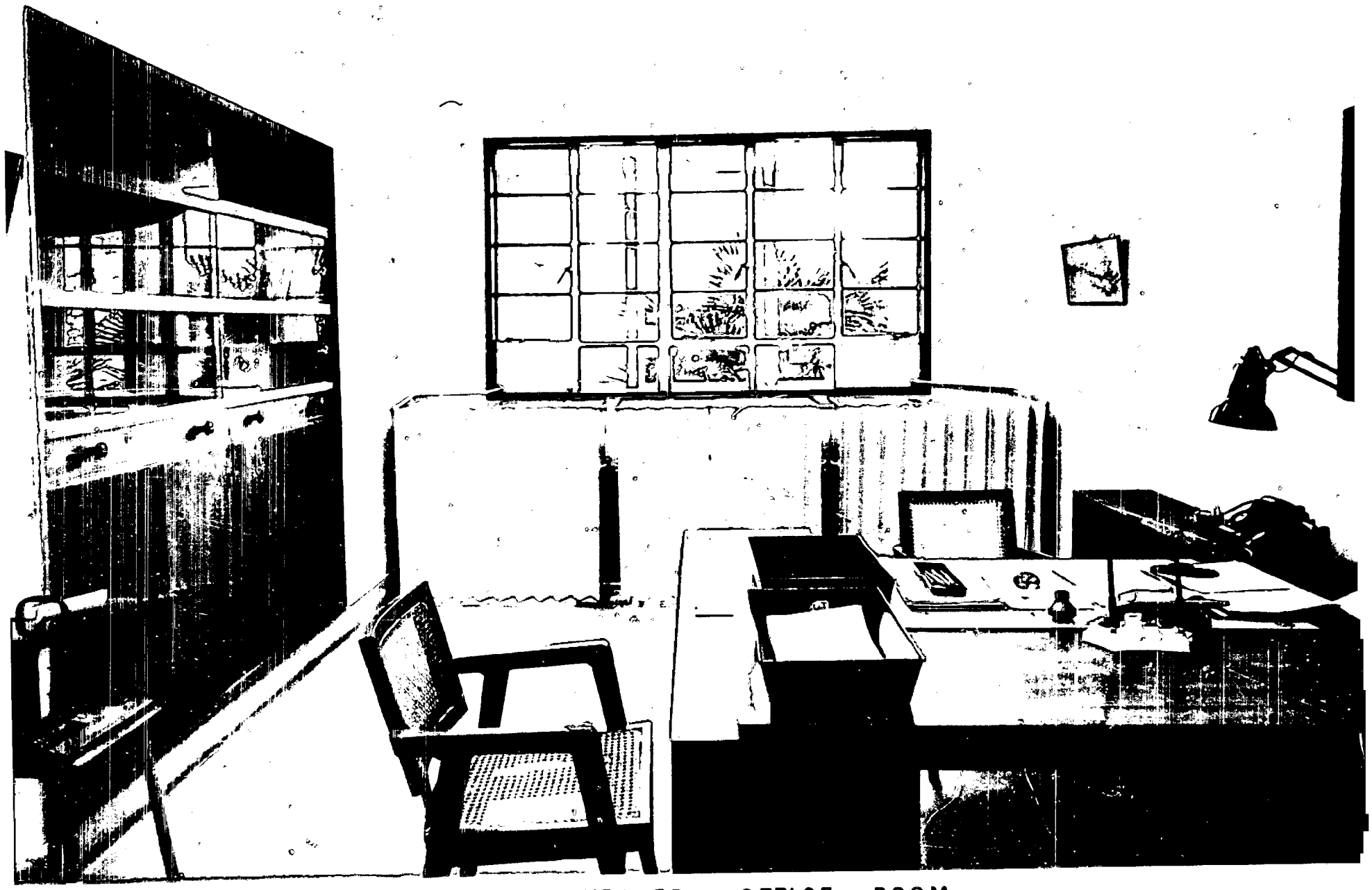

SOLAR HEATED OFFICE ROOM

C_E_R_T_I_F_I_C_A_T_E

Certified that the thesis entitled

' Application of solar energy for water and Room heating' which is being submitted by Shri H.P.Garg, M.Sc., for the award of the degree of Doctor of Philosophy in Physics of the University of Roorkee, is a record of his own work, carried out under our supervision and guidance. The matter embodied in this thesis has not been submitted for the award of any other degree of any university.

This is further to certify that he has worked for a period of about three years at the Central Building Research Institute, Roorkee, to prepare this thesis.

ICRRao

(K.R. Rao)
Head of Heat Transfer
Section,
Central Building Research
Institute,
Roorkee

RPmukerji

(Rajendra Prakash)
Professor of Mech. Engg.
Department,
University of Roorkee,
Roorkee.

SKJoshi.

(S.K. Joshi)
Professor and Head
Physics Department
University of Roorkee
Roorkee.

A C K N O W L E D G E M E N T S

The author wishes to express his deep appreciation to his advisors Dr.K.R.Rao, Scientist in charge, heat transfer section, Central Building Research Institute, Roorkee, Dr. Rajendra Prakash, Professor of the department of Mechanical Engineering, University of Roorkee and Dr.S.K.Joshi, Professor and Head of Physics Department, University of Roorkee for their valuable suggestions and general guidance throughout the work.

He is also indebted to Prof.Jinesh Mohan, Director and Dr.N.K.D.Choudhury, Assistant Director, Central Building Research Institute, Roorkee for the interest shown, encouragement given and facilities provided to carry out this study.

The author also expresses his thanks to Dr. C.L.Gupta, formerly a scientist at C.B.R.I., Roorkee for initiating the work on solar energy at C.B.R.I. and for the sustained interest shown in the present study.

The assistant rendered by the solar energy section staff at C.B.R.I., Roorkee and computer centre staff at C.B.R.I.C., Roorkee is gratefully acknowledged.

LIST OF PHOTOGRAPHS

SYNOPSIS OF THESIS

SYNOPSIS

The present work deals with the various studies carried out by the author on estimation of solar radiation, flat-plate solar energy collector design and its application for water heating and room heating. A summary of these studies are given below in brief :

1) ESTIMATION OF SOLAR RADIATION:

For a better utilisation of solar energy, the information regarding hourly rate of total and diffused solar radiation on horizontal and on various inclined surfaces on clear as well as on average days is needed. In India this type of data either measured or computed is not available. A method is therefore developed in this work, for the computation of hourly global and diffused solar radiation on horizontal surface from the actual measured sunshine hours data which is available for about 100 stations.

Solar radiation on various planes for all the orientations are measured under various sky conditions (overcast and clear) at Roorkee and are compared with the computed values. It is shown that even under overcast sky conditions the usual assumption of isotropy of sky radiation is not valid. An experimental method of

determining the albedo of the ground is described.

For various places the conversion factors that are to be applied to the total solar radiation on a horizontal surface in order to obtain the daily totals on the various inclined surfaces, are provided. These conversion factors include the direct, diffused and ground reflected components of solar radiation. With the methods and data provided, the availability of solar energy at any place can easily be estimated for a rational design of solar energy devices.

ii) [illegible]

A flat-plate collector was developed by the author and is optimized to give maximum efficiency per unit of cost. Expressions, for various parameters, such as plate efficiency factor, heat removal efficiency factor, effective transmissivity absorptivity product, overall heat loss coefficient from collector plate to outside air, etc. which affects the performance of the flat-plate collector, are derived.

Generalized performance curves for various configurations and operating temperatures of flat-plate collectors for a number of Indian cities are obtained. Expressions are also derived for arriving at optimum absorber size for various places.

A formula for the optimum tilt of flat-plate collector which takes into account, the direct and diffused solar radiation and also the variation of transmittance of glass cover with angle of incidence, is derived.

iii) SOLAR WATER HEATING:

(a) Small size, domestic type heaters:

A theoretical model for predicting the thermal performance of natural circulation type solar water heater is developed and experimentally validated for clear as well as cloudy weather. With the help of this model a prototype solar water heater (140 litres) capable to meet the requirements of an average Indian family of five persons is developed and its performance for a number of years under actual conditions, with different draw-off schedules during the day time, has been studied.

(b) Small size, low cost solar water heater:

A low cost solar water heater (90 litres) comprising a flat, shallow tank which performs the dual function of absorbing heat and storing the heated water, is developed. This heater is found ideal for daytime use. Various design and operating parameters are optimized with the help of the theoretical model developed for the purpose.

(c) Large size solar water heater:

To meet the demands of big establishments like hotels and hostels, large size solar water heaters are required. Such large installations introduce special problems which require investigations before arriving at a suitable design. The effect of mass flow rate and the various controls used for the operation of the water pump are experimentally studied. The various possible modes of inter-connections of large number of absorber banks such as in cascade, series, series parallel and parallel are experimentally studied and an optimum way of connecting them for a maximum efficiency at low cost, is found.

A prototype large size solar water heater (600 litres) is developed on the basis of above studies and its performance was studied for three years under actual conditions of use at a local hospital.

iv) SOLAR ROOM HEATER:

A theoretical study on a conventional solar air heater has been made. From this study, the mass flow rate and the duct depth in the absorber are optimised to give a maximum efficiency per unit of cost. Design curves are also developed from which the collector output for a given climate and operating conditions can be predicted.

An experimental study on the performance of various types of solar air heaters, for room heating purposes, has been made under various operating conditions at Roorkee. From this study, the practical numerical values of useful design parameters such as the effective transmissivity-absorptivity product, overall heat loss coefficient, plate efficiency factor, heat removal efficiency factor, etc, are brought out.

These air heaters, without the provision of storage are employed to heat a typical room during a severe winter period at Roorkee with a view to evaluate their performance. These studies indicate that with such a solar air heating system the room air temperatures can be raised by 8 to 10°C during sun-up hours on clear days. This method of heating rooms without storage is ideally suitable for office rooms as they are occupied during daytime.

For heating a room both day and night periods, by solar energy, an integrated storage cum radiant heating panel system with the flat-plate collectors using water as a medium has been developed. The performance of this system has been studied by heating a test room in winter months at Roorkee. The results were found to be

encouraging and the room temperatures could be maintained between 19 to 21^{o}C over a 24 hour period. Based on the experimental observations, design curves, for arriving at the absorber size and storage panel size for various heating requirements are developed.

TABLE OF CONTENTS

CHAPTER I

SCOPE OF WORK

1.1 INTRODUCTION

The world's population is increasing rapidly and the per capita demands for energy are increasing still more rapidly. The majority of the world's population which has been lagging behind are on the move towards rapid industrialisation. Consequently the requirements for fuel have increased enormously. Already some countries are beginning to feel the pinch of diminishing supplies of easily minable coal. It is also being realised that it is the time to start intensive research for fuel substitutes to cope with the future demands. The future generations may face a serious energy crisis due to the rapid rate of depleting the energy resources if new sources of energy are not brought into large scale use.

Sunshine is one of the greatest assets that the earth has ever known and infact is a real source of all fossil fuel. Since the beginning of human history, man has tried to use solar energy to improve his life. Yet, because of the difficulties involved in the efficient collection and effective storage of solar energy and moreover because of the ease and efficiency of fossil fael utilisation, not much effort has been devoted to the s cientific utilisation of solar energy.

Modern civilisation is completely dependent on cheap and abundant energy. The economic wealth and the material standards of living of a country are determined by the technologies and fuels which are available. Table 1.1 gives the per capita incomes and energy consumption from commercial sources (coal, oil, gas and hydro) in 1958 and also the per capita consumptions of non commercial fuels (wood, bagasse, dung among others). In the past few decades, large scale communication systems has increased the contact between the people of the world. This contact has stimulated the populations of under-developed areas to struggle for economical development. Most of these areas are in arid or semi-arid regions where sunshine is abundant and the expense of fossil fuel and hydroelectric power is prohibitively high. Here the effective utilisation of solar energy is most attractive.

In most of the under-developed countries, solar energy is more or less a part and parcel of their life. In under-developed countries the utilisation of solar energy is most likely to overcome the mental barriers which often resist the introduction of advanced technologies.

1.2 SOLAR ENERGY

1.2.1 Facts about Solar Energy

An important fact regarding the utilisation of solar energy is that it is the most abundant source of energy known to man, and is likely to last as far as

Energy consumption and per capita income (1948) for some selected countries.

	Per capita income (dollars)	Per capita consumption of coal. energy (tons of coal equivalent)	Per capita consumption of non-coal sources of (tons of coal equivalents)	Total energy consumption.
Australia	1123	3.03	0.43	4.06
Burma	40	0.64	0.25	0.89
Canada	1500	5.39	0.70	5.99
Ceylon	116	0.00	0.25	0.24
Chile	201	0.70	0.23	0.93
Denmark	837	2.81	0.35	2.76
Egypt	134	0.24	0.20	0.44
France	943	2.41	0.15	2.66
Germany	771	3.32	0.13	3.45
Greece	333	0.33	0.20	0.53
India	66	0.14	0.06	0.20
Iran	116	0.20	0.03	0.23
Italy	491	0.93	0.17	1.07
Japan	356	0.67	0.17	1.04
New Zealand	1101	1.93	0.09	2.17
Philippines	102	0.16	0.20	0.41
Spain	300	0.84	0.17	1.01
Switzerland	1267	1.67	0.15	1.82
South Africa	377	2.83	0.04	2.89
United Kingdom	939	4.73	0.02	4.75
United States	2006	7.05	0.40	8.05
Sweden	1169	2.98	0.53	3.51

Source : Statistical office of the United Nations.

man can comprehend.

A close examination of research and develepm t activities, the world over indicates that the greatest advances have been or are likely to be made in the utilisation of solar energy in relatively small unit. This factor is particularly important for serving the needs of the under-developed areas, and fits into the pattern of their rural economies. Small units can be tailored to the needs of individual communities and the availabilities of surplus manpower will largely obviate any need for mechanisation.

Availability, intermittance and storage are the most important consideration in the utilisation of solar energy.

Solar energy utilisation may not be practicable in all the locations or in all climates. The number of bright sunshine hours, solar radiation and the height of the sun in the sky are all factors which must be considered. Arid regions near to equator and which are actually short of cheap fuels have greatest possibilities for its use. Places situated between 40°N and 40°S latitude would be more suitable.

1.2.2 Symposia and Conferences

Within the past two decades, several international symposia have led to an active and rapidly increasing interest on the part of scientists and engineers, and of the general public as well, in the direct use of the

sun's energy. A symposium on space heating with solar energy[1] was held in 1950 at M.I.T., U.S.A. Symposia on solar energy were organised by the American Academy of Arts and Sciences[2] and Ohio Academy of Sciences[3], at University[4] of Wisconsin in 1953. In 1954 UNESCO and the Indian government sponsored a symposium[5] on solar energy and wind power in which various technical possibilities, social and political implications in the use of solar energy were discussed.

At the conference held at University of Arizona, at Tucson[6] in 1955, more stress was laid on basic research in solar energy. Another international conference in the same year 1955 was held in Phoenix[7] under the name of World symposium on applied solar energy.

In 1958 Professor F.Trombe organised an international symposium in France[8] emphasising the thermal aspects of solar energy in research and industry.

In April 1961, a symposium was organized by the National Academy of Sciences in Washington[9], in which economic restrictions in the use of solar energy were disregarded and an attempt was made to bring out new ideas and encourage research on solar energy that ight find practical application in the future.

A conference was held in Rome[10] in August 1961 and it attracted 500 scientists from over 50 countries. This conference was organised by the Social and Economic

Division of the United Nations. All phases of applied solar energy except agriculture were considered. In the same year 1961, another seminar on solar and aeoli energy was held at Sounion in Greece[11]. The main topics of discussion were generation of electricity, the large scale use of solar water heaters, and the production of power from methane obtained from the formation of algae.

An international solar energy society conference was held in March 2-6, 1970 at Melbourne[12], Australia. Recently an another International solar energy symposium was held in Washington[13], May 10-15, 1971. An International solar energy society was formed in 1954 and brings out the Journal of solar energy which is a forum for scientists working on solar energy applications.

1.3 SOLAR ENERGY DEVICES

A good deal of efforts have been devoted towards the utilisation of solar energy in various areas of human activities for the last two decades. Several theoretical and practical studies on various applications have brought out the feasibility of effective and economic utilisation of solar energy. Some of the direct application of solar energy are heating water, heating and cooling buildings, refrigeration, dehydration, cooking and baking, distilling water from sea or brackish sources. Solar energy can be converted into mechanical power through heat engines or directly into electricity through thermo-electricity and photo-voltaic conversion. On the biological side successful experiments have b done on

growing algae in solar ponds.

It can be said that while numerous applications have been demonstrated, very little commercial use is being made of the solar energy. Solar energy is the free gift of nature and more so in the hot and arid regions of the world than in the colder northern climates where this bounty of nature is not so plentiful.

1.4 PRESENT STUDY

The type of applications on which a country focusses its attention would depend mostly on its stage of technological advancement, economic standards, imbalances in energy resources etc. In the context of our special requirements and the availability of solar energy in abundance in most parts of the country, the problem appears to be the development of such devices which are cheap enough to find acceptability on a wide scale.

The low grade heat, that is, at a temperature below the normal boiling point of water, can be accomplished with relatively simple equipment, and with a collection efficiency of the order of 60 per cent. This low grade heat may be used for domestic hot water supply, house heating and cooling and distillation to provide drinking water from salt water, which would be of immediate application in tropical countries like India.

Solar energy collector is one of the most important item which is used in all solar energy utilization devices. These collectors are generally of two types-the flat-plate

type and focussing type. Various designs and their performances are discussed in a number of references[14,15,16,17,18,19]. The flat-plate collectors are most suited for temperatures below boiling point of water i.e.100°C. These collectors do not follow the sun, absorbers direct as well as diffused solar radiation and are cheaper than focussing type of collectors. So these collectors are preferred for water and space heating applications.

The present is an experimental study of the performance of the flat-plate collectors and their use for water heating and house heating. The results obtained not only show that solar energy utilisation is feasible but also that it is economical for under-developed countries to adopt them.

Methods have also been developed for estimating the hourly total solar radiation on any inclined surfaces of any orientation for those places where only sunshine hours data is available. This is essential for the correct designing of solar energy systems or any environmental control systems.

Various climatic, operating and design parameters which influences the performance of flat-plate collectors are studied in detail and are combined and optimised so that the collector works at optimum performance at low cost. Various design factors are experimentally determined. A formula for the optimum tilt taking into account the variation of glass transmittance with the angle of

incidence of sun's rays and th diffused solar radiation has been derived. Simple curves for obtaining optimum tilt at any place for anytime of the months are presented.

Simple design curves for arriving at optimum collector area for a given load are developed, based on measured and computed solar radiation data and other climatic factors. Further, simple emperical linear relations are given which are very useful for a quick assessment of the absorber area for any given situation.

1.4.1 Solar Water Heating

A mathematical model for predicting the performance of solar water heating systems is developed which has b . validated for clear as well as cloudy sky conditions. This model is used for studying the effect of a number of design parameters such as: height to diameter ratio of storage tank, stagnant water effect, circulation pipe diameter, height to width ratio of absorber, type of absorber, height of storage tank above the absorber's top etc. This model can be conveniently used for predicting the system temperatures, once the climatic and design conditions are given. Based on the above findings a domestic solar water heater capable of heating 140 litres of water upto 55°C in the winter evenings at Roorkee is developed and studied in a variety of ways so as to simulate the normal domestic usage conditions. The insulation used around the storage tank has been optimized to give an economic thickness.

A large size solar water heater for the industrial use have a number of other problems in addition to the probl encountered in domestic size. These problems are, inter-connection of absorber banks, flow rate effect, control for the pump operation, storage size and absorber size effect on each other. The effect of inter-connection of large number of absorbers such as in coscade, series, series parallel and true parallel on the overall performance is experimentally studied. It is observed that true parallel arrangement gives maximum efficiency and economy. This study is very useful and is directly helpful for places where large number of heating panels or radiators are used for heating the space.

The effect of flow rate on the overall performance has been experimentally observed and found that the flow rate has practically negligible effect on the performance in a closed circuit. This experimental fact goes against the theoretical findings where a number of assumptions and simplifications were made for predicting the effect of flow rate on the performance.

The effect of various controls, such as set temperature, set radiation, timeswitch and differential temperature, which are generally used for the control of pump operation, on the overall performance of the system, are experimentally studied. Such a comparative study has been made for the first time. It is observed that differential control as developed by the author gives maximum efficiency and minimum operating costs.

The effect of storage size on the performance for

a fixed absorber area and the effect of absorber area on the performance for a fixed storage size is theoretically studied, and experimentally proved. It is observed that for a fixed storage size there is an optimum absorber area at a given locality.

Based on the above studies a large size solar water heater of 600 litres capacity was designed and installed at a local hospital to study its performance. An immersion heater (3.0 KW) is fitted in the storage tank and connected in series with a safety thermostat and solar switch developed by a author. Thus the system becomes automatic and gives hot water for 24 hours either heated by sun if present or by electricity if sun is not shining. This unit is tested for a number of years under varying climatic and operating conditions.

A low cost solar water heater which is a built in storage type where a tank performs the dual function of absorbing and storing heat is also developed. This heater is mainly meant for day time use and does not store hot water for overnight. A theoretical model based on unsteady heat flow conditions is developed which can predict the mean storage temperature within an accuracy of 1°C. The model is used for optimizing the ratio of absorbing area to its capacity which determines the final temperature reached in the tank.

The performance of the heater is studied experimentally simulating various domestic usage conditions.

The effect of dirt deposition on the glass cover and plastic cover at various inclinations from the horizonta on the overall transmittance has been experimentally studied and correction factors for the dirt are determined both for glass and plastic covers. It is observed that more dust gets deposited on plastic as compared to glass sheet because of its electrostatic nature.

The economics of solar water heating as compared to water heating by electric geyser has been worked out for various power rates and various life expectencies of solar water heater. It is shown that solar water heating is economical as compared to electric heating of water for most of the Indian cities.

1.4.2 Solar Space Heating

The temperature required for heating houses is low, so it is not necessary to use the more expensive focussing and movable solar collectors. All solar space heating is done with flat-plate collectors mounted horizontally on a flat-roof, tilted toward the equator on a roof or placed vertically along the side of a building facing the equator.

Keeping this in mind four different types of solar air heaters such as corrugated type and Matrix type are developed and their performance are experimentally studied. Various design constants such as plate efficiency factor, heat removal efficiency factor, overall heat loss coefficient and effective transmissivity absorptivity product are experimentally determined. These values were not

available in the literature and are very helpful for designing these devices.

Flow friction characteristics of these air heaters responsible for their efficiencies as well as for circulating cost is optimized for maximum efficiency. The air gap or duct size between the rear and exposed absorber surface is also optimized.

Space heating by use of solar heated air from roof mounted collectors has been tested at the laboratory without any provision of storing heat. This system is found to be more economical and advantageous for buildings which are generally occupied during daytime and sun-up hours suhh as office buildings. This system is further tested for two winter seasons in an experimental room without having any insulation on the walls and roof. The performance data such as resulting rise in indoor air temperature, air circulating rate and cost, solar insolation rate and ambient air temperatures are measured and discussed.

Another type of a simple solar room heater suitable for single rooms has been developed and tested for two winter seasons once in an experimental room and then in an actual occupied office room. This system can be used even at those places where there is no electricity, as thermo-syphonaction can be made use of for circulation of water. The system uses a number of collectors placed at a convenient location and storage-cum-radiant panels

placed near the wall inside the room. These panels were specially designed to have more heat transfer area within a limited space. Radiative and convective heat loss from the panels which is a function of room air and surface temperatures is utilized in heating the room space. Curves for predicting the panel area and its water capacity for a given heat load requirement are developed. Linear curves for arriving at optimum collector area at different places which is a function of climatic, operating and design conditions for any required heating load are discussed.

The economic design and operation of space heating system is inter-linked with the type of construction and of building concerned. The effect of providing insulation lining on the inner side of the room, on the heating load and thereby on the solar heating system has been studied. The results show that for an insulated structure the solar space heating can be proved to be economically feasible.

-*-*-*-

C H A P T E R - 2.

THE NATURE AND ESTIMATION OF SOLAR ENERGY

CHAPTER-2

THE NATURE AND DISTRIBUTION OF SOLAR ENERGY

2.1. INTRODUCTION

The knowledge of long term average hourly values of solar radiation intensity on monthly mean basis is essential for rational design of solar energy utilisation devices and environmental control systems for any location. The increased use of flat-plate collectors for utilisation of solar energy for water and space heating and airconditioning has necessitated the measurement of solar radiations on inclined surfaces under different sky conditions. Measurement of direct and diffused solar radiation on sloped surfaces of any orientation, under clear, average and overcast days is not so far attempted in the tropics.

In India, there are only a few stations which continuously record the instantaneous values of total solar radiation intensity on a horizontal surface and only a couple of these are recording total and diffused components seperately.

For places where no measurements are made empirical methods have been proposed for estimating the solar energy available, based on other climatic data. The most direct approach has been to use actual sunshine hours which are widely measured by Campbell Stokes sunshine recorders. However, no records in most meteorological stations are limited to visual estimates of percent cloud cover, i.e. nebulocity, or duration

of sunshine, it is usual to resort to simple empirical relations, worked out on statistical basis from which the rates of total insolation on horizontal surfaces may be predicted. A correlation between the total radiation received on a horizontal surface during cloudy periods with the degree of cloudiness was first made by Kimball[1] in 1919. Later Angstrom[2] proposed the relation:

$$Q = Qc \ (a+bs) \qquad \text{--------(2.1)}$$

where Q = total radiation received on a horizontal surface on an average cloudy day.

Qc= total radiation received on a horizontal surface on a clear day.

a & b = constants

S = Ratio of actual to possible sunshine hours.

The constants a & b varies with the locality, prevailing cloud formation and the time of the year.

Cloud cover as estimated at weather stations[3] can be used for estimating solar radiation on average days[4,5].

No method is presently available by which one can calculate from theory alone the solar energy available during hazy or partly cloudy days. Theoretical methods developed for calculating solar radiation are primarily for cloudless skies only and are based on the amounts of dust, moisture and Ozone present in the atmosphere. The standard clear sky solar radiation curves given by Moon[6] (1940), Klein[7] (1948) and Pleijel[8] (1964) have found wide application. The atmospheric transmission curves given by Threlkeld and

Jordan[9] are used by Rao and Deshadri[10] for the computation of direct solar radiation for Indian latitudes for clear days.

There are statistical correlations developed for computing the diffused component in terms of the total radiation intensity, the altitude of the sun and atmospheric turbidity. Choudhury[11] has extended the applicability of Jordan's[12] method, based on the definition of cloudiness index, to tropical climates. Sharma and Pal[13] have extended Parmelee's[14] analysis, based on the definition of clearness number, to take into account clear as well as cloudy days. All these methods, however, require hourly radiation data, which are not available for most of the places in the country.

2.2. SOLAR RADIATION OUTSIDE THE EARTH'S ATMOSPHERE

The sun's intensity outside the earth's atmosphere consists of a temporarily invariant component known as solar constant. It is the rate at which energy is received upon a unit surface, perpendicular to the sun's beam, at the upper limit of our atmosphere for the earth's mean distance from the sun. During the last 30 years, estimates of this total solar irradiance have ranged from 1.90 to 2.05 cal per cm^2 per minute. At present, the evaluations that have found most support are those of Johnson[15] in the USA (2.0 cal per cm^2 per minute) and Nicolet in Europe (1.98 cal per cm^2 per minute). A summary of the various values of solar constant suggested from time to time are given in table (2.1).

TABLE 2.1:

SOLAR CONSTANT VALUES AS GIVEN BY VARIOUS WORKERS.

Year	Authority	Solar constant Cal/cm^2 minute.
1923-1952	ABBOT	1.94
1932	LINKE	1.94
1934-1936	MULLERS	1.95
1933	UNSOLD	1.90
1951	NICOLET	1.98
1951	ALLEN(16)	1.97
1954	JOHNSON	2.00
1955	UNSOLD	1.96
1956	STAIR & JOHNSON	2.06
1959	ALLEN	1.99
1970	THEKAEKARA(17)	1.94

Until now, all methods of deriving the integral wavelength solar constant and its spectral components have entailed extrapolation of measurements made at the earth's surface under clear sky conditions at different heights and at different solar altitudes.

Direct measurements made by satellites in recent years had produced converging evidence that the Johnson value of the solar constant was too high and the spectral distribution curve required significant revisions. Thekaekara[17] of N.A.S.A. Goddard space flight centre made a close study of the data and proposed a value of solar constant 1.94 cal per cm^2 per minute (1.353.KW/m^2) which is about 3 percent lower than the Johnson value of 2.0 cal per cm^2 per minute. The spectral distribution of extraterrestrial solar radiation, according to Thekaekara, is presented in fig 2.1.

The radiation intensity on horizontal surface (Ioh) outside the earth's atmosphere is a function of sun's zenith angle (θh), and is given as :

$$Ioh = Ion \cos \theta h \qquad \text{----------(2.3)}$$

where Ion = Solar constant

The incident angle, θh, can be written as :

$$\cos h = \cos L \cos \delta \cos v + \sin L \sin \delta \qquad \text{------(2.3)}$$

where L = latitude of the place.

δ = declination of sun

v = hour angle from solar noon.

The various angles are shown in fig (2.2).

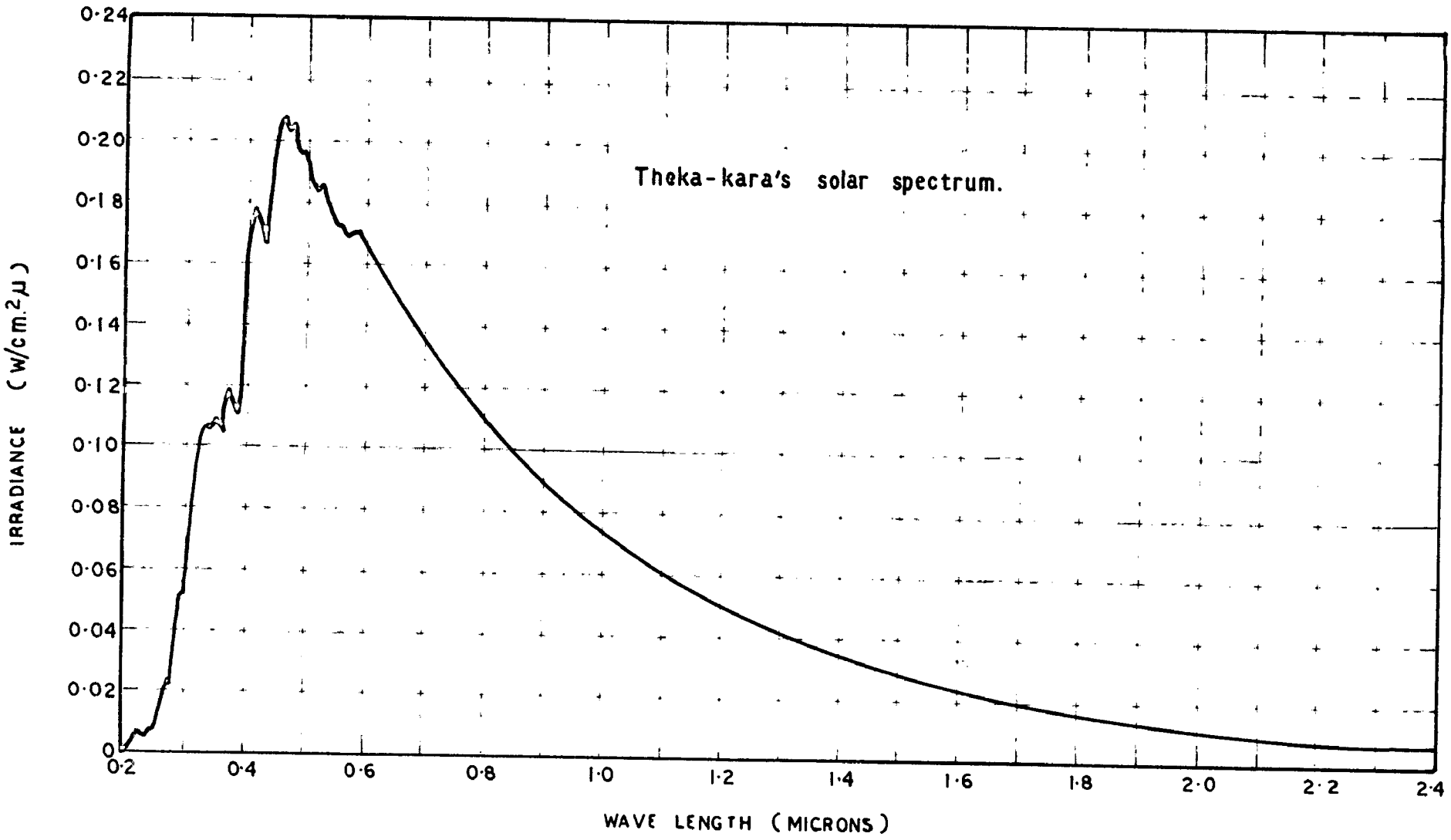

FIG. 2·1 SPECTRAL DISTRIBUTION OF THE EXTRATERRESTRIAL SOLAR RADIATION

The daily extraterrestrial radiation on a horizontal surface (Ho) can be determined by integrating equation (2.3) with respect to time for all hours when Cos θ_h is positive. Assuming Ion and δ to be constant for a day, we get the expression

$$Ho = Ion \int_{-\omega s}^{+\omega s} (\cos L \cos\delta \cos\omega + \sin L \sin\delta) \times d\left(\frac{24}{2\pi}\omega\right) \qquad \text{-------(2.4)}$$

$$= \frac{24}{\pi} Ion (\cos L \cos\delta \sin \omega s + \omega s \sin L \sin\delta) \text{---(2.5)}$$

$$= \frac{24}{\pi} Ion \sin L \sin\delta (\omega s + \tan \omega s) \qquad \text{-------(2.6)}$$

Where ωs is the sunset hour angle in radians and can be obtained by equation (2.3) by putting $\theta_h = 90^\circ$,

$$\cos \omega s = - \tan L \tan\delta \qquad \text{-------(2.7)}$$

It can be easily seen here that possible sunshine hours is given as

$$Sp = 2\omega s/15 \qquad \text{-------(2.8)}$$

By using the new value of solar constant as 1.94 cal/cm^2 minute, and applying the correction factor in it as given in table (2.2) the values of Ho and Sp are computed with the help of above equations and are shown in table 2.3 and 2.5 respectively.

The solar radiation on a tilted surface (Iot) outside the earth's atmosphere is given as :

$$Iot = Ion \cos\theta t \qquad \text{--------(2.9)}$$

TABLE 7.2: Solar constant correction factor

DAY OF MONTH	JAN.	FEB.	MAR.	APR.	MAY	JUNE	JULY	AUG.	SEPT.	OCT.	NOV.	DEC.
1	1.0335	1.0283	1.0173	1.0000	0.9841	0.9714	0.9636	0.9703	0.9883	0.9936	1.0164	1.0330
9	1.0326	1.0263	1.0160	0.9993	0.9793	0.9692	0.9670	0.9736	0.9902	1.0062	1.0297	1.0305
18	1.0310	1.0235	1.0193	0.9913	0.9757	0.9680	0.9680	0.9757	0.9930	1.0097	1.0223	1.0310
22	1.0300	1.0237	1.0057	0.9875	0.9737	0.9670	0.9698	0.9795	0.9949	1.0133	1.0287	1.0327

TABLE 2.3: Mean values for calendar months of extraterrestrial daily insolation(Langley/day) on a horizontal surface outside the earth's atmosphere for various latitudes.

(Solar constant = 1.94 langley/minute)

MONTH	LATITUDE: 8°N	10°	12°N	14°N	16°N	18°N	20°N	22°N	24°N	26°N	28°N	30°N	32°N	34°N	36°N	38°N
Jan.	751	729	707	686	661	637	613	587	562	535	510	482	454	427	399	371
Feb.	814	789	763	738	713	688	663	638	612	585	559	533	505	481	453	426
March	871	844	818	792	767	741	715	689	663	637	611	585	559	533	507	481
April	918	893	868	842	817	792	767	742	717	693	668	644	619	595	571	547
May	957	933	910	888	865	843	820	798	776	754	732	711	690	669	648	628
June	987	965	943	922	901	880	860	840	820	801	782	763	745	727	709	692
July	991	969	948	927	907	887	867	848	829	810	792	774	757	740	723	707
Aug.	957	939	915	901	883	866	849	832	816	800	784	769	754	739	725	711
Sept.	890	868	845	823	801	780	759	739	719	700	681	663	645	628	611	595
Oct.	814	793	772	751	731	711	692	673	655	637	620	603	587	571	556	541
Nov.	776	757	737	718	699	681	663	646	629	613	597	581	566	551	537	523
Dec.	734	711	688	664	639	614	590	565	539	514	489	464	439	414	390	367

TABLE 2.4: Conversion factor for direct solar radiation for outside the earth's atmosphere for various tilts.

MONTH	SOLAR DECLINATION (degrees)	10° North Latitude				20° North Latitude				30° North Latitude				40° North Latitude			
		ω_p (hrs)	H_b	$RD = HDT/H$		ω_p (hrs)	H_b	$RD = HDT/H$		ω_p (hrs)	H_b	$RD = HDT/H$		ω_p (hrs)	H_b	$RD = HDT/H$	
				D=L+15	D=L-15			D=L+15	D=L-15			D=L+15	D=L-15			D=L+15	D=L-15
JAN.	-21.00	11.47	723.7	1.26	1.00	1.12	10.91	610.6	1.49	1.10	1.33	10.20	489.0	1.08	1.41	1.63	9.45	362.0	2.02	2.01	2.22
FEB.	-13.01	11.68	789.3	1.14	1.00	1.07	11.35	708.4	1.28	1.06	1.20	10.97	609.7	1.51	1.23	1.41	10.60	474.0	1.91	1.81	1.70
MAR.	- 2.33	11.94	864.1	1.01	1.00	1.02	11.67	813.8	1.07	1.03	1.08	11.30	738.7	1.10	1.14	1.19	11.72	641.3	1.33	1.31	1.37
APR.	+ 9.33	12.22	903.9	0.87	1.00	0.97	12.45	903.7	0.87	1.00	0.97	12.78	877.0	0.89	1.03	1.01	12.06	824.3	0.96	1.00	1.03
MAY	+18.81	12.45	908.8	0.77	1.00	0.93	12.93	958.3	0.78	0.98	0.90	13.49	966.5	0.72	0.96	0.90	14.18	963.0	0.78	0.97	0.91
JUNE	+23.26	12.57	902.6	0.72	1.00	0.91	13.03	965.7	0.67	0.97	0.86	13.91	1005.3	0.64	0.89	0.84	14.01	1021.6	0.83	0.91	0.83
JULY	+21.69	12.53	905.3	0.73	1.00	0.92	13.10	961.1	0.69	0.97	0.87	13.73	992.5	0.67	0.94	0.86	14.60	1000.2	0.86	0.93	0.86
AUG.	+14.23	12.34	893.3	0.81	1.00	0.95	12.70	931.1	0.80	0.99	0.93	13.12	989.0	0.80	0.99	0.94	13.64	996.7	0.93	1.02	0.98
SEPT.	+ 3.41	12.08	838.6	0.94	1.00	1.00	12.16	868.7	0.96	1.01	1.03	12.26	910.7	1.03	1.03	1.09	10.30	734.3	1.13	1.19	1.21
OCT.	- 8.11	11.80	833.0	1.00	1.00	1.05	11.60	783.9	1.13	1.05	1.14	11.37	688.4	1.34	1.20	1.30	11.00	552.5	1.62	1.45	1.66
NOV.	-18.21	11.55	757.4	1.21	1.00	1.10	11.00	660.1	1.41	1.03	1.27	10.34	536.6	1.73	1.36	1.63	9.03	391.3	2.31	1.89	2.03
DEC.	-23.21	11.42	711.6	1.30	1.00	1.13	10.50	630.0	1.34	1.11	1.35	10.00	454.6	1.93	1.60	1.74	9.10	319.9	2.36	2.15	2.60

TABLE 2.5: Mean values for calendar months of possible sunshine hours on a horizontal surface for various latitudes.

LATITUDE (degrees) / MONTH	0°N	10°N	12°N	14°N	16°N	18°N	20°N	22°N	24°N	26°N	28°N	30°N	32°N	34°N	36°N	38°N
JAN.	11.58	11.47	11.36	11.20	11.14	11.03	10.91	10.79	10.66	10.54	10.40	10.26	10.12	9.96	9.80	9.63
FEB.	11.76	11.69	11.62	11.56	11.49	11.42	11.36	11.28	11.21	11.13	11.06	11.98	10.89	10.80	10.71	10.61
MARCH	11.96	11.94	11.93	11.91	11.90	11.89	11.87	11.86	11.86	11.83	11.82	11.80	11.79	11.77	11.75	11.73
APRIL	12.17	12.22	12.26	12.31	12.35	12.40	12.45	12.50	12.56	12.61	12.66	12.72	12.78	12.83	12.91	12.98
MAY	12.35	12.45	12.54	12.63	12.73	12.83	12.93	13.04	13.14	13.25	13.37	13.49	13.61	13.74	13.83	14.03
JUNE	12.46	12.57	12.69	12.81	12.94	13.06	13.19	13.33	13.46	13.61	13.75	13.91	14.07	14.24	14.42	14.61
JULY	12.42	12.53	12.64	12.76	12.87	13.00	13.10	13.22	13.35	13.47	13.62	13.76	13.91	14.07	14.23	14.40
AUGS	12.27	12.34	12.41	12.48	12.55	12.63	12.70	12.78	12.86	12.94	13.03	13.12	13.21	13.31	13.41	13.52
SEPT.	12.06	12.07	12.09	12.11	12.12	12.14	12.16	12.18	12.20	12.21	12.23	12.26	12.29	12.30	12.32	12.36
OCT.	11.94	11.91	11.77	11.73	11.69	11.64	11.59	11.56	11.51	11.47	11.42	11.37	11.32	11.26	11.21	11.15
NOV.	11.64	11.56	11.49	11.37	11.29	11.18	11.08	10.93	10.87	10.77	10.66	10.54	10.42	10.29	10.15	10.01
DEC.	11.54	11.42	11.30	11.18	11.06	10.93	10.80	10.67	10.53	10.39	10.24	10.09	9.93	9.76	9.58	9.39

where θt = angle of incidence of solar rays on the tilted surface.

If the surface is tilted β degrees from the horizontal towards the equator i.e. facing south in the northern hemisphere then the cosine of the angle of incidence on the tilted surface is given as

$$\cos\theta t = \cos(L-\beta)\cos\delta\cos\omega + \sin(L-\beta)\sin\delta \quad \text{----(3.10)}$$

The sunset hour angle for the tilted surface is given as

$$\cos\omega st = -\tan(L-\beta)\tan\delta \quad \text{--------- (3.11)}$$

The daily extraterrestrial radiation on the tilted surface (H_{ot}) can be determined by integrating equation (3.9) with respect to time and is given as :

$$H_{ot} = \frac{24}{\pi} I_{on}\left[\cos(L-\beta)\cos\delta\sin\omega_s + \sin(L-\beta)\sin\delta\right]$$

$$\omega_s \leq \omega st \quad \text{----------(3.12)}$$

and $$H_{ot} = \frac{24}{\pi} I_{on}\left[\cos(L-\beta)\cos\delta\sin\omega st + \omega st\sin(L-\beta)\sin\delta\right]$$

$$\text{---------(3.13)}$$

when $\omega st \leq \omega_s$

Thus the conversion factor (R_D) for converting direct solar radiation from a horizontal surface to a tilted surface at outside the earth's atmosphere is given as :

$$R_D = \frac{H_{ot}}{H_o} = \frac{\cos(L-\beta)}{\cos L}\left(\frac{\sin\omega_s - \omega_s\cos\omega st}{\sin\omega_s - \omega_s\cos\omega_s}\right) \text{ when } \omega_s \leq \omega st$$

$$\text{--------(3.14)}$$

and $$R_D = \frac{H_{ot}}{H_o} = \frac{\cos(L-\beta)}{\cos L}\left(\frac{\sin\omega st - \omega st\cos\omega st}{\sin\omega st - \omega_s\cos\omega_s}\right) \text{ when } \omega st \leq \omega_s$$

$$\text{--------(3.15)}$$

Table 2.4 gives the value of Hot/Ho for various latitudes computed from equation (2.14) or (2.15). Here those tilts are considered which are usually used in case of flat-plate collectors. The value of solar declination, and the equation of time used for above computations were for 15th of each month and were seen from Nautical Almanac[18].

The optimum tilt for the flat-plate collector can be seen from table (2.4) for the desired season of use. For example, for a collector at 30°north latitude and tilted at 45°from the horizontal plane, this ratio i.e. H_{ot}/H_o is 1.98 during December. The ratio increases to as much as 2.86 for a collector at 40° north latitude and tilted at 65°from the horizontal surface. Although these ratios are worked out for extraterrestrial radiation only, the conclusions drawn will still hold good when the effect of the earth's atmosphere is taken into consideration. However, the actual quantitative values may be different.

2.3. SOLAR RADIATION AT THE EARTH'S SURFACE:

As has been seen, the intensity of beam radiation at the top of the atmosphere is known to a high degree of accuracy and remains sensibly uniform from sunrise to sunset throughout the year, the only variation being due to the slight ellipticity of the earth's orbit. The energy reaching the ground, however, varies progressively with latitude, altitude, season and time of day and may change rapidly and discontinuously with changes in local meteorological conditions. During its passage downwards

through the atmosphere the solar beam is split up into four parts. One part is reflected back into space mainly by clouds, another is scattered in all directions by molecules of dry air, water vapour, carbon dioxide and ozone, while the remainder is transmitted through the atmosphere, being received at the ground as beam or direct radiation. As a consequence of the absorption of solar energy the component particles of the atmosphere are heated and emit long wave radiation in all directions. The fraction of the latter which eventually reaches the earth's surface together with the incident scattered radiation (short wave) comprises the incoming diffused radiation. The ground also emits long-wave radiation and reflects part of the incident direct and diffused radiation. All the separate processes of scattering and absorption are functions of the wave-lengths of the incident radiant energy. Due to this spectral selectivity the solar beam is both reduced in intensity and altered in wavelength distribution in a complex manner. As an exact analysis of this problem will lead to an extremely unwieldly solution of limited practical application meteorologists[19,20,21] have adopted a semi-empirical approach based upon a simplified physical picture of the atmosphere, each effect being considered separately as if none of the other

components were present and the overall effect is obtained by superposition.

3.31 Direct Radiation

In United States an analytical approach has been adopted, the effect of each component being considered separately in an attempt to evaluate a comprehensive formula from which the beam radiation or direct radiation at any location may be predicted in the absence of any local radiation measurements. The early work of Fivball[22,23,24,25] has been extended by Moon[26] and more recently by Threlkeld and Jordan[27]. Moon's relation between the monochromatic transmission and the intensities of the various depleting agents may be expressed by the following equations :

$$\log T_\lambda = \log \frac{I_{N\lambda}}{I_{o\lambda}} = m \frac{o3}{2.5} \log T_{\lambda o3} + m \frac{p}{760} \log T_{\lambda a} + m \frac{w}{20} \log T_{\lambda wa} + m \frac{w}{20} \log T_{\lambda wa} + m \frac{d}{500} \log T_{\lambda d} \quad \text{-----(2.16)}$$

Here the first term of the right side accounts for absorption by Ozone, the second Rayleigh scattering by clean, dry air, the third and fourth scattering and absorption by water vapour and the last term attenuation by dust. The component transmission factor, T, refer to standard amounts of 2.5 mm Ozone, 760 mm barometric pressure, 20 mm precipitable water vapour and 500 dust

TABLE 2.6: Atmospheric Conditions affecting air mass

Workers	Precipitable water (cm)	Dust particles (per cm^3)	Ozone Partial press. (cm Hg)	Solar constant Btu/ft^{2}hr
Moon (1940)	20	200	2.8	419
Gaton(1963)	10	200	3.5	448
Threlkeld & Jordan (1958)	Variable 7.8 mid winter 2.8 mid summer	clear sky 200 Industrial 800	2.5	442

TABLE 2.7: Variation of direct solar radiation (normal to sun's rays in Btu/ft^{2}hr) with air mass.

Workers	AIR MASS								
	0	1.0	1.5	2.0	3.0	4.0	5.0	6.0	8.0
	corresponding solar altitude (degrees)								
	=	90.0	41.8	30.0	19.6	14.6	11.5	9.3	7.8
Moon		419	334	283	230	196	169	149	133	197
Gaton		446	307	239	192	143	107	83	63	41
Threlkeld and Doe/Jan.	=	301	314	293	257	216	183	162	130	
Jordan Mar/Oct.	=	320	298	274	233	204	172	143	129	
June/July	=	330	259	233	194	150				
Sept.	=	310	220	253	214	170				
Nov/Feb.	=	321	308	228	250	216				

For the design of solar energy utilisation devices, the diffused radiation should also be given due weightage. It has been reported by Desikan, Iyer and Mahalkar[29] that at Delhi the diffused radiation on horizontal surface varies from 19 percent (November), to 30 percent (June) of the total solar radiation, on clear days and it varies from 34 percent (November) to 59 percent (July) for all days. It indicates that in tropical regions diffused radiation forms a high percentage and thus plays an important role.

Precise information concerning the intensity of diffused radiation and its variability in different parts of the world is severely limited and any formulae which have been proposed apply only to the particular locations. The scattering functions involved in diffuse radiation are extremely complicated and have only recently been evaluated numerically from Mie's theory[29] using special assumptions about the compositions of the aerosols. The work of Deirmendjain[30] and Sekera and Ashburn[31] has shown that it is possible to estimate the total diffused sky radiation (Dr) on a horizontal plane with the aid of the following simple formula proposed earlier by Albrecht[32]

$$Dr = K_p\,(I_{o,r} - I_r)\,\sin r \qquad \text{--------(3.17)}$$

$Sa/_{Sp}$, for Poona. Mooley[35] et-al and Lof[36] et-al have worked out this relation between the ratios, $H/_{Ho}$, and $Sa/_{Sp}$ where Ho is the daily total extraterrestrial radiation. The constants for the later relationship between, $H/_{Ho}$, and $Sa/_{Sp}$ have been worked out for Delhi, Poona, Calcutta and Madras by the author. Further, curves for determining the hourly values of total and diffused radiation are drawn following Whillier[37] and Liu and Jordan's[38] procedure. The hourly data reported by Anna Mani[39] et-al have been employed to obtain these curves. The proposed method for determination of hourly total and diffused solar radiation for average days on a horizontal surface is given below.

2.41 Relation between sunshine hours and global radiation:

The ratio of daily solar radiation on the earth's horizontal surface and the daily extraterrestrial radiation $H/_{Ho}$, is determined for those stations for which daily values of total solar radiation are measured and correlated them with the corresponding values of $Sa/_{Sp}$. The values of actual sunshine hours, Sa, for a number of Indian stations as given by Ram Dass[32] et-al are shown in table (2.5).

The linear equation should be of the form:

$$\frac{H}{Ho} = a + b\,\frac{Sa}{Sp} \qquad \text{----------(2.19)}$$

Sl. No.	Station	NOV	DEC	ANNUAL
1.	Trivandrum	6.5	8.6	6.4
2.	Kodaikanal	6.2	7.7	6.2
3.	Coimbatore	6.8	8.4	7.5
4.	Bangalore	7.5	8.4	7.0
5.	Madras	7.0	8.6	7.7
6.	Raichur	9.8	9.8	8.2
7.	Sholapur	10.2	10.1	7.9
8.	Poona	9.6	9.5	8.0
9.	Bombay	9.7	9.6	7.4
10.	Akola	10.3	9.9	8.5
11.	Jalgaon	10.3	9.9	8.6
12.	Nagpur	9.7	9.2	7.6
13.	Surat	10.1	10.0	8.8
14.	Baroda	10.3	9.9	8.5
15.	Calcutta	8.3	8.4	7.1
16.	Ahmedabad	10.4	9.8	8.7
17.	Allahabad	9.3	9.2	8.1
18.	Jodhpur	10.0	9.2	9.0
19.	Jaipur	9.9	9.0	8.4
20.	Agra	9.5	8.5	8.5
21.	Delhi	8.7	8.3	8.0
22.	Jullundur	8.6	7.6	8.3
23.	Srinagar	7.6	2.9	6.8

where

$\frac{H}{Ho}$ = cloudiness index (K_T),

$\frac{n}{Np}$ = ratio of actual to possible sunshine hours,

a&b = constants.

It has been shown by Hooley[36] et-al that the daily values of the constants a & b for Madras have not significantly altered from the mean monthly values of a & b. As such, monthly mean values on daily basis have been considered following Liu and Jordan[38].

The above type of relation has been studied in detail by Berg[40] and Monteith[41]. They showed that for high cloud cover conditions, the linear relationship is not valid strictly and as such this relation will give only the design values on a monthly mean basis. The linear relationship between $H/_{Ho}$ and $n/_{Np}$ obtained by a least square analysis by the author is shown in fig (2.3). The correlations derived for a few major Indian cities are given below :

For Delhi $H = Ho\ (0.10+0.82\ \frac{n}{Np})$ ------(2.20)

For Poona $H = Ho\ (0.28+0.53\ \frac{n}{Np})$ ------(2.21)

For Calcutta $H = Ho\ (0.39+0.26\ \frac{n}{Np})$ ------(2.22)

For Madras $H = Ho\ (0.24+0.52\ \frac{n}{Np})$ ------(2.23)

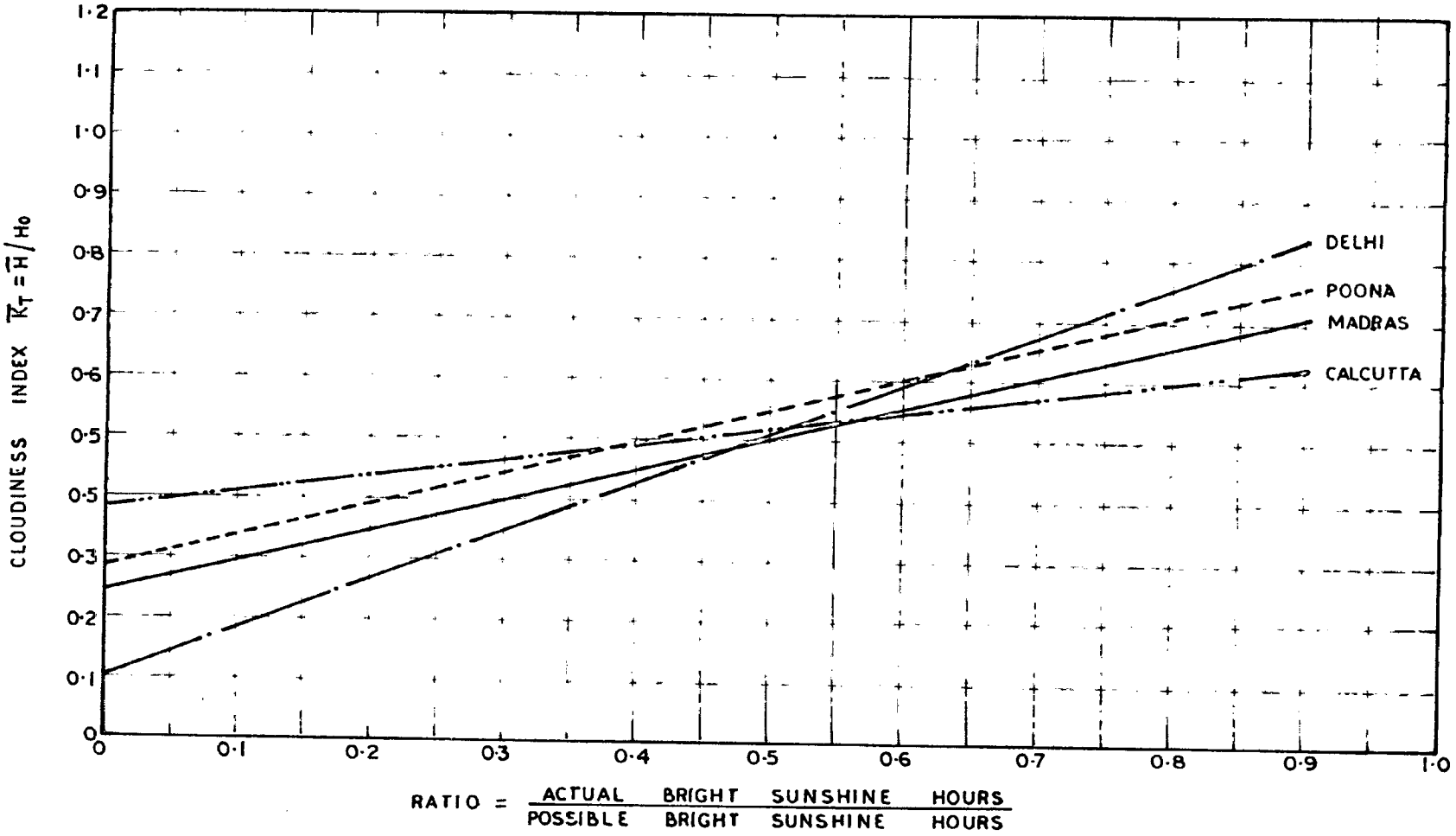

FIG. 2·3 RELATION BETWEEN CLOUDINESS INDEX AND RATIO OF ACTUAL POSSIBLE SUNSHINE HOURS

Once these relations are known, they can be utilized to determine H for all the places, for which only actual sunshine hours, So, are known and which have a cloudiness pattern similar to any of these four types. The values of Ho, Cp and Ko can be seen for various latitudes from table 2.3, 2.5 and 2.8, respectively. A comparison between the measured and computed values of daily total radiation for Delhi, Poona, Calcutta and Madras is made in Table (2.9). It can be seen that there is a good agreement between the measured and computed values. In 75 percent of cases the error is below 6 percent and in 25 percent of cases the error is from 5 to 10 percent.

2.42. Relation between daily diffused and daily global radiation:

The values of cloudiness index defined as the fraction of the extraterrestrial radiation reaching the earth's surface, K_T, as discussed earlier were determined on monthly mean basis and are given in table 2.10. These values are found to be between 0.4 and 0.8. Following Liu and Jordan's[12] procedure a relationship between the ratio of daily diffused radiation, D, to daily total radiation, H, and the cloudiness index, K_T, for Delhi, Poona, Calcutta and Madras has been obtained and is shown in Fig.(2.4). Using this curve, average daily diffused radiation, D, can be determined if the values of daily total radiation are known. The ratios of measured D to H for a number of Indian

TABLE 2.2: Comparison of computed and measured values of total solar radiation on horizontal surface. (langley/day)

PLACE		JAN	FEB	MAR	APR	MAY	JUNE	JUL.	AUG.	SEP.	OCT.	NOV.	DEC.
DELHI	MEAS.	341	421	530	621	636	563	423	405	471	430	371	321
	COMP.	350	430	496	581	581	560	450	446	451	516	419	362
POONA	MEAS.	458	533	562	622	600	505	371	389	430	456	444	396
	COMP.	470	544	601	624	652	616	426	417	463	462	435	445
CALCUTTA	MEAS.	355	432	466	542	646	411	393	389	366	400	382	330
	COMP.	339	401	461	513	535	450	436	403	406	399	364	329
MADRAS	MEAS.	428	537	571	576	556	500	452	472	479	420	380	364
	COMP.	410	510	570	579	536	481	418	432	459	422	399	419

TABLE 2.9: Comparison of computed and measured values of total solar radiation on horizontal surface. (langley/day)

PLACE		JAN.	FEB.	MAR.	APR.	MAY	JUNE	JUL.	AUG.	SEPT.	OCT.	NOV.	DEC.
DELHI	MEAS.	341	421	530	621	636	633	429	405	471	460	371	321
	COMP.	350	430	496	581	601	660	450	446	451	516	419	352
POONA	MEAS.	462	533	502	622	600	505	371	389	430	455	444	396
	COMP.	470	544	501	624	652	616	426	417	463	462	435	440
CALCUTTA	MEAS.	355	432	406	542	646	411	393	363	366	400	333	330
	COMP.	339	401	461	513	595	450	436	403	406	359	364	329
MADRAS	MEAS.	488	537	571	576	566	500	452	472	479	420	380	364
	COMP.	410	510	570	579	536	481	418	432	459	423	359	419

TABLE 2.10:

Monthly average cloudiness index $K_T = H/H_0$

H = average daily total insolation on the earth's horizontal surface (langley/day)

H_0 = daily extraterrestrial radiation on the horizontal surface (langley/day)

PLACE	JAN	FEB	MAR	APR	MAY	JUN	JUL	AUG	SEP	OCT	NOV	DEC
POONA	0.70	0.71	0.64	0.66	0.61	0.51	0.37	0.40	0.42	0.57	0.66	0.63
DELHI	0.66	0.68	0.67	0.68	0.63	0.55	0.41	0.42	0.55	0.65	0.66	0.66
MADRAS	0.59	0.67	0.65	0.61	0.59	0.52	0.47	0.49	0.52	0.50	0.50	0.52
DUMDUM	0.60	0.61	0.57	0.58	0.56	0.40	0.39	0.38	0.41	0.52	0.57	0.58
TRIVANDRUM	0.65	0.62	0.61	0.60	0.52	0.46	0.46	0.46	0.53	0.49	0.54	0.55
SHILLONG	0.57	0.70	0.49	0.47	0.46	0.38	0.36	0.41	0.39	0.52	0.56	0.67
AHMEDABAD	0.68	0.69	0.73	0.69	0.66	0.50	0.39	0.39	0.50	0.67	0.69	0.62
NAGPUR	0.70	0.70	0.63	0.62	0.61	0.56	-	-	-	-	-	-
VISAKHAPATNAM	0.64	0.67	0.62	0.62	0.61	0.43	0.42	0.45	0.46	0.65	0.68	0.61

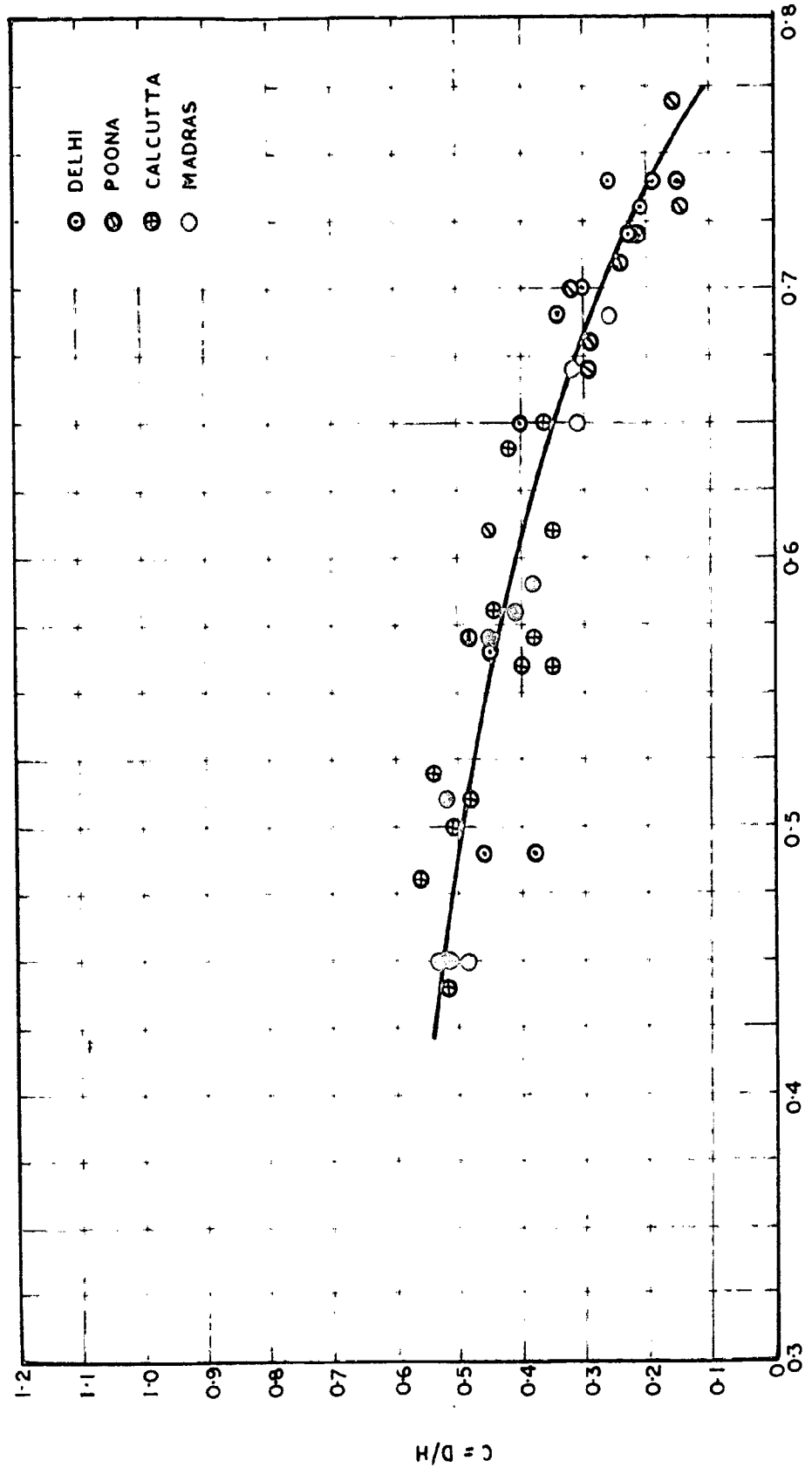

FIG. 2·4 RELATION BETWEEN CLOUDINESS INDEX AND RATIO OF DIFFUSED TO TOTAL SOLAR RADIATION ON HORIZONTAL SURFACE

stations are given in table 2.11. It is seen that this ratio is large during monsoon season and small during winter season, showing that winters are mostly clear. The measured value of daily diffused radiation on horizontal surface for various cities are given in table 2.12. A comparison between the measured and computed values of daily diffused radiation is shown in table 2.13. It can be seen that the maximum error is of the order of 10 to 12 percent.

2.43 Relation between daily and hourly total and diffused solar radiation.

Hourly radiation values are more useful in calculating the performance of flat-plate collectors than daily radiation values, since flat-plate collectors are usually placed in a fixed orientation and the dirunal motion of the sun in the sky requires that the performance of a collector be evaluated on an hour to hour basis. It has been shown by Whillier[37] that average hourly values of both direct and diffused radiation can be determined from the daily total values for any place or month characterized by the duration of possible sunshine hours, by taking the mean hourly position of the sun into consideration. The relationship between RT and Rp, Rd and Dp are shown in fig 2.5 and 2.6 respectively. These are based on the experimental observations for two Indian cities. The deviation of individual points from the mean curve was

TABLE 2.11: Ratio of mean daily values of diffused to total solar radiation on horizontal surface for all days (d/H)

PLACE	JAN.	FEB.	MAR.	APR.	MAY	JUNE	JULY	AUG.	SEPT.	OCT.	NOV.	DEC.	ANN
POONA	0.21	0.10	0.24	0.27	0.32	0.59	0.76	0.74	0.67	0.31	0.26	0.26	0.3
DELHI	0.29	0.29	0.30	0.22	0.30	0.51	0.69	0.56	0.33	0.25	0.24	0.20	0.3
MADRAS	0.30	0.27	0.23	0.30	0.39	0.49	0.69	0.54	0.44	0.45	0.46	0.47	0.4
BOMBAY	0.34	0.31	0.39	0.33	0.46	0.63	0.66	0.64	0.57	0.36	0.33	0.30	0.4
GOA	0.18	0.18	0.22	0.24	0.30	0.54	0.73	0.64	0.62	0.33	0.29	0.17	0.3
TRIVANDRUM	0.31	0.33	0.33	0.35	0.50	0.53	0.61	0.56	0.47	0.49	0.42	0.42	0.4
SHILLONG	0.36	0.24	0.43	0.42	0.60	0.75	0.76	0.80	0.63	0.43	0.34	0.39	0.5
AHMEDABAD	0.27	0.24	0.23	0.27	0.29	0.60	0.73	0.77	0.43	0.26	0.20	0.20	0.3
NAGPUR	0.31	0.20	0.30	0.27	0.32	0.40	-	-	-	-	-	-	-
VISAKHAPATNAM	0.22	0.30	0.27	0.27	0.33	0.49	0.53	0.60	0.43	0.25	0.23	0.29	0.3

TABLE 2.12: Mean daily values of diffused solar radiation on horizontal surface for all days (H_d) (Langley/day)

PLACE	Period to which data refer.	JAN	FEB	MAR	APR	MAY	JUN	JUL	AUG	SEP	OCT	NOV	DEC	ANNUAL
POONA	1963-67	96	93	136	169	192	178	282	238	246	141	111	90	177
DELHI	1963-67	99	118	163	199	229	230	263	227	179	115	09	03	171
MADRAS	1962-67	167	146	160	173	217	243	262	255	211	159	171	171	197
BURDWAN	1964-67	121	134	182	206	248	259	266	238	209	140	116	100	186
GOA	1964-67	93	100	130	146	211	244	222	271	231	161	121	79	167
TRIVANDRUM	1960-67	167	173	193	217	241	246	261	270	239	210	163	176	214
SHILLONG	1967	111	112	162	186	233	236	279	278	227	166	118	110	193
AHMEDABAD	1967	103	116	172	173	189	253	230	202	212	132	93	100	175
JAIPUR	1967	91	101	153	167	192	225	-	-	-	-	-	-	-
VISAKHAPATNAM	1967	136	103	144	168	197	203	220	240	203	131	119	109	164

found to be less than 5 percent, between 9.0 A.M. to 3.0 P.M. These curves are found to be similar to those given by Liu and Jordan[33] except that the diffused component is slightly higher in the hours about sunrise and sunset. The ratio, RT, versus possible sunshine hours, Sp, is plotted in Fig 8.6.

where,

$$RT = \frac{\text{Average hourly total radiation on horizontal surface}}{\text{Average daily total radiation on horizontal surface.}}$$

$$= \frac{I_{Th}}{H} \qquad \text{--------(8.24)}$$

So by knowing the value of H as from article 2.41, it is possible to find out the value of I_{Th} at any hour counted from solar noon on either side.

Fig.(8.6) shows a relation between Rd and Sp, where

$$Rd = \frac{\text{Average hourly diffused radiation on horizontal surface}}{\text{Average daily diffused radiation on horizontal surface}}$$

$$= \frac{I_{dh}}{D} \qquad \text{--------(8.25)}$$

So much, knowing the value of D as from article 2.42, one can determine the hourly value of diffused radiation, Idh, to a reasonable degree of accuracy.

In Fig (2.14) shows a comparison between the measured and computed values of hourly total radiation at Delhi. It is seen that for 70 percent of the values, the error is within 5 percent and the maximum error is not more than 10 percent.

TABLE 2.12: Mean daily values of diffused solar radiation on horizontal surface for all days ($\bar{d}_H$) (Langley/day)

PLACE	Period to which data refer.	JAN	FEB	MAR	APR	MAY	JUN	JUL	AUG	SEP	OCT	NOV	DEC	ANNUAL
POONA	1933-67	96	93	136	109	102	273	282	238	246	141	111	90	177
DELHI	1953-67	99	118	163	199	220	269	263	237	179	115	99	93	171
MADRAS	1962-67	107	145	160	173	217	245	262	255	211	159	171	171	197
BOMBAY	1964-67	121	134	152	206	248	259	256	238	209	149	116	100	188
GOA	1964-67	96	100	130	146	211	244	222	271	231	161	121	79	167
TRIVANDRUM	1964-67	157	173	198	217	241	246	261	270	239	210	163	176	214
SHILLONG	1967	111	112	152	136	233	206	270	276	227	165	116	110	193
AHMEDABAD	1967	103	116	172	173	199	253	230	202	212	132	93	100	175
JAIPUR	1967	91	101	153	167	192	225	-	-	-	-	-	-	-
VISAKHAPATNAM	1967	136	163	144	168	197	203	230	246	203	131	119	109	164

TABLE 2.13: Comparison of computed and measured values of daily diffused radiation on a horizontal surface(Langley/day)

PLACE		JAN.	FEB.	MAR.	APR.	MAY	JUNE	JULY	AUG.	SEPT	OCT.	NOV.	DEC.
DELHI	MEAS.	99	118	166	199	250	300	268	227	170	116	89	98
	COMP.	109	128	161	189	229	277	249	223	197	156	119	105
POONA	MEAS.	96	96	135	163	192	278	252	203	245	141	111	90
	COMP.	119	119	153	180	214	237	263	268	225	165	122	111
CALCUTTA	MEAS.	121	134	162	206	246	259	256	233	209	140	116	109
	COMP.	138	151	200	227	246	236	242	229	205	160	125	118
MADRAS	MEAS.	167	146	160	173	217	245	262	255	211	180	171	171
	COMP.	175	162	184	190	228	236	241	246	235	190	186	178

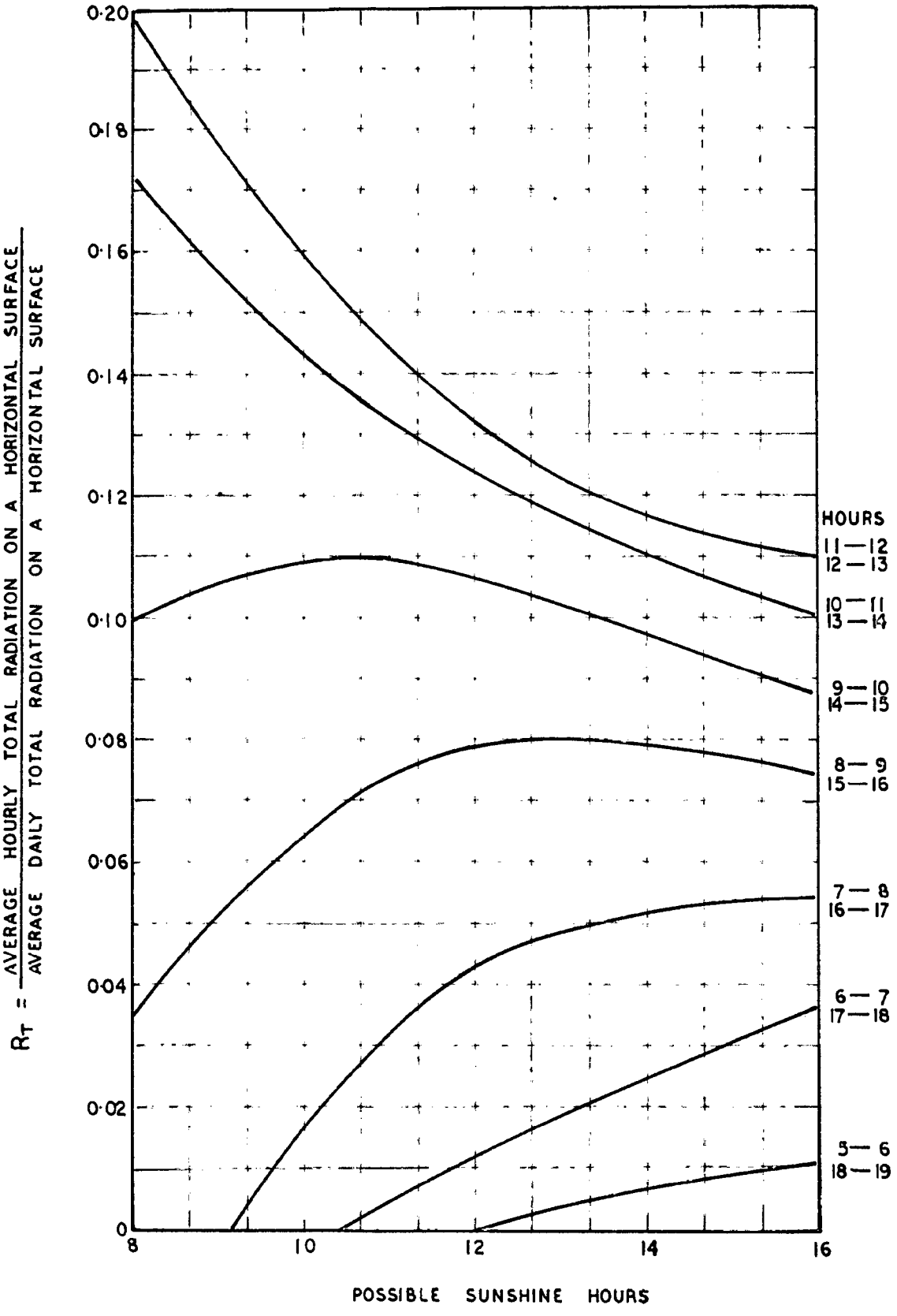

FIG.2·5 RELATION BETWEEN POSSIBLE SUNSHINE HOURS AND R_t

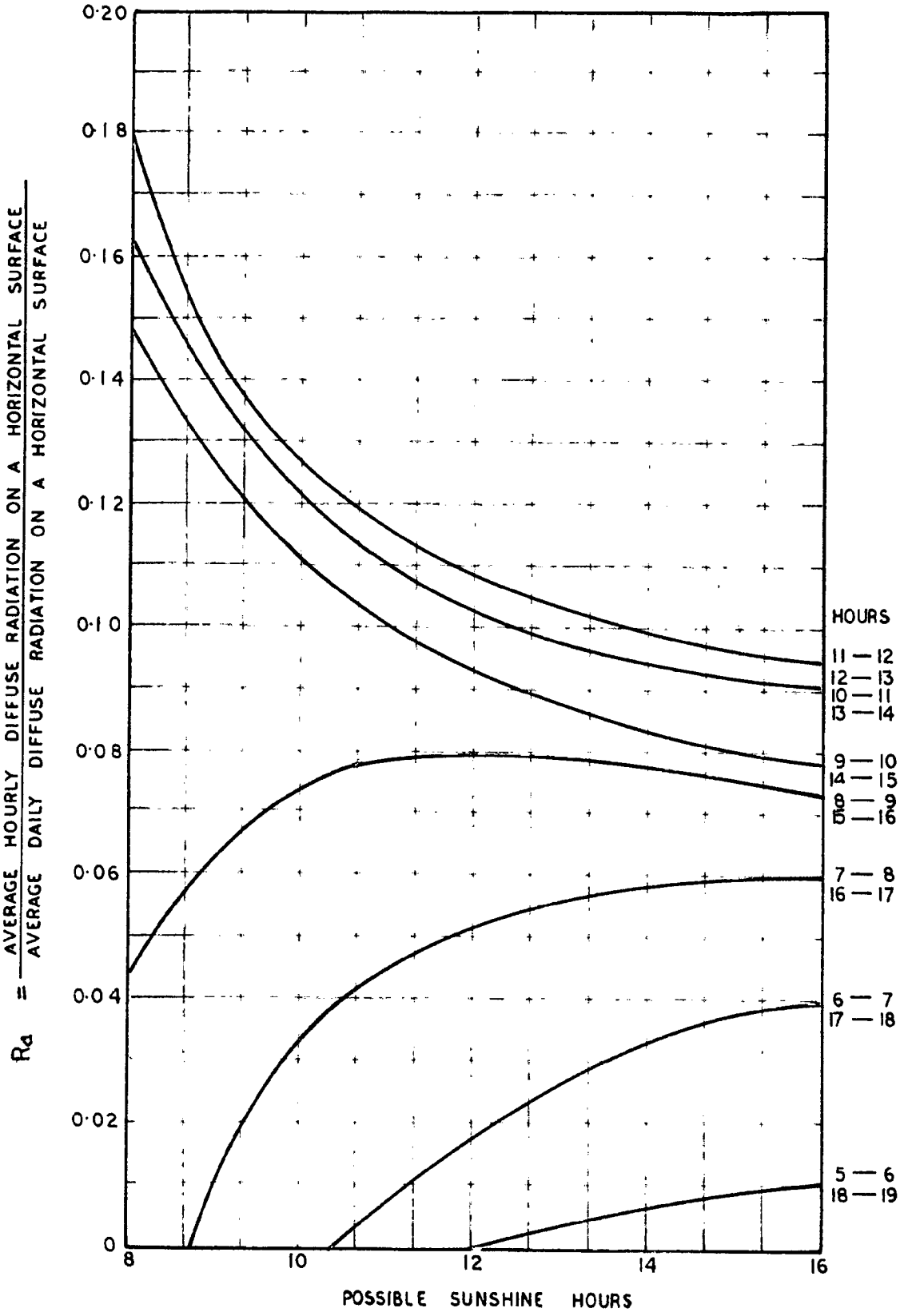

FIG.2·6 RELATION BETWEEN POSSIBLE SUNSHINE HOURS AND R_a

found to be less than 6 percent, between 9.0 A.M. to 3.0 P.M. These curves are found to be similar to those given by Liu and Jordan[33] except that the diffused component is slightly higher in the hours about sunrise and sunset. The ratio, RT, versus possible sunshine hours, Sp, is plotted in fig 8.6.

where,

$$RT = \frac{\text{Average hourly total radiation on horizontal surface}}{\text{Average daily total radiation on horizontal surface.}}$$

$$= \frac{I_{Th}}{H} \qquad \text{--------(8.24)}$$

So by knowing the value of H as from article 8.41, it is possible to find out the value of I_{Th} at any hour counted from solar noon on either side.

Fig.(8.6) shows a relation between Rd and Sp, where

$$Rd = \frac{\text{Average hourly diffused radiation on horizontal surface}}{\text{Average daily diffused radiation on horizontal surface}}$$

$$= \frac{I_{dh}}{D} \qquad \text{--------(8.25)}$$

As such, knowing the value of D as from article 8.42, one can determine the hourly value of diffused radiation, Idh, to a reasonable degree of accuracy.

Table (8.14) shows a comparison between the measured and computed values of hourly total radiation at Delhi. It is seen that for 70 percent of the values, the error is within 6 percent and the maximum error is not more than 10 percent.

TABLE 5.4: Comparison of observed and computed values of average hourly total radiation on horizontal surface (I_{Th}) for DELHI (Langley/hr).

MONTH	HOUR(IST)	5-6	6-7	7-8	8-9	9-10	10-11	11-12	12-1	1-2	2-3	3-4	4-5	5-6	6-7
JAN.	OBS.	0.0	0.4	9.7	25.8	40.2	50.0	58.4	57.3	49.6	39.9	24.6	9.1	0.5	0.0
	COM.	0.0	0.34	8.8	23.6	39.6	49.4	53.2	53.2	49.4	38.5	23.6	8.8	0.34	0.0
FEB.	OBS.	0.0	2.5	17.8	38.7	55.3	66.3	72.6	72.1	65.1	53.2	33.8	16.0	2.9	0.0
	COM.	0.0	2.1	15.2	34.0	49.7	59.9	63.4	63.4	59.9	49.7	34.8	15.2	2.1	0.0
MAR.	OBS.	0.0	6.4	24.6	44.2	60.9	71.3	77.7	77.6	71.7	59.2	43.9	24.6	6.7	0.0
	COM.	0.0	5.4	23.3	41.8	58.6	67.0	73.2	73.2	67.0	58.6	41.8	23.3	5.4	0.0
APR.	OBS.	1.1	12.3	30.4	49.9	61.4	72.4	76.3	75.3	71.6	61.6	45.2	28.4	11.9	1.3
	COM.	1.2	12.4	31.6	51.1	63.1	74.7	78.4	78.4	74.7	63.1	51.1	31.6	12.4	1.2
MAY	OBS.	3.0	16.4	33.6	52.5	67.1	77.4	83.0	82.6	76.7	68.3	52.4	35.3	17.6	3.7
	COM.	2.6	15.3	32.4	50.6	64.6	75.7	80.3	80.8	75.7	64.6	50.6	32.4	15.3	2.6
JUNE	OBS.	2.0	15.0	31.2	47.1	58.6	69.0	72.7	74.4	69.0	59.0	45.7	28.0	10.6	1.2
	COM.	2.3	14.2	29.5	45.3	56.6	64.6	70.7	70.7	64.6	56.6	45.3	29.5	14.2	2.3
JULY	OBS.	1.6	9.4	22.6	39.7	49.3	57.0	60.1	58.4	54.2	40.7	29.3	17.8	10.1	2.4
	COM.	1.3	9.0	21.5	34.3	46.6	54.7	58.6	58.6	54.7	45.6	34.3	21.5	9.0	1.3
AUG.	OBS.	0.8	9.2	20.1	33.2	43.4	51.3	62.2	60.9	57.1	42.8	23.4	23.0	10.8	1.6
	COM.	0.6	7.3	18.6	30.9	40.2	49.2	57.1	55.3	45.2	40.2	30.9	18.6	7.3	0.6
SEPT.	OBS.	0.2	6.5	18.9	33.1	43.6	54.6	58.9	57.0	49.9	47.1	32.3	21.4	5.7	0.2
	COM.	0.3	7.0	20.0	36.0	49.0	58.1	65.1	65.1	58.1	49.0	36.0	20.6	7.0	0.3
OCT.	OBS.	0.0	3.3	17.5	35.3	49.0	58.8	64.7	62.5	57.8	46.6	33.0	15.0	2.7	0.0
	COM.	0.0	3.2	17.9	36.3	50.6	60.2	66.1	66.1	60.2	50.6	36.3	17.9	3.2	0.0
NOV.	OBS.	0.0	0.0	11.5	28.4	42.6	56.3	59.0	59.3	55.3	41.6	25.4	10.3	0.5	0.0
	COM.	0.0	0.7	10.7	27.1	40.4	54.1	60.7	60.7	54.1	40.4	27.1	10.7	0.7	0.0
DEC.	OBS.	0.0	0.2	7.6	22.0	36.8	47.3	50.3	52.2	47.4	36.3	23.2	8.1	0.3	0.0
	COM.	0.0	0.2	7.1	21.6	34.9	45.0	51.1	51.1	45.0	34.9	21.6	7.1	0.2	0.0

Table (2.15) shows a comparison between the measured and computed values of hourly diffused radiation at Delhi. Here also in most of the cases there is a good agreement and the maximum error is about 12 percent.

A similar comparison of measured and computed values of I_{Th} and I_{dh} for Poona is made in tables 2.16 and 2.17 respectively.

Based on these relationships established, hourly values of total and diffused solar radiation on horizontal surface for Madras and Calcutta were computed for all the twelve months. These values are given in Table (2.18) and (2.19) for Madras and Calcutta respectively.

2.5. COMPUTATION OF SOLAR RADIATION ON INCLINED SURFACES.

An inclined surface not only receives the direct and diffused radiation but also the reflected radiation from the nearby ground. For the design and feasibility studies on flat-plate collectors, it is essential to know the total incident solar radiation including the ground reflection. The importance of this in arriving at an optimum tilt corresponding to the critical season of use will be discussed in chapter 3. For this purpose, it is convenient to know the conversion factors for tilted surfaces for a single representative day of each month. Liu and Jordan[42] have tabulated these conversion factors only for direct radiation at outside the earth's atmosphere while Page[43] has assumed an empirical relation for the ratio of diffused to total radiation to get such values

TABLE : 2.10:

Comparison of observed and computed values of average hourly diffused radiation on horizontal surface (I_{gb}) for Delhi (Langley/hr).

MONTH		5-6	6-7	7-8	8-9	9-10	10-11	11-12	12-1	1-2	2-3	3-4	4-5	5-6	6-7
JAN.	OBS.	0.0	0.2	3.5	6.9	9.3	10.3	10.3	10.6	10.6	9.3	7.5	4.1	0.3	0.0
	COM.	0.0	0.2	4.0	7.2	10.0	11.5	11.6	11.6	11.5	10.0	7.2	4.0	0.2	0.0
FEB.	OBS.	0.0	1.3	6.3	9.3	10.6	11.8	12.3	13.1	12.6	12.3	10.4	6.3	1.5	0.0
	COM.	0.0	1.4	6.8	10.2	11.6	12.9	13.5	13.6	12.9	11.6	10.2	6.8	1.4	0.0
MARCH	OBS.	0.0	3.6	8.4	10.9	13.5	14.6	15.7	16.3	16.3	15.3	11.9	8.9	3.4	0.0
	COM.	0.0	3.9	9.3	11.1	14.1	16.3	16.6	16.6	15.3	14.1	11.1	9.3	3.9	0.0
APRIL	OBS.	0.9	6.8	9.6	13.1	15.5	16.6	16.6	17.3	17.3	16.5	15.1	11.7	6.4	0.7
	COM.	0.9	6.6	10.5	14.9	16.3	19.3	18.5	18.5	19.3	16.3	14.9	10.5	6.6	0.9
MAY	OBS.	2.0	10.4	10.5	16.7	16.3	19.7	20.3	20.9	20.5	19.6	17.2	13.3	8.9	2.3
	COM	2.0	11.5	11.6	17.8	17.7	21.2	21.8	21.8	21.2	17.7	17.8	11.6	11.6	2.0
JUNE	OBS.	2.5	0.2	14.0	18.4	21.7	23.6	25.0	25.2	27.0	25.8	22.3	14.6	10.9	3.0
	COM.	2.6	10.4	12.2	20.2	22.9	26.2	27.5	27.6	26.2	22.0	20.2	12.2	10.4	2.6
JULY	OBS.	1.2	7.7	16.8	25.6	28.3	31.5	31.1	30.2	29.9	28.3	20.4	14.7	8.5	1.9
	COM.	1.0	6.8	14.9	24.0	28.8	29.0	28.8	28.8	29.0	26.8	24.0	14.9	6.8	1.0
AUGUST	OBS.	0.5	4.8	10.3	15.3	20.1	22.9	25.9	27.6	29.7	18.3	14.4	11.0	6.3	1.0
	COM.	0.4	5.2	11.3	17.0	21.4	24.6	27.9	27.8	24.6	21.4	17.0	11.3	5.2	0.4
SEPT.	OBS.	0.1	3.8	7.8	9.8	13.1	13.7	21.0	15.0	10.0	10.2	11.63	9.2	3.4	0.1
	COM.	0.1	3.7	8.4	10.4	15.0	20.0	24.1	24.1	20.0	15.0	10.0	6.4	3.7	0.1
OCT.	OBS.	0.0	2.0	6.3	9.0	10.8	11.9	13.2	12.0	11.1	10.0	8.5	6.1	1.5	0.0
	COM.	0.0	2.1	7.1	10.2	12.1	13.2	13.9	13.8	13.2	12.1	10.2	7.1	2.1	0.0
NOV.	OBS.	0.0	0.4	3.7	5.7	6.9	6.8	7.3	7.1	7.3	6.8	5.8	3.2	0.2	0.0
	COM.	0.0	0.5	4.5	7.2	8.0	8.8	9.5	9.6	8.8	8.0	7.2	4.5	0.5	0.0
DEC.	OBS.	0.0	0.1	3.5	6.4	8.7	10.7	11.8	12.1	19.4	0.1	7.0	3.6	0.1	0.0
	COM.	0.0	0.1	3.9	7.1	9.6	11.8	13.1	13.1	11.8	8.0	7.1	3.9	0.1	0.0

TABLE 2.16a

Comparison of observed and computed values of average hourly total radiation on horizontal surface (I_{gh}) for Poona (Langley/hour)

HOURS(IST) / MONTH		5-6	6-7	7-8	8-9	9-10	10-11	11-12	12-1	1-2	2-3	3-4	4-5	5-6	6-7
JAN.	OBS.	0.0	1.8	15.9	34.1	49.0	59.7	67.9	68.3	69.4	48.6	31.9	16.1	2.0	0.0
	COMP.	0.0	2.2	15.4	34.2	49.8	59.6	65.1	65.1	59.6	49.2	34.3	15.4	2.2	0.0
FEB.	OBS.	0.0	3.4	20.4	43.7	63.2	70.6	77.4	76.3	72.3	60.6	43.7	33.1	4.8	0.0
	COMP.	0.0	4.2	20.2	42.1	63.1	68.2	75.1	75.1	69.8	58.1	43.1	30.2	4.2	0.0
MARCH	OBS.	0.0	6.5	26.2	47.3	64.3	76.8	83.8	83.6	77.6	64.7	47.4	30.7	7.2	0.0
	COMP.	0.0	6.7	24.7	44.9	61.1	72.1	78.7	78.7	72.1	61.1	44.9	24.7	6.7	0.0
APRIL	OBS.	0.0	9.1	29.9	48.1	65.0	74.5	83.2	81.6	65.0	59.9	42.3	23.1	10.9	0.0
	COMP.	0.0	8.3	23.6	40.7	65.3	74.6	78.6	79.6	74.6	65.3	49.7	28.6	9.3	0.0
MAY	OBS.	1.3	12.9	31.4	53.2	67.6	77.6	82.3	77.6	74.9	57.3	47.2	31.0	13.0	2.2
	COMP.	1.3	10.0	30.8	49.2	69.6	73.2	79.4	78.4	73.2	63.8	49.2	29.9	10.0	1.3
JUNE	OBS.	1.5	10.0	26.6	41.1	57.6	65.9	67.7	70.6	63.9	50.8	33.6	23.2	9.3	1.4
	COMP.	1.0	9.0	24.7	40.4	54.6	60.6	63.1	63.1	60.6	54.6	40.4	24.7	9.6	1.9
JULY	OBS.	0.6	7.6	16.5	28.8	35.9	44.0	50.8	49.0	41.1	23.6	24.0	15.9	6.6	0.6
	COMP.	1.0	6.7	18.1	29.6	36.2	43.0	45.0	45.0	43.0	36.2	29.6	18.1	6.7	1.0
AUGUST	OBS.	0.5	6.8	18.0	31.6	41.3	50.0	53.5	51.7	44.4	31.2	26.7	14.9	6.3	0.5
	COMP.	0.8	6.2	18.3	31.1	40.4	46.9	50.1	50.1	45.9	40.4	31.1	18.3	6.8	0.8
SEPT.	OBS.	0.0	5.4	18.8	32.8	43.3	53.1	55.3	53.0	51.3	37.8	30.5	17.0	4.8	0.0
	COMP.	0.0	5.5	19.3	34.4	43.5	53.4	55.0	55.0	53.4	43.8	34.4	19.3	5.5	0.0
OCT.	OBS.	0.0	3.0	18.4	36.2	51.7	61.8	65.0	63.1	59.9	50.2	32.0	17.4	3.8	0.0
	COMP.	0.0	4.5	18.2	36.4	49.1	59.8	63.4	63.8	63.8	49.1	36.4	18.2	4.5	0.0
NOV.	OBS.	0.0	1.6	13.5	30.0	43.7	53.8	61.5	60.9	55.0	44.7	31.1	15.0	1.8	0.0
	COMP.	0.0	2.1	15.3	31.6	46.4	57.7	62.8	62.8	57.7	45.6	31.8	15.3	2.1	0.0
DEC.	OBS.	0.0	1.1	12.8	30.3	40.4	57.2	63.6	64.0	57.0	47.2	31.3	13.5	1.1	0.0
	COMP.	0.0	1.8	13.0	29.7	44.1	53.7	58.9	59.9	53.7	44.1	29.7	13.0	1.8	0.0

TABLE 2.17: Comparison of observed and computed values of average hourly diffused radiation on horizontal surface (I_{dh}) for Poona (Langley/hr)

MONTH	HOUR (IST)	5-6	6-7	7-8	8-9	9-10	10-11	11-12	12-1	1-2	2-3	3-4	4-5	5-6	6-7
JAN.	OBS.	0.0	1.2	5.5	9.0	9.3	11.3	11.1	11.3	12.0	10.5	9.2	6.4	1.2	0.0
	COM.	0.0	0.9	4.5	7.6	9.5	10.3	11.2	11.2	10.5	0.5	7.0	4.5	0.96	0.0
FEB.	OBS.	0.0	2.0	6.4	8.7	9.6	9.9	9.9	9.0	9.9	9.2	8.1	6.3	2.6	0.0
	COM.	0.0	1.6	5.7	7.0	9.3	10.1	10.9	10.0	10.1	9.3	7.9	5.7	1.6	0.0
MAR.	OBS.	0.0	3.7	8.9	11.1	12.8	13.5	13.9	13.6	14.1	13.0	11.9	9.5	4.1	0.0
	COM.	0.0	2.6	7.1	10.0	12.5	13.0	14.8	14.8	13.9	12.6	10.8	7.1	2.6	0.0
APR.	OBS.	0.0	5.5	11.2	14.9	17.3	17.6	19.4	20.6	20.8	18.9	12.3	12.1	6.5	0.0
	COM.	0.0	3.8	10.0	13.4	16.1	16.8	18.2	18.2	16.8	16.1	13.4	10.0	3.8	0.0
MAY	OBS.	1.2	7.5	14.2	19.3	19.5	20.5	21.6	21.3	20.5	19.7	16.6	14.3	8.5	1.9
	COM.	0.7	6.8	11.9	16.3	18.7	18.0	19.9	19.9	18.9	18.7	16.3	11.8	6.8	0.7
JUNE	OBS.	1.1	6.4	14.1	19.3	22.1	24.1	25.0	27.9	25.1	22.0	19.4	13.6	6.8	1.1
	COM.	1.1	7.5	15.6	21.9	25.9	26.8	28.6	28.6	26.0	23.0	21.9	15.6	7.5	1.1
JULY	OBS.	0.6	7.2	14.7	23.6	27.1	25.5	28.7	27.1	24.3	27.3	20.5	14.3	5.0	0.5
	COM.	0.8	6.2	13.7	22.6	26.3	31.3	32.6	33.6	31.3	26.3	22.6	15.7	6.2	0.8
AUG.	OBS.	0.5	6.3	15.9	26.6	31.4	37.1	35.1	36.3	35.1	31.6	23.2	13.4	5.3	0.4
	COM.	0.5	6.0	15.3	24.0	28.3	32.5	35.2	35.2	32.5	28.3	24.0	15.3	6.0	0.5
SEP.	OBS.	0.0	4.3	11.1	18.2	26.2	30.3	34.8	30.1	30.4	25.3	17.6	11.1	4.1	0.0
	COM.	0.0	4.9	12.3	19.6	24.6	28.9	31.7	31.7	29.3	24.6	19.6	12.3	4.3	0.0
OCT.	OBS.	0.0	2.3	7.1	11.2	14.4	18.3	18.9	20.0	19.6	17.2	12.6	6.0	2.2	0.0
	COM.	0.0	2.2	7.0	11.2	13.4	16.6	16.8	16.0	16.3	13.4	11.2	7.0	2.3	0.0
NOV.	OBS.	0.0	1.2	5.9	9.6	12.0	15.3	16.6	19.1	16.8	13.1	8.9	6.3	1.2	0.0
	COM.	0.0	1.2	3.3	7.0	10.6	12.9	14.3	14.8	12.9	10.3	8.8	5.3	1.3	0.0
DEC.	OBS.	0.0	0.9	4.1	6.1	7.2	8.1	8.3	9.1	7.9	7.8	6.1	3.8	0.7	0.0
	COM.	0.0	0.0	4.5	7.8	9.0	9.6	10.2	10.2	9.6	9.0	7.8	4.6	0.0	0.0

TABLE 2.19:

Computed values of average hourly total (I_{Th}) and diffused (I_{dh}) radiation on horizontal surface for Kolaba (Langley/hr)

MONTH	HOUR(I.S.T.)	5-6	6-7	7-8	8-9	9-10	10-11	11-12	12-1	1-2	2-3	3-4	4-5	5-6	6-7
JAN.	I_{Th}	0.0	3.78	17.93	37.28	51.45	59.94	65.14	65.16	60.04	51.45	37.28	17.93	3.78	0.0
	I_{dh}	0.0	2.01	7.56	12.36	14.20	16.37	17.60	17.00	16.37	14.02	12.36	7.56	2.01	0.0
FEB.	I_{Th}	0.0	6.15	22.91	44.72	60.37	69.87	64.91	64.01	60.87	50.37	44.72	22.91	6.15	0.0
	I_{dh}	0.0	2.38	7.17	11.16	13.14	14.53	15.61	15.51	14.60	13.14	11.16	71.13	2.38	0.0
MAR.	I_{Th}	0.0	7.09	26.00	47.28	63.84	72.10	77.42	77.42	72.10	63.84	47.28	26.00	7.09	0.0
	I_{dh}	0.0	2.03	8.30	12.73	14.68	16.23	17.20	17.33	16.20	14.68	12.76	8.20	2.03	0.0
APR.	I_{Th}	1.12	6.20	24.47	47.60	63.87	72.20	73.20	73.16	71.60	62.47	47.60	27.27	8.02	1.19
	I_{dh}	0.38	4.19	10.20	15.23	16.05	19.04	20.37	20.37	19.04	16.85	15.23	10.20	4.19	0.38
MAY	I_{Th}	1.04	9.93	26.21	47.63	60.78	64.47	68.26	63.26	64.49	55.78	43.63	26.21	9.93	1.04
	I_{dh}	0.64	5.32	11.71	17.04	18.50	20.50	22.16	22.16	20.18	18.53	17.04	11.71	5.32	0.64
JUNE	I_{Th}	1.57	9.41	25.63	41.07	53.07	60.07	64.30	64.33	60.67	53.07	41.04	25.03	9.41	1.57
	I_{dh}	0.71	5.12	12.60	10.03	19.04	22.63	24.24	24.24	22.03	19.64	19.63	12.60	5.10	0.71
JULY	I_{Th}	2.09	8.89	25.10	41.04	53.7	61.19	64.06	64.26	61.13	53.07	41.04	25.10	8.89	2.09
	I_{dh}	0.67	6.60	12.65	17.04	19.50	21.97	23.31	23.32	21.97	19.50	17.04	12.65	6.60	0.67
AUG.	I_{Th}	0.04	5.47	19.84	33.76	43.09	49.79	53.17	53.17	49.79	43.89	33.76	19.84	5.47	0.04
	I_{dh}	0.43	3.53	12.63	10.23	20.06	22.34	23.32	23.34	23.34	20.06	10.23	12.53	3.53	0.43
SEPT.	I_{Th}	0.50	7.34	23.14	40.24	52.81	60.36	64.38	64.38	60.36	52.31	40.24	23.14	7.04	0.50
	I_{dh}	0.46	5.04	13.36	10.31	20.70	23.29	24.49	24.49	23.29	20.70	18.31	12.36	5.04	0.46
OCT.	I_{Th}	0.00	4.43	15.80	29.52	39.49	45.39	48.71	48.71	45.20	39.43	29.52	15.06	4.43	0.00
	I_{dh}	0.00	3.37	9.27	14.17	16.47	18.02	19.43	19.43	18.07	16.04	14.17	9.21	3.37	0.00
NOV.	I_{Th}	0.00	3.73	14.98	29.47	40.38	46.62	51.73	51.73	43.03	40.38	29.47	24.02	3.73	0.00
	I_{dh}	0.00	3.16	10.03	15.62	18.78	20.76	22.34	22.34	20.76	18.70	18.03	10.03	3.16	0.00
DEC.	I_{Th}	0.00	3.18	15.00	31.36	43.27	50.42	54.79	54.79	50.42	43.27	31.36	15.00	3.18	0.00
	I_{dh}	0.00	2.33	7.72	13.25	16.07	17.60	18.90	18.90	17.63	16.07	13.76	7.72	2.30	0.00

TABLE 2.19: Computed values of average hourly total (I_{th}) & diffused (Idh) radiation on horizontal surface for Calcutta (Langley/hr)

Month		6-7	6-7	7-8	8-9	9-10	10-11	11-12	12-1	1-2	2-3	3-4	4-5	5-6	6-7
January	I_{th}	0.0	1.36	10.61	26.43	37.29	45.00	49.03	49.83	49.09	37.29	26.43	10.61	1.36	0.0
	I_{dh}	0.0	1.07	6.36	12.06	15.36	17.03	16.15	15.15	17.03	15.06	12.06	6.06	1.07	0.0
February	I_{th}	0.0	3.15	14.97	30.78	42.06	50.49	54.77	54.77	50.43	42.06	30.78	14.07	3.16	0.0
	I_{dh}	0.0	1.99	7.53	12.29	14.03	16.44	17.67	17.67	16.44	14.80	12.29	7.53	1.99	0.0
March	I_{th}	0.0	5.07	21.03	39.12	52.32	60.15	64.56	64.65	60.15	52.32	39.12	21.03	5.07	0.0
	I_{dh}	0.0	3.26	8.09	13.06	15.01	17.46	18.92	18.92	17.45	15.01	13.06	8.09	3.25	0.0
April	I_{th}	1.0	6.09	23.78	40.49	53.02	59.71	63.76	63.76	59.71	53.02	40.49	23.78	6.09	1.0
	I_{dh}	0.6	4.08	11.41	16.39	17.95	19.36	21.78	21.78	20.78	17.95	16.39	11.41	4.08	0.0
May	I_{th}	2.17	10.04	27.10	43.36	54.76	62.33	67.12	67.12	62.33	54.76	43.36	27.10	10.04	2.17
	I_{dh}	0.73	5.16	10.60	14.56	15.66	17.50	18.79	18.79	17.60	15.66	14.56	10.60	5.16	0.73
June	I_{th}	2.36	10.06	24.77	37.29	47.2	53.34	56.64	56.64	53.34	47.2	37.29	24.07	10.06	2.36
	I_{dh}	1.34	6.06	15.69	21.23	23.31	25.27	25.53	25.53	25.27	23.31	21.23	15.69	6.06	1.34
July	I_{th}	2.27	10.44	23.15	35.37	45.40	51.30	54.49	54.49	51.30	45.40	35.37	23.15	10.44	2.27
	I_{dh}	1.10	7.15	15.02	18.03	19.70	22.40	23.07	23.07	22.40	19.78	18.03	15.02	7.15	1.10
August	I_{th}	1.03	8.14	23.07	38.63	49.06	55.79	59.10	59.10	55.79	49.06	38.63	23.07	8.14	1.03
	I_{dh}	0.69	6.69	15.06	19.66	20.06	22.39	24.03	24.03	22.39	21.06	19.66	15.06	6.69	0.69
September	I_{th}	0.85	6.40	19.64	34.16	44.83	51.26	54.66	54.66	51.24	44.83	34.16	19.64	6.40	0.85
	I_{dh}	0.44	5.11	11.09	17.76	19.76	22.20	23.76	23.76	22.20	19.76	17.76	11.09	5.11	0.44
October	I_{th}	0.0	3.96	16.24	31.66	42.77	49.60	53.06	53.06	49.60	42.77	31.60	16.24	3.96	0.0
	I_{dh}	0.0	3.67	11.00	17.86	20.27	22.43	23.04	23.04	22.43	20.87	17.26	11.00	3.67	0.0
November	I_{th}	0.0	2.36	13.76	30.26	42.84	51.09	55.81	55.81	51.09	42.84	30.26	13.76	2.36	0.0
	I_{dh}	0.0	1.06	8.11	13.62	16.56	18.42	19.60	19.60	18.42	16.06	13.62	8.11	1.06	0.0
December	I_{th}	0.0	1.45	10.09	26.06	38.03	45.91	57.26	57.36	49.91	38.03	26.50	10.69	1.45	0.0
	I_{dh}	0.0	0.93	6.21	10.83	14.07	15.83	16.85	16.85	15.83	14.07	10.89	6.21	0.93	0.0

has computed the actual value of

as a function of latitude. Van Straaten[41] ~~for some~~ radiation received by tilted surfaces for south Africa and Morse[45] for some cities of Australia. They have assumed the diffused radiation as a part of the direct radiation and applied the formula meant for direct radiation. This assumption is not justified. No such data, for tilted surfaces taking into account the diffused radiation as well, relevant to the tilts used for solar devices, is available so far.

2.51. Conversion factor determination:

The hourly conversion factor for direct radiation [46] for a tilted surface with any general orientation with reference to normal radiation intensity in terms of celestial co-ordinates is given by the equation:

$$\frac{I_{Dt}}{I_N} = \cos\theta t \qquad \text{-------(2.26)}$$

where I_{Dt} = hourly direct solar radiation on tilted surface.

I_N = hourly normal solar radiation.

and $\cos\theta t$ = $(\cos\beta \sin L - \sin\beta \cos L \cos\phi) \sin\delta$

$+ (\cos\beta \cos L + \sin\beta \sin L \cos\phi) \cos\delta \cos w$

$+ \sin\beta \sin\phi \cos\delta \sin w$ -------(2.27)

where β = tilt with respect to horizontal,

L = latitude of place,

ϕ = azimuth angle with respect to south direction,

δ = solar declination

and w = solar hour angle from solar noon.

or a horizontal surface, which can be treated as a special case of $\beta = 0$, the angle of incidence is :

$$\text{Cos}\,\theta_h = \text{Cos}\,L\,\text{Cos}\,\delta\,\text{Cos}\omega + \text{Sin}\,L\,\text{Sin}\,\delta \quad \text{----(2.28)}$$

The direct radiation on a horizontal surface (I_{DA}) then would be

$$I_{DA} = I_D \ \text{Cos}\,\theta_h \quad \text{------(2.29)}$$

From equation (2.27) and (2.29), we get

$$\frac{I_{Dt}}{I_{Dh}} = \frac{\text{Cos}\,\theta_t}{\text{Cos}\,\theta_h} = R_{Dh} \quad \text{-------(2.30)}$$

where

R_{Dh} = hourly conversion factor for direct radiation.

Assuming the isotropy of sky radiation, the hourly conversion factor for diffused radiation Rdh is given by

$$R_{dh} = \left(\frac{1+\text{cos}\beta}{2}\right) \quad \text{-------(2.31)}$$

Now if h and H_t are the daily total radiation on horizontal and inclined surfaces respectively, the daily conversion factor, R_T, will then be

$$R_T = \frac{H_T}{H} = \frac{\Sigma(I_{Dh})^+}{\Sigma(I_h)} \quad \text{------(2.32)}$$

where the summation is for all hours when (I_{th}) is positive and where Ith and I_h are the hourly total radiation on tilted and horizontal surfaces respectively. If radiation reflected from the ground is neglected, then Ith consists

of direct radiation from the sun and the scattered radiation from the sky vault.

$$I_{th} = (I_h - I_{dh}) R_{bh} + I_{dh} R_{dh} \quad \text{----------(2.33)}$$

where

I_{dh} = hourly diffused radiation on horizontal surface.

By using IBM 1620 computer the value of RT is computed for various useful tilts. Using the measured hourly total and diffused values of solar radiation for Delhi and Poona and the computed values for Madras and Calcutta, the hourly conversion factors have been obtained for total, direct and diffused radiation and the daily conversion factor for total solar radiation on tilted surfaces. The tilts considered were (L+15°), (L-15°) and 0.9L for orientation due south. Conversion factors for three azimuths (15°, 30°, 45°) with respect to south orientation for the tilt corresponding to 0.9 times the latitude are also calculated for Delhi and Madras.

Fig (2.7, 2.9, 2.10) show the month by month variation of the daily conversion factors for the various tilts for south orientation for the above mentioned cities. It can be seen that from march to october, the tilt (L-15°) gives the maximum conversion factor which is almost equal to unity throughout the period. On the other hand for winter season, the tilt (L+15°) gives the maximum conversion factor and these occur fortunately in the called months of

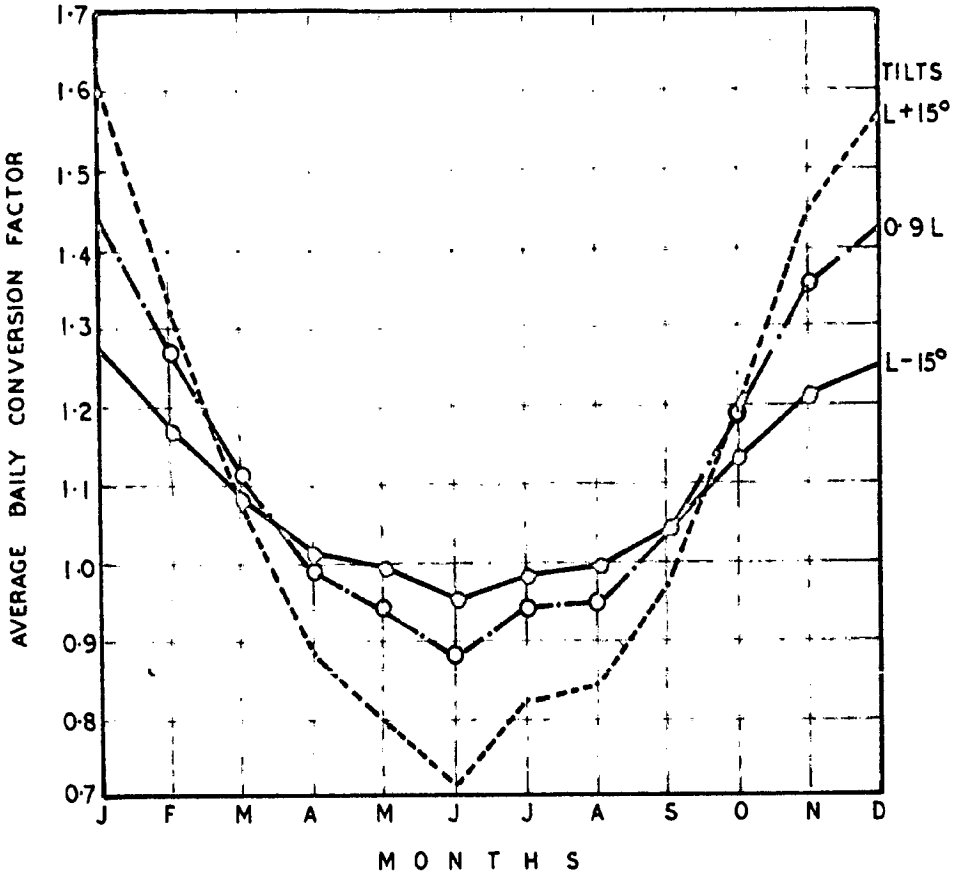

FIG. 2·7 DAILY CONVERSION FACTORS FOR VARIOUS TILTS WITH ORIENTATION DUE SOUTH FOR DELHI

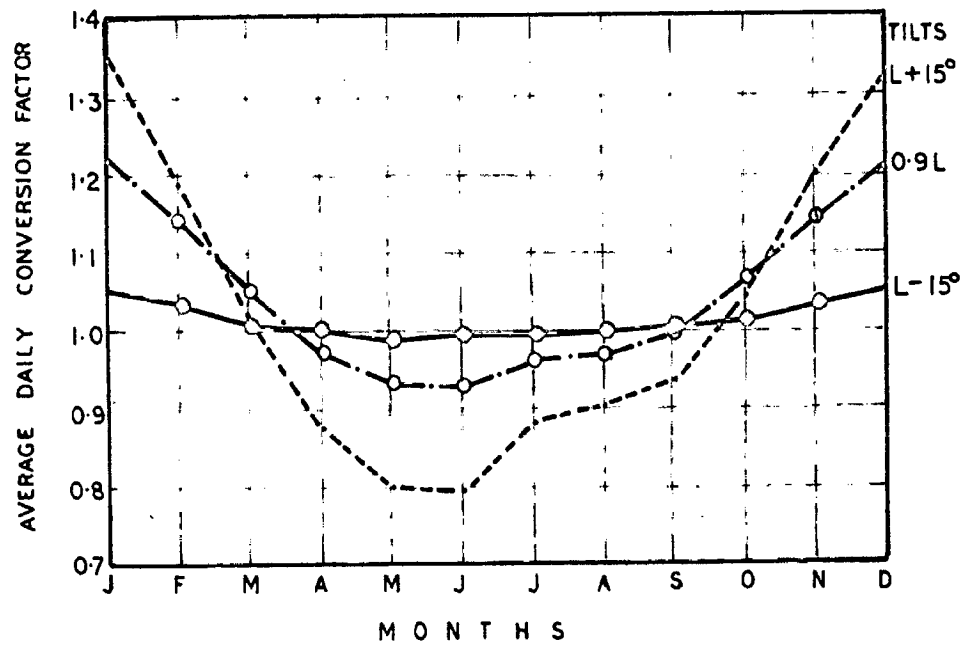

FIG. 2·8 DAILY CONVERSION FACTORS FOR VARIOUS TILTS WITH ORIENTATION DUE SOUTH FOR POONA

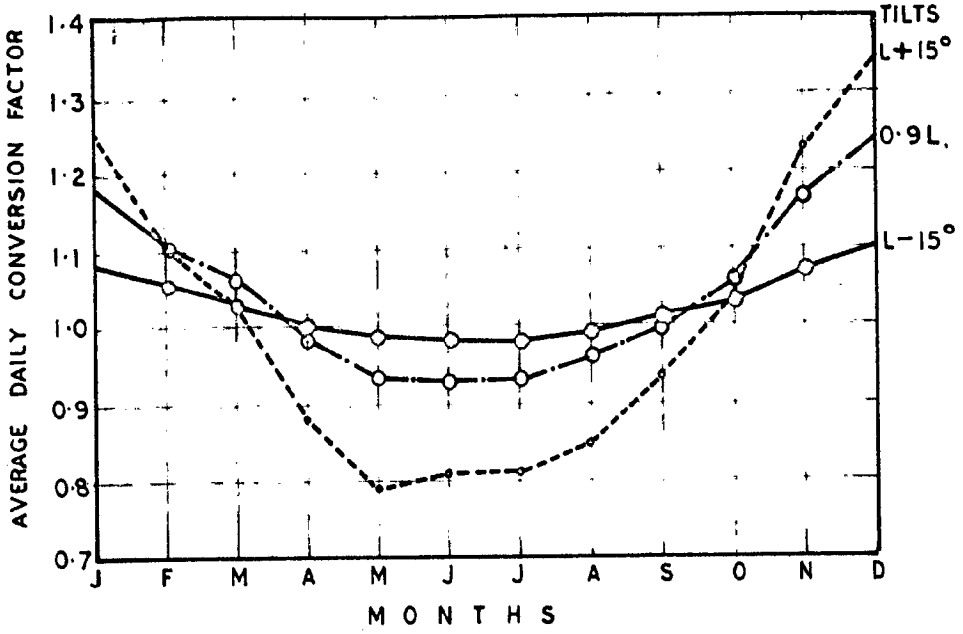

FIG. 2·9 DAILY CONVERSION FACTORS FOR VARIOUS TILTS WITH ORIENTATION DUE SOUTH FOR CALCUTTA

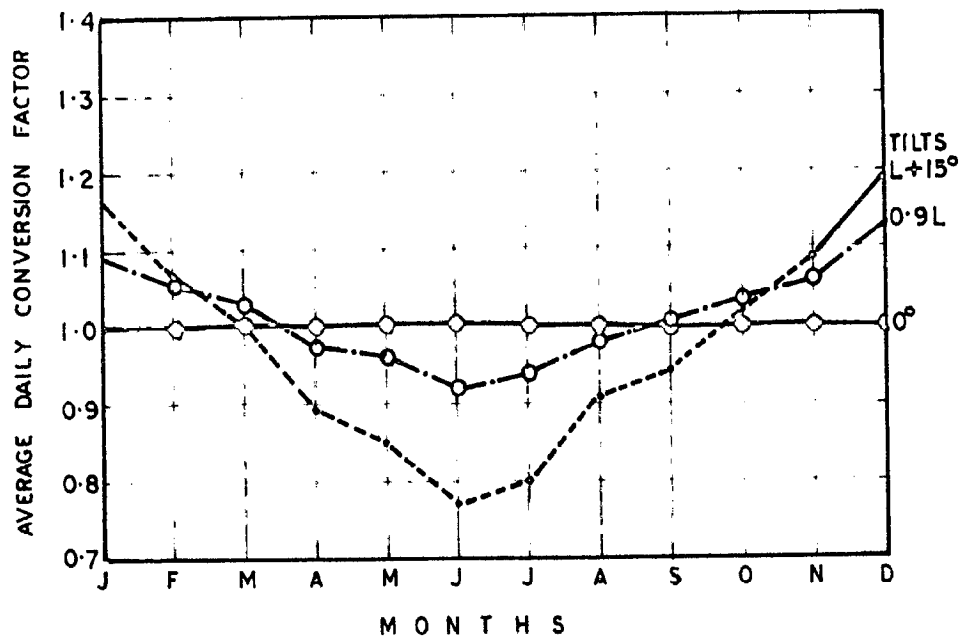

FIG. 2·10 DAILY CONVERSION FACTORS FOR VARIOUS TILTS WITH ORIENTATION DUE SOUTH FOR MADRAS

December and January when the daily solar radiation on a horizontal surface has the low values. The maximum value, however, varies with the latitude and is fortunately higher with higher latitudes, the range being from 1.2 for Madras to 1.62 for Delhi. The curves for the tilt (0.9L) are in the middle of the curves of the above tilts.

The effects of varying the orientation from south are shown in figs (3.11) and (3.12) for the highest and lowest latitude corresponding to Delhi and Madras for a tilt 0.9 L. It can be seen that except for November and December in Delhi a deviation of azimuthal shift of 45° from south towards west is not only permissible but is beneficial. However, for November and December there is a reduction upto 6 percent for a shift of 30° and upto 10 percent for a shift of 45° west.

3.2. Comparison of measured and computed solar radiation:

Average daily radiation for a vertical surface and for a surface inclined 45° from the horizontal and facing south is computed for all the twelve months for Delhi as follows :

The hourly total radiation on a tilted surface is given as

$$I_{Tt}=(I_{Th}-I_{dh})\,R_b+(\frac{1+\cos\beta}{2})\,I_{dh}+(\frac{1-\cos\beta}{2})\,RI_{Th} \qquad \text{--------(3.34)}$$

where R = Albedo of the ground.

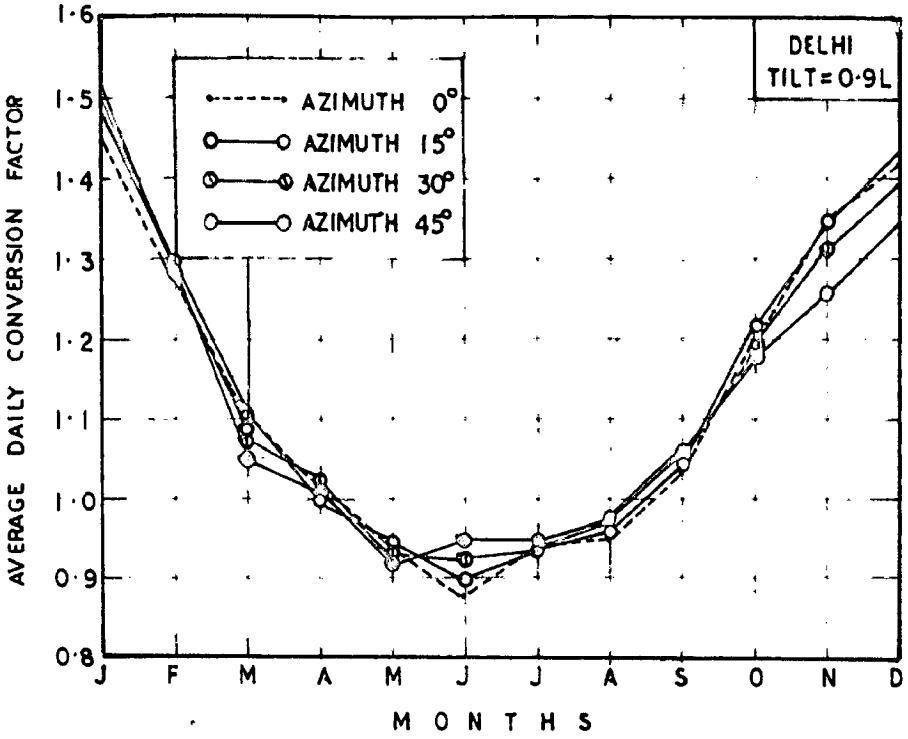

FIG. 2·11 DAILY CONVERSION FACTORS FOR VARIOUS AZIMUTHS FOR DELHI

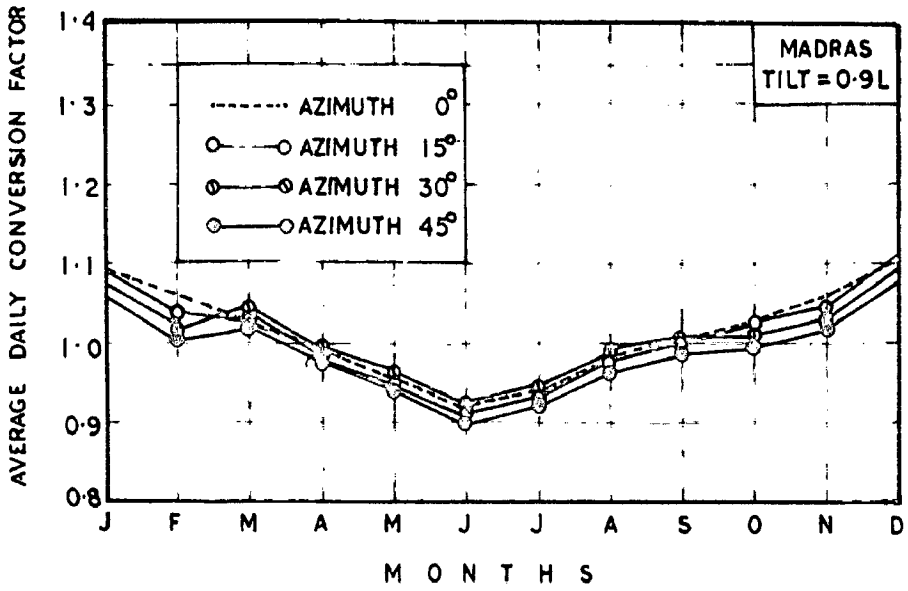

FIG. 2·12 DAILY CONVERSION FACTORS FOR VARIOUS AZIMUTHS FOR MADRAS

Here in the computation the value of R is assumed as 0.22, the justification of which is discussed in article 2.62. The above calculation is made for one representative day i.e. 15th of each month.

The values of daily total radiation at Delhi for β equal to 0°, 45° and 90° are shown in fig (2.13). It is seen that a surface inclined at 45° facing south receives maximum radiation during winter months. A horizontal surface receives more radiation during summer months. A south oriented vertical surface though receives more radiation during winter months as compared to a horizontal surface, still receives less than for a surface inclined at 45° of same orientation.

A comparison is made between the computed and the measured values of daily total radiation on a surface inclined at 45° from the horizontal at Roorkee. All the days chosen were clear days. As mentioned earlier in the computation it is assumed that the sky is isotropic and the albedo of the ground is 0.22. This comparison is shown in Table 2.20. It can be seen that the maximum error is of the order of 6 percent. The measured values of hourly total radiation on inclined and horizontal surfaces and diffused radiation on horizontal surface are shown in fig (2.14) for a typical winter day. The formula used for the computation here is the same as given in equation 2.34.

TABLE 3.29 Comparison of computed and measured total solar radiation received on a surface inclined 46° to the horizontal and facing south

DAY OF MONTH	Measured		Computed		Error percent
	H_H Langley/day	d_H Langley/day	H_T Langley/day	H_T Langley/day	
16th Nov	330	78	610	601	-3.0
16	378	70	605	400	-2.0
17	350	88	490	498	+1.0
18	345	85	488	498	+2.0
19	382	76	601	612	+2.0
20	351	89	603	500	-1.0
21	378	78	610	628	+3.0
22	378	70	609	630	+4.0
23	307	88	596	636	+3.0
24	406	87	620	640	+4.0
25	409	88	630	645	+2.0
26	412	86	643	670	+3.0
27	401	88	640	660	+4.0
28	390	86	496	610	+3.0
29	396	83	610	630	+4.0
30	390	81	609	633	+3.0

H_H = Measured daily total solar radiation on horizontal surface (langley/day)

d_H = Measured diffused solar radiation on horizontal surface (langley/day).

H_T = Daily total radiation on a surface inclined 46° to the horizontal (langley/day).

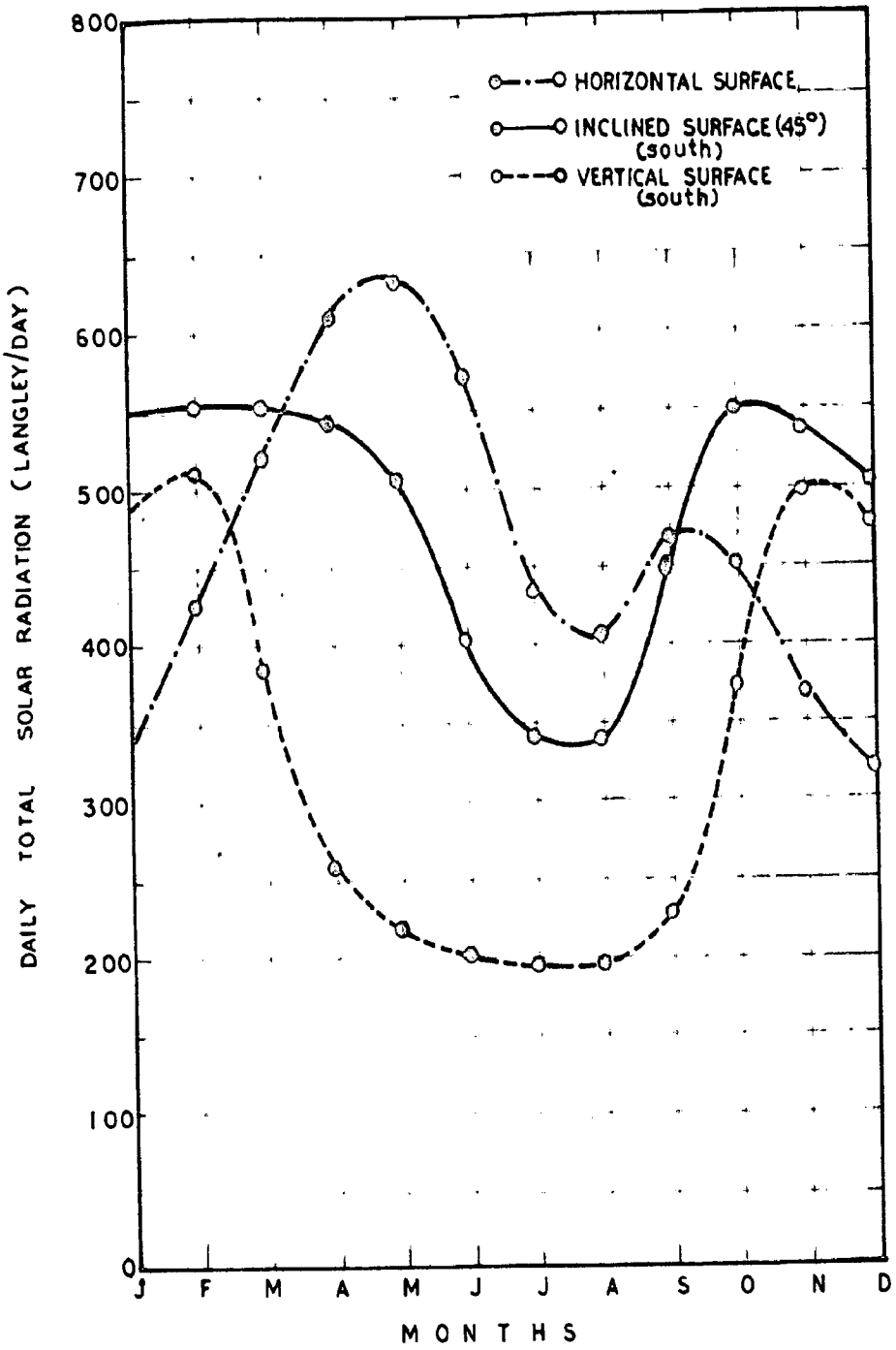

FIG. 2·13 MONTHLY MEAN VALUE OF TOTAL SOLAR RADIATION ON INCLINED SURFACES

2.6. MEASUREMENT OF TOTAL SOLAR RADIATION ON INCLINED SURFACES:

Measurement of direct and diffused solar radiation on sloped surfaces of any orientation has not been so far attempted in the tropics. The total radiation received on any day, by an inclined plane is dependent on the cloudiness, the atmospheric turbidity and the albedo of the ground. Unfortunately in tropics not much measured data is available on any of the above factors. If such data based on measurements spread over long periods is available, the estimation of solar radiation on a horizontal surface can be made to a fair degree of accuracy. However, in case of vertical and inclined surfaces, a knowledge of the distribution of diffused radiation over the sky vault is also necessary.

Kondratyev and Monolva [46] suggest that for an overcast sky an azimuthal isotropy can be assumed, while Moon and Spencer[47], Hegwood[48] and Parmelee[49] consider that as in the case of clear sky conditions, the anisotropy of the sky radiation should be taken into account.

Observations made at Roorkee for overcast sky conditions are presented here alongwith its measuring technique. It has been shown earlier in this chapter that in the tropical regions diffused radiation forms a high percentage and thus plays an important role.

2.61 Apparatus used for the measurement:

Moll-Gorczynski pyranometers and Cambridge recorders are used for the measurement of total and diffused solar radiation on a horizontal surface. The diffused solar radiations are measured by using a suitable shield over the thermopile which cuts off direct solar rays throughout the day. The shield is a circular flat-ring 3 cms wide and 35 cms. in diameter and can be clamped at any point along two parallel bars, inclined to the horizontal at angle equal to the latitude of the place. Errors due to the shade ring[60] are taken into account and diffused part is corrected accordingly.

For the measurement of solar radiation on inclined surfaces, a Kipp-pyranometer is mounted on a universal stand, which enabled it to be tilted at any angle in the vertical plane between the horizontal and vertical positions and can be rotated to any azimuthal orientation in the horizontal plane. A detachable semi-circular screen painted with lamp-black is also used to prevent the reflected ground radiation reaching the instrument. By keeping the screen horizontal irrespective of the inclination of the pyranometer, the radiation reflected from the ground can be excluded. The e.m.f. output of the pyranometer was observed with a sensitive D.C.Microvoltmeter which can read to 1.0 microvolt. The pyranometer with the universal mount and the ground reflection screen is shown in fig (2.16).

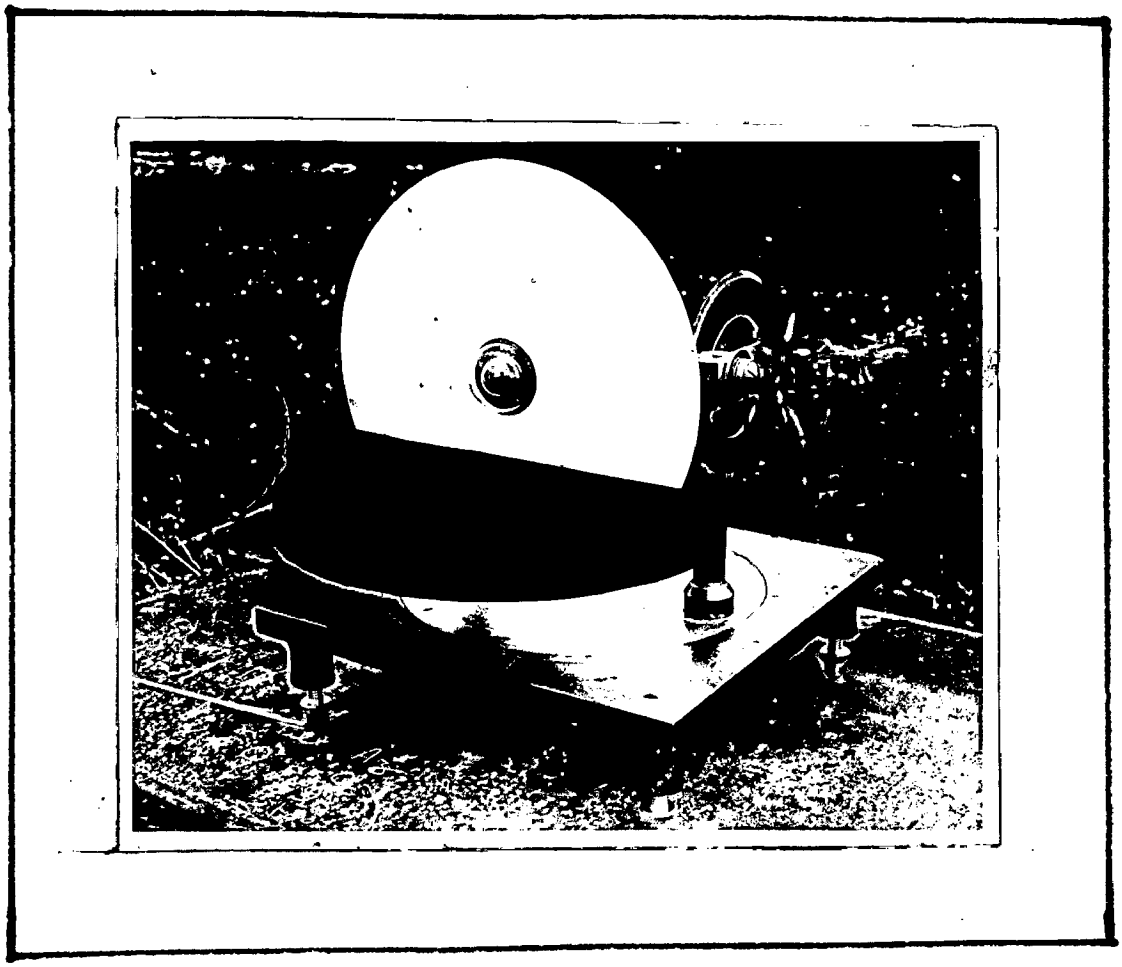

FIG.2.15: CLOSE UP VIEW SHOWING SOLARIMETER WITH GROUND REFLECTION SCREEN MOUNTED ON STAND.

2.62 Measurement of albedo of the ground:

It is known that an inclined surface receives direct solar radiation, diffused solar radiation and also the radiation reflected from the ground. Measured data on the ground reflected radiation for sloping surfaces of different inclinations is not usually available. However, it can be obtained from the measurements made with and without the ground reflection screen and the total solar radiation on horizontal surface. From these observations the albedo of the ground could be computed as shown below :

The total radiation (I_{GT}) received by an inclined surface is given by

$$I_{GT} = D_T + d_T + I_H \rho \sin^2 \beta/2 \qquad \text{----------(2.36)}$$

where D_T = direct solar radiation on inclined surface,

d_T = diffused solar radiation on inclined surface,

I_H = total solar radiation on horizontal surface,

ρ = albedo of the ground,

and β = tilt of plane from horizontal.

When a screen is used to cut-off the ground reflected part, equation (2.35) reduces to

$$I_T = D_T + d_T \qquad \text{----------(2.36)}$$

From equation (2.36) and (2.36) we get the albedo of the ground, as

$$\rho = \frac{I_{2R} - I_S}{I_H \sin^2 \beta/2} \qquad \text{--------- (2.37)}$$

About 80 observations are made for computing albedo of the ground. The ground surface at which the observations were made was fully covered by green grass. These results indicate that for a ground covered by green grass, the albedo varies from 0.20 to 0.24 around the average value of 0.22.

2.63. Radiation on inclined surfaces on overcast days:

Number of observations of total solar radiation were made on inclined surfaces of different slopes and orientations, at Roorkee during several overcast days. It may be mentioned here that these studies were spread over several overcast days and these days were so selected that the sky conditions were similar. The type of cloud cover may be classified as thick altrostratus (C_3) as per world meteorological organisations' (W.M.O.) classification. As the sun was not visible, the altitude and the azimuth of the sun at the time of observations were computed. The azimuthal orientation with respect to sun is then obtained from the azimuthal position of the seen and the solar azimuth with respect to the true south.

The data collected has been analysed in terms of the ratios of (I_{E/I_H}) radiation on inclined (with ground reflection accounted) to a horizontal surface for various solar altitudes and azimuthal orientation. In this study, azimuthal orientation of the surface is measured with respect to the position of the sun at any time. These observations cover a range of solar altitudes from 20 degrees to 80 degrees. The tilts selected for the study were 30°, 45°, 60° and 90° from the horizontal. The ratios of I_E/I_H were plotted against solar altitude for various azimuthal orientations. Fig (2.16) illustrates the effect of solar altitude on these ratios for a few typical cases. It can be seen from fig (2.16), that though the effect of solar altitude on these ratios is very small there appear to be a linear variation with solar altitude. The ratios of I_E/I_H for all the solar altitudes from 20° to 80° at intervals of 10° for the above four tilts as obtained from these plots are given in table (2.21). It can be seen from the table that the ratios vary linearly with the solar altitude, though this variation is small (of the order of 4 to 6 percent). It may also be noted that for a given solar altitude, these ratios vary considerably with the azimuthal orientation and tilt angle. As much as 30 to 40 percent fall is found for variation in azimuthal orientation from 0° to 180° in the case of 30° and 90° respectively.

TABLE 2.31: Ratios of total solar radiation on various inclined surfaces to total solar radiation on horizontal surface for different solar altitudes and azimuth angles under overcast sky conditions for Roorkee.

Tilt of plane from horizontal (degrees)	Azimuth of plane relative to sun (degrees)	Ratio Altitude of sun (degrees) 20	30	40	50	60	70	80	$\bar{\rho}_{cos}$
30	0	1.03	1.03	1.02	1.00	0.99	0.99	0.98	
	45	1.00	0.99	0.99	0.98	0.97	0.96	0.96	
	90	0.93	0.92	0.92	0.91	0.90	0.90	0.89	
	135	0.86	0.86	0.86	0.86	0.86	0.84	0.84	0.93
	180	0.83	0.81	0.80	0.80	0.79	0.79	0.79	
45	0	0.96	0.96	0.96	0.94	0.94	0.93	0.93	
	45	0.90	0.89	0.90	0.90	0.89	0.88	0.87	
	90	0.86	0.84	0.84	0.83	0.83	0.82	0.82	0.86
	135	0.79	0.78	0.78	0.77	0.77	0.76	0.76	
	180	0.71	0.70	0.70	0.70	0.69	0.69	0.68	
60	0	0.87	0.86	0.86	0.86	0.84	0.83	0.83	
	45	0.77	0.78	0.78	0.78	0.74	0.73	0.73	
	90	0.64	0.63	0.63	0.62	0.61	0.61	0.60	0.75
	135	0.53	0.57	0.58	0.58	0.58	0.54	0.53	
	180	0.53	0.53	0.51	0.50	0.49	0.49	0.49	
90	0	0.63	0.63	0.62	0.62	0.61	0.61	0.61	
	45	0.67	0.63	0.63	0.66	0.64	0.64	0.63	
	90	0.49	0.48	0.48	0.48	0.47	0.47	0.46	0.60
	135	0.33	0.37	0.37	0.38	0.38	0.36	0.36	
	180	0.34	0.33	0.33	0.33	0.33	0.34	0.34	

$\bar{\rho}_{cos}$ by Liu and Jordan's formula, where the sky is assumed as isotropic.

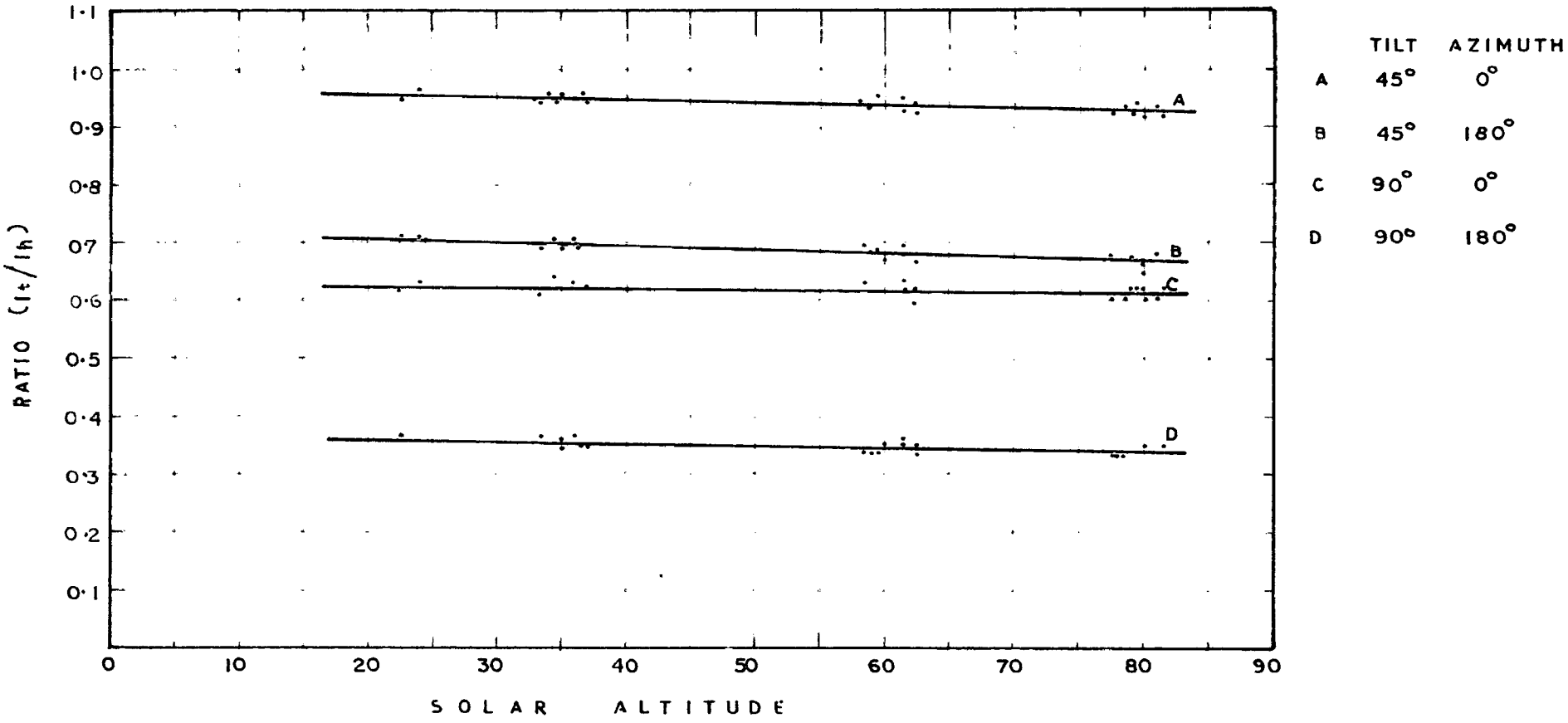

FIG. 2·16 VARIATION OF RATIO OF (I_t / I_h) WITH SOLAR ALTITUDE UNDER OVERCAST SKY CONDITIONS

Typical azimuthal variation of total solar radiation for a fixed solar altitude of 30 degrees is shown on a polar diagram (Fig.2.17) for different tilts. Fig.(2.18) shows the variation of the ratios (I_T/I_H) for various tilts with the azimuthal orientation for a solar altitude of 60 degrees. This study clearly brings out that even for overcast sky conditions anisotropy exists and the assumption of isotropic sky is not strictly valid in the estimations of total solar radiation on inclined and vertical surfaces.

2.7 MEASUREMENT OF SOLAR RADIATION ON VERTICAL SURFACES UNDER CLEAR SKY CONDITIONS

For a rational assessment of the heating and cooling loads of buildings, reliable information on the magnitude of the various radiation components which together make up the net radiation exchange at the outside surface of an exposed building element is a basic requirement. In tropics most of the meteorological data is available only for horizontal surfaces. For building design purposes, however, radiation data are required with respect to vertical and inclined surfaces and additional measurements are, therefore, necessary if a realistic interpretation of the influence of radiation on the thermal performance of buildings is to be made.

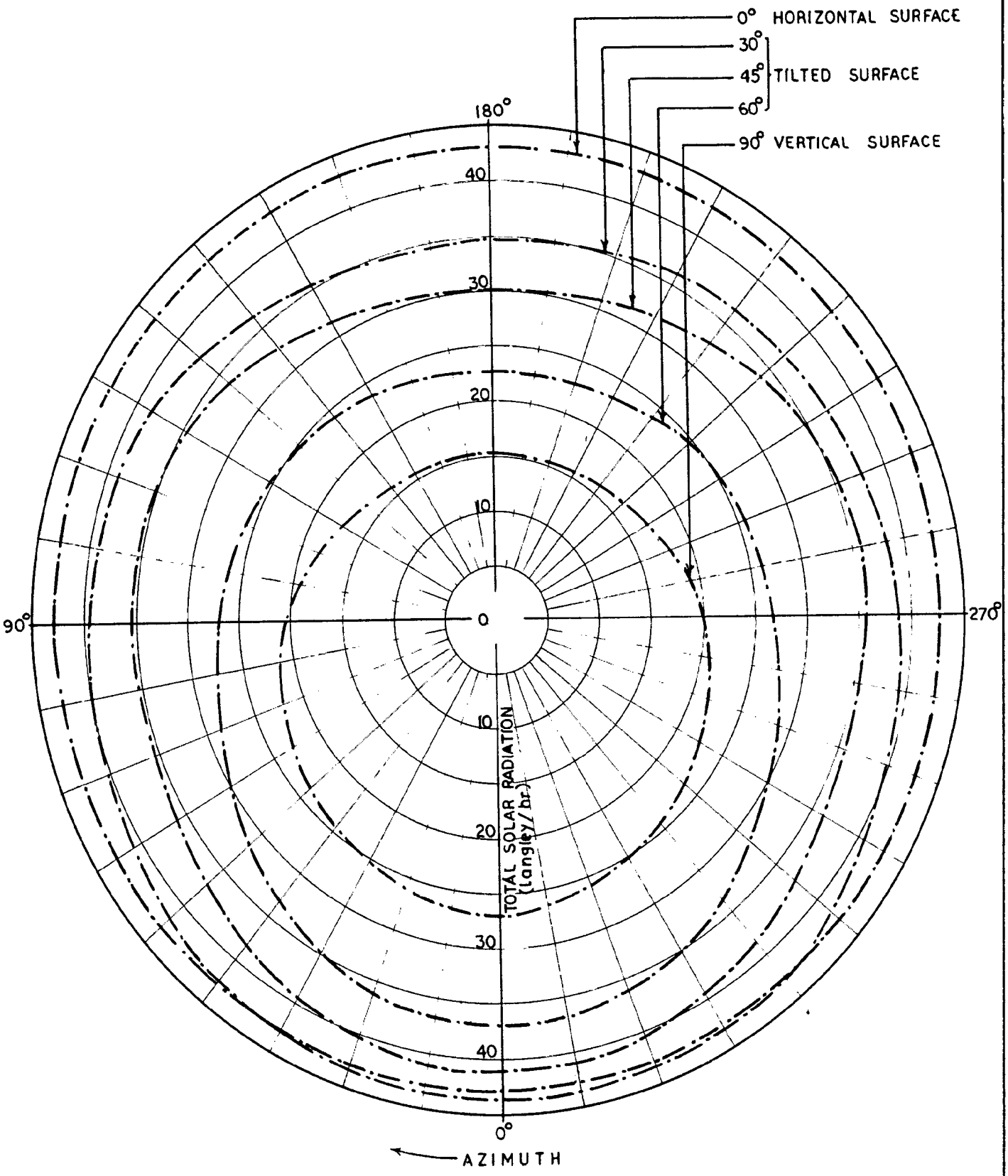

FIG. 2·17 POLAR DIAGRAM SHOWING VARIATION OF TOTAL SOLAR RADIATION ON INCLINED SURFACE WITH AZIMUTHAL ORIENTATION UNDER OVERCAST SKY CONDITIONS

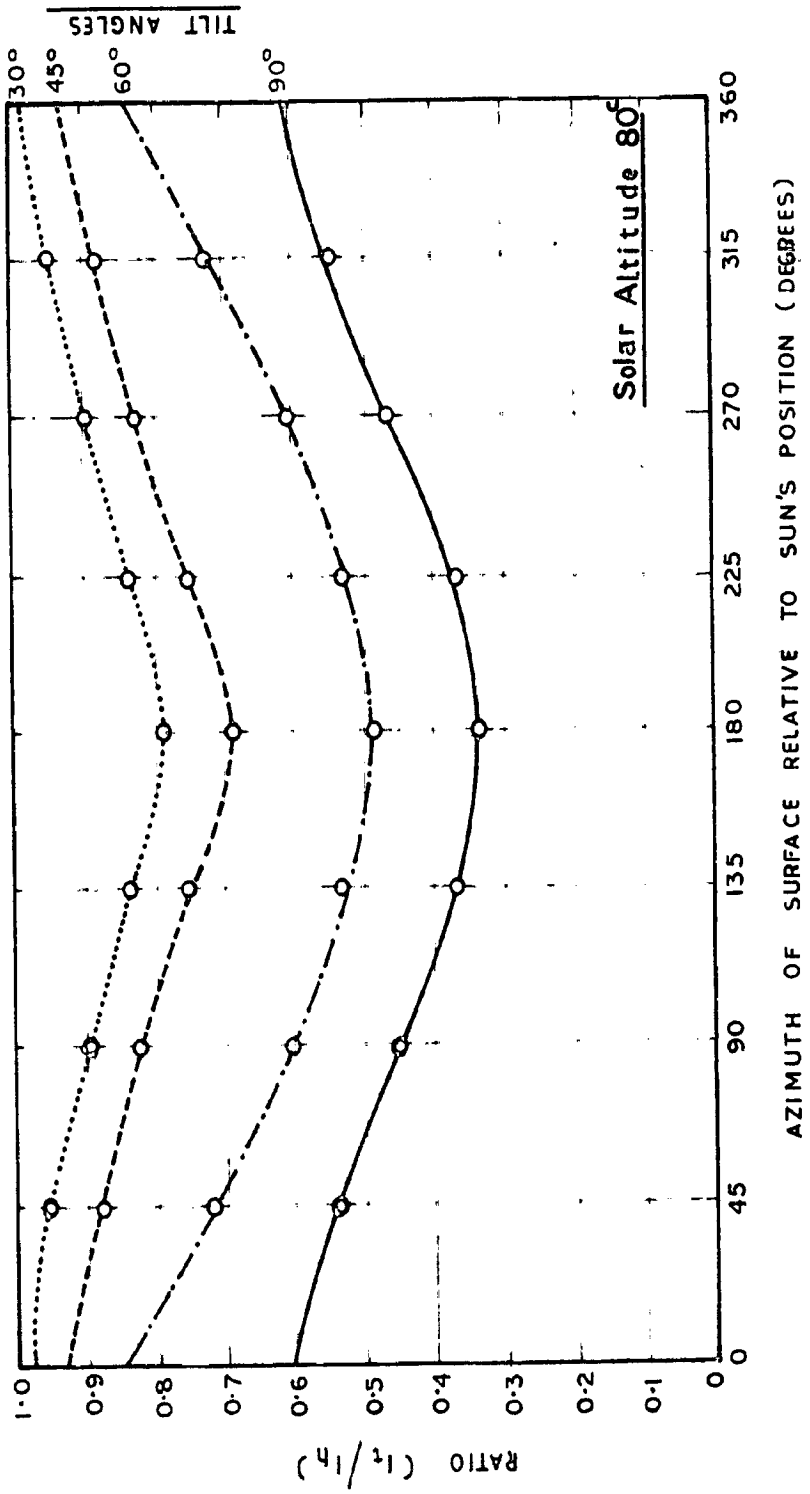

FIG. 2·18 VARIATION OF RATIO OF I_t/I_h WITH THE AZIMUTHAL ORIENTATION.

The instruments used for this study is the same as discussed in article (2.61).

For this study 20 days with clear sky conditions were selected. The ground surface at which the observations are made was fully covered by green grass having albedo of 0.22 as mentioned in article 2.62. The altitude and azimuth of the sun at the time of observations were computed. The observations were made for eight cardinal directions, i.e. S, SW, W, NW, N, NE, E, SE. The solar altitudes covered here are from 20 degrees to 70 degrees. Finally the total solar radiation on vertical surface is observed in terms of wall solar azimuth angle. The direct radiation was computed on the vertical surfaces of various azimuthal orientations from the measured direct radiation on horizontal surface. By calculating the direct sun component on the different surfaces, the diffused plus reflected component was derived by subtraction as done by Van Doventer and Gold[61].

The measured values of direct, diffused and total solar radiation on horizontal surfaces (Langley/hr) for various solar altitudes for clear days at Roorkee are shown in fig (3.10). These curves are drawn from the power-series[62] developed by the author on the basis of measured values.

Moon's values are also plotted in fig (3.10) to compare them with the experimental observations. It is seen that Moon's values are higher from the measured values at

TABLE 2.23: Ratios of diffused sky plus ground reflected radiation on vertical surfaces to diffused sky radiation on a horizontal surface for different solar altitudes and wall solar azimuth angles under clear sky conditions for Roorkee.

Wall Solar azimuth (degrees)	ALTITUDE OF SUN (degrees)					
	20	30	40	50	60	70
0	2.33	2.10	1.80	1.60	1.30	1.09
45	2.02	1.84	1.59	1.46	1.23	1.06
90	1.03	1.04	1.05	1.03	1.03	1.02
135	1.00	1.00	1.00	1.00	1.00	1.00
180	1.00	1.00	1.00	1.00	1.00	1.00

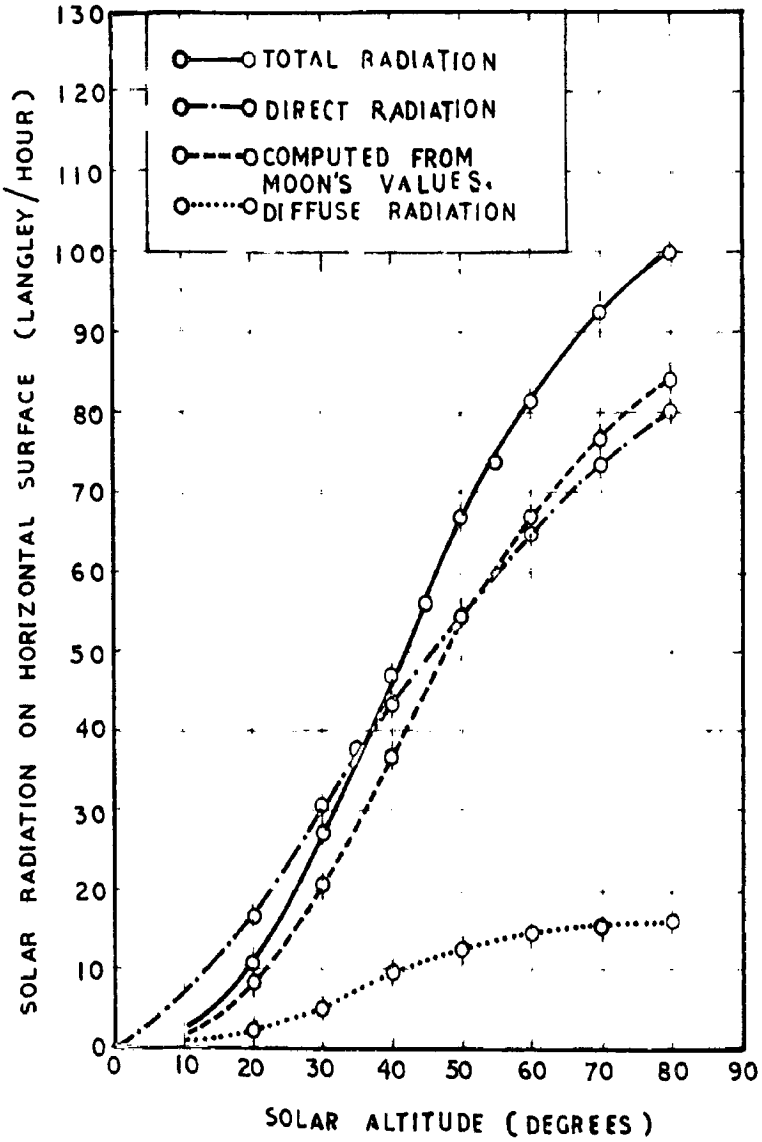

FIG. 2·19 VARIATION OF DIRECT & DIFFUSED SOLAR RADIATION ON HORIZONTAL SURFACE WITH THE SOLAR ALTITUDE AT ROORKEE

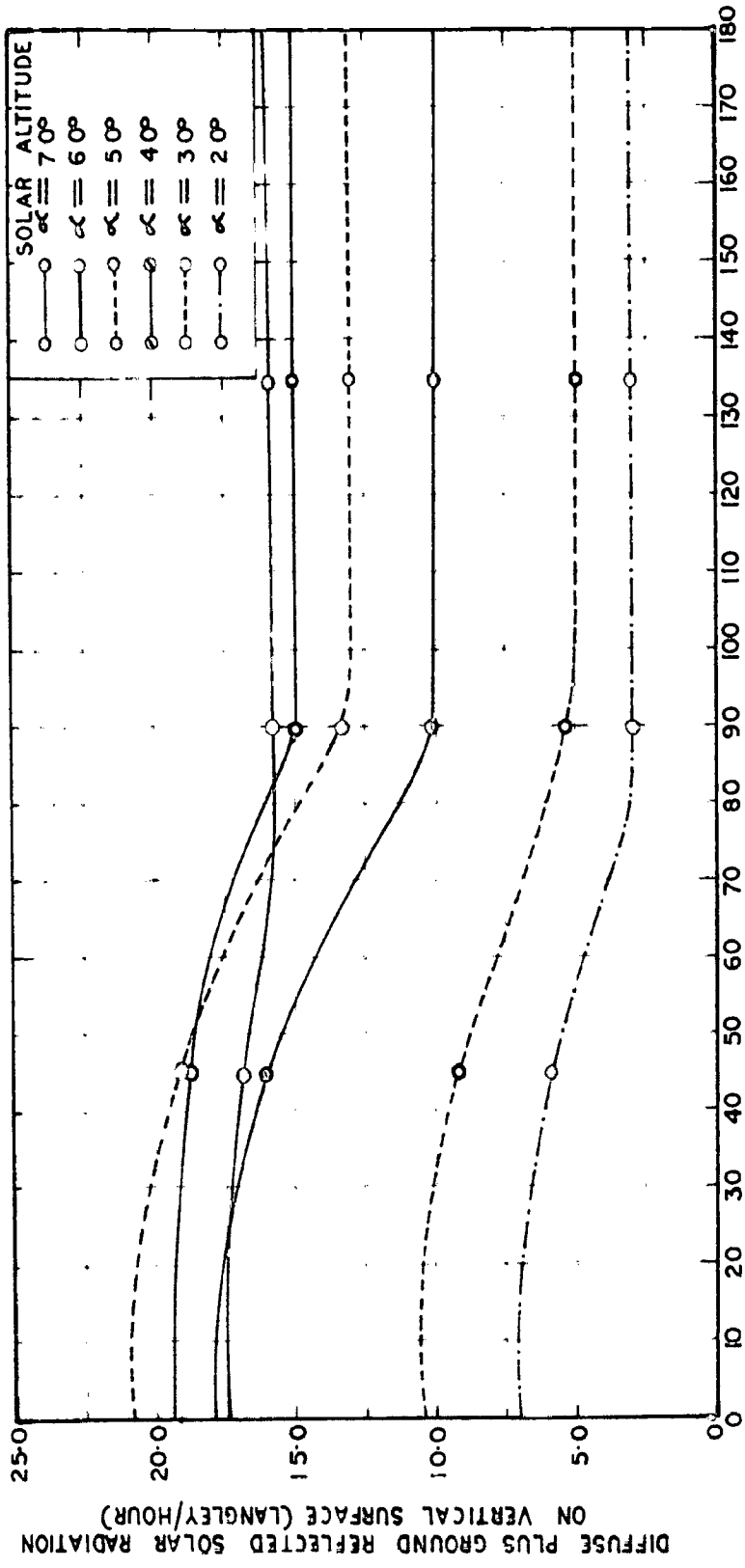

FIG.2·20 VARIATION OF DIFFUSED SOLAR RADIATION ON VERTICAL SURFACE WITH ALTITUDE OF SUN AND WALL SOLAR AZIMUTHAL ANGLES

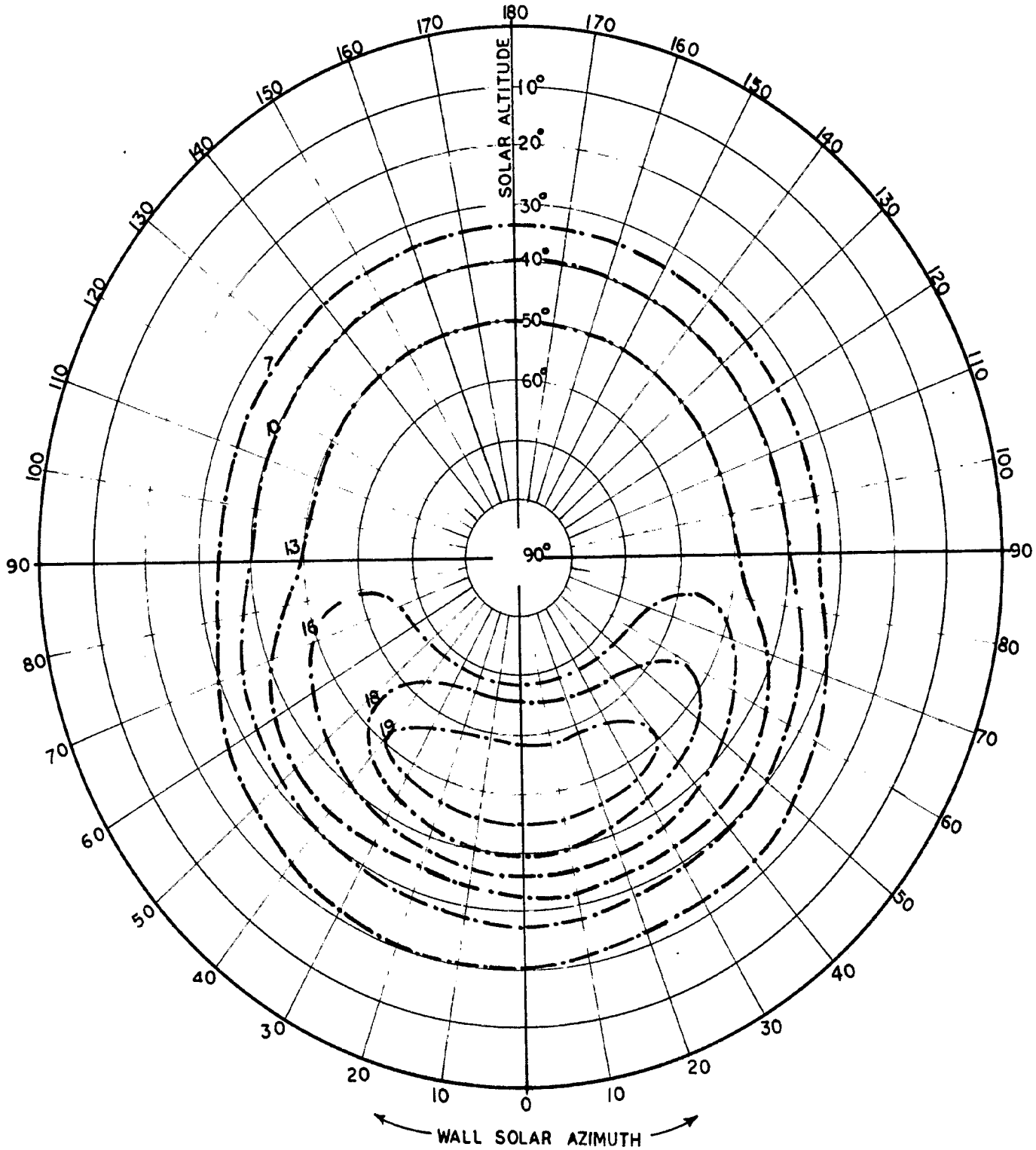

FIG. 2·21 POLAR DIAGRAM SHOWING THE VARIATION OF DIFFUSED RADIATION ON VERTICAL SURFACE WITH AZIMUTHAL ORIENTATION UNDER CLEAR SKY CONDITIONS

low altitude and low at high altitudes.

Fig.(2.20) shows the influence of solar altitude and wall solar azimuth angle on the diffused plus reflected radiation on the vertical surface. This curve clearly shows that a vertical surface facing the sun receives more diffused radiation than a surface opposite the sun. This is because of the strong circumsolar radiation near the sun.

The azimuthal variation of diffused plus reflected radiation on a vertical surface for various solar altitude is shown on a polar diagram(2.21). Here it again confirms that the surface which is in the quadrant of the sun receives more diffused radiation.

The ratios of diffused sky plus ground reflected radiation on vertical surfaces to diffused sky radiation on horizontal surface for various solar altitudes and wall solar azimuth angle were determined for the above study and are given in table 2.2. It can be seen that the vertical surface receives more diffused radiation i.e. diffused plus ground reflected radiation, than a horizontal surface. The ratio varies from 1.0 to 2.33. This high ratio at low solar altitude can be explained on the basis that at low solar altitude there is a strong circumsolar diffused radiation which has a small angle of incidence with the pyranometer.

C H A P T E R - 3.

COLLECTION OF SOLAR ENERGY

C H A P T E R - 3.

COLLECTION OF SOLAR ENERGY

3.1 INTRODUCTION

A flat-plate collector has a number of advantages over the focussing type of collectors such as (i) it absorbs direct, diffused and reflected radiation (ii) it is of low cost (iii) it is easy to fabricate and (iv) it does not require any sun path following arrangement. It is generally used in applications where temperatures below 100°C are encountered. A flat-plate solar energy collector consists of a flat metallic plate painted black on the side facing the sun to increase its absorption for the solar radiation, and insulated on the reverse side to reduce the backward heat losses. Above and parallel to the collector plate are mounted one or more air-spaced glass plates, glass being a material which is capable of transmitting the shortwave solar radiation but is opaque to the longwave re-radiation from the collector plate. Provision is made to remove the energy absorbed in the collector by circulating water through tubes soldered to the collector plate.

3.2 ABSORPTION OF ENERGY BY COLLECTORS:

A flat-plate collector is simply a heat exchanger which absorbs the heat from the sun and transfers this heat

to the fluid flowing within. The absorbed energy, q_a, depends on :

i) insolation rate on the absorber,

ii) the transmittance properties of the cover,

iii) losses due to dirt on the cover,

iv) shading of the absorber plate by the side walls of the absorber,

and v) absorptivity of the plate for solar radiation.

The flat-plate collectors are always oriented and tilted (fixed) such that they receive maximum solar radiation during the desired season of use. But the solar radiations are generally measured on horizontal surfaces so these values require conversion to use on tilted surfaces.

In unit time on unit area of the absorber will absorb energy, q_a, given as

$$q_a = \left[(I_{Th}-I_{dh})\, R_b \tau_b \alpha_b + I_{dh}\, R_d \tau_d \alpha_d + I_{Th} R_R \tau_R \alpha_R \right] \quad \text{---------(3.1)}$$

where I_{Th}, I_{dh} = hourly total and diffused solar radiation on horizontal surface respectively,

τ_b, τ_d, τ_R = transmittance of cover for direct, diffused and reflected radiation respectively,

$\alpha_b, \alpha_d, \alpha_R$ = absorptivity of plate for direct, diffused and reflected radiation respectively,

R_b, R_d, R_R = conversion factor for direct, diffused and reflected radiation respectively for converting from horizontal to tilted surface,

D = dirt correction factor,

and S = shading correction factor.

For practical purposes α_b, α_d and α_R are assumed to be same i.e. α. The significance and expressions for R_b, R_d and R_R are already discussed in chapter 2. The values of τ_b, τ_d and τ_R will be discussed later in this chapter. The dirt correction factor (D) for various inclined surfaces will also be discussed in this chapter. The shading correction factor (S) are computed (Fig.3.1) for various hours from solar noon for a latitude 30°N. Here it has been assumed that the collector is facing southern and makes an angle from the horizontal equal to (latitude of place + 10 degs.). The dimensions of the absorber are assumed as length = 2 width = 10 height.

Thus the equation (3.1) can be written as :

$$q_a = \left[(I_{Tb} - I_{Rb}) R_b \tau_b \alpha + I_{Rh} R_d \tau_d \alpha + I_{Th} R_R \tau_R \alpha \right] D.S. = H (\tau\alpha)_e$$

----------(3.2)

where H = solar energy per unit time and area falling on the outer surface of the collector,

and $(\tau\alpha)_e$ = suitable mean value of transmittance and absorptance product. This term here includes allowance for dirt and shading.

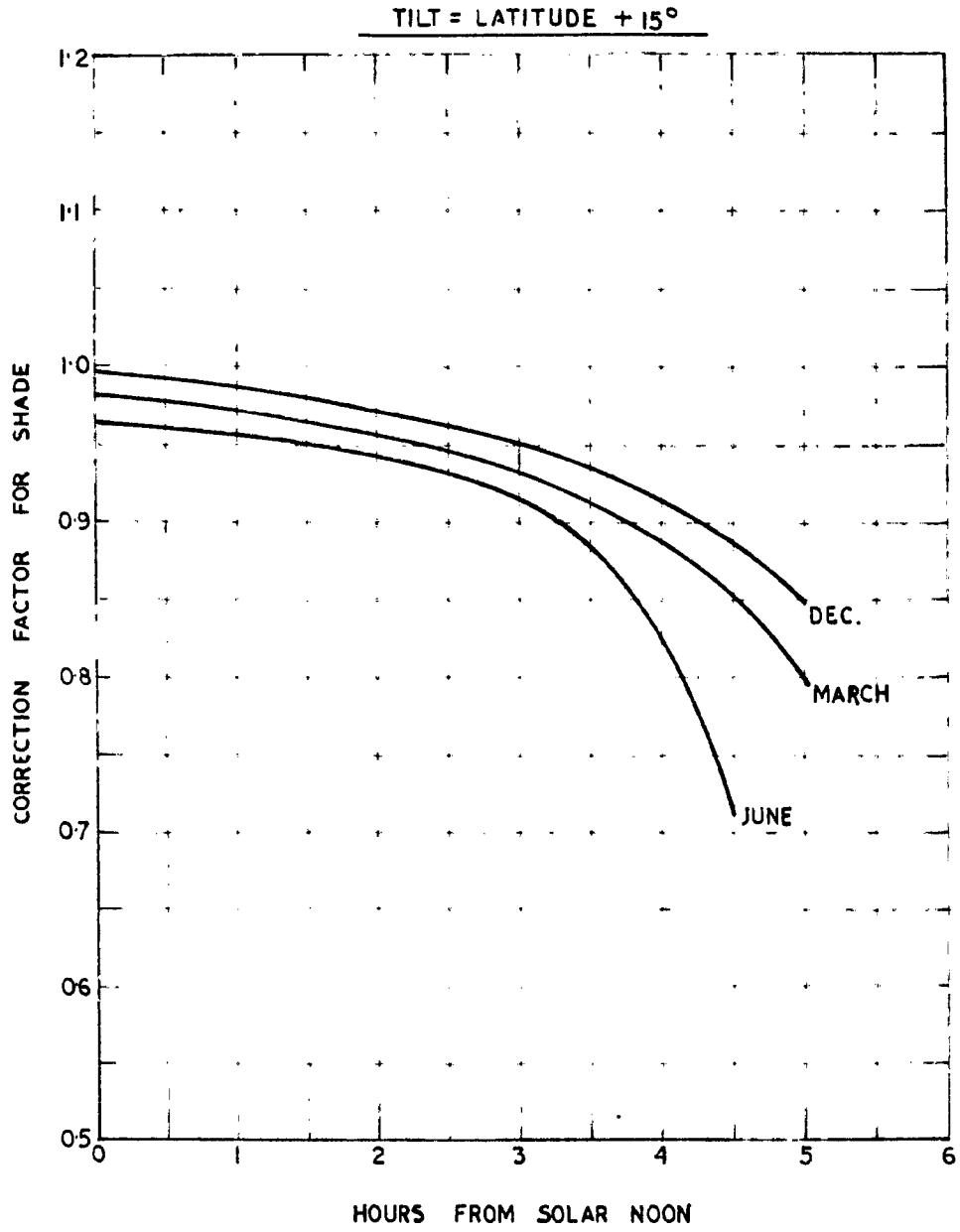

FIG. 3·1 SHADING CORRECTION FACTOR FOR VARIOUS HOURS.

There are a large number of designs of flat-plate collector. Some of the commonly used collectors are shown in fig (3.3). Under steady state conditions, the rate of useful heat collection is the difference between the rate at which solar energy is absorbed by the blackened plate and the rate at which energy is lost due to difference in temperature of the blackened plate and the ambient air. The heat balance of the absorber is given by the simple equation:

(useful heat collected) = (Heat absorbed by the plate) − (Heat losses)

$$\text{or} \quad q_u = H(\tau\alpha)_o - U_L (t_p - t_a) \qquad \text{——————(3.3)}$$

where q_u = rate of useful heat collection per unit area,

U_L = overall heat loss coefficient from the collector plate to ambient air,

and t_p, t_a = average plate and ambient air temperature respectively.

Usually the average plate temperature, t_p, is not known. So it would be convenient to put the equation in terms of the inlet fluid temperature or the average fluid temperature, which can be easily measured. The above equation can be put in terms of inlet temperature , t_i, by using a heat removal efficiency factor, F_R, as

$$q_u = F_R \left[H(\tau\alpha)_o - U_L (t_i - t_a) \right] \qquad \text{——————(3.4)}$$

The expression for F_R shall be derived later. The equation

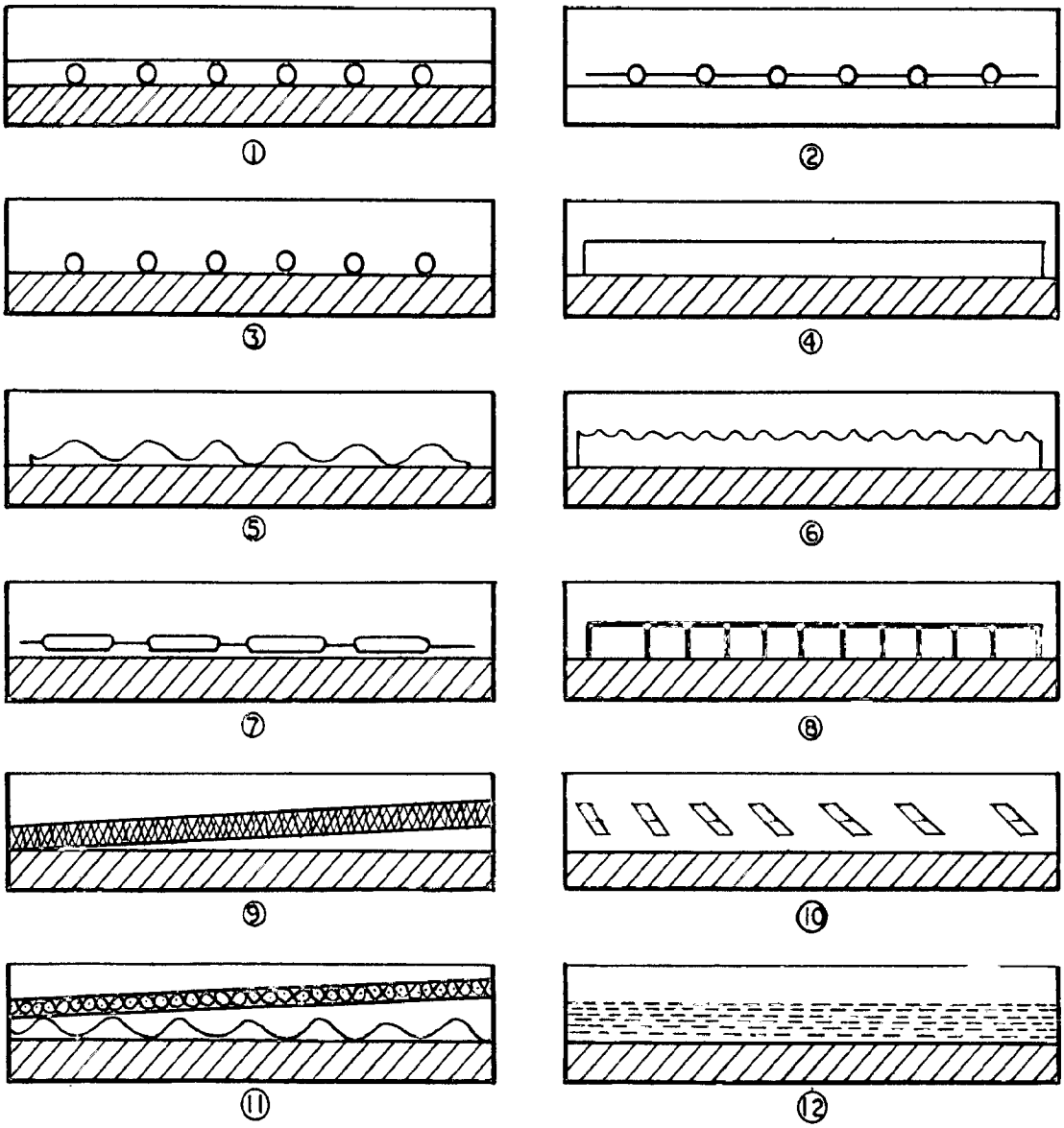

FIG.3-2 VARIOUS DESIGNS OF FLAT PLATE COLLECTOR

(3.3) may be put in terms of plate efficiency factor, F_p, as

$$q_u = F_p \left[H (\tau\alpha)_e - U_L (t_{av} - t_a) \right] \quad \text{------(3.6)}$$

where t_{av} = average fluid temperature
$= \frac{t_1 + t_2}{2}$

and t_2 = outlet fluid temperature.

The expression for rate of useful energy per unit area (q_u) can also be written as :

$$q_u = C C_p (t_2 - t_1) \quad \text{------(3.6)}$$

where C = mass flow rate of fluid (Kgm/m^{2}hr)

C_p = specific heat of fluid.

The collection efficiency (η) of the absorber is defined as the ratio of useful energy collected to that of incident energy i.e.

$$\eta = \frac{C C_p (t_2 - t_1)}{H} \quad \text{------(3.7)}$$

From equation (3.3), the efficiency can be given as :

$$\eta = \frac{q_u}{H} = \left[(\tau\alpha)_e - \frac{U_L}{H} (t_p - t_a) \right] \text{----(3.8)}$$

From this expression the collection efficiency can be computed provided the right hand side values are known.

The effect of glass cover on the collector efficiency as computed from equation (3.8) for various plate temperatures

are shown in fig (3.3). In this computation, following conditions are assumed.

U = 800 Kcal/m^{2}hr.

t_a = 25^{0}C

τ = 0.80
α = 0.95
ϵ = 0.88

Blackened absorber with one glass cover.

τ = 0.83
α = 0.95
ϵ = 0.88

Blackened absorber with two glass cover.

The values of U_L are read from the curve which shall be discussed later in this chapter.

It is seen from fig (3.3) that the choice of the multiple glass cover depends on the temperature of use. For low temperature applications such as water heating and space heating, one glass cover is adequate. But where large temperatures are required such as in absorption refrigeration cycles two glass covers must be used.

The effect of selective paint over an ordinary black paint is shown in fig (3.4). Here it has been assumed that for selective paint α = 0.93 and ϵ = 0.20. It is seen from this figure that the selective paint is more advantageous over the black paint as far as the efficiency is concerned, and this advantage goes on increasing as the plate temperature increases.

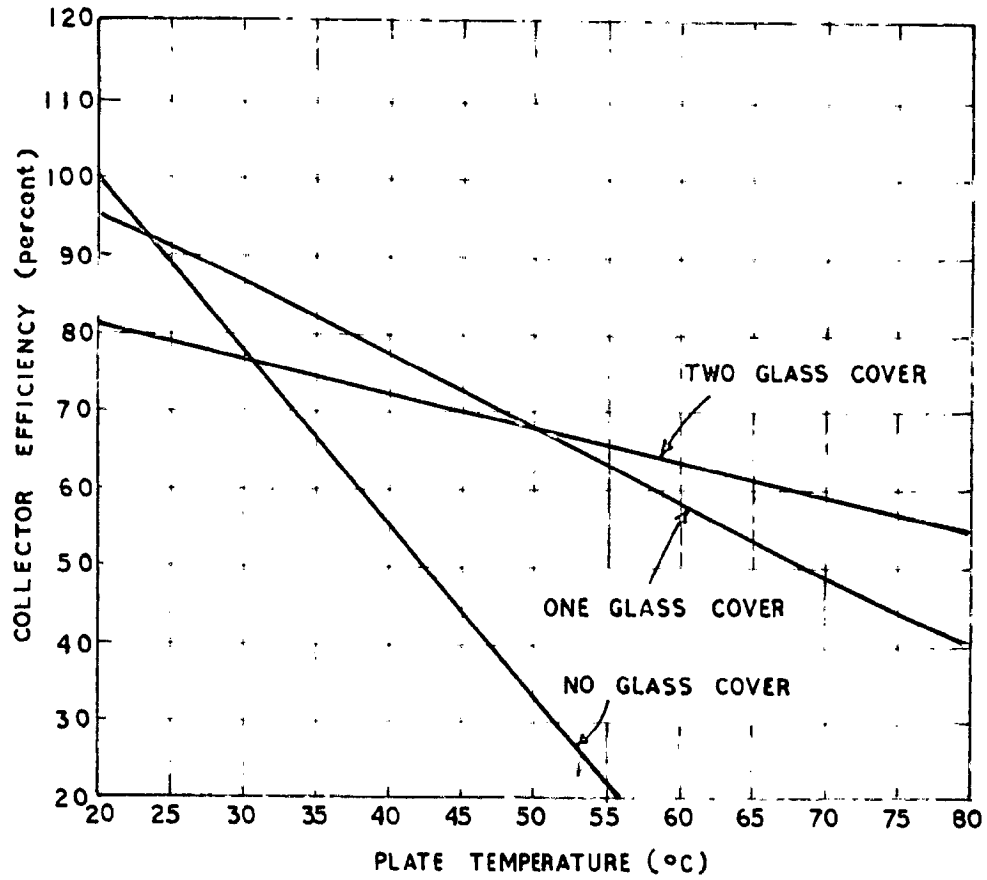

FIG. 3·3 EFFECT OF USING NUMBER OF GLASS COVERS

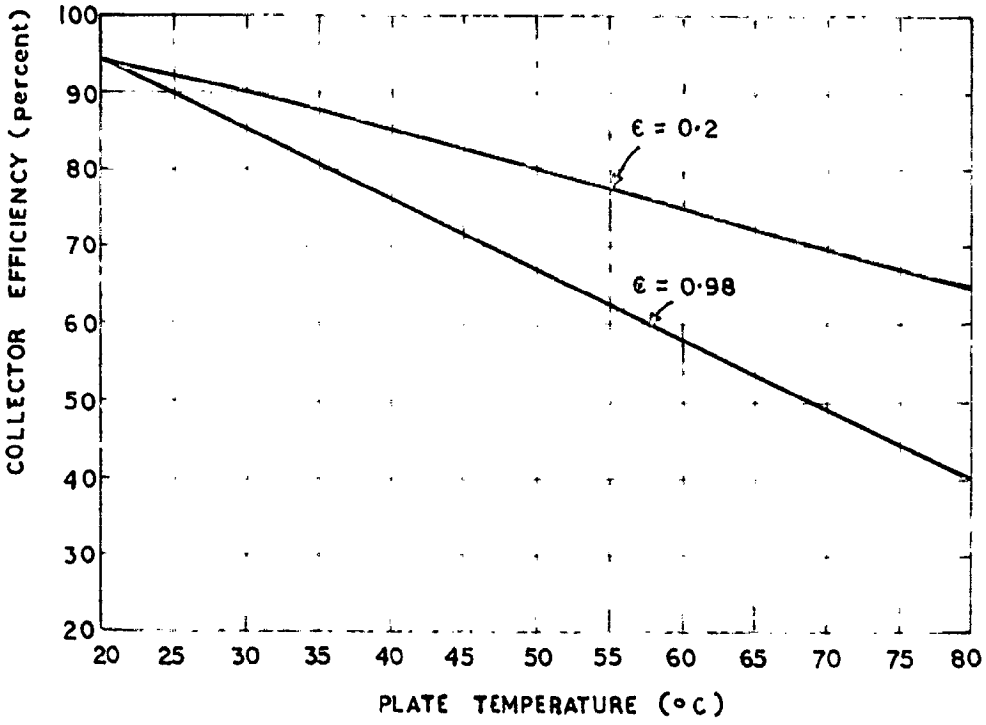

FIG. 3·4. EFFECT OF SELECTIVE OVER NONSELECTIVE ABSORBER

The effect of mass flow rate (Kgm/m^2hr) on the outlet temperature (^oC) for various amounts of absorbed energy ($Kcal/m^2hr$) is shown in fig (3.3). It is seen from this figure that at a constant amount of absorbed energy, the outlet temperature decreases as the flow rate increases. This difference is more at higher energy absorbed rate. These curves are plotted for a single glass cover absorber having black painted plate.

3.3 OPTICAL PROPERTIES OF TRANSPARENT MATERIALS

The overall transmittance (τ) of any transparent material for a beam of solar energy depends upon surface reflection and internal absorption in the material, which in turn depend upon the angle of incidence of the beam. The solar range of wavelength at the earth's surface lies between 0.3 to 2.5μ and its transmission through transparent material is complicated by the fact that all wavelengths do not suffer equal attenuation. Fig (3.6) shows the spectral transmittance[1] for ordinary window glass of 3 mm thick. It is seen that transmittance remains nearly constant upto 2.7 microns then it falls sharply and becomes zero at about 4.5 microns. Fig.(3.7) shows the spectral absorbance for polyethylene (80 microns) and polystrene (110 microns) tested at National Chemical Laboratory at Poona at the author's request. From this it is evident that both the films are transparent upto 0.6 microns after which the polystrene becomes opaque but polyethylene remains transparent. From

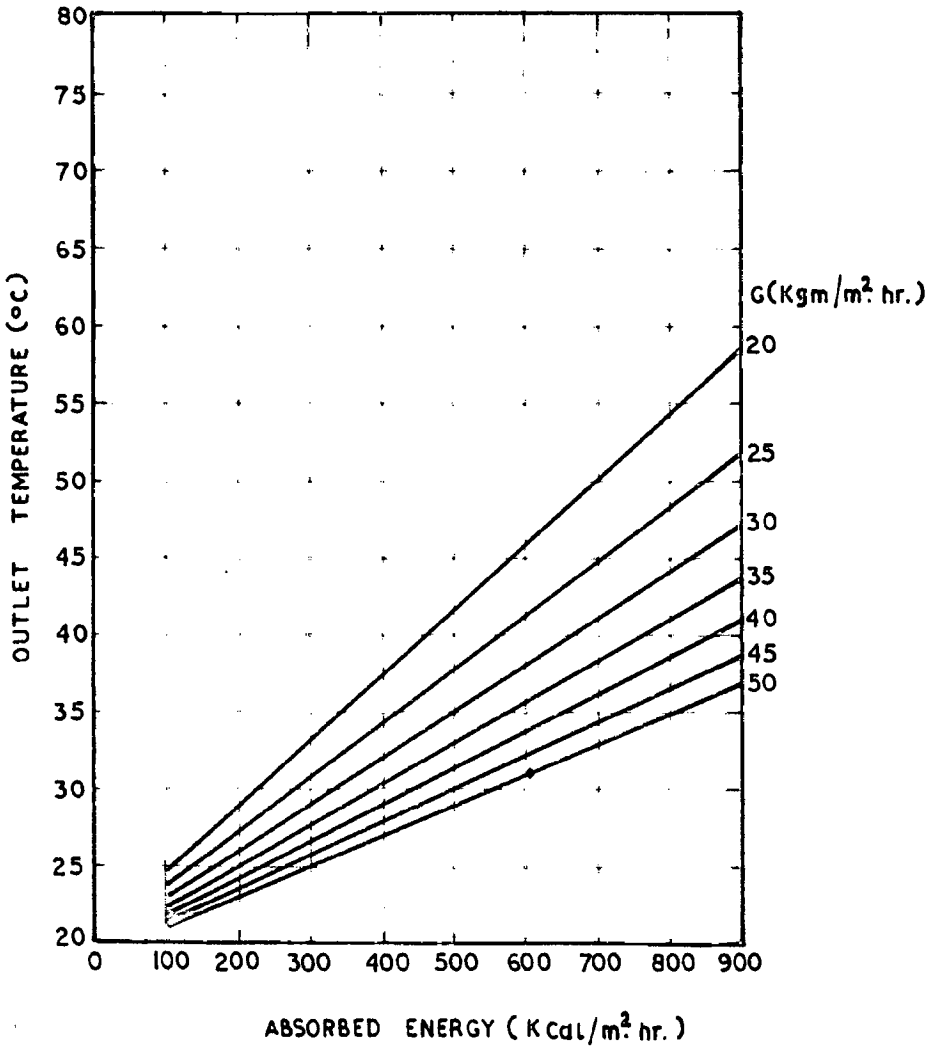

FIG. 3·5 EFFECT OF MASS FLOW RATE ON THE OUTLET TEMPERATURE

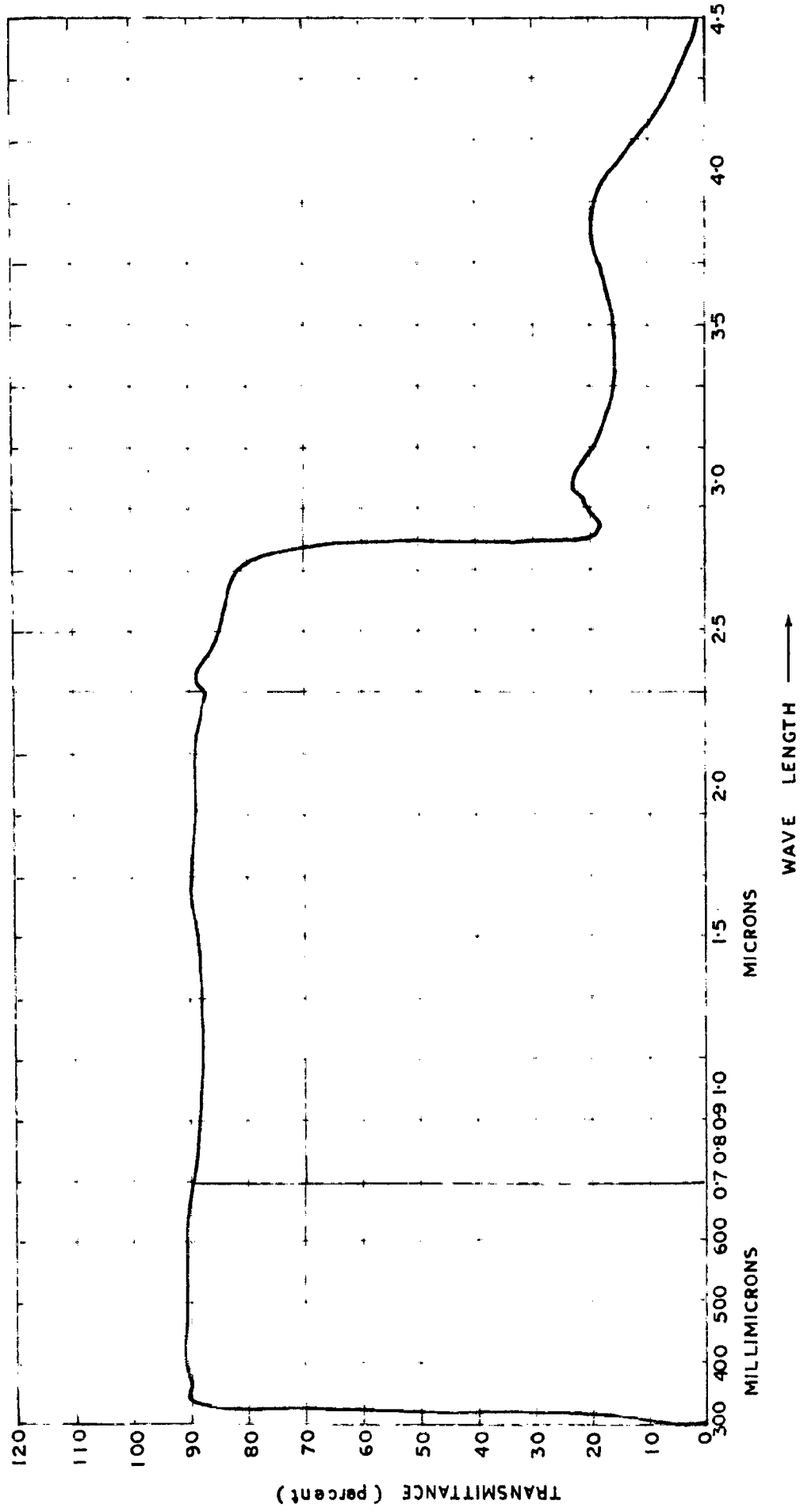

FIG. 3·6 SPECTRAL TRANSMITTANCE OF GLASS HAVING LOW IRON CONTENT

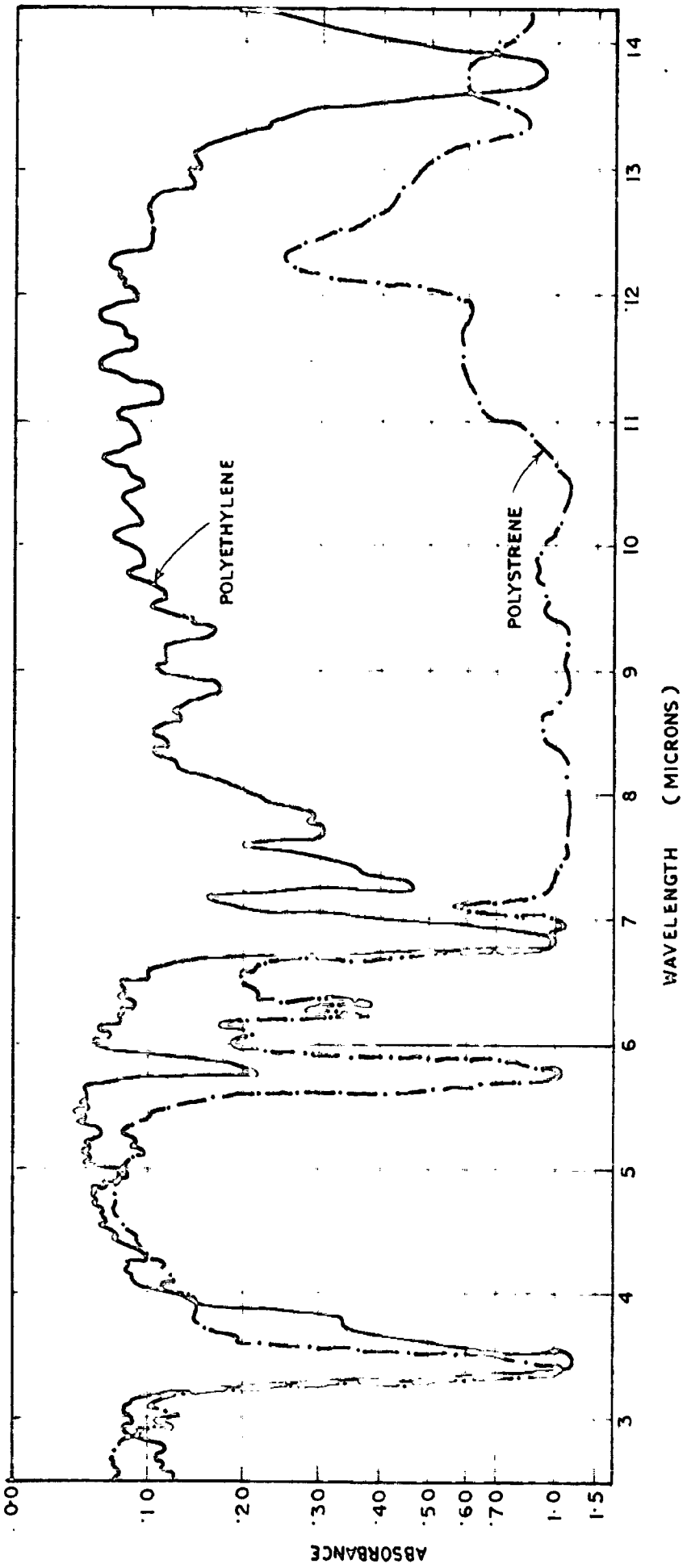

FIG. 3·7 SPECTRAL ABSORBANCE OF PLASTIC FILMS

these observations it can be concluded that glass plate and polystrene can be used as a cover for the collection since they do not allow the longwave thermal re-radiation from the heated plate to the atmosphere.

Surface reflection, r_s Natural light may be assumed to be consisted of equal amounts of two plane polarised light one having vibrations parallel to the plane of incidence while other perpendicular to the plane of incidence. Fresnel[2] has shown that surface reflection (r) is given as:

$$r = \frac{1}{2}\left[\frac{\sin^2(i-i')}{\sin^2(i+i')} + \frac{\tan^2(i-i')}{\tan^2(i+i')}\right] \qquad \text{-------(3.9)}$$

This relationship is shown graphically in fig (3.9) for glass having an index of refraction $n' = 1.525$.

For normal incidence, $i = 0$, then

$$r = \left(\frac{n'-n}{n+n}\right)^2 \qquad \text{-------(3.10)}$$

and if $n = 1$ i.e. one of the medium is air, then

$$r = \left(\frac{n'-1}{n+1}\right)^2 \qquad \text{------ (3.11)}$$

It can be seen from equation (3.11) or from curve of fig (3.8) that at normal incidence, $r = 0.0432$.

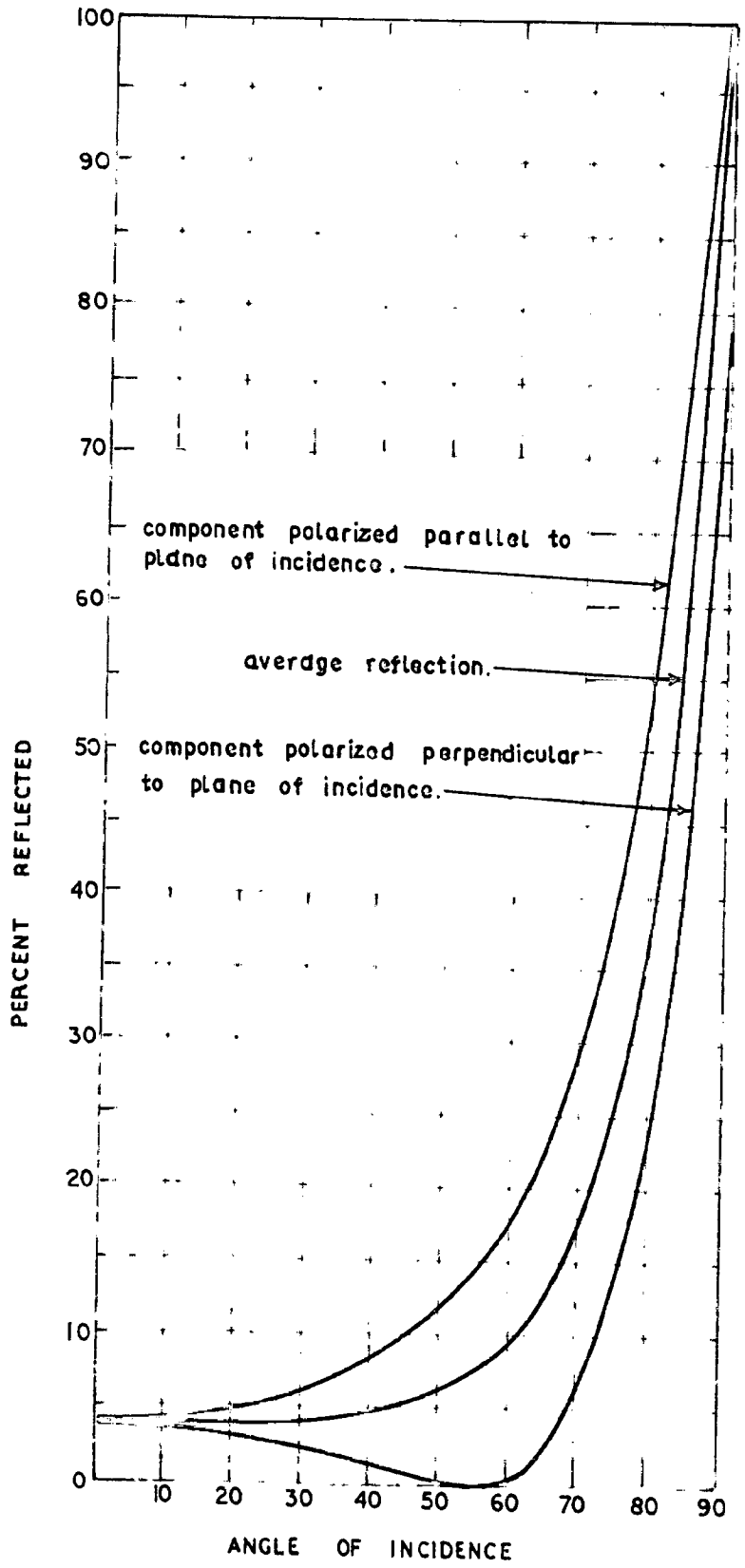

FIG. 3·8. REFLECTION VERSUS ANGLE OF INCIDENCE CURVES FOR POLARIZED AND NATURAL LIGHT. $n = 1{\cdot}525$ (glass)

Absorption in glass :

The absorption of solar radiation in glass which is due to Fe_2O_3 can be calculated from Bouger's law, $\frac{dI}{dx} = -KI$, which says that the decrease in light intensity is KI in traversing a distance of dx. Where K is known as extinction or absorption coefficient. The above equation can be put as

$$\tau_a = e^{-Kx} \qquad \text{-------(3.12)}$$

where τ_a = transmission of glass allowing for absorption losses only.

It can also be shown easily that the transmittance (τ) allowing for reflection and absorption losses is

$$\tau = \left(\frac{1-r}{1+r}\right) e^{-Kx} \qquad \text{-------(3.13)}$$

Thus for the available glass in India, where $\tau = 0.90$ and $x = 0.3$, the absorption coefficient comes out to be 0.062 per cm.

The value of K can be more precisely determined with the help of the following formula

$$\frac{\tau_2}{\tau_1} = e^{-K(x_2 - x_1)} \qquad \text{-------(3.14)}$$

where x2 and x1 are the thickness of two plates of same glass having transmittance τ_2 and τ_1 respectively.

3.31 Transmittance of two or more parallel plates

Sometimes two glass covers or even more covers are used over the absorber to reduce the losses from the absorber plate. Stokes[3] has developed expressions for the combined effects of reflection and absorption by one or more sheets. For a single sheet the transmittance (τ_1) is

$$\tau_1 = \frac{(1-r)^2 e^{-Kx}}{1-r^2(e^{-Kx})^2} \qquad \text{--------(3.15)}$$

and the reflectance is

$$\rho_1 = r + \frac{r(e^{-Kx})^2(1-r)^2}{1-r^2(e^{-Kx})^2} \qquad \text{--------(3.16)}$$

For small values of the extinction coefficient, K, and surface reflectance, r, this expression is simplified to

$$\tau_1 = \left(\frac{1-r}{1+r}\right) e^{-Kx} = \tau_{1r}\,\tau_{1a} \qquad \text{--------(3.17)}$$

the subscript 1 referring to a single sheet. Similarly for a number of glass covers (parallel), one can write

$$\tau = \tau_a\,\tau_r \qquad \text{--------(3.18)}$$

where τ = overall transmittance,

τ_a = transmittance allowing for absorption losses only,

and τ_r = transmittance allowing for reflection losses only.

This expression is found to be most accurate for problems of solar heat collector design.

3.33 Measurement of transmittance:

Hipp and Reman pyrheliometer is used for the measurement of color transmittance for direct color radiation at various angles of incidence. The measured data are shown in fig (3.8), together with the calculated curve and a curve allowing for reflection losses only. There is a fair agreement between the calculated curve and experimental curve. It is seen that as the angle of incidence increases from 0^0 to 30^0 the reflectance or transmittance does not change much. Between 30^0 and 40^0 the transmittance drops off with increasing rapidity as the incidence angle increases. The absorptivity of glass also begins to increase because of the increasing path length traversed. For values of the incident angle greater than 45^0, the transmittance drops off very rapidly because of the increase of reflectivity at such angles. When incidence angle approaches 90^0, the reflectivity becomes 100 percent.

Fig (3.10), shows the computed values of the transmittance for the sun-rays for normal incidence for a number of airspaced glass roots of extinction coefficient 0.063 per cm. Curve (A) is drawn for comparison which is the transmittance curve taking into account the reflection losses only. Curve B is the transmittance curve which takes into account the reflection as well as the absorption losses.

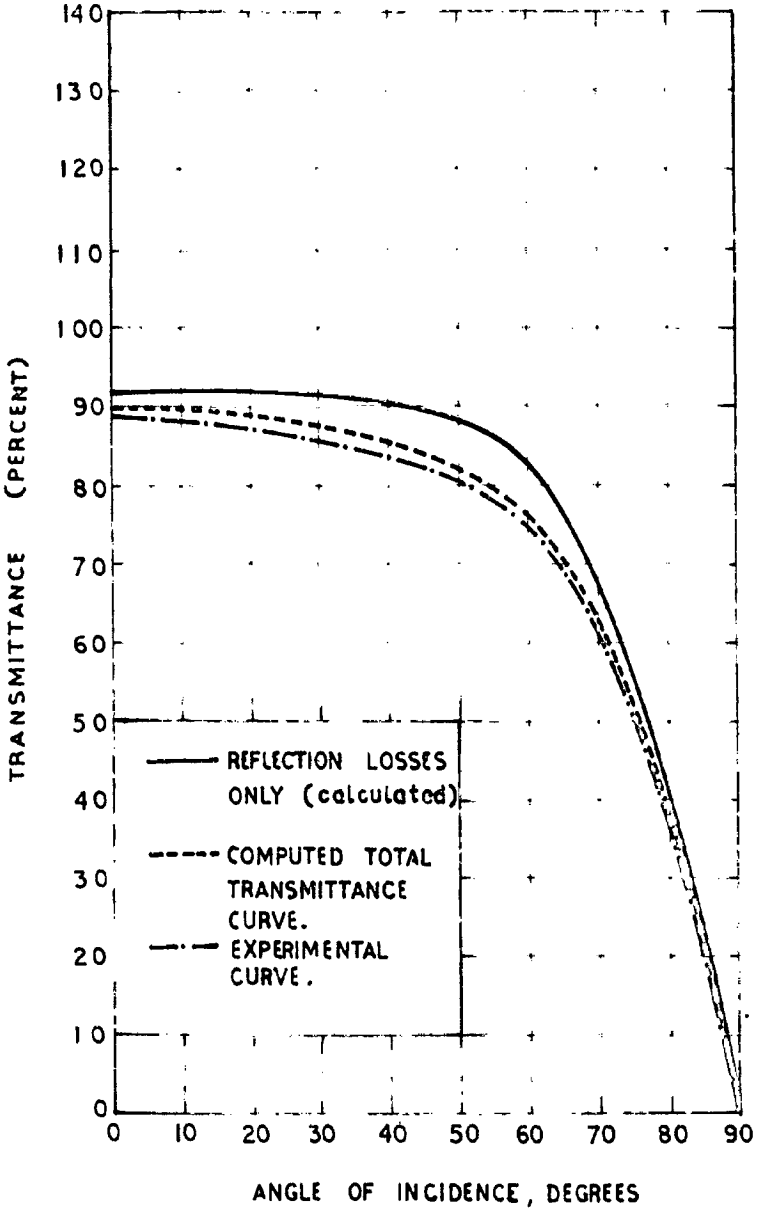

FIG. 3·9. COMPUTED AND EXPERIMENTAL TRANSMITTANCE CURVE FOR SINGLE GLASS (0·3 cm.)

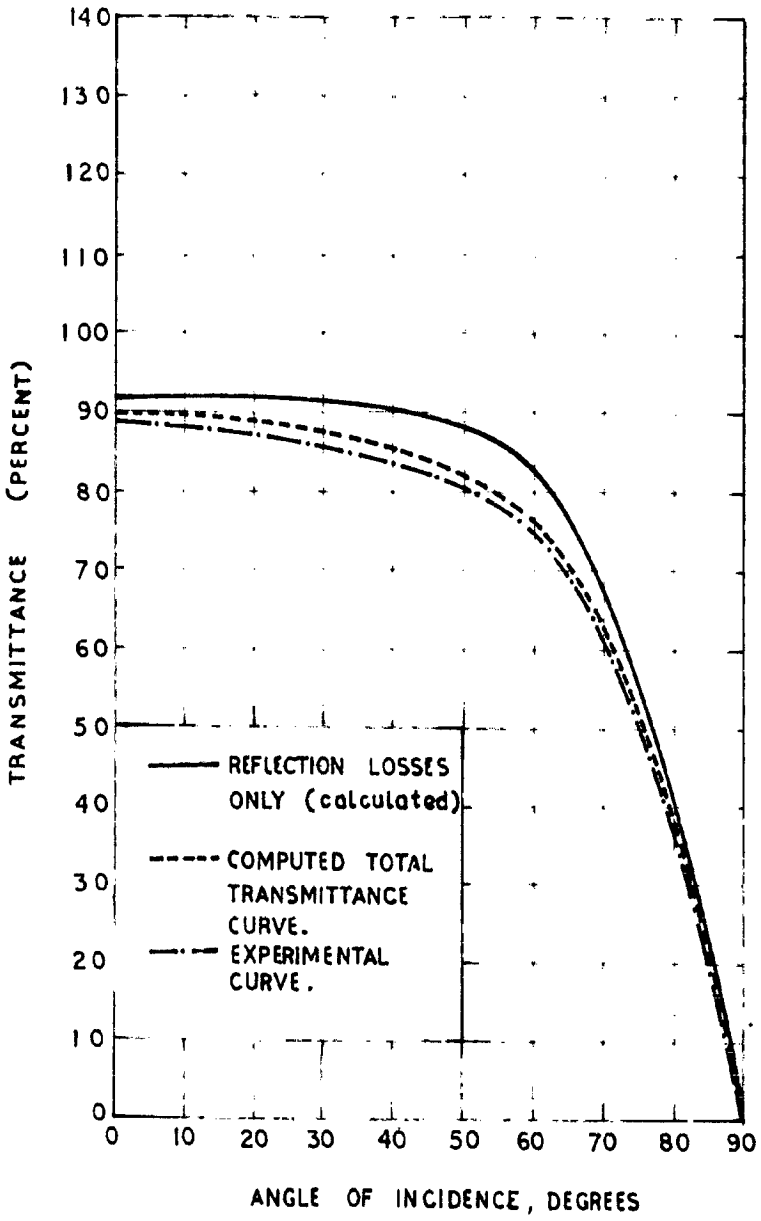

FIG. 3·9. COMPUTED AND EXPERIMENTAL TRANSMITTANCE CURVE FOR SINGLE GLASS (0·3 cm.)

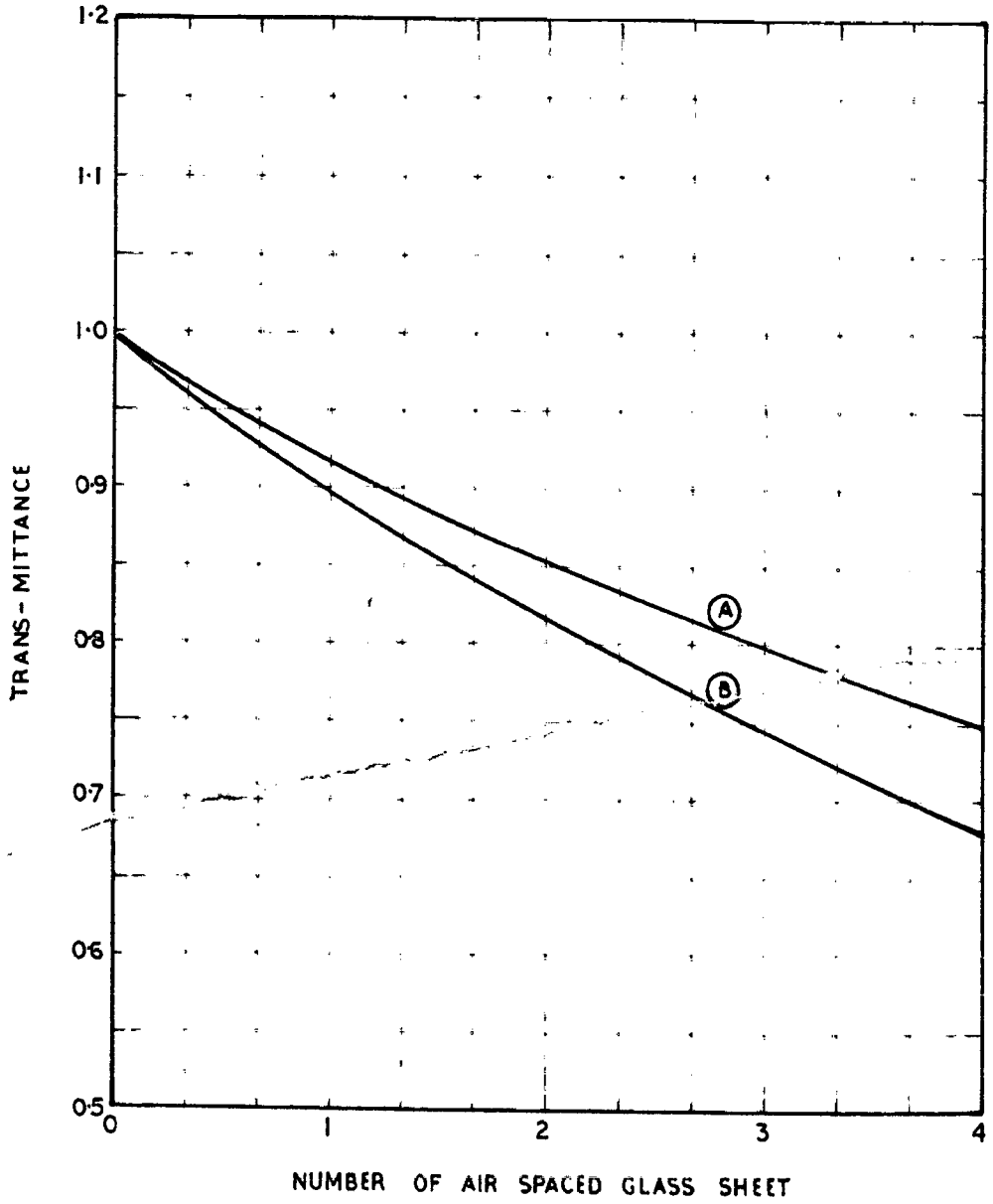

FIG. 3·10 TRANS-MITTANCE AT NORMAL INCIDENCE FOR SUNLIGHT

3.33 Transmission characteristic of glass and plastics:

Upto now glass was the only material used for absorber cover but recently a number of plastics are developed which may replace the glass. Their use depends on the availability, cost and life. Recently three plastic films, namely Tedlar, Mylar and Teflon produced by dupont (4,5,6,7,8) can be used as alternatives to glass. The more important physical properties of these plastics and polyethylene and polystrene and of glass are compared in Table (3.1).

Only glass, polyethylene and polystrene are available in India. In the solar range of wavelength i.e. 0.3 to 2.6 microns, both glass and plastics have very good transmittence. Longwave radiation is not transmitted by window glasses whereas polyethylene transmits upto 50 microns radiation.

The suitability of polyethylene and polystrene as a cover was tested for two years and found that they do not give satisfactory performance because of their poor weathering properties. Further, polyethylene can not be used at higher temperatures. However, polystrene can be used satisfactorily in combination with glass which should form the top cover.

3.4 EFFECT OF DIRT ON TRANSMITTANCE COVER:

In the computation of overall performance of flat-plate collector, the effect of dirt on the transmittence of

TABLE 3.1: Physical properties of some of the transparent materials used as a cover.

		Glass	Polyethylene	Polystyrene	Mylar	Tedlar	Teflon
1.	Thickness, cm	3.0	0.03	0.11	0.10	0.10	0.10
2.	Density, $gm/_{cc}$	2.47	0.90	1.30	1.30	1.37	2.15
3.	Tensile strength (PSI)	-	2000	6000	24000	8000	3000
4.	Temperature limit °C	-	80	150	150	150	200
5.	Coefficient of thermal expansion $^{cm}/_{cm}$ per °C	0.043×10^{-6}	540×10^{-6}	-	27×10^{-6}	43×10^{-6}	100×10^{-6}
6.	Refractive index	1.526	1.50	1.48	1.64	1.457	1.34
7.	Surface reflectivity (normal)	0.043	0.040	0.038	0.053	0.0353	-
8.	Solar transmittance (normal)	0.90	0.923	0.95	0.874	0.943	0.977
9.	Extinction Coefficient per cm.	0.073	0.40	1.2	1.36	1.2	0.40
10.	Cost U.S. dollars per m^2	1.5	0.20	0.40	-	-	-
11.	Expected life, years.	20	1	2	2	4	10

glass or plastic cover should be taken into account. Hottel and Woertz[9] carried out some tests to assess the effect of dirt on collector performance and concluded that the dirt setting on glass in an industrial area reduces collector performance only by about one percent. This correction factor seems to be too low as pointed out by themselves and as the collector performance depends on a number of factors, it is important to study the effect of dirt on transmittance alone. Hence the dirt factor or correction factor due to dirt is studied in detail as follows :

Ten identical wooden boxes 15x15x10 cms having a sliding glass window were kept at various inclinations from horizontal ranging from 0 to 90 degrees in steps of 10 degrees and facing south in the solar energy yard of the Institute. The transmittance of various such inclined glasses were measured for normal incidence after every five days and these are graphically represented in Fig(3.11). It can be seen that the transmittance decreases very rapidly with days for a horizontal glass as compared to the vertical one.

For finding out the correction factors for the dirt, certain days (10 days here) are arbitrary fixed after which glass cover is cleaned. The dirt factor or correction factors so obtained are given in fig.(3.12) for various inclined glass sheets. It can be seen from the figure that

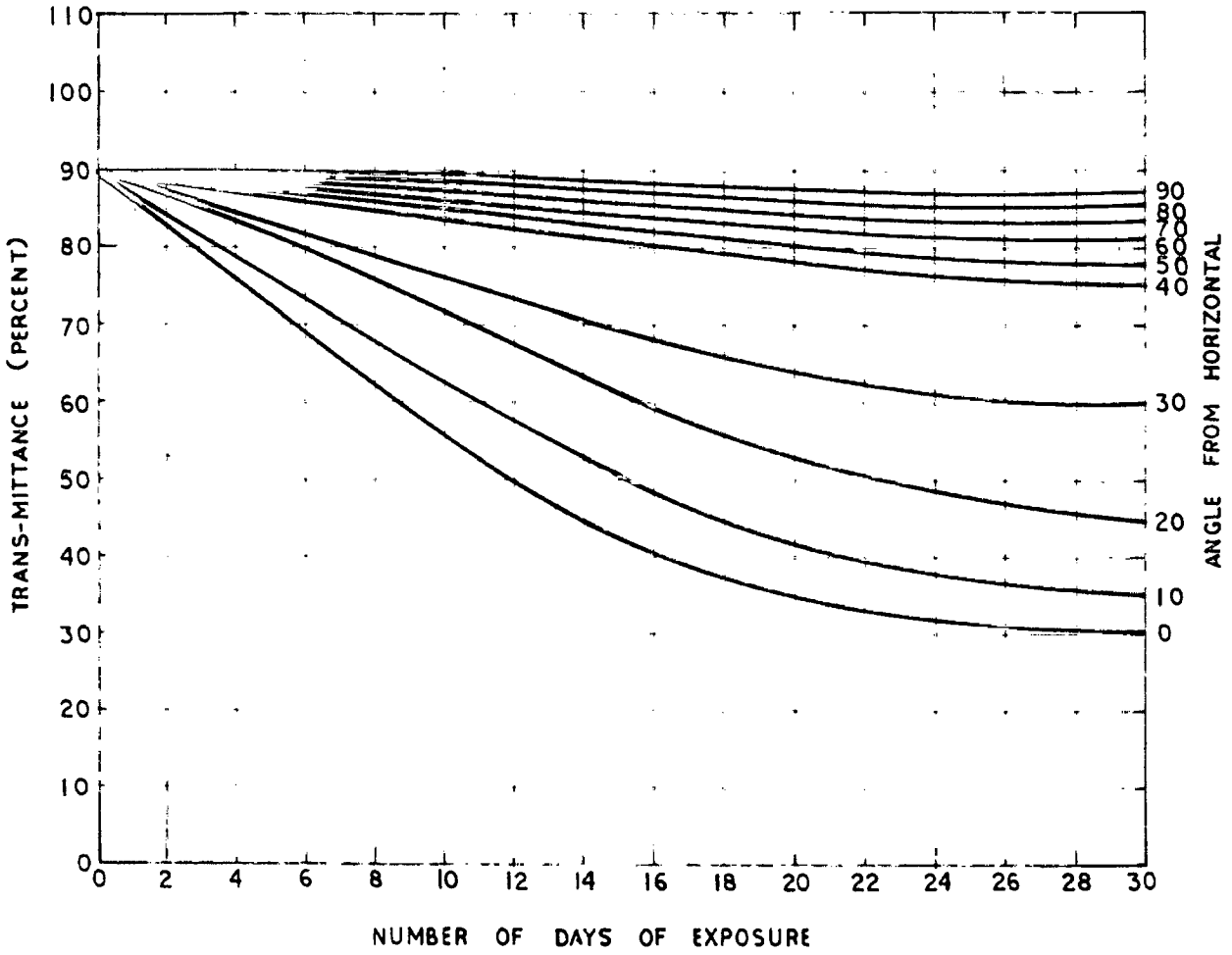

FIG. 3·11 EFFECT OF DIRT ON THE TRANSMITTANCE OF VARIOUS INCLINED GLASS PLATES WITH DAYS OF EXPOSURE

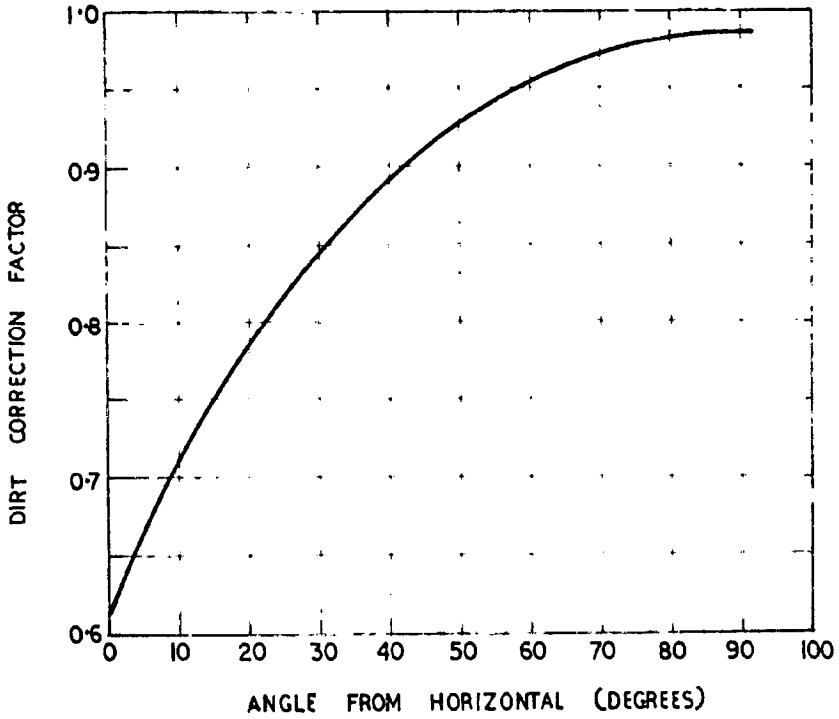

FIG. 3·12 DIRT CORRECTION FACTORS FOR VARIOUS INCLINED GLASS PLATES

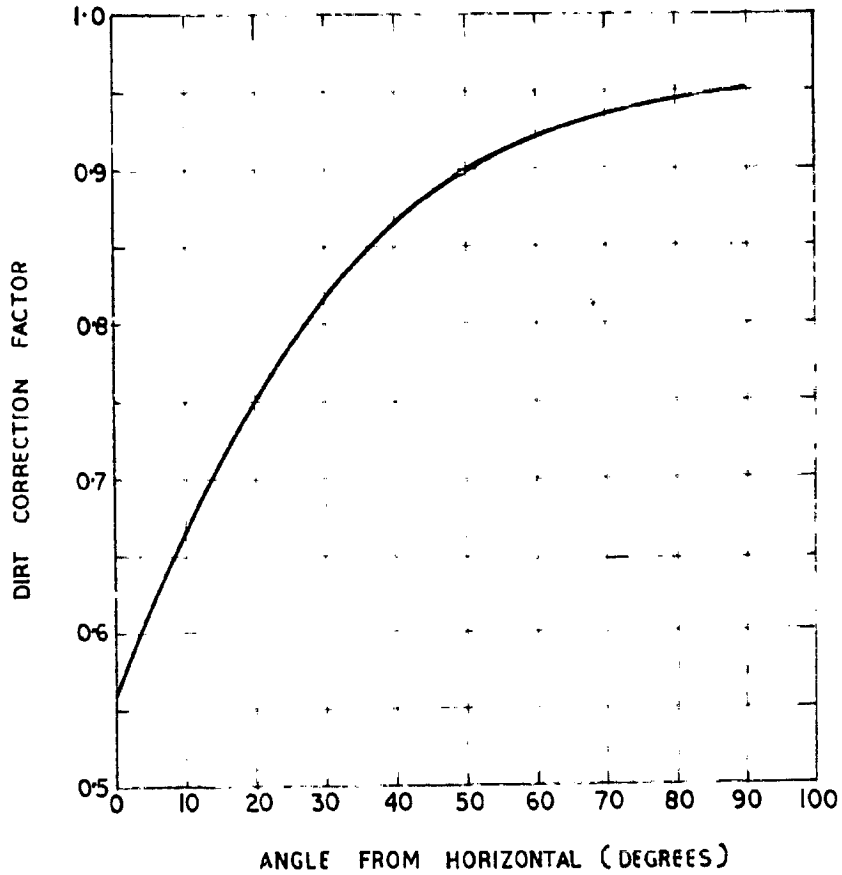

FIG. 3·13 DIRT CORRECTION FACTORS FOR VARIOUS INCLINED PLASTIC FILMS

the correction factor for glass sheet inclined at an angle of 45 degrees from the horizontal should be 0.95 which is a very high value as compared to the value of 0.99 given by Hottel and Woertz.

The same observations are repeated in case of a plastic film. The correction factors for dirt as obtained are plotted in fig 3.13. It can be seen that the correction factor in the case of plastic film is more as compared to glass sheet for any inclination. This may be because of the fact that plastics have a strong tendency to be electrostatic.

3.5 HEAT LOSSES FROM SOLAR ENERGY COLLECTORS:

An important factor in the computation of solar collector performance is the determination of the rate at which heat is lost from the hot absorbing plate. This loss depends on a number of factors, such as (i) temprature of the absorber plate, (ii) the emissivity of collector plate, (iii) temperature of ambient air and sky conditions, (iv) number of glass plates their properties and spacing, (v) insulation property and its thickness on the edges and rear side, (vi) tilt of the collector from horizontal and (vii) wind speed over the absorber.

While deriving the heat balance equations, it has been assumed that the heat absorbed by the glass plate

is negligible as compared to either the heat loss from the absorber plate to the glass or from the glass to the outside air. It has also been assumed that the absorber plate and the glass are at uniform temperatures and the temperature drop across the thickness of the glass plate is negligible. This has been verified by experiments also and will be discussed later.

3.61. Convection Losses from the absorber plate :

The calculation of free convection loss is fairly well established for bodies of regular shape in an infinite space and is adequately dealt with by Mc Adams[10], Richardson and Saunders[11], Brown and Marco[12], Mikheyev[13] and others. Here the problem is complicated since the space is not infinite and heating and cooling takes place very near to each other between absorber plate and glass cover.

The Nusselt number, Nu, responsible for convection loss is given as,

$$Nu = C\,(Gr.\,Pr)^n \qquad \text{---------(3.19)}$$

where Gr = Grashof number = $L^3 g \beta \Delta t / \nu^2$

Pr = Prandtl number = $C_p \mu / K$.

and Nu = Nusselt number = $\frac{h_c L}{K}$

here L = spacing between the plates (metres)

g = acceleration due to gravity (m/sec^2)

β = coefficient of Volumetric expansion of air (per ^{o}C)

ν = Kinematic Viscosity (sq.m/sec).

C_p = specific heat of air (Kcal/Kgm^{o}C)

μ = coefficient of viscosity of air (Kgm-sec/Sqm)

K = thermal conductivity of air (Kcal/m hr^{o}C)

h_c = film heat transfer coefficient (Kcal/m^{2}hr^{o}C)

Fishenden and Saunders has given the values of C and n as 0.15 and 0.25 respectively for vertical air spaces. But it has been shown by Mikheyev by plotting all the available experimental data, that these values fairly remain unchanged with the slope of the surface. Thus the expression

$$Nu = 0.15\ (Gr.Pr)^{1/4} \qquad \text{----------(3.20)}$$

has been used for estimating convective heat losses, from collector plate to glass cover.

If q_c is the rate of free convection loss per unit area of surface having temperature difference Δt, then

$$q_c = h_c.\Delta t \qquad \text{----------(3.21)}$$

$$= 0.15 \frac{K}{L}\left(\frac{L^3 g \beta \rho^2}{\mu^2}\ \frac{C_p \mu}{K}\right)\Delta t^{5/4}$$

putting all these values of K, β, ρ, μ, Cp for air at a mean temperature of about 50^{o}C and L = 0.05 m, we get,

$$q_c = 0.094\ (\Delta t)^{5/4} \qquad \text{----------(3.22)}$$

3.62 Convection losses from the glass surface to atmosphere:

The solar energy collector is generally exposed to atmosphere and the heat losses are dependent on wind conditions. Mikheyev has plotted the experimental values on a chart for forced convection and from this he concluded that for turbulent flow i.e. $Re > 10^5$, the following equation should be used for the computation of convective losses.

$$Nu = 0.032\ Re^{0.80} \qquad \text{--------(3.23)}$$

and for laminar flow i.e. $Re < 10^5$,

$$Nu = 0.66\ Re^{0.50} \qquad \text{--------(3.24)}$$

where $Re = \frac{v l}{\nu}$

v = Velocity of air (m/sec),

l = length of plate (m)

and ν = Kinematic Viscosity (sqm/sec)

But $q_c = h_c \Delta t$

or $q_c = \frac{k}{l} (0.66\ R_e^{0.50} \Delta t)$ ---(3.26)

if $R_e < 10^5$

and $q_c = \frac{k}{l} (0.032\ Re^{0.80} \Delta t)$ ---(3.25)

if $Re > 10^5$

As an example consider a typical collector where glass temperature and air temperatures are 32°C and 21°C respectively. The length of collector is 1.2 m and wind is blowing at a speed of 10 miles/hr or 16 Km/hr.

From the above data we get h_c = 10.06 Kcal/m²hr °C.

3.63 Radiation losses from glass surface to sky:

The loss of heat from the glass surface to the environment by radiation is very complicated. If the mean radiant temperature of the surroundings is T_{MR}, then T_{sky} is given by Brunt[14] equal to

$$T_{sky} = T_a (\epsilon')^{\frac{1}{4}} \qquad \text{--------(3.37)}$$

where ϵ' is the emissivity of the sky and is given as

$$\epsilon' = (a+bp^{\frac{1}{2}}) \qquad \text{-------- (3.38)}$$

where a and b are constants and are found to be

a = 0.56, b = 0.33 for horizontal exposure

and a = 0.39, b = 0.0163 for vertical exposure.

and p = atmospheric partial water vapour pressure (Inches of Hg)

Thus the net radiation exchange between the glass surface and sky is

$$q_r = \epsilon\sigma \left(T_g^4 - T_{sky}^4 \right) \qquad \text{--------(3.39)}$$

where ϵ is the emissivity of the glass plate.

If we consider the dry bulb temperature as 31°C, wet bulb temperature as 18°C and emissivity of glass as 0.88 then

$$q_r = 129.31 \text{ Kcal/m}^2 \text{ hr}$$

or Radiation Coefficient $h_r = \dfrac{q_r}{(t_g - t_{mR})}$

$$= 4.7 \text{ Kcal/m}^2 \text{ hr}^\circ\text{C}.$$

Thus the total one side heat loss coefficient (h_o) is the sum of convective and radiative heat transfer coefficient.

Thus

$$h_o = h_c + h_r$$

$$= 30.70 \text{ Kcal/m}^2 \text{ hr}^\circ\text{C}.$$

3.34 Conduction losses from the absorber plate :

The conduction loss takes place from the rear side of the collector which is not exposed to solar radiation. This loss is usually known as rear loss, q_{rear}. If insulation is provided adequately, then this loss can practically be eliminated. The rate of loss of heat per unit of area can be computed from the formula :

$$q_{rear} = \frac{K}{d} (t_p - t_b) \qquad \text{------(3.30)}$$

where K = mean thermal conductivity of the insulating material (Kcal/m hr$^\circ$C)

t_p = temperature of the plate ($^\circ$C)

t_b = temperature of the back of the frame ($^\circ$C)

d = thickness of insulation (m)

But in practical calculations the temperature of the back of the frame may be assumed to be the temperature of air, t_a, then

$$q_{rear} = \frac{K}{d} (t_p - t_a) \qquad \text{------(3.31)}$$

This heat loss is usually negligible as compared to the upward heat loss.

3.03 Radiation losses between the absorber plate and glass plate.

The radiation loss per unit of area per unit of time from a grey surface when surrounded by a large enclosure is given as

$$q_p = \epsilon_p \sigma (T_p^4 - T_o^4) \qquad \text{----------(3.33)}$$

where ϵ_p = emissivity of the surface,

T_p = absorber plate temperature (^oK)

T_o = temperature of enclosure (^oK)

σ = Stephan-Boltzmann Constant

= (4.07×10^{-8} Kcal/m^2 $hr\,^oK^4$)

when a body is surrounded by an envelope of the size of the body, then it becomes

$$q_p = \epsilon_e \sigma (T_p^4 - T_o^4) \qquad \text{--------(3.333)}$$

where ϵ_e = effective emissivity of the body

$$= \frac{1}{\frac{1}{\epsilon_p} + \frac{1}{\epsilon_q} - 1} \qquad \text{------(3.34)}$$

where ϵ_p = emissivity of the body

and ϵ_q = emissivity of the glass envelope.

In the present case, the glass is used as an envelope so $\epsilon_q = 0.88$ and plate is painted with lamp black with $\epsilon_p = 0.93$. So effective emissivity becomes

$\epsilon_e = 0.84$

and for a selective surface where $\epsilon_p = 0.2$, the effective emissivity is

$\epsilon_e = 0.20$.

3.63 Overall losses from the collector plate :

The loss from the absorber plate to the first glass cover is given as :

$$q = C\left(t_p - t_{g1}\right)^{5/4} + \frac{\sigma\left(T_p^4 - T_{g1}^4\right)}{\frac{1}{\epsilon_p} + \frac{1}{\epsilon_g} - 1} \qquad \text{---(3.35)}$$

Similarly from the first glass to the next glass will be

$$q = C\left(t_{g1} - t_{g2}\right)^{5/4} + \frac{\sigma\left(T_{g1}^4 - T_{g2}^4\right)}{\frac{2}{\epsilon_g} - 1} \qquad \text{---(3.36)}$$

Similar relations can be written upto the top glass plate. At the outermost cover(nth sheet) , the heat loss would be

$$q = h_a\left(t_{gn} - t_a\right) + h_r\left(t_{gn} - t_a\right) \qquad \text{---------(3.37)}$$

The values of the constants C , h_a, h_r, K, d, ϵ_p , ϵ_g and σ are already discussed. If there are n glass covers, there would be (n+1) such equations.

The heat loss from the absorber plate can be reduced as :

i) by using additional glass cover

ii) by using spectrally selective surface.

iii) by evacuating the space between the plate and glass.

Generalised relationships between the term ϵ_p and the overall heat loss coefficient U_L have been worked out by solving the above equations by covering the practical range of the variables.

The values of overall heat loss coefficient are computed as

$$U_L = \frac{q}{(t_p - t_a)} \qquad \text{-------(3.33)}$$

for a single and double glass cover for various values of t_p and t_a and are shown in fig (3.14). In the above calculations the absorber plate is assumed to have an emissivity of 0.95. As it is also a practice to use a selective black coat on the absorber plate the values of U_L for a single glass cover and plate having emissivity as 0.2 are also shown computed and are presented in the same figure.

3.6. HEAT TRANSFER THROUGH FINNED SURFACES.

Heating surfaces are finned in order to intensify heat transfer. Fins may be of different sizes and shapes depending on the type of use. Consider a simple fin of length (2L) of uniform thickness (M) attached to two tubes as shown in fig (3.15). The thermal conductivity of the material of the fin is K. The temperature of the fin varies along the length i.e. $t = f(x)$. Let the temperature of the fin base $t = t_b$ (it is in excess over the surrounding temperature t_a). Let the temperature at distance along the fin be t_p (which is also excess over t_a). Consider an

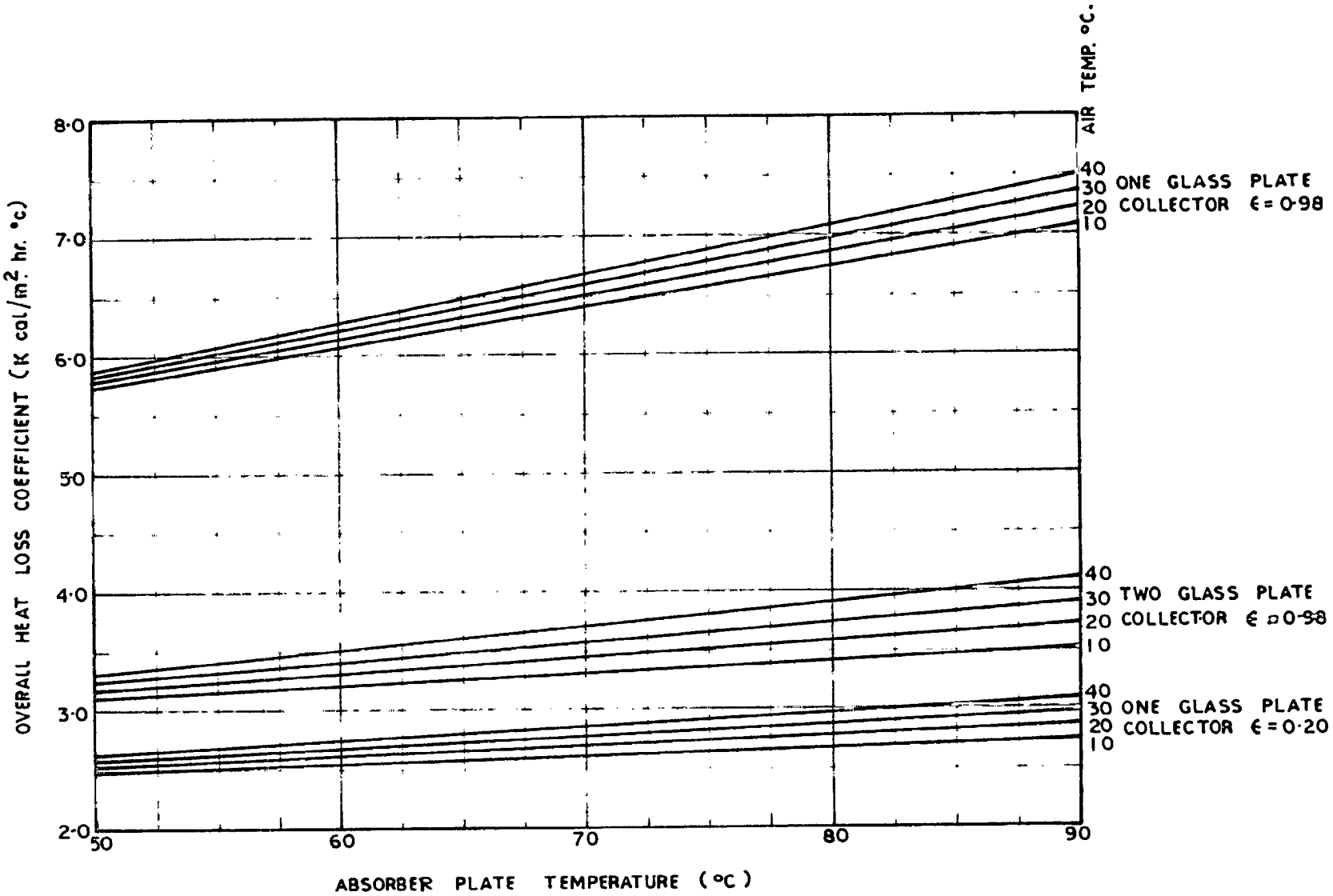

FIG. 3·14 OVER ALL HEAT LOSS COEFFICIENT

$\alpha = 0.95$

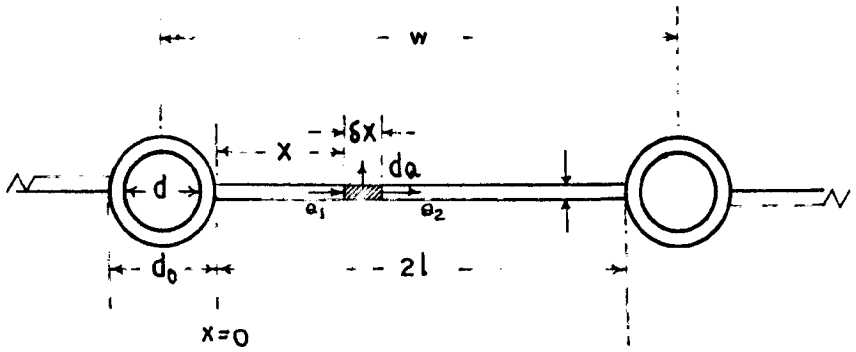

FIG. 3·15 HEAT EXCHANGER WITH A STRAIGHT FIN.

element of the fin of length δx (fig 3.15) and of unit depth normal to paper. Here to have assumed (i) steady state heat flow (ii) one dimensional heat conduction in the fin (iii) uniform outside temperature, and (iv) constant film heat transfer coefficient (h).

If dQ is the heat loss from the element, then it is seen that

$$dQ = Q_1 - Q_2$$

From Fourier's law

$$Q_1 = -KA \frac{dt_f}{dx}$$

and $$Q_2 = -KA \frac{d}{dx}\left(t_f + \frac{dt_f}{dx}\delta x\right)$$

so heat loss to the surroundings is

$$dQ = -KA \frac{dt_f}{dx} + KA \frac{d}{dx}\left(t_f + \frac{dt_f}{dx}\delta x\right)$$

$$= KA \frac{d^2 t_f}{dx^2}\delta x \qquad \text{-------(3.39)}$$

But dQ can also be written as

$$dQ = h\,\delta x\, t_f \qquad \text{-------(3.40)}$$

or $$KA \frac{d^2 t_f}{dx^2} = h\,\delta x\, t_f$$

or $$\frac{d^2 t_f}{dx^2} - \frac{h}{KA} t_f = 0$$

or $$\frac{d^2 t_f}{dx^2} - a^2 t_f = 0 \qquad \text{-------(3.41)}$$

where $a = \sqrt{\frac{h}{KA}}$ = Constant

The solution to equation (3.41) is

$$t_f = C_1 \cosh ax + C_2 \sinh ax \quad \text{-------(3.42)}$$

The boundary conditions are

$$at\ x = 0 \quad ; \quad t_f = t_b$$

$$at\ x = L \quad ; \quad \frac{dt_f}{dx} = 0 \quad \text{(neglecting heat transfer from the middle of fin)}$$

we get $C_1 = t_b$

and $C_2 = -t_b \frac{\sinh aL}{\cosh aL}$

Thus the temperature distribution is given as,

$$t_f = t_b \cosh ax - t_b \frac{\sinh aL}{\cosh aL} \sinh ax$$

$$\text{or} \quad t_f = t_b \frac{\cosh a(L-x)}{\cosh aL} \quad \text{----------(3.43)}$$

Now the flow of heat into the fin at $x = 0$ is given by

$$q_0 = -2KH\left(\frac{dt_f}{dx}\right)_{x=0}$$

$$= -2KH\, t_b \frac{d}{dx}\left(\frac{\cosh a(L-x)}{\cosh aL}\right)_{x=0}$$

$$= 2aKH\, t_b \left(\frac{\sinh a(L-x)}{\cosh aL}\right)_{x=0}$$

$$= 2aKH\, t_b \tanh aL \quad \text{--------(3.44)}$$

Now the efficiency of the fin (η) is defined as the ratio of the heat actually transferred through the fin to the heat that would be transferred by convection

or radiation from the base area if the fin was removed.

From equation (3.44) the fin efficiency is given by

$$F = \frac{2\,a\,K\,H\,t_b \tanh a\,L}{2b\,L\,t_b}$$

$$\text{or} \quad F = \frac{a\,K\,H \tanh a\,L}{b\,L}$$

$$= \frac{a\,K\,H}{a^2\,K\,H\,L} \tanh a\,L$$

$$\text{or} \quad F = \frac{\tanh aL}{a\,L} \qquad \text{-----(3.45)}$$

where $a = \sqrt{b/KH}$

Here $b = U_L$ = overall heat loss coefficient from fin to air.

$$\text{So} \quad a = \sqrt{U_L/KH} \qquad \text{-----(3.46)}$$

The temperature at the centre line of the fin (i.e. $x = L$) will be from equation (3.43) as,

$$t_f \text{ centre} = \frac{t_b}{\cosh a\,L} \qquad \text{------(3.47)}$$

The value of L can be put in terms of the spacing S (centre to centre) as

$$S = 2L + d_o$$

$$\text{or} \quad L = \frac{S - d_o}{2} \qquad \text{------(3.48)}$$

The values of fin efficiency for various spacings for Copper, Aluminium and steel fin of three thicknesses 24, 26 and 28 gauges for three values of U_L (2.6, 3.4 and 6.2 Kcal/ m^2 hr ^oC) for a tube of 10 mm outside diameter are computed and are

shown in fig (3.16). It is seen that as the tube spacing increases the fin efficiency decreases . It is also seen that a fin of high conductivity material gives high fin efficiency.

3.7 PLATE OR ANNULAR FINS:

Consider a simple fin as shown in fig (3.16). Suppose a fluid of specific heat (C_p) flows in tube at temperature (t) with mass flow rate (m). The heat balance equations are

$$C_p \frac{dt}{dx}\,\delta x = h\,\pi\, d\,\delta x (T' - T) \qquad \text{-----(3.60)}$$

$$= \frac{\pi d k' (T'' - T')}{m}\,\delta x \qquad \text{-----(3.61)}$$

$$= K_b \frac{(b\,\delta x)}{y} (T_b - T'') \qquad \text{-----(3.62)}$$

$$= (b \times 2L \times 1)\,\delta x \left[\frac{q_A}{A} - U_L (T_b - T_a)\right] \qquad \text{-----(3.63)}$$

where δ = bond thickness ,

T' and T'' = inside and outside tube temperatures respectively,

h = tube inside film heat transfer coefficient,

t_a = air temperature,

do = tube outside diameter,

m = thickness of tube,

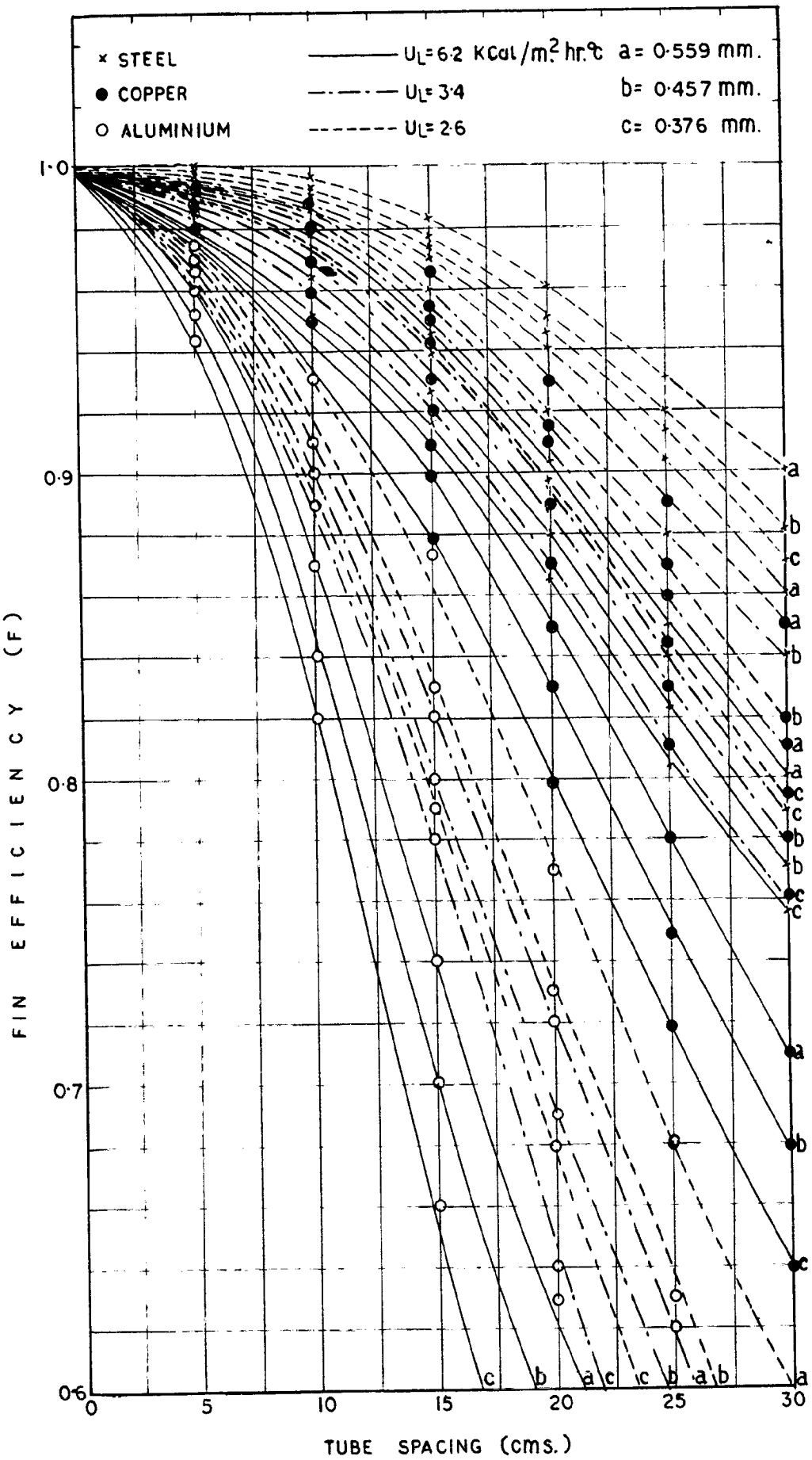

FIG. 3·16 EFFECT OF TUBE SPACING, MATERIAL AND OVERALL HEAT LOSS COEFFICIENT ON THE FIN EFFICIENCY

K' = thermal conductivity of tube material

and K_b = thermal conductivity of bond material.

From equation (3.60)

$$T' = \frac{WC_p \frac{dT}{dx}}{h \pi d} + T$$

On putting this value of T' in equation (3.61), T'' is given as

$$T'' = \frac{mWC_p \frac{dT}{dx}}{\pi d K'} + \frac{WC_b \frac{dT}{dx}}{h \pi d} + T$$

On putting this value of T'' in equation (3.63), T_b is given as

$$T_b = \frac{(1-m)WC_p \frac{dT}{dx}}{K_b b} + \frac{m WC_p \frac{dT}{dx}}{\pi d K'} + \frac{WC_b \frac{dT}{dx}}{h \pi d} + T$$

on putting this value of T_b in equation (3.63), we get

$$WC_p \frac{dT}{dx} = (b+2LP)\left[\frac{q_A}{A} - U_L\left\{\frac{(1-m)WC_p \frac{dT}{dx}}{K_b b} + \frac{m WC_p \frac{dT}{dx}}{\pi d K'} + \frac{WC_p \, dT/dx}{\pi d h} + T - T_a\right\}\right]$$

$$\text{or } WC_p \frac{dT}{dx}\left[1 + \frac{(b+2LP)(1-m)U_L}{K_b b} + \frac{(b+2LP)mU_L}{\pi d K'} + \frac{(b+2LP)U_L}{\pi d h}\right]$$

$$= (b+2LP)\left[\frac{q_A}{A} - U_L (T-T_a)\right]$$

$$\text{or} \quad W C_b \frac{dT}{dx} = \frac{\frac{S}{A} - U_L (T - T_a)}{\frac{1}{(b + \pi D) F} + \frac{W U_L}{K_b b} + \frac{m U_L}{\pi d K'} + \frac{U_L}{\pi d h}}$$

$$= F_p \left[\frac{S}{A} - U_L (T - T_a) \right] \qquad \text{------(3.64)}$$

$$\text{where} \quad F_p = \frac{1}{\frac{U_L}{\pi d h} + \frac{U_L}{\pi d K'/_m} + \frac{U_L}{C} + \frac{U_L}{(b + \pi D F) U_L}}$$

$$\text{where} \quad C = \frac{K_b b}{S} = \text{bond conductance.}$$

If W is the spacing between the tubes centre to centre then

$$F_p = \frac{1}{\frac{W U_L}{\pi d h} + \frac{W U_L}{\pi d K'/_m} + \frac{W U_L}{C} + \frac{W U_L}{(b + \pi D F) U_L}}$$

$$\text{----------(3.65)}$$

The plate efficiency factor (F_p) can be defined from equation (3.64) as the ratio of actual heat collected to that one that would have been collected if the average water temperature was the same as the average plate temperature. As has been seen that it is mainly dependent upon the geometry of the collector surface, and hence is a useful design constant for collector performance evaluation.

From equation (3.65) we see that (F_p) is a function of the tube spacing (U), tube outer diameter (do) and its thickness (n), tube thermal conductivity (K'), plate thickness (H), plate conductivity (K), bond width (b), bond conductance (C), overall heat loss coefficient (U_L) and the heat transfer coefficient (h) from the inner surface of the tube to the fluid inside the tube. Here in our case as shown in figure the bond width (b) is taken as the outer diameter of the tube (do) and a single glass cover is assumed with a non-selective paint. The values of the constants used for the computation of F_p are as follows

$$C = 22.0 \text{ Kcal/m hr}^{\circ}\text{C}.$$
$$U_L = 0.2 \text{ Kcal/m}^2 \text{ hr}^{\circ}\text{C}.$$
$$h = 300.0 \text{ Kcal/m}^2 \text{ hr}^{\circ}\text{C}.$$

The value of U_L has been discussed earlier. The values of C and h and their dependence on operating conditions are determined by the author by separate experiments.

For the purpose of comparison their dependence upon climatic and operating conditions are neglected. The following combinations and geometry of materials have been tried with the help of 1620 digital computer :

W = 2.3, 5.0, 7.5, 10.0, 12.5, 15.0 cms.

d = 12.5, 19.0, 25.0 mm (nomial diameters of C.I.pipes)

M = 0.66, 0.45, 0.37 cm.

Plate material=Copper, Aluminium and G.I.sheet.

The computed values of plate efficiency factors for various combinations are shown in Table 2. It can be seen that for maximumefficiency, spacing should be less, diameter should be large, plate should be thick and its material should be of high thermal conductivity such as Copper.

3.8. FLOW PASSAGE

Suppose two parallel plates of length (L) and of width unity perpendicular to the plane of the paper as shown in fig (3.17). Suppose it is exposed to solar radiation. Water enters at x = 0 at temperature t_1 and leaves it at x = L at temperature t_2. Let us consider an element of length δx at a distance x. The temperature of water at its two sides are twx and $t_{wx} + \frac{d}{dx}(t_{wx})\,\delta x$. Let the temperature of plate at x = 0 is t_{px} and of air t_a.

Now useful heat collected at a distance of x is given as

$$q_{ux} = q_A - U_L (t_{px} - t_a) \qquad \text{--------(3.56)}$$

Where q_A = absorbed energy,

and U_L = overall heat loss coefficient from the plate to the air.

G.I. Tube diameter mm	CEG. 12.0
25	0.9484
	0.9450
	0.9342
	0.9342
	0.9264
	0.9075
	0.8194
	0.8121
	0.7602
19	0.9156
	0.9131
	0.8986
	0.8960
	0.8930
	0.8880
	0.7969
	0.7706
	0.7195
12.5	0.9004
	0.8734
	0.8645
	0.8649
	0.8552
	0.8357
	0.7675
	0.7353
	0.6309

This useful heat goes to the fluid flowing within. So

$$q_{ux} = h_c (t_{px} - t_{vx}) \qquad \text{-------(3.57)}$$

where h_c = inside surface coefficient.

Eliminating t_{px} between equation (3.53) and (3.57), we get

$$q_{ux} = \frac{h_r}{h_c + U_L} \left[q_A - U_L (t_{vx} - t_a) \right] \qquad \text{-------(3.58)}$$

The average rate of useful heat collected for the entire length L is

$$q_u = \frac{1}{L} \int_0^L q_{ux}\, dx$$

$$= \frac{h_r}{h_c + U_L} \left[q_A - U_L \left(\frac{1}{L} \int_0^L t_{vx}\, dx - t_a \right) \right]$$

But $\frac{1}{L} \int_0^L t_{vx}\, dx = t_v$ (average water temperature)

or $q_u = \frac{h_r}{h_c + U_L} \left[q_A - U_L (t_v - t_a) \right]$

But according to the definition of fin efficiency (F_p)

$$F_p = \frac{h_r}{h_c + U_L} \qquad \text{-------(3.59)}$$

Now equation (3.60) can be written as

$$q_{ux} = F_p \left[q_A - U_L (t_{vx} - t_a) \right] \qquad \text{-------(3.60)}$$

differential of this is

$$d\,q_{ux} = -F_p\,U_L\,dt_{ux} \qquad \text{-------(3.61)}$$

Now if G is mass flow rate (Kgm/m^2hr) and L is the area (m^2) of plate, then the mass flow rate over the entire area is GL (Kgm/hr).

Hence the useful heat gain associated with the area $\delta x \times 1$ ($= \delta x$) may be equated to the gain to the fluid, as it flows under that area

$$q_{ux}\,\delta x = G\,C_p L\,\frac{dt_{ux}}{dx}\,\delta x \qquad \text{-----(3.62)}$$

Dividing (3.61) by (3.62), we get

$$\frac{q_{ux}}{q_{ux}} = -\frac{F'_{UL}}{G\,C_p L}\,d\,x \qquad \text{----(3.63)}$$

Integrating this equation and applying the boundry condition as $x = 0$, $q_{ux} = q_{uo}$, we get

$$q_{ux} = q_{uo}\,e^{-\frac{F_p\,U_L}{GC_pL}\,x}$$

The average useful heat collection is given as,

$$q_u = \frac{1}{L}\int_0^L q_{ux}\,dx$$

$$= \frac{q_{uo}}{L}\int_0^L e^{-\frac{F_p\,U_L}{GC_pL}\,x}\,dx$$

$$= q_{uo} \frac{CC_p}{F_p U_L} \left(1 - e^{-\frac{F_p U_L}{CC_p}}\right) \quad \text{---(3.64)}$$

From equation (3.60), at $x = 0$, $q_{ux} = q_{uo}$ and $t_{ux} = t_1$, we get

$$q_{uo} = F_p \left[q_A - U_L (t_1 - t_a)\right]$$

putting this value in equation (3.64), we get

$$q_u = F_p \frac{CC_p}{F_p U_L} \left(1 - e^{\frac{-F_p U_L}{CC_p}}\right) \left[q_A - U_L (t_1 - t_a)\right]$$

------(3.65)

Here t_1 is the entering fluid temperature.

or

$$q_u = F_R \left[q_A - U_L (t_1 - t_a)\right] \quad \text{------(3.66)}$$

where F_R is known as the heat removal efficiency factor and can be defined with the help of equation (3.66).

$$F_R = F_p \frac{CC_p}{F_p U_L} \left(1 - e^{\frac{-F_p U_L}{CC_p}}\right) \quad \text{------(3.67)}$$

$$= F_p F_f \quad \text{------(3.68)}$$

where

$$F_f = \frac{CC_p}{F_p U_L} \left(1 - e^{-F_p U_L / CC_p}\right) \quad \text{------(3.69)}$$

= flow rate factor. ------(3.70)

The factor F_R is found of much use and its importance shall be discussed in chapter 4.

3.9. OPTIMIZATION OF TILT:

The maximum solar heat is collected if the flat-plate collector is kept always normal to the sun rays which requires a costly and cumbersome heliostatic mounting. An alternative for collecting more solar heat is to find an average optimum tilt of the collector for any desired month of the year. Two methods are available in the literature for the determination of optimum tilt for flat-plate collector. Baumann[16] experimentally determined the performance of collectors in cambridge, tilted southward at various angles and with two and three glass-plates. Here no general formula could be made for other cities and time of the year. The another approach[17] is to assume a constant atmospheric transmittance of unity and no diffused radiation, and to evaluate the resultant total incidence of radiation on a surface of specified tilt for a specified time of year.

In the method developed here the effect of direct and diffused solar radiation and the variation of transmittance of glass cover with angle of incidence is considered. The measured value of direct and diffused radiation and transmittance of glass cover are used. The method is described in the following steps :

(1) Total radiation received by a collector:

The total radiation received by a tilted collector

is the sum of direct color radiation (I_{Dt}) and the diffused color radiation (I_{dt}).

Those are given as :

$$I_{Dt} = (\tau\alpha)_D \, R_D \, (I_{Th}-I_{dh}) \qquad \text{--------(3.71)}$$

and $$I_{dt} = (\tau\alpha)_d \, R_d \, I_{dh} \qquad \text{--------(3.72)}$$

where $(\tau\alpha)_D$ and $(\tau\alpha)_d$ = effective transmittance-absorptance product for direct and diffused solar radiation respectively.

R_D and R_d = Conversion factor for direct and diffused solar radiation respectively.

and I_{Th} and I_{dh} = Hourly total and diffused solar radiation on horizontal surface respectively.

All the above factors are highly dependent on the angle of incidence of sun's rays at any time and the atmospheric conditions. For simplicity, mean monthly average hourly values of (I_{Th}) and (I_{dh}) can be used in equation (3.71) and (3.72). It has been shown in chapter (7) that for a south facing surface tilted at an angle (β) to the horizontal, the expressions for R_D and R_d are given by

$$R_D = \frac{\cos\theta_t}{\cos\theta_h} \qquad \text{--------(3.73)}$$

and $$R_d = \frac{(1+\cos\beta)}{2} \qquad \text{--------(3.74)}$$

where

$\cos\theta_t$ = Cosine of the angle of incidence on tilted surface

= $\cos(L-\beta)\cos\delta\cos U + \sin(L-\beta)\sin\delta$ ----------(3.76)

and $\cos\theta_h$ = Cosine of the angle of incidence on horizontal surface

= $\cos L\cos\delta\cos U + \sin L\sin\delta$ ----------(3.76)

where

L = latitude of place,

δ = declination

and U = hour angle from solar noon.

Substituting all these values in equation (3.71) and (3.73), the total radiation on tilted surface (I_{Tt}) becomes :

$$I_{Tt} = I_{bt} + I_{dt}$$

$$= I_{Th}\left[(\tau\alpha)_b \frac{\cos\theta_t}{\cos\theta_h}\left(1-\frac{I_{dh}}{I_{Th}}\right)+(\tau\alpha)_d\left(\frac{1+\cos\beta}{2}\right)\frac{I_{dh}}{I_{Th}}\right]$$

----------(3.77)

(ii) EXPRESSION FOR OPTIMUM TILT:

The optimum tilt will be given by the value of β for which the first derivate of (I_{Tt}) with respect to β vanishes. Assuming that the absorptivity of black paint is invariant with respect to angle of incidence, $(\tau\alpha)_b$

versus $(1/\cos\theta_t)$ curve has been worked out. This straight line curve is represented by the equation

$$(\tau\alpha)_D = 0.88 - \frac{0.115}{\cos\theta_t} \qquad \text{-----(3.78)}$$

For a uniform sky, following Hottel and Woertz[9], the value of $(\tau\alpha)_d$ for diffused radiation is taken corresponding to an incident angle of 55^0, and given by

$$(\tau\alpha)_d = 0.72 \qquad \text{------(3.79)}$$

Substituting equations (3.78) and (3.79) in equation (3.77), one gets for a single glass cover collector in the tropics,

$$I_{Tt} = I_{Th}\left[\left(\frac{0.88\cos\theta_t - 0.115}{\cos\theta_h}\right)\left(1 - \frac{I_{dh}}{I_{Th}}\right) + 0.36\right.$$

$$\left.(1+\cos\beta)\frac{I_{dh}}{I_{Th}}\right] \qquad \text{------(3.80)}$$

using equations (3.76) and (3.79) in equation (3.80), and maximizing I_{Tt} with respect to β, one gets the expression for optimum value of the tilt (β_o) as,

$$\beta_o = \tan^{-1}\left[\left(1 - \frac{I_{dh}}{I_{Th}}\right)\frac{(\sin L\cos\delta\cos\omega\cos L\sin\delta)}{\left\{1-0.62\left(\frac{I_{dh}}{I_{Th}}\right)\cos\theta_h\right\}}\right]$$

$$\text{------(3.81)}$$

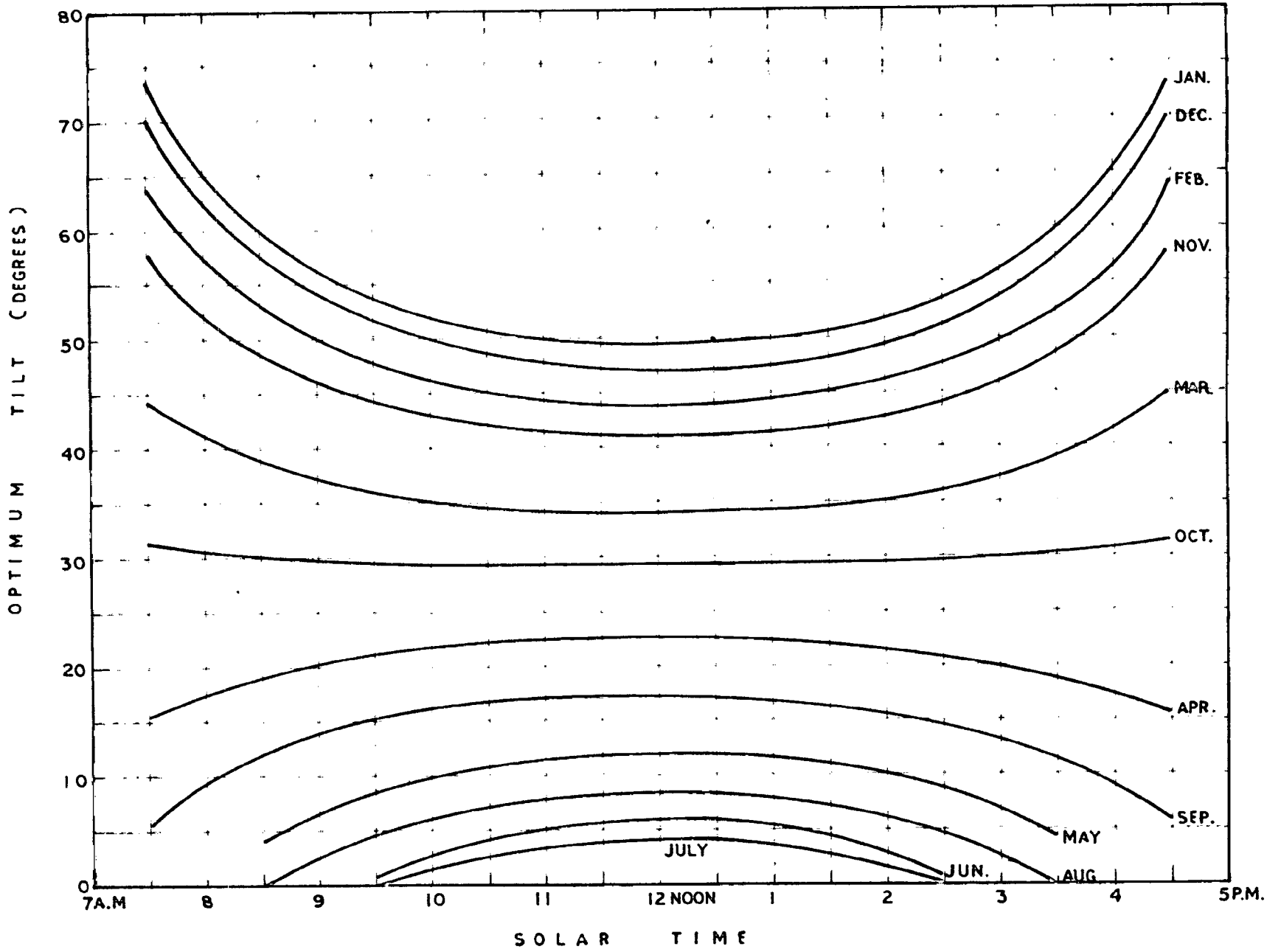

FIG. 3-18 OPTIMUM TILT CURVES FOR FLAT PLATE COLLECTORS AT DELHI

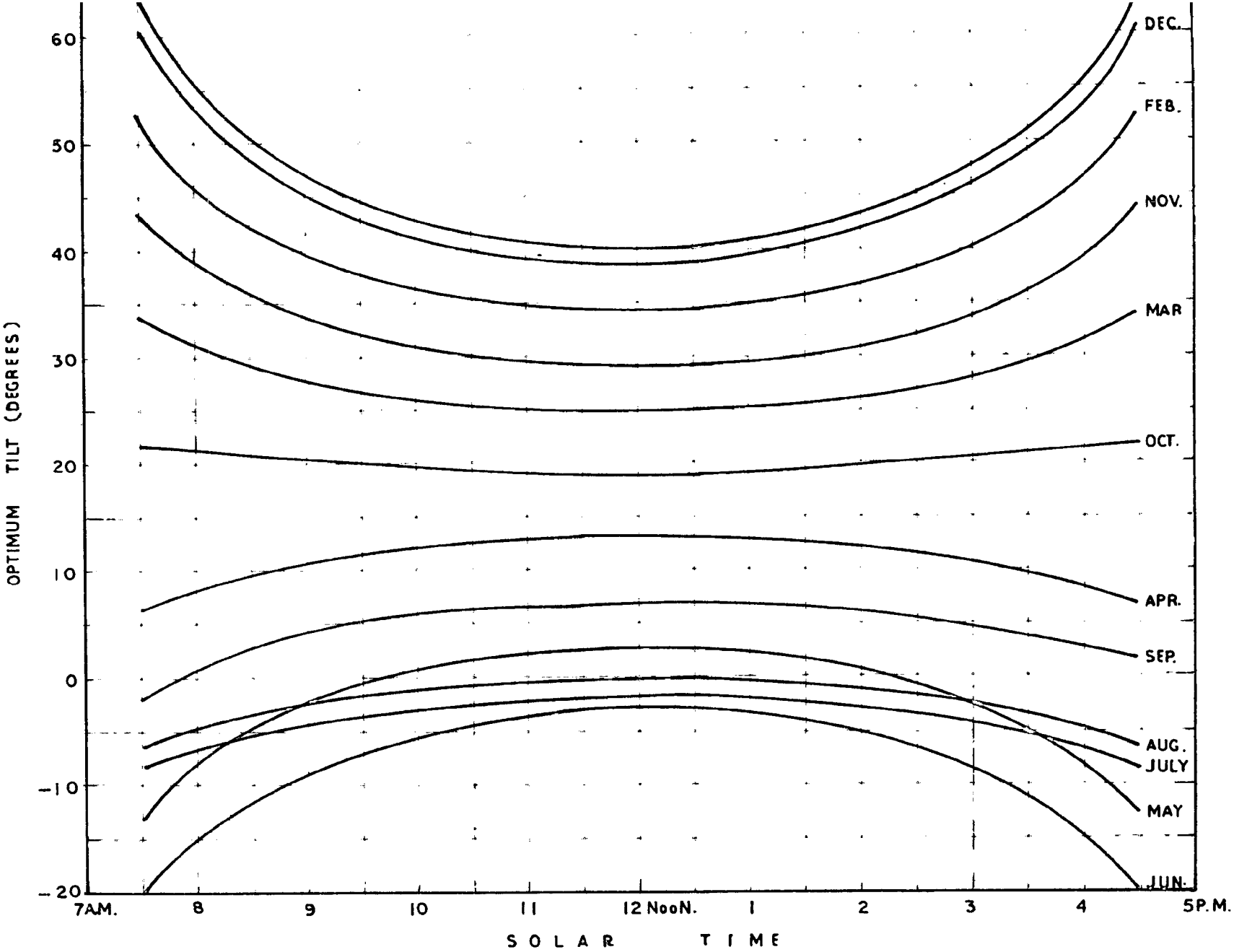

FIG. 3·19 OPTIMUM TILT CURVES FOR FLAT PLATE COLLECTORS AT POONA

(iii) Determination of Optimum tilt:

On examining equation (3.01), one finds that β_o can be determined for any place, time and month if the latitude (L), hour angle (H), solar declination (δ) and the corresponding values of (I_{dh}/I_{Th}) are known. The values of L, H, and δ can be taken from the geographical atlas and nautical almanac. If the measured values of I_{dh} and I_{Th} are not available for any place then these can be determined by the method described in Chapter (2). Here the measured values of I_{dh} and I_{Th} are used in computation of optimum tilt for Delhi and Poona. The optimum tilt curves for various months for Delhi and Poona are shown in fig (3.18) and (3.19) respectively. The results for Delhi ($L = 28^0 35'$) are slightly lower when compared to results for 30^0 latitude given by Souka and Safwat[18]. This is primarily because the results of Souka and Safwat are for an assumed cloarness number of unity, which does not always occur in practice.

It can be easily seen from the optimum tilt curves that for the average winter and summer performance the optimum tilts are (latitude angle + 15^0) and (latitude angle-15^0) respectively. For the year round performance the best tilt is 0.9 times the latitude angle.

CHAPTER-4

SOLAR WATER HEATING

CHAPTER-4

4.1. INTRODUCTION

During the last two decades there has been unprecedented progress in the field of development of solar water heating for domestic use. It has not been widely accepted in developing countries because of its high initial cost, although it has practically no fuel costs and can be proved economical, in the long run, especially when compared with conventional electrical heating.

Solar water heaters have become popular in Japan, Israel, Australia, South Africa and Latin American countries. Solar heaters are commonly divided into three types, based on the size and usage. They are :

a) Domestic solar water heater: In this type the storage tank and absorbers are separate and the water is circulated by natural circulation. These are popular in Israel[1], Australia[2] and Latin America.

b) Large size solar water heater: These heaters are developed for coping with larger demand of hostels, hotels and hospitals and other community uses. These heaters are under development in Australia[3].

c) Built-in storage type solar water heater: In this type the storage tank and the absorber are integrated as a single unit with a view to reduce the cost. Different versions are in vouge and about two million of solar water heater of this type are reported to

in use in Japan[4]. Such units are also developed in South Africa[5] for low income group people. There is a large scope for economic solar water heating in India too. However, no systematic study on the design and optimisation of various parameters and cost has been carried out so far. With this in view all the above three types of solar water heaters are developed by the author, and optimised in terms of cost and efficiency under Indian climates.

4.2 OPTIMISATION OF COLLECTOR:

So far as the water heating is concerned two types of flat-plate collectors are in common use.

1. Corrugated sheet type flat-plate collector,

and 2. tube in plate type flat-type collector.

Though the corrugated type[6] of flat-plate collector has the higher efficiency, it suffers from many other defects such as bulging under high hydrostatic pressure, leaking through the rivets and comparatively shorter life. Some of these defects have been overcome by the author and it is discussed in a special publication of C.S.I.R., Roorkee[7]. Different types of tube in plate-type collectors are used and are discussed here. These are mainly :

1. Soldered bond type,

and 2. Contact bond type.

The soldered bond type is expensive, its bond may crack with time due to heating and cooling[6]. There is also considerable difficulty in soldering tubes to a thin sheet and whole of the frame with plate has to be discarded[1] if there is scale formation in the tubes. Contact bond type is therefore preferred. The displant is a wire wound type developed here and shown in fig.4.1.

As has been seen (chapter 3) that the plate efficiency factor F_p would be large if spacing between the tube is less, diameter of tube is large, plate is thick and is of high conductivity material such as copper. But such an optimisation would result in an uneconomical absorber. So the problem is to find out the sheet thickness and tube spacing which would give the maximum ratio of efficiency per unit of capital cost for any particular choice of sheet material. If C is the cost of collector per unit of area and F_p is its efficiency then C/F_p should be minimum.

By experience the cost can be broken into four components as follows :

(a) a fixed cost per m^2 of collector, which includes framing, insulation, glass, supports, painting etc.

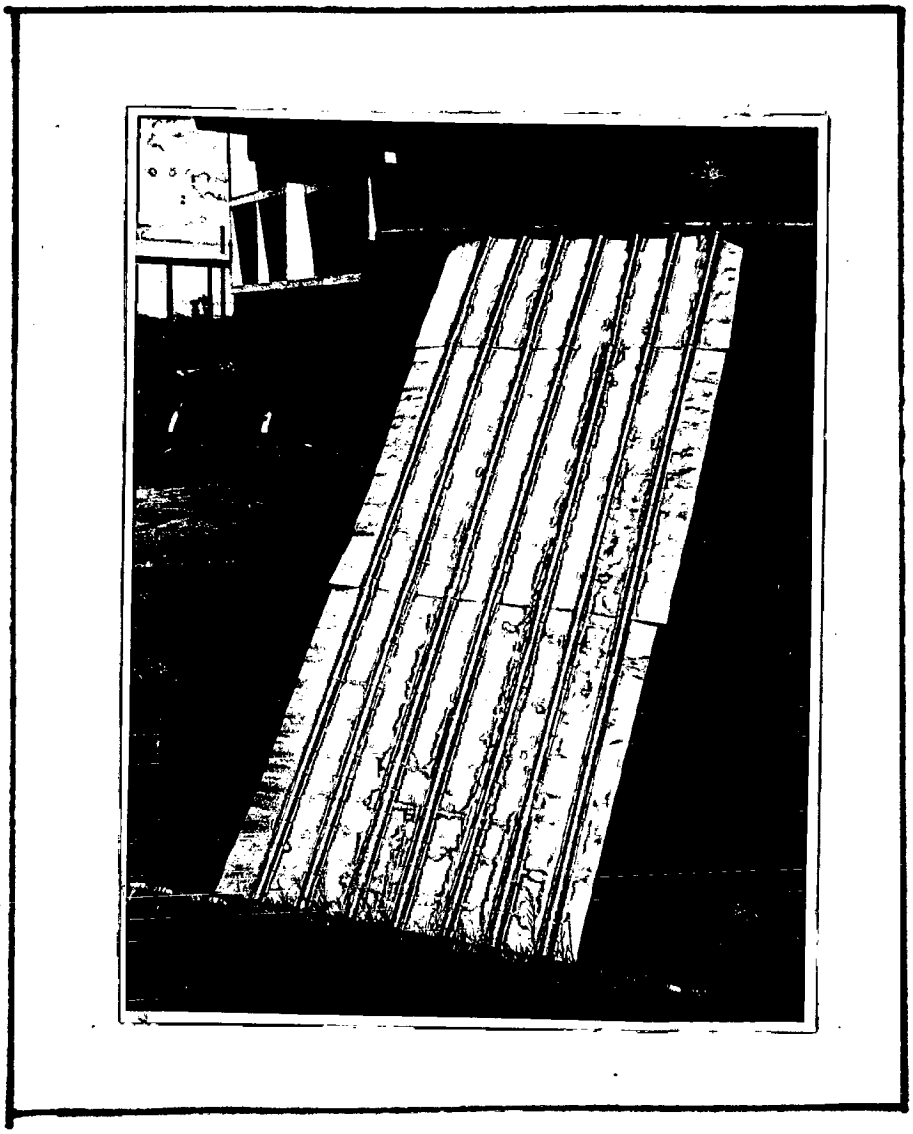

FIG. 4.1 TUBE IN PLATE TYPE COLLECTOR

(b) the cost of the metal sheet for the collector which varies directly for a metal to its thickness.

(c) the cost of the tubes and binding wires etc. which varies directly to the length of the tube.

(d) the cost of the headers which is also proportional to its length.

At any particular place, with a knowledge of the rates of the materials, the total cost can be computed for any combination of materials. A computer programme has been developed and used for computing plate-efficiency factor, cost per m^2 and cost to efficiency ratio for the following combinations:

Tube spacing: 2.5, 5.0, 10.0, 12.5, 15.0 cms.
G.I.Tube diameter: 12.5, 19.0, 25 mm
Plate thickness: 0.63, 0.46, 0.37 mm.
Plate material : Copper, Aluminium and G.I.sheet.

The above theoretical study brings out that the maximum efficiency per unit of cost is obtained for the following combinations:

G.I.Tube diameter	= 19.0 mm.
Plate material	= Aluminium.
Thickness of plate	= 0.37 mm (28 SWG)
Tube spacing	= 10.0 cms.

This combination has the plate efficiency factor as 0.94. The corresponding values for this combination are shown in figure 4.2. It is seen that cost/efficiency (S/F_p) decreases first rapidly with the increase in tube spacing and gives minimum value at 10 cms and then slightly increases.

—

4.3 STANDARD TEST SET UP AND EXPERIMENTAL STUDIES:

(4.31) Effect of different types of collectors:

The experimental test set up developed is similar to one suggested by Whillier[9]. Two collectors one consisting of corrugated and of plane G.I.sheet and another of pipe in plate type described earlier (4.2) are chosen for test, as they are basically of two different types of collectors. Water was allowed to flow in each absorber through a seperate constant head tank. The flow rate was controlled using a rotameter as an indicator and the actual flow rate was determined by accurately measuring the water collected in graduated vessel for a known time. Copper constantan thermocouples (32 S.W.G.) were used as temperature sensors and the corresponding thermal emf's were measured manually at regular intervals on a potentiometer having a least count of ten microvolts. Instantaneous total solar radiation incident on the collector surface was measured with a pyranometer placed in the plane of the collector, so that ground reflected radiation component is also included.

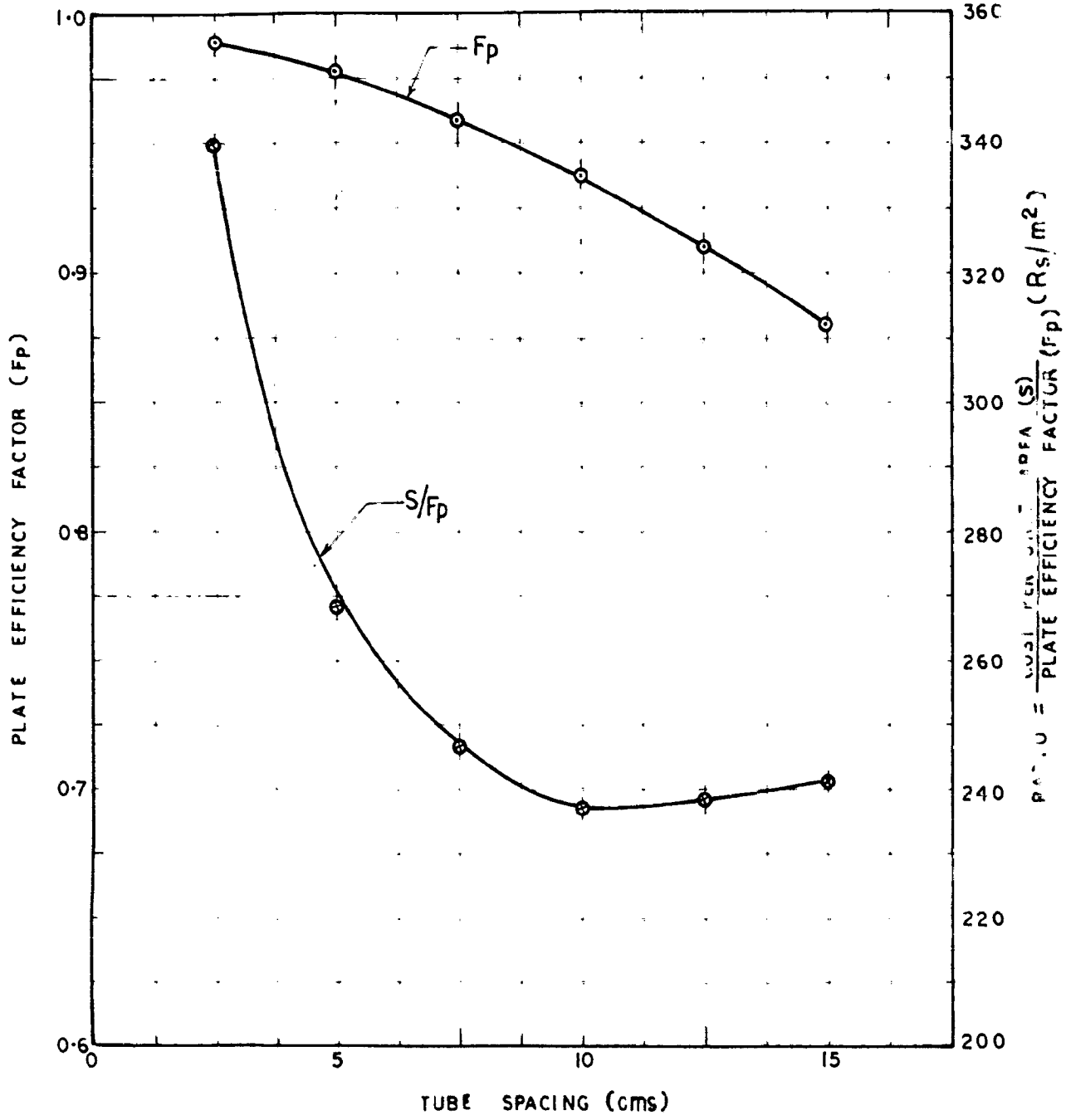

FIG. 4·2 OPTIMIZATION OF COLLECTOR CONFIGURATION

The observations were recorded from morning to evening simultaneously on both the heaters on several days in the month of January.

Fig.4.8(a) shows the solar radiation on the absorber surface from morning to evening for a typical day of test. The maximum solar radiation on the collector surface is about 800 Kcal/m^2hr which occurs at about 12.00 hours. The Fig 4.8(b) shows the hourly variation of outlet temperature for two different types of collectors when the inlet temperature was kept constant i.e.16°C and mass flow rate in both the collectors was maintained at 30 Kgm/m^2hr. Both these collectors were kept side by side so as to expose under identical conditions. It is seen that the outlet temperature is maximum at 13.0 hours and that corrugated type of collector gives higher outlet temperature as compared to the pipe type collector, the maximum difference being of the order of 8°C.

The collector efficiency (η) for sun up hours of the day are also computed from the above observations as shown below :

$$\eta = \frac{\text{Useful energy}}{\text{Radiation incident}} = \frac{Q_u}{H} \qquad \text{------(4.1)}$$

$$= \frac{G\,C_p(t_2 - t_1)}{H} \qquad \text{------(4.2)}$$

where G = 30.0 Kgm/m^2 hr°C (fixed)

t_1 = 15°C.

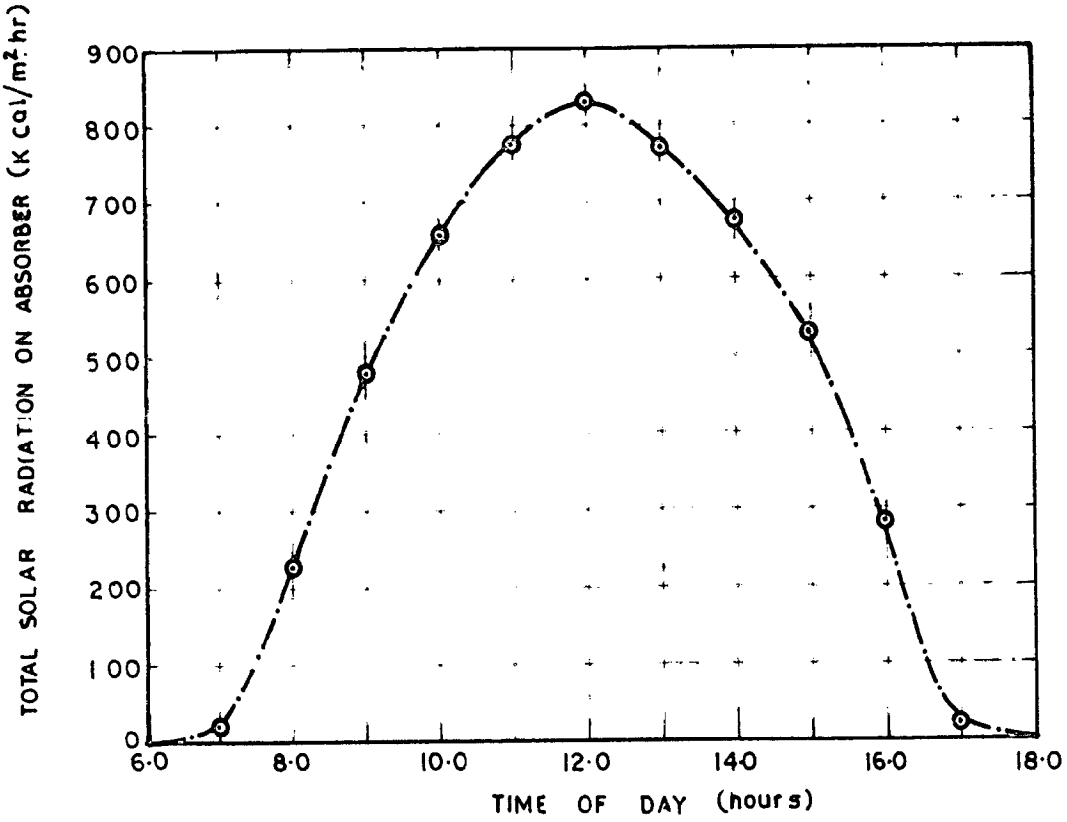

FIG.4·3(a) SOLAR INSOLATION ON ABSORBER SURFACE FOR THE DAY OF TEST

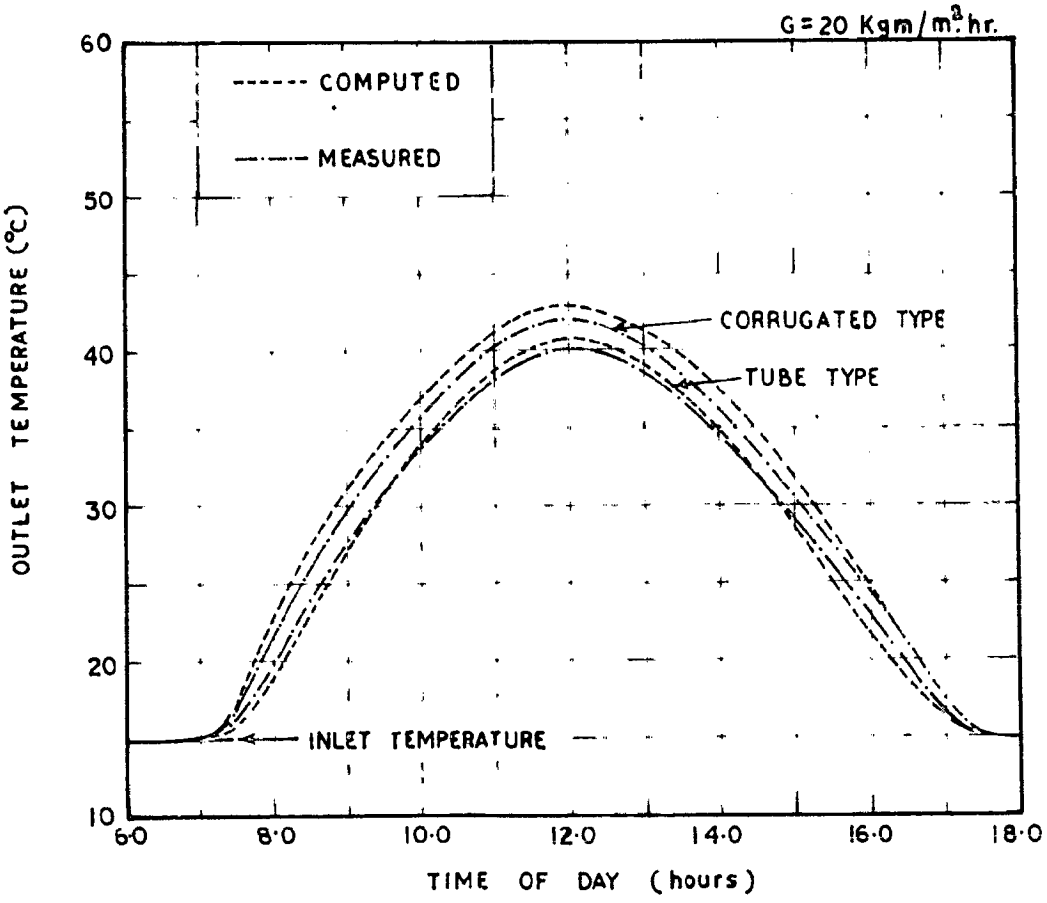

FIG.4·3 (b) HOURLY VARIATION OF OUTLET TEMPERATURE FOR CORRUGATED AND TUBE IN PLATE TYPE COLLECTOR

It can be seen from the efficiency curve of fig 4.4 that the efficiency of tube in plate-type collector varies from 55 to 60 percent while for corrugated type collector it varies from 60 to 65 percent. From these observations it can be concluded that the corrugated type of flat-plate collector gives about 5 percent higher efficiency as compared to pipe type collector.

4.32 Effect of mass flow rate:

It has already been shown (chapter 3) that flow rate has a considerable effect on the efficiency of the flat-plate collector system. If the inlet temperature is fixed, for a given solar insolation the efficiency increases with the increase of flow rate. It is obvious that the temperature difference between the outlet and inlet will be inversely proportional to flow rate, for a given situation. At higher flow rates the thermal losses from the plate are reduced, and hence the efficiency is increased.

Observations were also made for the two collectors at various mass flow rates ranging from 10 to 80 Kgm/m^2 hr. From these sets of observations, average collector efficiencies were computed and are shown in fig 4.8. It can be seen that the efficiency increases very rapidly as the flow rate increases say upto 20 Kgm/m^2hr. With a flow rate

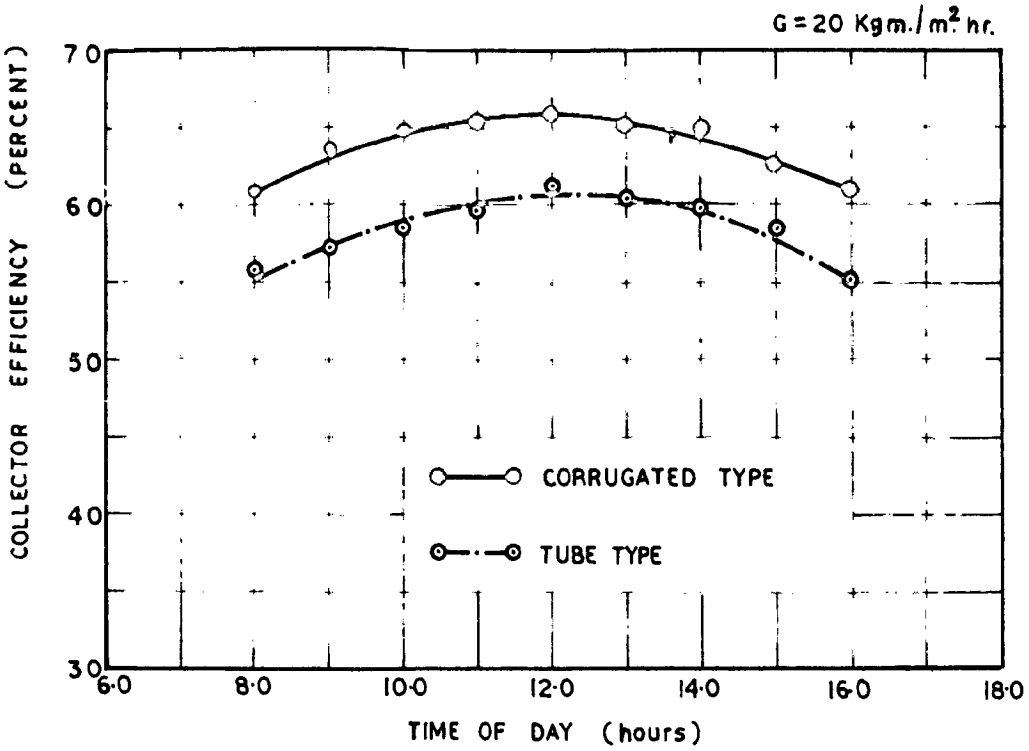

FIG. 4·4. VARIATION OF EFFICIENCY WITH TIME

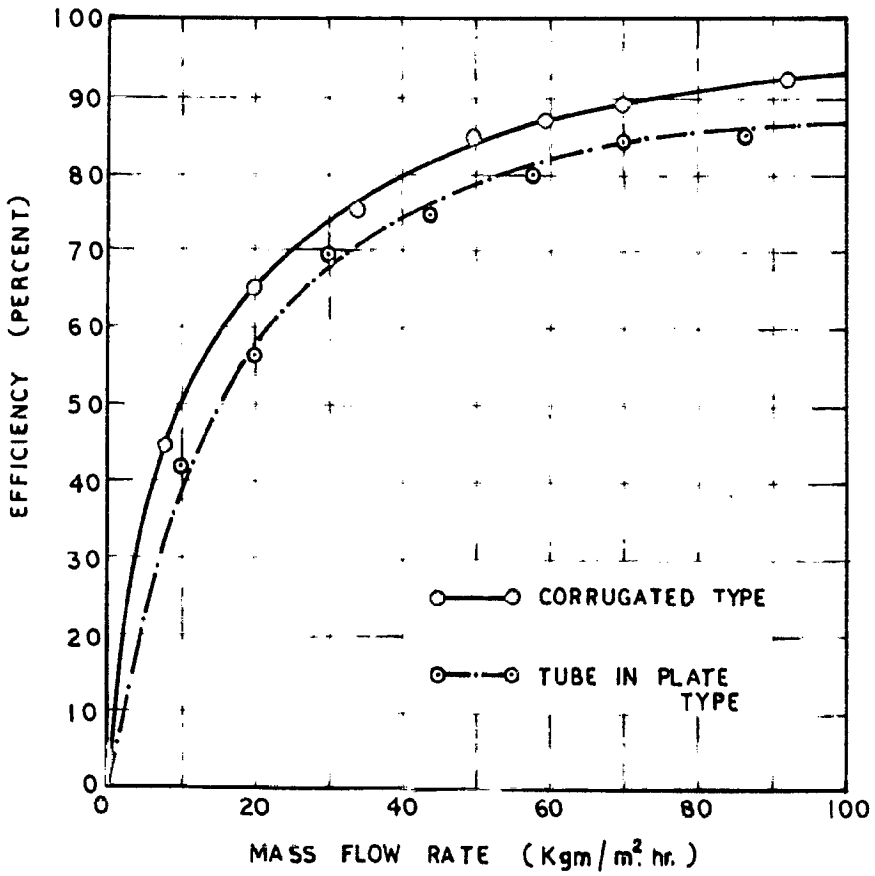

FIG. 4·5 FFFECT OF MASS FLOW RATE ON THE COLLECTOR EFFICIENCY

of 30 to 60 Kgm/m^2 hr the increase in efficiency is slow. After 60 Kgm/m^{2}hr there is very little further increase in efficiency. From these observations it can be concluded that there will not be of much use by increasing the flow rate beyond 60 Kgm/m^{2}hr. It can also be seen that the corrugated type of collector gives higher efficiency as compared to tube type at all the mass flow rates.

The measured temperature difference (t_2-t_1) is plotted for various solar insolation rates at different flow rates in fig 4.6. It is clear that temperature difference increases with the radiation intensity at a particular flow rate and decreases wit.. flow rate at a particular radiation intensity. Based on the above data design curves for tube in plate type collector are plotted in fig.4.7. With the help of these curves, for any radiation intensity and flow rate, the temperature difference and the average daily efficiency can easily be found.

The outlet temperature (t_2) can be computed by the following expression which was derived earlier in chapter 3 :

$$G\ (t_2-t_1) = F_p \left[H\tau\alpha - U_L\ (T_{av}-t_a)\right] \quad \text{-----(4.3)}$$

where $$t_{av} = \frac{t_1 + t_2}{2} \quad \text{-----(4.4)}$$

From this expression, the hourly outlet temperatures are computed and compared with the measured values in

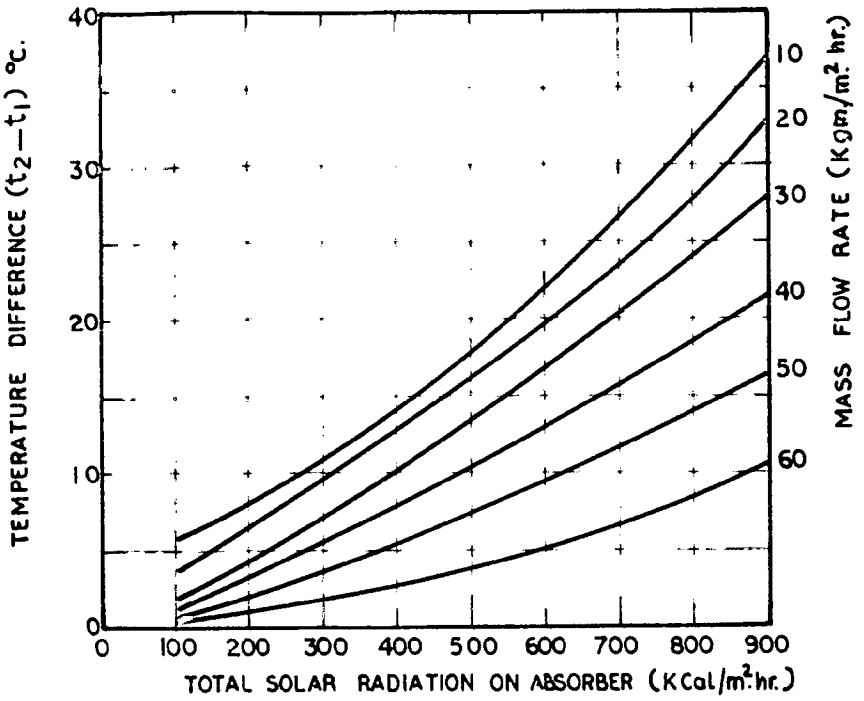

FIG. 4·6. EFFECT OF MASS FLOW RATE & SOLAR INSOLATION ON THE TEMP. RISE OF WATER

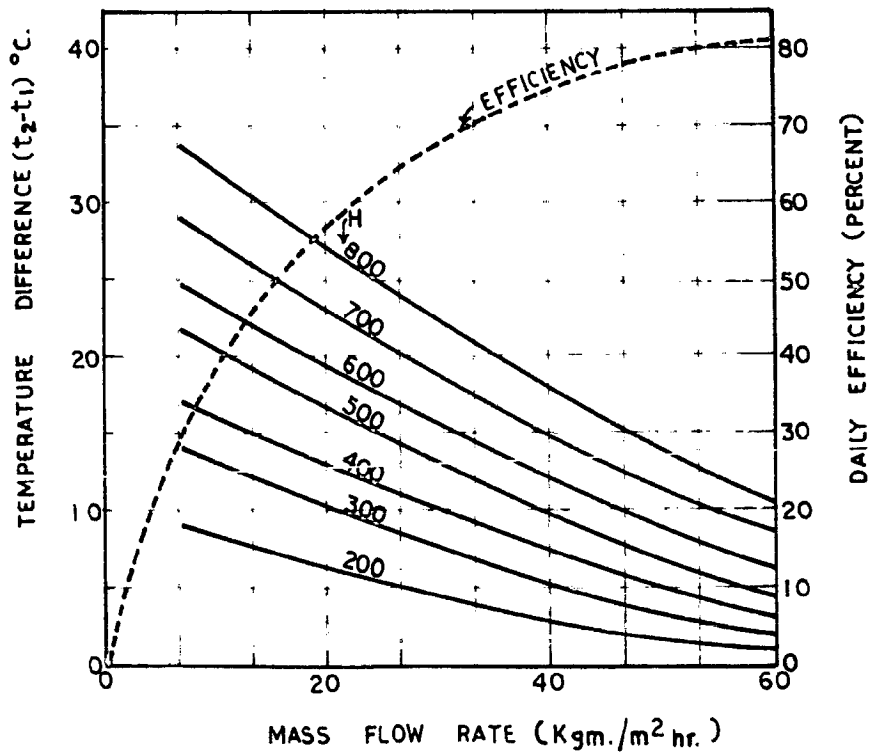

FIG. 4·7. DESIGN CURVES FOR SOLAR WATER HEATING.

fig 4.3(b). It can be seen that there is a close agreement between the measured and computed values.

4.33 Effect of multiple transparent cover:

The effect of multiple glass or plastic covers has also been studied in this test set up. A thermocouple was fixed at the centre of each absorber which will correspond to the average plate temperature. The collector efficiencies are computed as before for a single glass, double glass and glass and plastic film combination with plastic film on inner side, and are shown in fig.4.5. The life of plastic sheet is increased when it is used below the glass sheet.

It is observed that under field exposure conditions almost all the available plastic films in India become brittle and yellowish in less than two years period. But if the plastic film is kept between the glass sheet and the absorber plate it does not deteriorate so rapidly.

It can be seen from fig 4.6 that at lower plate temperatures the absorber having single glass cover gives higher efficiency but as the plate temperature increases the double glass cover gives higher efficiency. One glass plus one plastic gives still higher efficiency as compared to double glass cover. This is due to the fact that the plastic sheet has a higher transmittance as compared to that of glass-sheet.

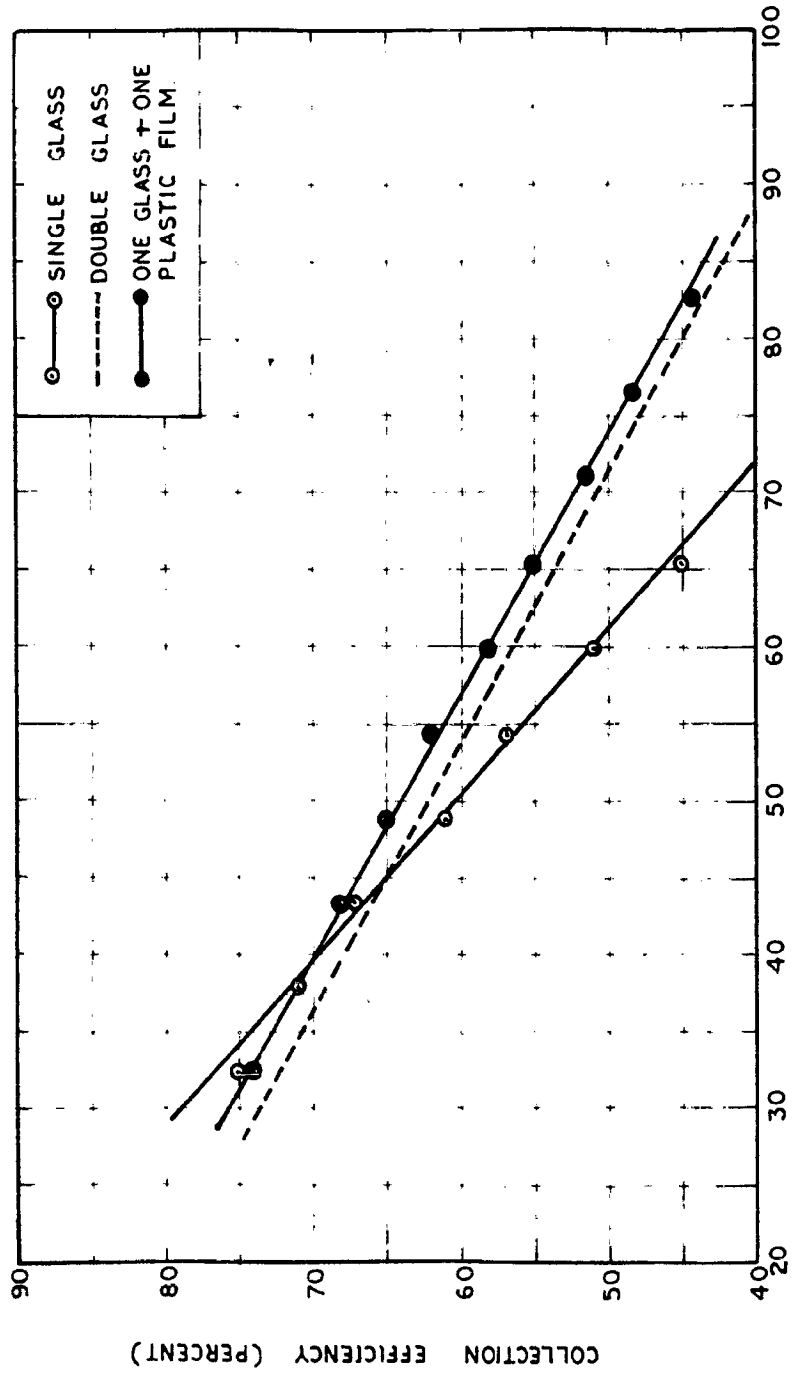

FIG. 4.8 EFFECT OF GLAZING ON THE COLLECTOR PERFORMANCE

4.34. Effect of Honeycomb.

It is recommended in the literature[10,11] that by using some honeycomb consisting of transparent material, the efficiency of flat-plate collector can be increased. By using this it is hoped that the convective movement of the air will be prevented to a large extent. For this purpose two types of honey-comb were made out of transparent thin p.v.c. sheet. One was of cylindrical cell of about 1.0 cm diameter and about 4.0 cm height as shown in Photograph fig 4.9. The other honeycomb is made out of flat-strips of p.v.c. sheet of 4 cm width jointed at suitable intervals and stretched to take the honeycomb shape as shown in photograph of fig. 4.10.

A test set up to study the effect of honey-comb on the collector efficiency when placed in the space between the absorber plate and the inner glass sheet was made and shown in photograph Fig.4.11. The test set up consists of two identical absorber plates each having an area of 0.1 m^2, fixed in an insulated glass covered box. A number of thermocouple are fixed outside and inside the glass surface, absorber plate, inlet and outlet of the absorber and in the insulation on the rear side of the absorber plate for measuring the temperatures at the respective points. Initially the two absorbers were exposed to sun, simultaneously and were checked for their similar behaviour. In both the absorbers a constant flow rate of 60 Kgm/m^2 hr was maintained. The

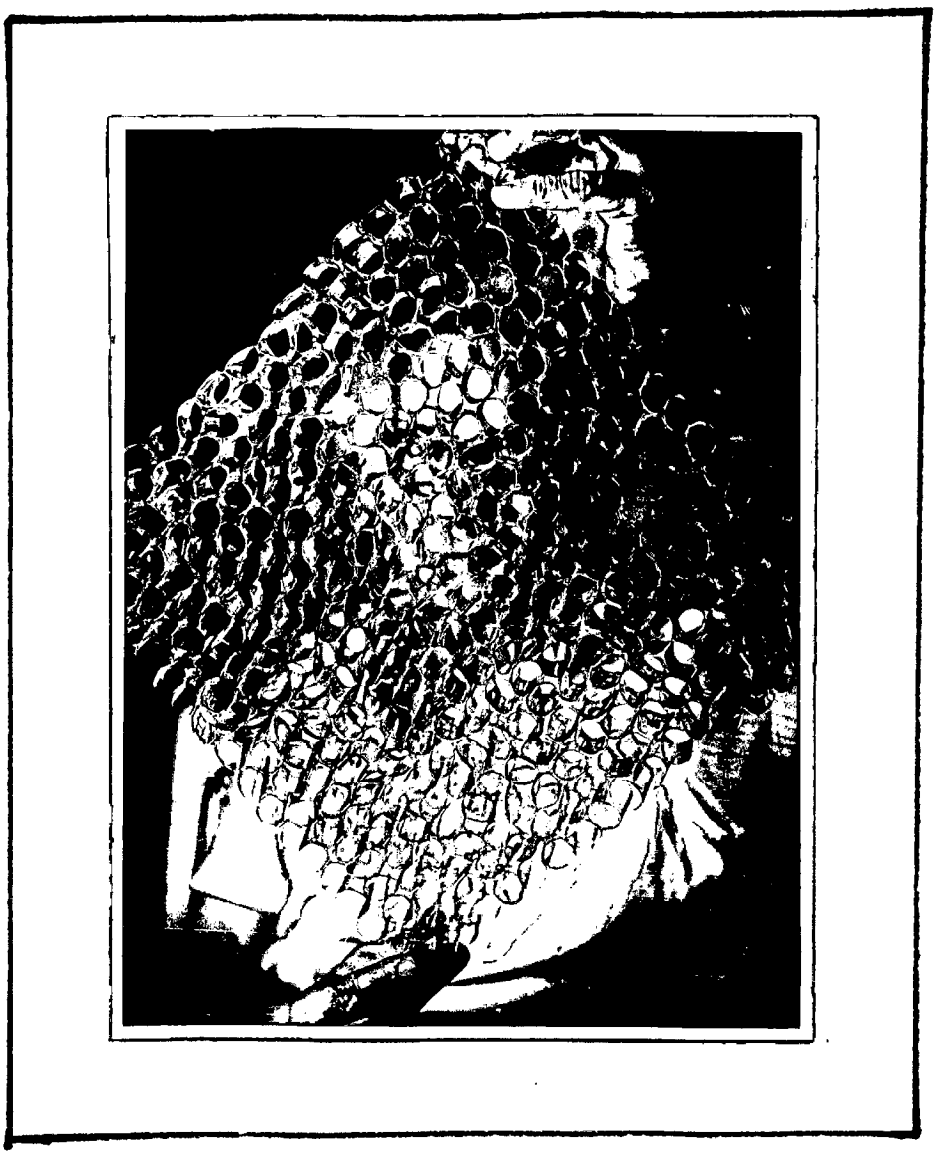

FIG.4.9: CYLINDRICAL CELL TYPE HONEYCOMB.

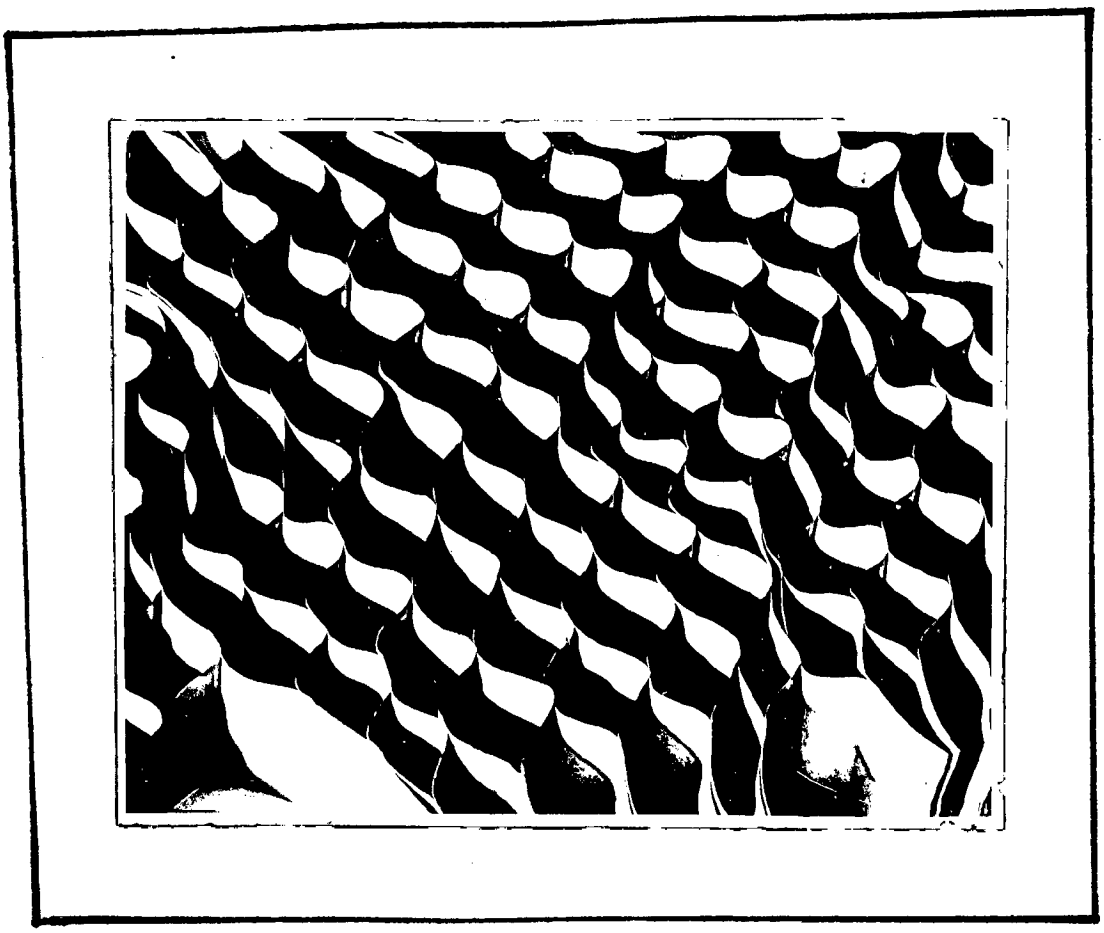

FIG.4.10: STRETCHED STRIP TYPE HONEYCOMB.

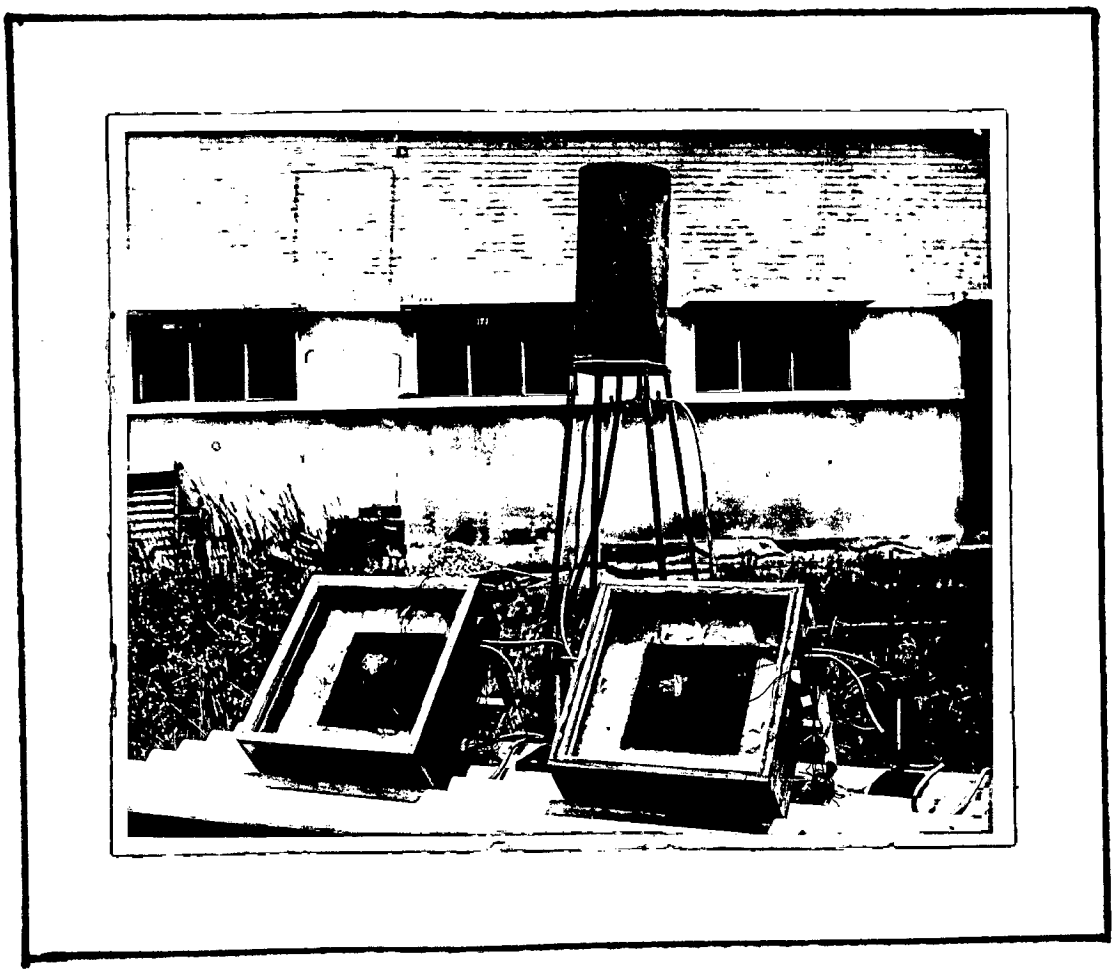

FIG.4.11: TEST SETUP USED FOR STUYDING THE EFFECT OF HONEYCOMB.

total solar radiation on the absorber surface in Kcal/m^2 hr on the day of test is shown in fig 4.12.(a). The comparative behaviour of the two absorbers i.e. the plate, outlet and inlet temperatures are shown in fig.4.12(b). It is seen that both the absorbers behave identically and thus do not require any correction factor.

The effect of honeycomb on the outlet temperature was studied by placing them between the absorber plate and glass cover of one of the test units, the other being left untreated. The results are shown in fig 4.13. It can be seen that by providing the honeycomb the outlet temperature increased by 1 to 2°C. The circular cell honeycomb gives slightly higher values as compared to other type of honeycomb. The honey-comb as is seen does not increase the efficiency markedly and hence the addition of honeycomb with its extra cost is not fully justified.

4.4 DEVELOPMENT OF DESIGN CURVES FOR WATER HEATING:

To be more realistic, in order to find out the overall efficiency of the system, one should integrate the hourly performance over a number of days of the season. Hence the useful energy is to be computed on the long term basis. The hourly rate of useful energy collection per unit area of the flat-plate collector as shown earlier (chapter 3) is given by the expression,

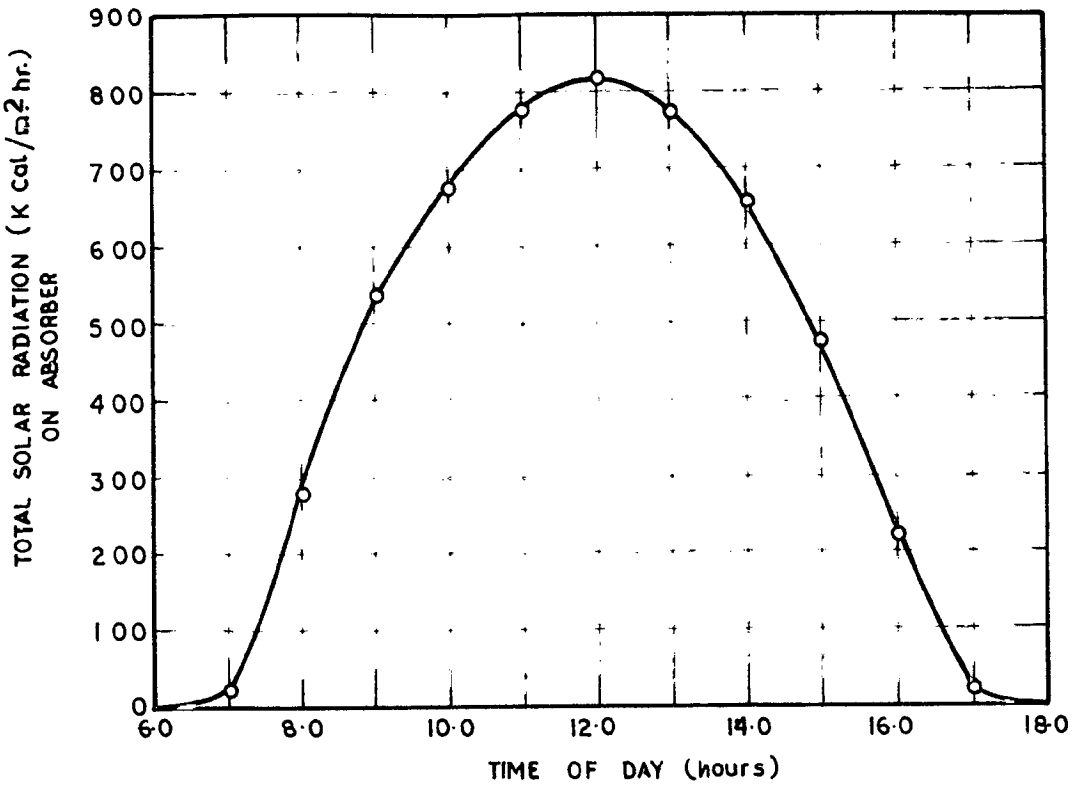

FIG. 4·12(a) SOLAR INSOLATION ON ABSORBER SURFACE FOR THE DAY OF TEST

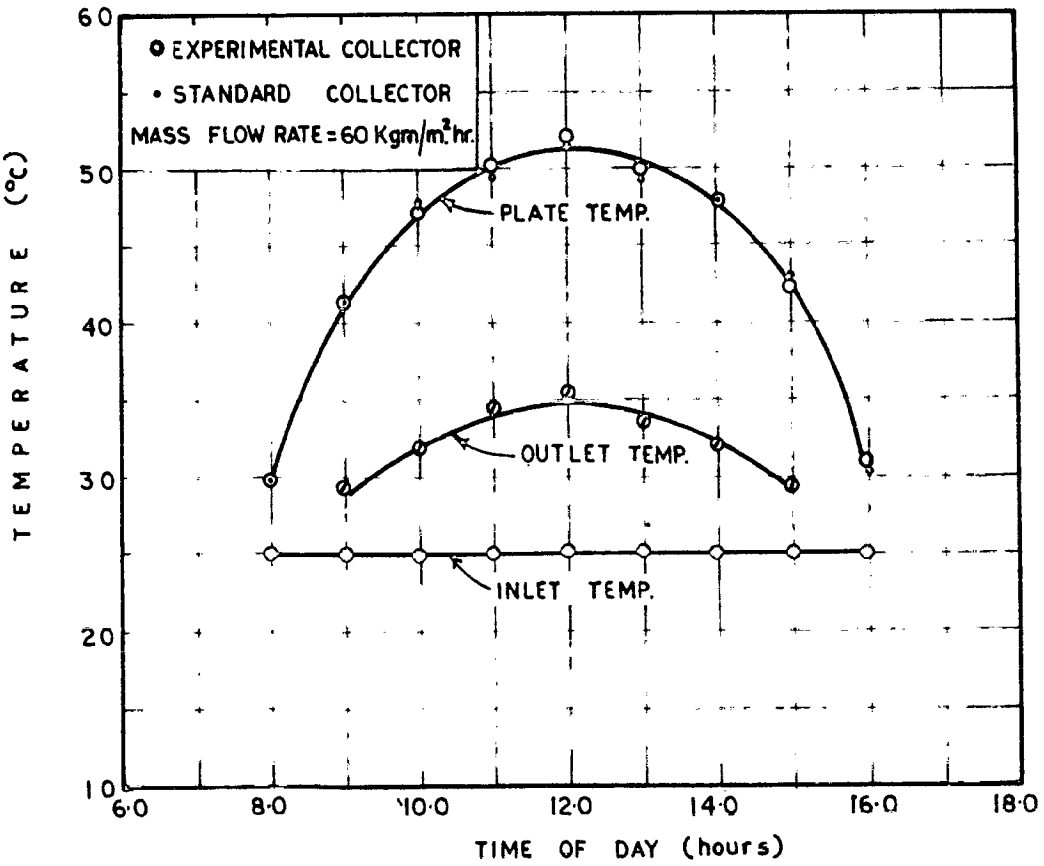

FIG. 4·12 (b) CALIBERATION OF TEST SET UP

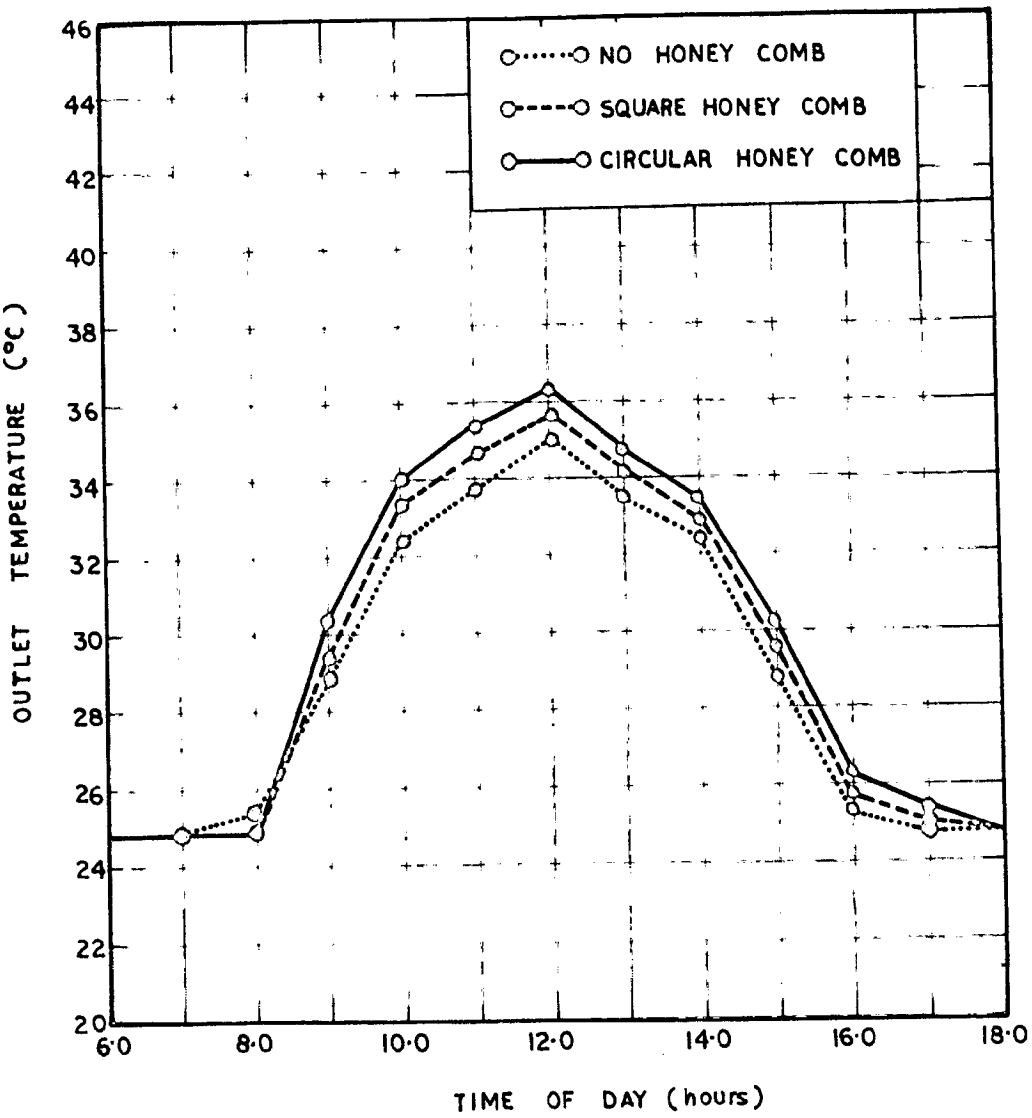

FIG. 4·13 EFFECT OF HONEY COMB ON THE OUTLET TEMP.

$$q_u = F_R \left[I_{Tt} \ (\tau\alpha) \ - U_L \ (t_1 - t_a) \right] \quad \text{-----(4.6)}$$

From this equation it becomes clear that there is a critical rate of solar radiation (I_C) above which only the best collection should be attempted, and this is given as

$$I_C = \frac{U_L \ (t_1 - t_a)}{(\tau\alpha)} \quad \text{-----(4.6)}$$

The equation 4.6 can be rewritten as

$$q_u = F_R(\tau\alpha) \quad (I_{Tt} - I_C) \quad \text{------(4.7)}$$

Here F_R can be assumed constant for a particular design system and flow rate. As it can be assumed that for a month at any particular hour the angle of incidence of sun's rays does not change appreciably, the hourly rate of useful energy collection, q_u, during the month (n-days) can be obtained as follows :

$$q_u = F_R \ (\tau\alpha) \ \frac{1}{n} \ \Sigma \ (I_{Tt} - I_C)^+ \quad \text{------(4.8)}$$

The long term average daily rate of useful energy collection can now be determined by summing the average hourly rate of useful energy collection, q_u, for all hours (h) from sunrise to sunset,

$$q_u = \sum^{h} q_u \quad \text{-----(4.9)}$$

If a new parameter, ϕ, utilisability defined by Whillier[12] is introduced in equation (4.8), then we get

$$q_u = F_R(\tau\alpha)\ \bar{I}_{Tt}\ \phi \qquad \text{---------(4.10)}$$

where $$\phi = \frac{1}{n}\Sigma\left(\frac{I_{Tt}}{\bar{I}_{Tt}} - \frac{I_C}{\bar{I}_{Ct}}\right)^{*} \qquad \text{---------(4.11)}$$

Further, Liu and Jordan[13] have shown that the monthly frequency distribution curves on daily basis are only a function of the average transmission coefficient and do not depend significantly upon the latitude or the declination. As such, the generalised curves prepared by them for utilizability as a function of cloudiness index, K_T, have been employed here for the determination of ϕ. The hourly radiation on inclined surfaces (I_{TC}) are computed as discussed in chapter 3.

Four widely distant places in India, viz., Delhi, Poona, Calcutta and Madras have been selected to be representative of the cross-section of Indian climate[14]. The monthly average daily total radiation on a horizontal surface, $\bar{H}$, the atmospheric transmission factor, K_T, and the maximum and minimum temperatures for these places along with their latitudes, L, are given in Table 4.1, for the months of January and May.

Based on these data from weather records and the generalised design data, design curves, fig 4.14-4.17, for the four regions have been obtained. These show th

---

* Positive values of $(I_{Tt}-I_C)$ are only to be taken.

TABLE 4.1: Weather data for Indian cities

PLACE	Latitude	K_T		$\bar{H}$ Cal/cm^2/day		t_{max} (°C)		t_{min} (°C)	
		Jan.	May	Jan.	May	Jan.	May	Jan.	May
DELHI	28° 35'	0.66	0.63	341	636	21.4	40.4	6.3	26.0
CALCUTTA	22° 32'	0.60	0.55	365	546	26.4	36.3	12.5	25.3
POONA	18° 32'	0.70	0.61	462	600	30.3	37.1	11.7	22.4
MADRAS	13° 04'	0.69	0.59	620	556	29.6	38.5	19.5	27.6

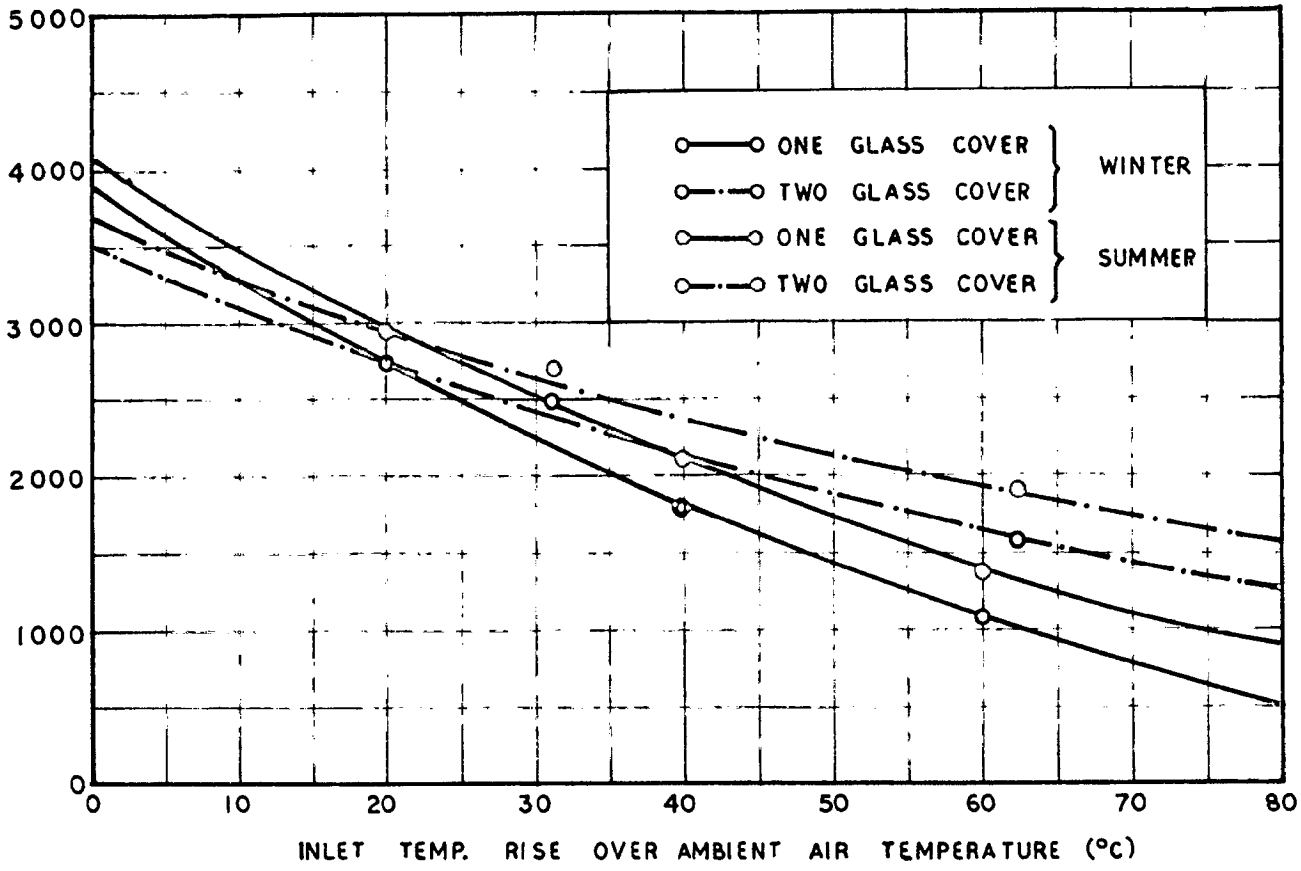

FIG. 4·14 SOLAR ENERGY COLLECTION AT DELHI

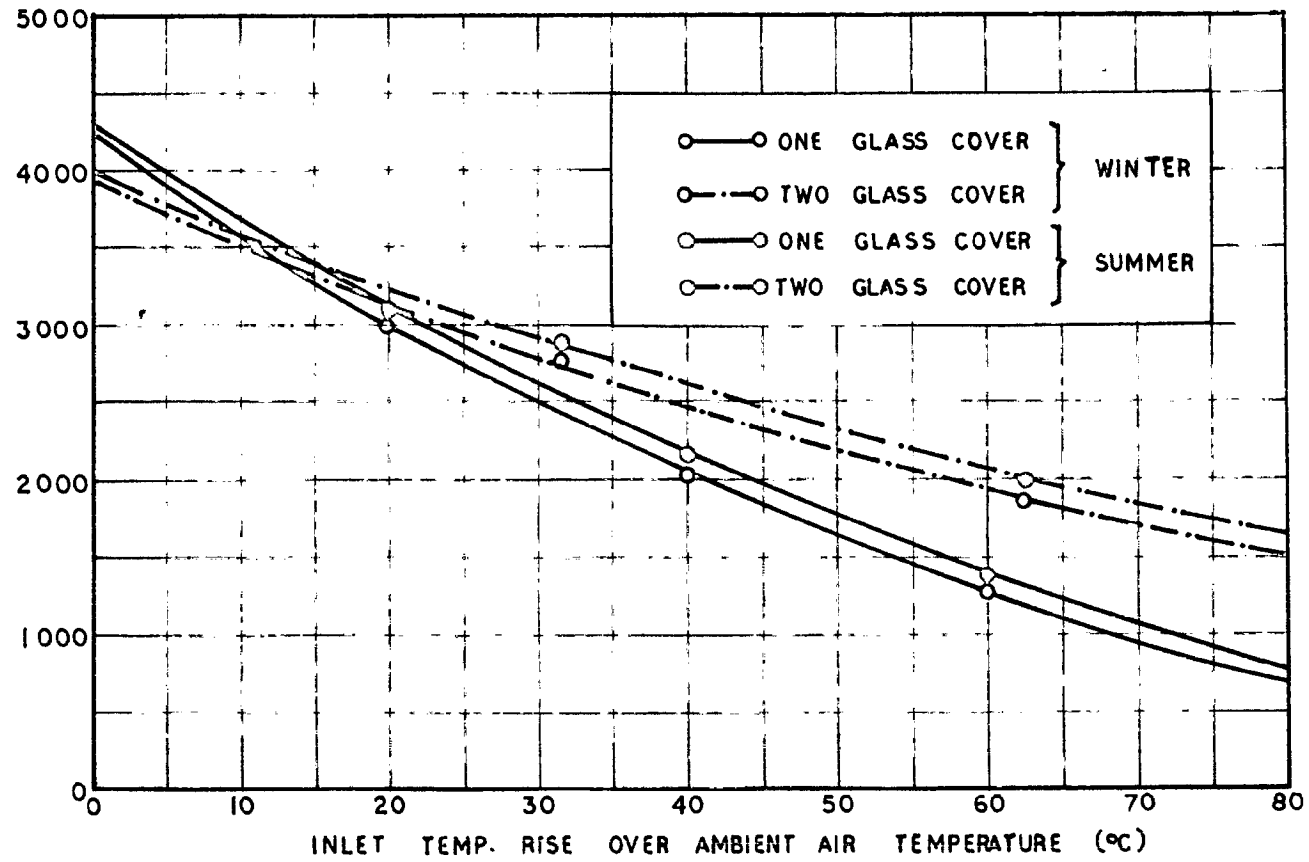

FIG. 4·15 SOLAR ENERGY COLLECTION AT POONA

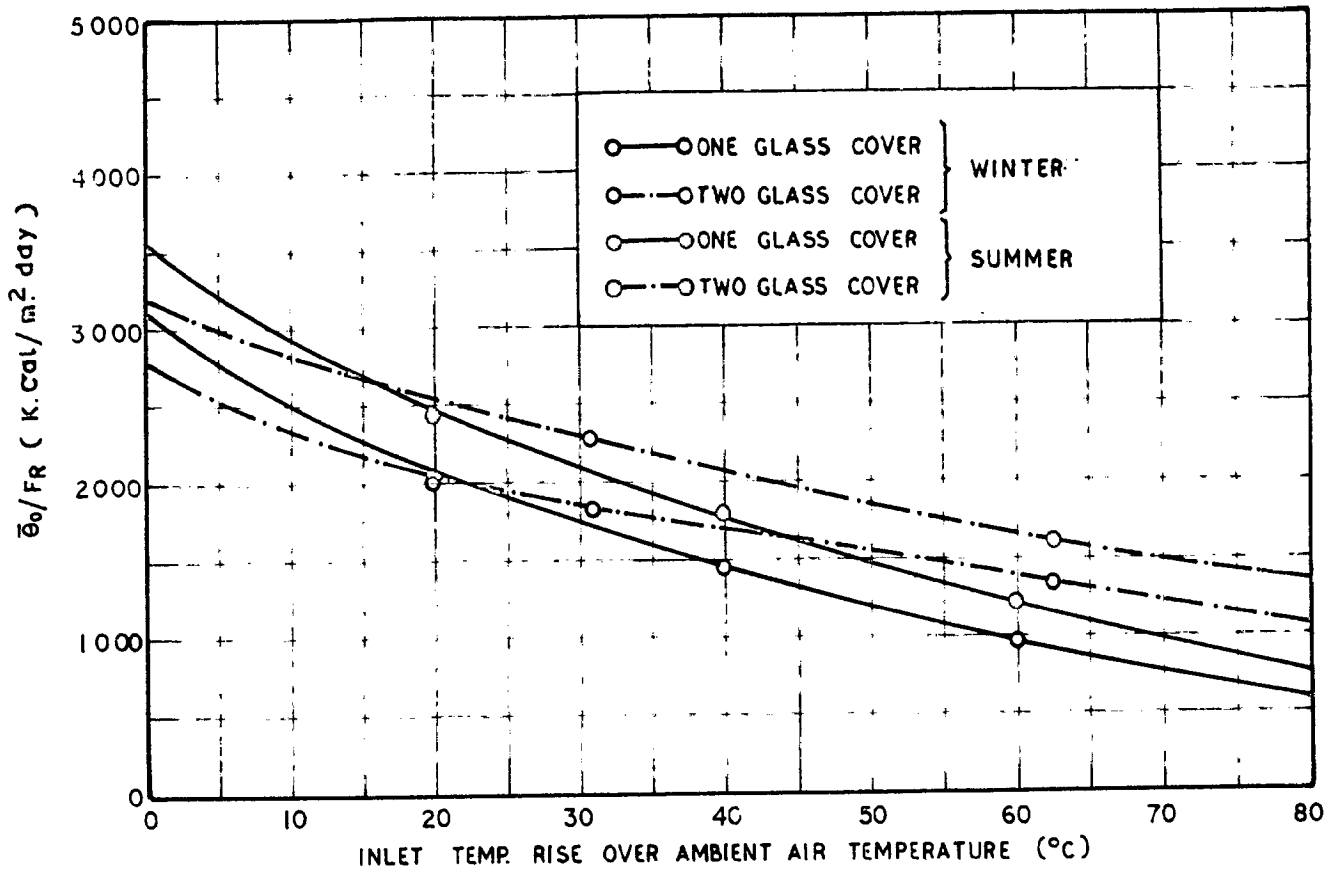

FIG. 4·16 SOLAR ENERGY COLLECTION AT CALCUTTA

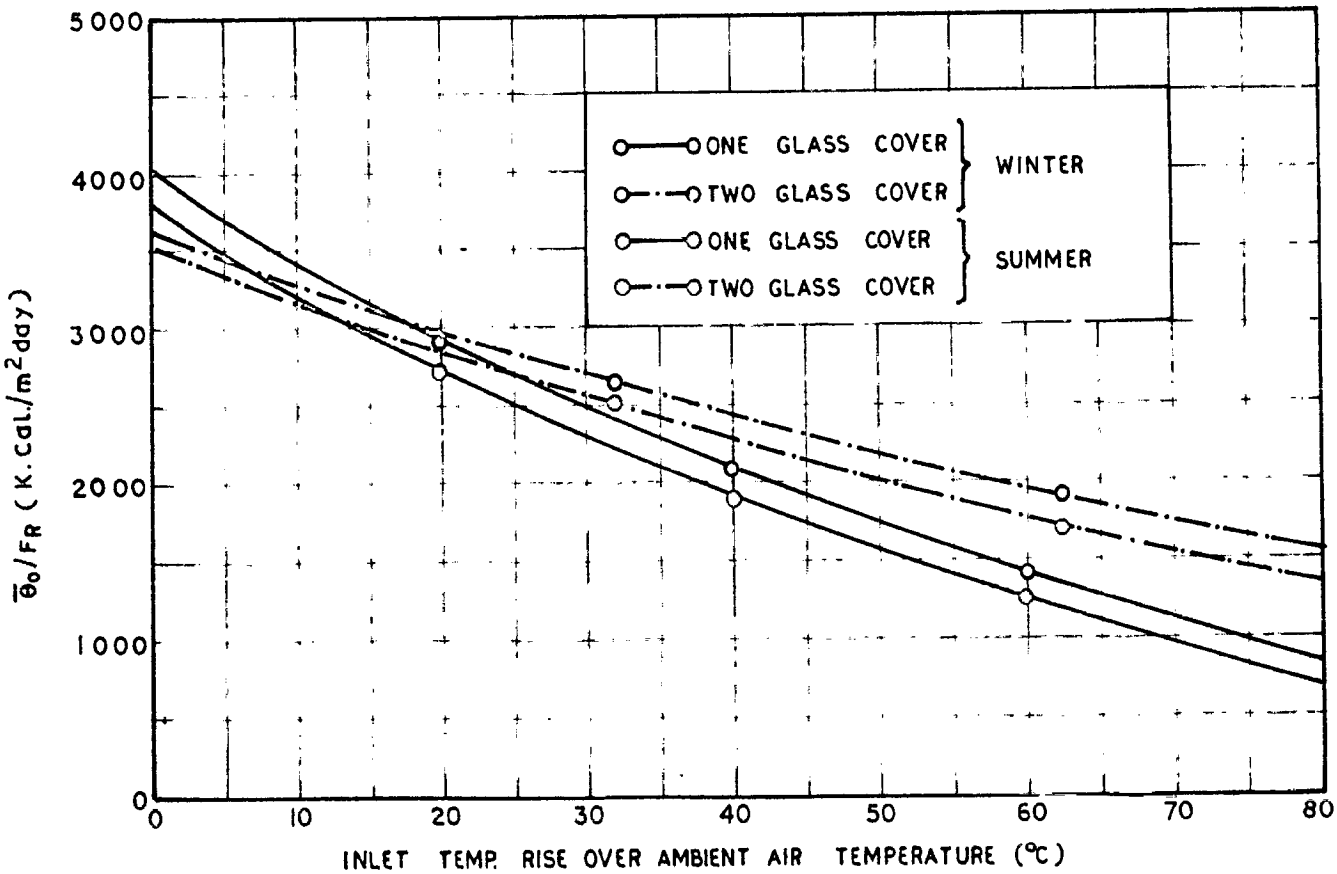

FIG. 4·17 SOLAR ENERGY COLLECTION AT MADRAS

daily average useful collection as a function of the temperature of collection, the number of glass cover plates, flow conditions and for two representative months, January and May, for collectors having angle of eastward tilt equal to 0.9 times the latitude in summer and latitude angle plus 15 degrees in winter. The temperature of collection is defined as the difference between the temperature of the fluid stream entering the collector, i.e. the storage temperature and the ambient temperature. Further, the flow conditions are to be maintained such that the solar collection is always positive. This condition is automatically satisfied in natural circulation type solar systems. It is evident from the curves that if the temperature level of the collection is less than 18°C, one glass cover is sufficient. This is in agreement with the experimental findings as discussed earlier.

6.41. APPLICATION OF DESIGN PROCEDURE:

In designing a solar heating installation with insulated thermal storage at any place, following steps are to be undertaken:

1) load calculation: The load is calculated by knowing the required amount of fluid and the design maximum fluid temperature.

Q_L (load) = mass of fluid x specific heat x (design maximum fluid temperature - morning fluid temp. in storage).

v) Average daily collection:

Consulting the appropriate design curves for the particular locality and season and the number of covers and temperature level of operation decided upon in steps (i) and (iii), the value Qu/F_R is obtained. Using the value of F_R, computed in step (iv), average daily collection per meter^2, Qu Kilocalories is then known.

vi) Area calculation:

$$\text{Area}(m^2) = \frac{\text{load in Kcal}(\ )_L}{\text{Average daily collection}(\ )u}$$

Though design curves can be used for finding out the absorber area graphically in steps, for a quicker calculation empirical expressions[15] are obtained as given below:

For Delhi Area $= \frac{M}{2.3\ F_R} \tan (0.86\ \text{temp.} - 12.0)$ ---(4.12)

For Poona Area $= \frac{M}{2.2\ F_R} \tan (0.80\ \text{temp.} - 16.6)$ ---(4.13)

For Calcutta Area $= \frac{M}{2.2\ F_R} \tan (0.86\ \text{temp.} - 14.0)$ ---(4.14)

For Madras Area $= \frac{M}{2.3\ F_R} \tan (0.84\ \text{temp.} - 19.7)$ ---(4.15)

where, M, is the amount of water in litres to be heated to a desired temperature (temp.), and F_R can be computed from design constants. For example, the tube in plate type collector will have an F_R value of equal to 0.87.

The absorber areas that are required for various water capacities and temperatures for few Indian cities as computed with the help of above expressions are given in Table 4.2.

4.64 CLOSE'S MODEL FOR SOLAR WATER HEATER:

It is needless to stress the importance of establishing a mathematical model and of theoretical methods of solving it in predicting the overal performance of a solar water heater. The methods[16-21] developed upto now can give the performance of the system only in a single pass-circuit. However, if the same water is recirculated through a tank and an absorber as it happens in natural circulation type solar water heater then the problem becomes difficult. Close[22] has worked out an analytical model of such a system for clear weather and no drain-off during the day, assuming sine function expression for the solar radiation and ambient temperature. Chiampa[23] described an alternative scheme for including the solar radiation data by taking cumulative partial sum's every hour. De Jan[24] has considered the whole system as water, contained in an insulated vessel being heated by the sun, without taking into account the system geometry and the thermosyphon flow.

Here the basic model due to Close has been modified so as to take into account the system capacity and heat

AMOUNT OF WATER		ROORKEE			
gallons	litres	60°C	60°C	65°C	60°C
30	137	2.04	1.98	2.43	2.70
40	182	2.72	2.64	3.24	3.60
50	227	3.40	3.30	4.05	4.50
60	273	4.08	3.96	4.86	5.40
70	318	4.76	4.62	5.67	6.30
80	364	5.44	5.28	6.48	7.20
90	409	6.12	5.94	7.29	8.10
100	454	6.80	6.60	8.10	9.00
120	545	8.16	7.92	9.72	10.80
130	590	8.84	8.58	10.53	11.70
140	636	9.52	9.24	11.34	12.60
150	681	10.20	9.90	12.15	13.50
160	726	10.88	10.56	12.96	14.40
170	772	11.56	11.22	13.77	15.30
180	817	12.24	11.88	14.58	16.20
190	863	12.92	12.54	15.39	17.10
200	908	13.60	13.20	16.20	18.0

and ambient temperature have been included as Fourier series. These modifications make the model valid for cloudy weather as well, as is verified by experimental studies. Design studies for various system parameters like circulating pipes diameter and layout, collector configuration, absorber length/breadth ratio and tank height/dia.ratio are reported here.

A schematic diagram of natural circulation type solar water heater is shown in Fig 4.15, various parameters of system geometry are indicated therein.

With reference to Fig 4.16, the instantaneous heat balance equations for the absorber and the pipes, considered as one unit, and the insulated storage tank are :

$$M_c C_p \frac{dt_3}{d\theta} = F_p AC\left[H(\tau\alpha) - U_c(t_m - t_a)\right] - W_c \frac{dt_c}{d\theta} - W_p \frac{dt_c}{d\theta} - U_p(t_p - t_a) \quad \text{--------(4.16)}$$

$$M_c C_p \frac{dt_s}{d\theta} = U_T(t_n - t_a) + M_T \frac{dt_T}{d\theta} + M_{WT} \frac{dt_n}{d\theta} \quad \text{----(4.17)}$$

where t_3 & t_{t5} = temperature at level 3 and at 5 in fig 4.16 respectively (^oC)

t_m & t_a = mean temperature of water in the collector and tank respectively (^oC)

t_c = mean collector plate temp.(^oC)

t_n = ambient temperature (^oC)

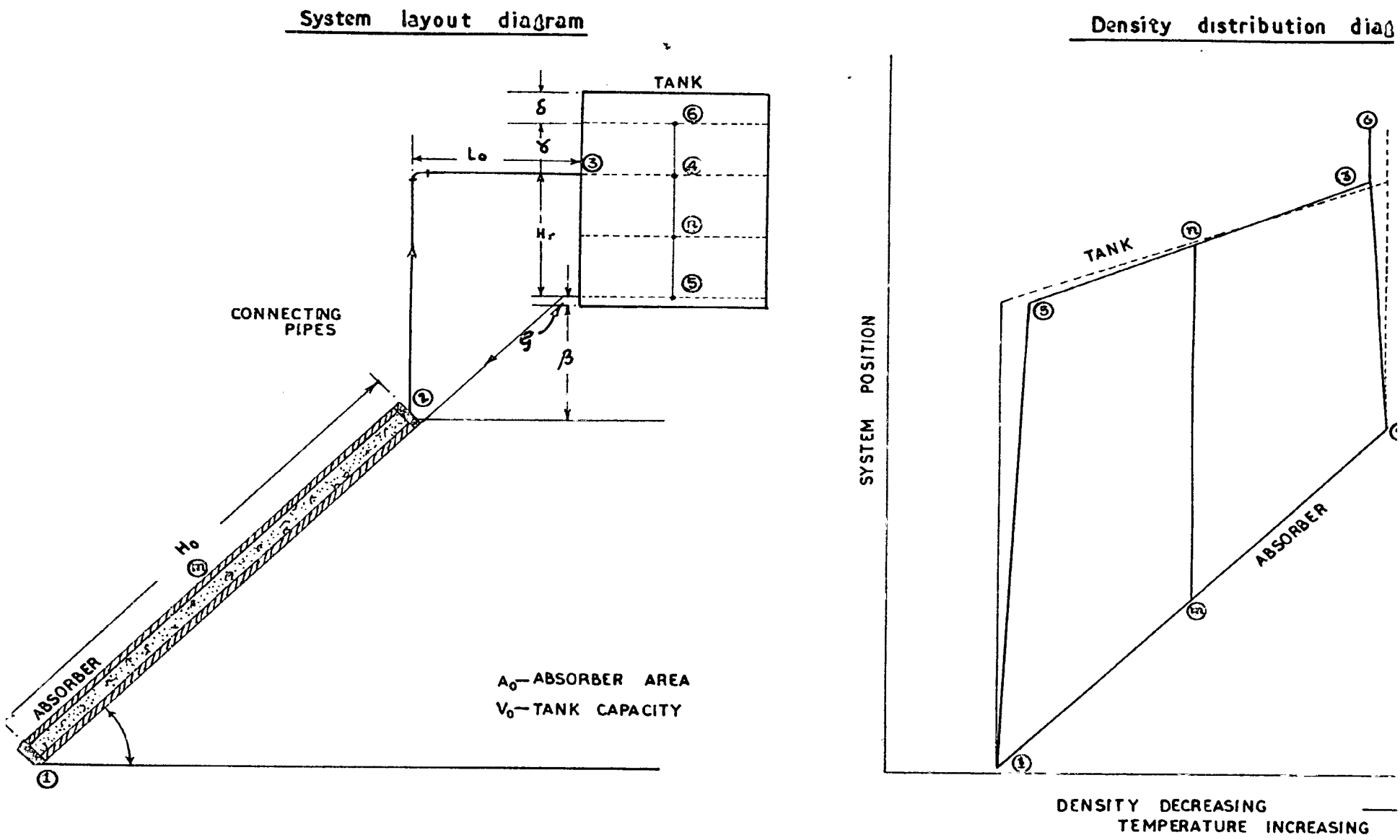

FIG.4-18 LAYOUT DIAGRAM OF THERMOSYPHON SYSTEM

t_g = mean pipe body's temp.(^oC)

t_p = mean temperature of water in pipes (^oC)

t_T = mean tank body temp.(^oC)

U_o = mass flow rate (Kg/hr)

C_p = specific heat (Cal/gm^oC)

F_p = plate efficiency factor

A_C = collector area (m^2)

$(\tau\alpha)$ = effective transmissivity absorptivity product

I = radiation intensity on tilted surface (Kcal/m^2hr)

U_C = collector loss coefficient (Kcal/m^2hr^oC)

U_p = pipes overall loss coefficient (Kcal/m^2hr^oC)

U_T = tank overall loss coefficient (Kcal/m^2hr^oC)

M_C = collector's thermal capacity with water in it (Kcal/^oC)

M_p = pipes thermal capacity with water in it (Kcal/^oC)

M_T = tank's thermal capacity (Kcal/^oC)

M_{WT} = weight of water in tank (Kg).

It can be assumed that the body temperatures of the collector and the tank are equal to the respective water temperatures. Thus, the equations become on putting $t_a = t_n$ and $t_g = t_p$

$$W_o C_p (t_3 - t_5) = F_p A_c \eta (\quad) = \left[F_p A_c U_c (t_m - t_a) + U_p (t_p - t_a) + U_c \frac{dt_R}{d\theta} + U_p \frac{dt_n}{d\theta} \right] \text{---(4.18)}$$

$$W_o C_p (t_3 - t_5) = (U_{WT} + U_T) \frac{dt_n}{d\theta} + U_T (t_n - t_e) \text{ ------- (4.19)}$$

As reported by Close[22], on the basis of experimental observations, the mean water temperature in the tank is the same as the mean water temperature in the absorber during sun up hours. This will be true for the pipe temperatures also, if the mean of both the pipes is considered. As such, putting $t_m = t_n = t_p$ and eliminating W_o from 4.18 and 4.19 by equating their right-hand sides, the equation for mean system temperature (t_n) during sun up hours becomes

$$W \frac{dt_n}{d\theta} + U (t_n - t_a) = F_p A_c H (\tau\alpha) \text{ ------(4.20)}$$

$$U = U_c + U_p + U_T + U_{WT} \text{ --------(4.21)}$$

$$U = F_p A_c U_c + U_T + U_p. \text{ --------(4.22)}$$

In this analysis, the system has been considered uncoupled at night ($F=0$). Therefore, the absorber mean water temperature (t_n) and tank water temperature have to be determined separately for the night by solving the modified set of equations

$$U_1 \frac{dt_a}{d\theta} + U_1 (t_m - t_a) = 0 \qquad \text{--------(4.23)}$$

and $$U_2 \frac{dt_a}{d\theta} + U_2 (t_m - t_a) = 0 \qquad \text{--------(4.24)}$$

where $U_1 = U - U_2$; $U_2 = U_T + U_{JT}$ --------(4.25)

$U_1 = U - U_2$; $U_2 = U_T$ --------(4.26)

Equations 4.20, 4.23 and 4.24 are first order inhomogeneous differential equations with constant coefficients and can be easily solved with the help of an integrating factor. Using the Fourier series expressions for U and t_a, obtained by harmonic analysis, we have

$$T = A_0 + \sum_{n=1}^{N} (A_n \cos n\omega\theta + B_n \sin n\omega\theta)$$

$$= A_0 + \sum_{n=1}^{N} \text{Real} \quad (A_n - jB_n)\, e^{jn\omega\theta} \qquad \text{----(4.27)}$$

and

$$t_a = C_0 + \sum_{n=1}^{N} (C_n \cos n\omega\theta + D_n \sin n\omega\theta)$$

$$= C_0 + \sum_{n=1}^{N} \text{Real} \; (C_n - jD_n)\, e^{jn\omega\theta} \qquad \text{------(4.28)}$$

$j = \sqrt{-1}$, $\omega = 2\pi/24$

The solution of equation 4.20 becomes

$$t_n = \frac{E_o}{x}\left[1-e^{-x(\theta-\theta_o)}\right] + t_o\, e^{-x(\theta-\theta_o)}$$

$$+ \sum_{n=1}^{N} \frac{(xE_n - nvF_n)(\sin nv\theta - e^{-x(\theta-\theta_o)}\cos nv\theta_o}{(x^2 + n^2 v^2)}$$

$$+ \frac{(nvE_n + xF_n)(\sin nv\theta - e^{-x(\theta-\theta_o)}\sin nv\theta_o}{(x^2 + n^2 v^2)} \qquad \text{-------(4.29)}$$

where t_o is the initial temperature at time θ_o, corresponding to the draw-off time when fresh water is filled in, and

$$x = \frac{U}{J}\ ;\ E_n = xA_n + y\,C_n,\ n = 0, 1, \text{-------N}$$

$$y = \frac{F_n\, A_o(\tau\alpha)}{W}\ ;\ F_n = x\,B_n + yD_n,\ n=1\text{-------N}.$$

$$\text{--------(4.30)}$$

For solution of equations 4.23 and 4.24 corresponding values of U and V are taken to compute X and Y. These are to be taken as zero, when no sun is present.

Hence equation 4.29 gives the mean system temperatures during all the hours, when proper values of constants are taken and no reverse thermosyphon flow is allowed to take place at night.

4.61 Thermosyphon flow:

To determine the rate of flow, due to thermosyphon action, generated by heating of water in the collector and

the consequent movement by natural convection, it is necessary to consider the density at various points of the flow circuit at any instant. The same is shown in fig 4.18. For purposes of computation, it is assumed that the collection and tank density distribution are linear and that losses in the pipe are negligible as compared to the heating in the collector. Following Close[22] and assuming a quadratic density temperature relationship.

$$\rho = at^2 + bt + c \qquad \text{--------(4.31)}$$

it can be shown that the thermal pressure head generated by solar heating, i.e. the area of density distribution diagram, is given by

$$h_t = \frac{(t_3-t_3)}{2}\left[2\,\Delta t_n + B\right] f(s) \qquad \text{-------(4.32)}$$

where $f(s)$ is the system function determined in terms of system geometry parameters like pipe layout (β, δ, ξ), height of water in the tank (H_t), absorber length and tilt (L_b, ξ) by the relation

$$f(s) = L_b \sin\xi + 2\beta + (H_t - r) \qquad \text{---(4.33)}$$

and $$t_n = \frac{(t_3-t_5)}{2} \qquad \text{---(4.34)}$$

Eliminating (t_3-t_5) from 4.19 and 4.32

$$h_t = \frac{(U_{LT} + U_T)(dt_{n/de}) + U_T(t_n - t_a)}{2\,\cos\phi}\left[2\Delta t_n + B\right] f(s)$$

$$\text{----(4.36)}$$

Now the thermosyphon flow rate will be such that at every instant, the thermal pressure head is balanced by the frictional head loss (h_f) in the flow circuit. Using Darcy Weishach's equation, the frictional head loss is

$$h_f = \frac{f\, l\, u^2}{2\, g\, d_p}$$

where f = 0.035 for laminar flow.

l = equivalent length of flow circuit (m)

g = acceleration due to gravity (m/hr^2.)

d_p = internal diameter of circulation pipes (m)

Using velocity (u) in terms of the mass flow rate (H_o)

$$h_f = \frac{D\, H_o^{\,2}}{d_p^{\,5}} \quad (l) \qquad \text{-------(4.36)}$$

Where D is a known constant and (l) is the effective length of the flow circuit of internal diameter d_p, which depends upon the collector configuration and the pipe layout. For a collector having parallel tubes between headers and with pipe layout as shown in fig 4.1,

$$l = \left[\frac{nH_o}{B_c}\left(\frac{dh}{dc}\right)^5 + B_c\left(\frac{dn}{dh}\right)^5\right] + \left[H_o + H_t + \gamma + \beta\left(1+2\operatorname{cosec}\xi\right)\right] + l_c + L_o \qquad \text{---(4.37)}$$

From equations 4.35 and 4.36, one gets the thermosyphon

flow equation

$$v_o^3 = -\left(\frac{1}{\frac{\partial p}{\partial x}\rho g_p}\right)\left[(v_{wT}+v_T)\frac{dt_n}{d\theta} + J_c\,(t_n - t_a)\right]$$

$$\left[\beta\,\Delta t_n + B\right]\, f(\beta) \quad \text{---(4.33)}$$

where S = pipes spacing in the absorber (m),

L_c = header length (m),

d_c = internal diameter of absorber pipes (m),

d_h = internal diameter of header pipes (m),

H_t = Height of water in the tank above the cold pipe (m),

γ = water above hot pipe in tank (m)

β = (tanks' cold outlet-collector's hot outlet) m,

ξ = Collector's tilt (degrees),

L_o = horizontal length of circulation pipes (m),

and J_c = equivalent length for constriction like bends, T's etc. (m)

Equation 4.33 is cubic in v_o and knowing the values of t_n and $dt_n/d\theta$ from equation 4.30 and after proper substitutions, v_o can be determined.

Knowing v_o and t_n and using equations 4.19 & 4.34 the inlet and outlet temperatures t3 and t5 can also be determined. From these, the collector efficiency, the system efficiency can be computed.

To incorporate the above system analysis a number of programmes written in Fortran II were developed, namely

1. A programme for computing the solar radiation on the absorber surface;

2. A programme for the harmonic analysis of ambient temperature and solar radiation on inclined surface upto 12 harmonics,

3. A programme for computing the heat exchanger efficiency of the absorber (F_p),

and 4. A final programme which determines the effect of all design variables (about 40), on the tank room temperatures. The complete details of analysis are given in the publication[25].

4.62 Experimental Verification:

The experimental installation is shown in fig 4.10. It is designed to be flexible so that the collector type and area, tilt and orientation, and the system parameters $\beta, \gamma, \xi, \delta$ and the circulation pipe diameter can be changed as required. The galvanised iron tank is insulated with 10 cms thick fibre glass insulation and a cover shell is provided to protect it from the weather.

The temperature of the water in the tank were measured at various points as marked in fig 4.12. 33 SWG Copper constantan thermocouples were used and observations taken hourly on a manually operated portable cambridge potentiometer with a resolution of 10 microvolt.

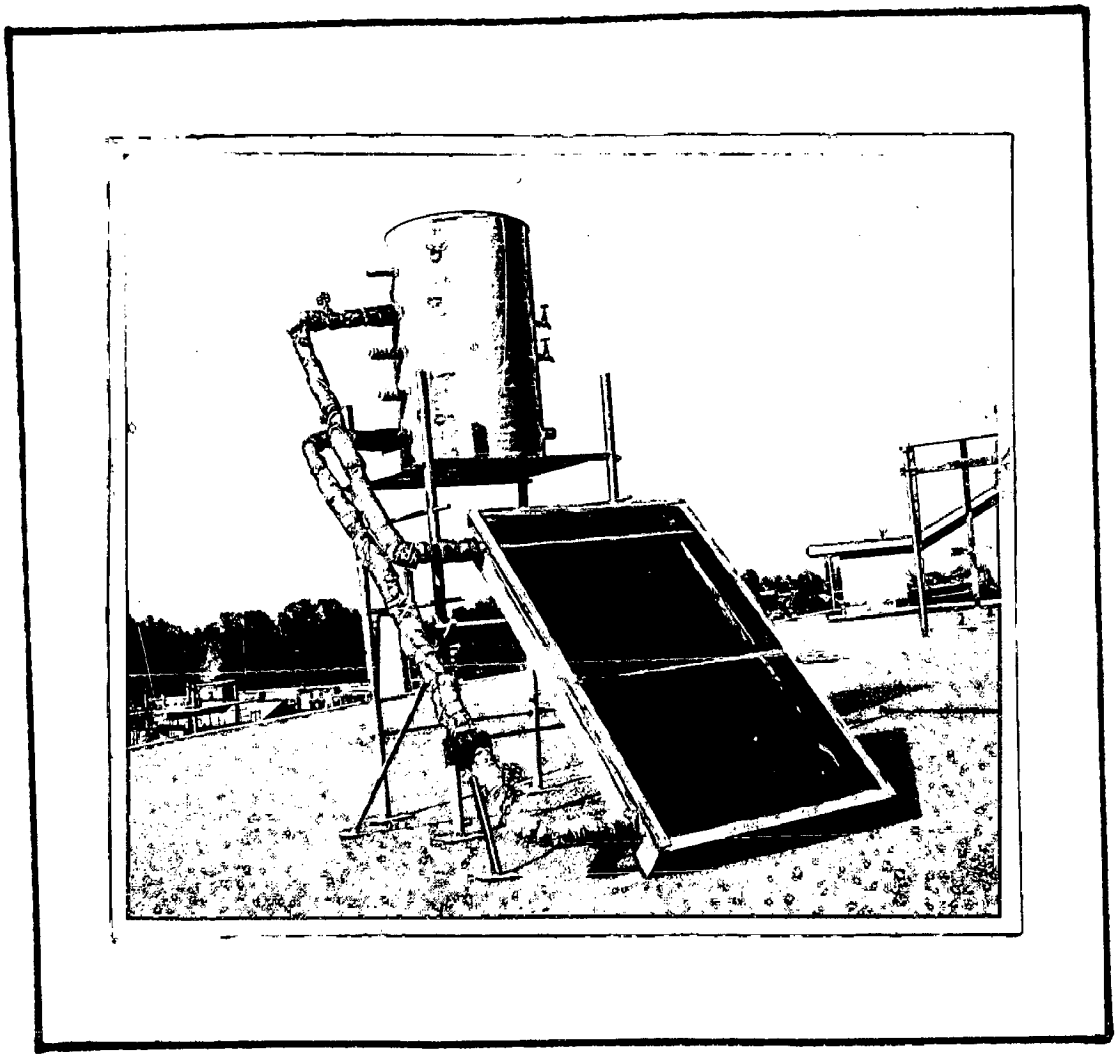

FIG.4.19. EXPERIMENTAL TEST INSTALLATION

A galvanized sheet corrugated collector with a net area of 1 m^2 and a length of 1.16 m and having a single glass cover, alongwith a circulation pipe of 25 mm nominal diameter and insulated with 25 mm mineral wool insulation, were installed. The observations were first taken on a clear day and later for a cloudy day.

For a clear day fig 4.20 shows the measured values of mean tank temperature alongwith the computed values and the ambient temperature. During the daytime, the agreement is found to be very close. Similar results for the cloudy day are shown in fig 4.21. Here also a close agreement is observed for day time.

However for the night time, the computed values are higher than those observed. This may be due to the fact that the system is here assumed as uncoupled during night hours, in the theoretical model while there may be reverse circulation bringing a cooling effect. However, if the system is treated as coupled one during both day and night then the computed temperatures come out to be lower, as shown in fig 4.20. This may be due to the non-confirmity of the assumption of (t_n=t_m) for night time as well. A good agreement between computed and observed values were also obtained in the case of a tube and plate type of collector heating system for daytime performance. The analytical model, having been proved by experiments for clear and cloudy days, is sufficiently general and can now be used for any

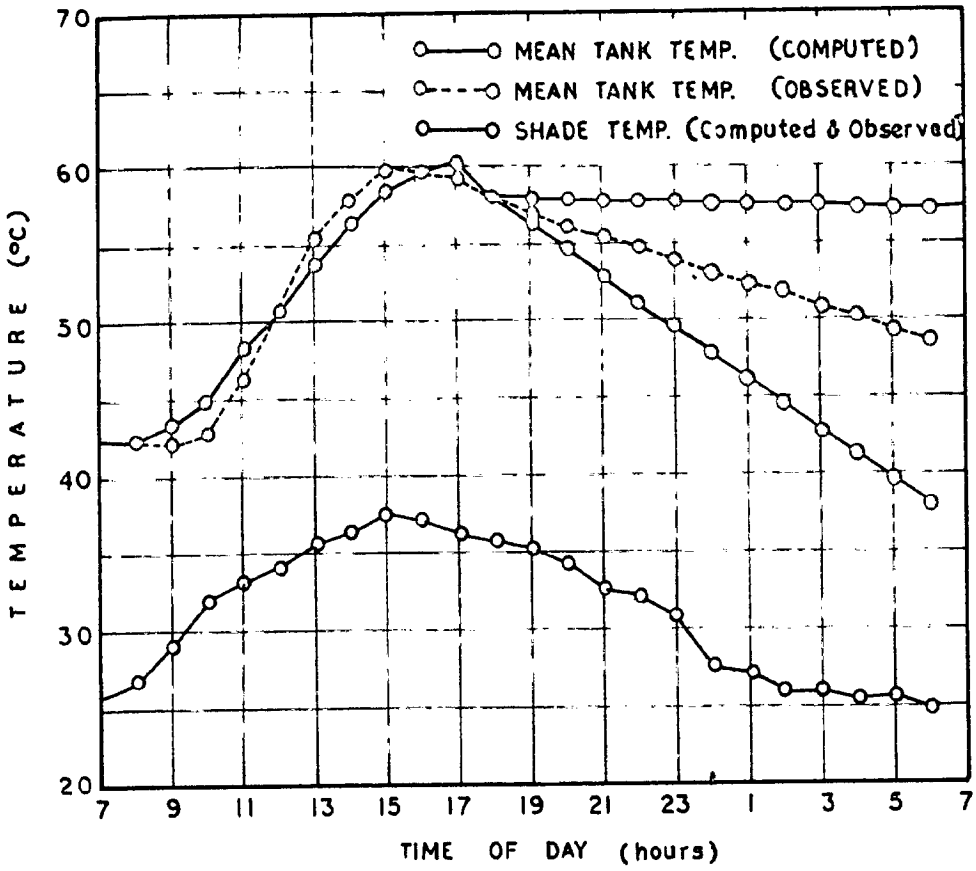

FIG. 4·20 MEAN TANK TEMPERATURES FOR A CLEAR DAY - CORRUGATED ABSERBER

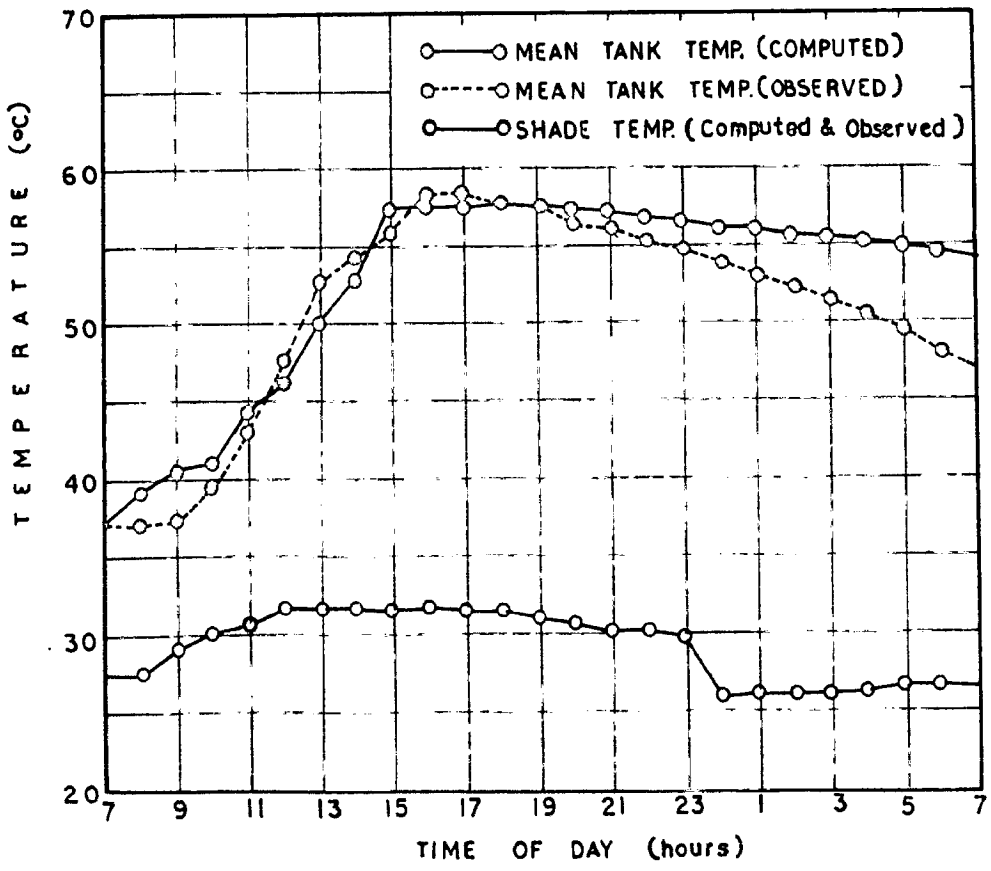

FIG. 4·21. MEAN TANK TEMPERATURE FOR A CLOUDY DAY. - (Computed & Observed)

climate and place, to evaluate any collector and system lay-out, for sun up hours, within engineering accuracy.

4.3 ECONOMIC THICKNESS OF INSULATION:

The required thickness of insulation for any specified application depends upon the characteristics of the insulating material and upon the permissible heat loss of the system. The costs to be considered are :

1. The cost of heat loss from the system prevented by the insulation during its period of use.

and 2. the cost of insulation and application during the same period of use.

For a given installation there will be some optimum thickness of insulation above which the cost of any further increase would not be justified by the additional heat saved. This optimum thickness is often termed as economic thickness.

Cost of Insulation:

Cost of insulation is given by the expression

$$\lambda \pi (r_2^2 h_2 k_2 - r_1^2 h_1) \quad \text{----------(4.39)}$$

where λ is rate of insulation (Rs/m^3). r1, h1 and r2, h2 are the radius and height of the inner and outer cylindrical tanks. In this case the insulation thickness is considered to be same throughout.

$$\text{thickness of insulation} = (r_2 - r_1) = \frac{h_2 - h_1}{2} \quad \text{----(4.40)}$$

Cost of heat loss: Under steady state conditions the rate of heat loss from an insulated cylindrical tank is given as

$$\frac{2\pi K h_1 (t_1-t_2)}{\log_e(r_2/r_1)} + \frac{2\pi K r_1^2 (t_1-t_2)}{(r_2-r_1)}$$

where K is the thermal conductivity of insulating material (Kcal/m hr^{0}C) and (t_1-t_2) is the temperature difference on the two sides of the insulation.

The maximum temperature in the storage tank reaches at about 4.0 pm and the hot water is usually drawn at about 8.0 on next day. So total heat loss from the tank in 16 hours will then be,

$$32\pi K (t_1-t_2) \left[\frac{h_1}{\log_e r_2/r_1} + \frac{r_1^2}{(r_2-r_1)}\right] \text{Kcal/day}$$

This heat loss is to be converted in terms of the absorber cost. In our design an absorber area of 1 m^2 costs about Rs.200/- and collects energy equal to 2800 Kcal/day. So the cost of heat loss in rupees is given as

$$\left(\frac{200}{2800}\right) 32\pi K (t_1-t_2) \left[\frac{h_1}{\log_e r_2/r_1} + \frac{r_1^2}{(r_2-r_1)}\right] \quad \text{---(4.41)}$$

Thus the total cost (C) will be

C = cost of insulation + cost of heat loss

$$= A\pi (r_2^2 h_2 - r_1^2 h_1) + \left(\frac{200}{2800}\right) 32\pi K (t_1 - t_2) \left[\frac{h_1}{\log_e r_2/r_1} + \frac{r_1^2}{(r_2 - r_1)} \right]$$

----------(4.42)

For obtaining the optimum thickness of insulation the total cost (C) is to be minimized.

The final expression for the optimum thickness is given as :

$$\pi r_2 (3 r_2 - 2r_1 + h_1) - 1.141 K (t_1 - t_2) \left[\frac{h_1}{r_2 (\log_e r_2/r_1)} + \frac{r_1^2}{(r_2 - r_1)^2} \right] = 0 \quad \text{------(4.43)}$$

In the present case

r_1 = 0.285 m,

h_1 = 0.730 m,

R =176.6 Rs/m^3,

K = 0.032 Kcal/m hr^0C,
(for fibreglass)

and $(t_1 - t_2)$ = (55-15) = 40^0C.

A graphical method has been employed Fig.4.22 for the determination of the optimum value of r_2. It can be seen from the figure that economic thickness of insulation for the case studied comes out to be 7.5 cms.

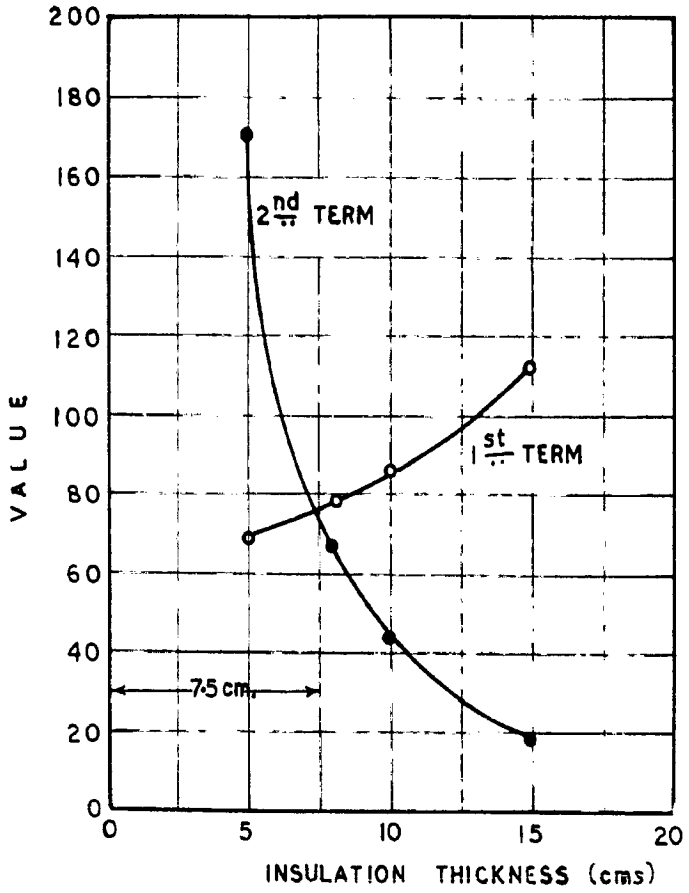

FIG. 4·22 OPTIMIZATION OF INSULATION THICKNESS

4.7. BASIC OF SOLAR WATER HEATER (DOMESTIC TYPE):

All solar water heaters basically consist of an absorber unit for collecting the incident solar radiation during the day hours and an insulated tank which stores the heated water. In most conventional systems these two components are separate and connected through circulation pipes, as shown in fig 4.23.

The large variety of designs of absorber units are available. However the flat-plate collector is the most commonly employed one. A general description of this type of collector is given below:

(a) Absorber unit: The following four components are known collectively as the absorber unit :

1) flat-plate collector,
2) insulation,
3) transparent cover,
4) absorber box.

1) Flat-plate collector: Flat-plate collectors are simple in operation, easy to fabricate, absorb diffuse as well as direct radiation intensity and are of low cost, though the temperature attained is below the boiling point of water. Flat-plate collector consists of more or less flat sheets in which channels are formed for the circulation of water. The exposed surface is specially treated such that

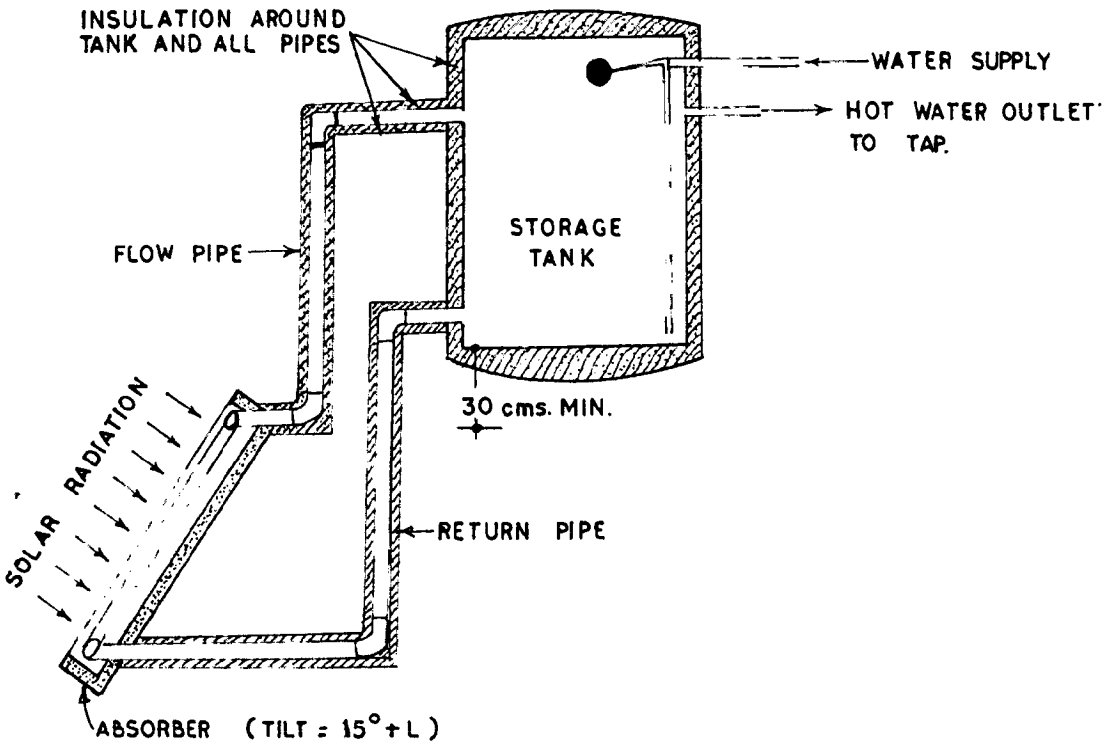

FIG. 4·23 SOLAR WATER HEATER

it absorbs maximum solar radiation but emits back little. Such selective coatings[26] require specialised methods and are costly. On the other hand matt black paints absorb maximum solar radiation but emit-low temperature radiation as well. The main advantage of this treatment is that it is cheap and can easily be applied on do-it-yourself basis.

The absorber unit consists of seven number of galvanised iron pipes of 19 mm diameter and fitted at 10 cms centre to centre on to two (GI) pipe headers 25 mm diameter. A 36 SWG aluminium sheet is wrapped on to the pipe network overlapping half the diameter for each pipe and then tied to this with a G.I.binding wire. This ensures that each tube is in good thermal contact with the plate. Two fine coats of lamp-black paint (lamp black dispersed in spirit shellac solution) with an additive (zinc dust) to make the paint more adhesive and thermally stable are sprayed to the absorber plate. It has already been shown(in sect on 4.2) that the type of collector gives maximum efficiency per unit cost. It is estimated that for an average family of five persons of a household in India, 140 litres of water at a temperature of 50°C is the requirement. Two absorbers each of area 1.0 m^2 are adequate to cope with the above demand.

2. Insulation: Conduction heat losses from the rear of the collector plate are reduced by lagging with suitable insulation on the back side. A number of insulating materials

are available in the country. Table (4.3) presents a list alongwith their thermal conductivity values at normal temperatures.

3. Transparent cover: The purpose of the transparent cover is to trap the sun's heat and to prevent the low temperature radiation loss from the absorber surface.

Loss of heat from the absorber plate is restricted in two ways by the transparent cover. Firstly, convective heat losses as a result of air movement are minimized and, secondly, heat losses due to low temperature radiation are decreased because the glass cover is opaque for long wave radiation.

The effect of one glass cover or plastic cover and two glass cover, on the overall performance is studied and will be discussed later.

4. Absorber box: The absorber box provides a weather proof container for the flat-plate collector and insulation and provide a support for the transparent cover. It may be constructed of wood, mild steel or glass reinforced plastic. Because of perishable nature of wood mild steel boxes are recommended.

The overall dimensions of the box are 130x92x16 cm.

4.71 STORAGE TANK:

The size of the storage tank depends on the daily demand of hot water and also on the radiation intensity

TABLE 4.3:

Thermal Conductivity(K values) of some insulating materials at medium temperature.

Material	Density (Kgm/m^3)	Thermal Conductivity (Kcal/m hr^oC)
Vermiculite (Loose)	264	0.069
Thermocole	22	0.027
Cork Slab	173	0.037
Saw dust	188	0.044
Mineral wool slab	192	0.035
Glass wool	65	0.032
Crown fibreglass	32	0.032
Straw	-	0.049
Foam plastic	24	0.027

available at the place. Because of the Indian custom of taking a bath in the morning hours, the tank should be well insulated.

Galvanized iron tank of 67 cms diameter and 73 cms height is taken. Float valve is fitted at a height so that the water capacity of tank becomes 140 litres. This tank is insulated all around by 7.5 cms fibreglass which in turn protected from weather by a cover of 24 gauge G.I.sheet.

The temperature is controlled by a safety thermostat fitted at the middle of the tank, which is set at 60°C. An immersion heater is fitted at one third the height of the tank so that on cloudy days or when the load is more than the design value this can be pressed into service.

Cold water enters the tank through a float valve which maintains the level of water in tank. Beneath the float outlet is fitted G.I.pipe of 15 mm diameter. The other end of pipe goes up to the bottom of tank so that cold water rose directly to the bottom.

The storage tank is placed over a stand such that its bottom is atleast 30 cms above the top header of the absorber.

It is a common practice to connect the flow pipe (fig 4.23) to the storage tank at a height equal to about two-thirds the height of the tank. The reason for this are

two fold, viz, to promote stratification of the water and to increase the head of water causing the circulation pressure.

4.72. Circulation system:

Various methods of circulating the heated water have been proposed. The simplest for normal domestic conditions would appear to be a system depending on natural convection in which the heated water rises naturally towards the top of the circuit, and is replaced beneath by colder water. Such a system has the advantage that it functions automatically whenever the solar heat input is high enough to heat the water in the absorber to a temperature above that of the water at the bottom of the storage tank. This makes it necessary to place the whole of the absorber at least 30 cms below the level of the bottom of the tank. It also requires that the connecting pipes should be as short as practicable, and should be effectively insulated.

4.73. Location of collector and tank:

The collector should be inclined to the horizontal to an optimum angle which depends on the latitude of the place as discussed in chapter 3. It should also face towards the south, with a distinct preference for an orientation a few degrees towards the west, to take advantage of the greater heating effect of the afternoon sun as discussed in chapter 3.

With a house having a roof of suitable slope and elevation of ridge, the collector might conveniently be located on the roof, towards the lower edge of a section facing south to south-west. If the ridge height will permit, the storage tank could then be located in the attic space above the ceiling, near the point where the ridge is highest. But whatever positions are chosen for the two components, their relative positions must conform to the requirements mentioned earlier, i.e. a rise of atleast 30 cms must be allowed between the top of the collector and the bottom of the tank.

Another favourable position for the collector might be as an awnings or louvre mountings at top windows in a southward facing wall. The tank may be located between roof and the ceiling, without extending the piping system unduly.

In case of flat or low-pitched roofs extra framework is necessary for the installation of the collector and tank, as shown in fig 4.24.

4.3 TESTING OF DOMESTIC SOLAR WATER HEATER:

In order to assess the performance of efficiency of solar water heater a testing programme was devised in which a number of practical domestic conditions were simulated by drawing off various quantities of water at different times during the day. The test programme is summarised in Table (4.3).

TABLE 4.4: Performance testing programme for domestic solar water heater (140 litres).

Test No.	Time (Hours)	Nature of test.
1.	09.0	Fresh water filled
	16.0	Run off all hot water
2.	03.0	Fresh water filled
	09.0 (next day)	Run off all hot water
3.	09.0	Fresh water filled
	13.0	Run off 30 litres hot water
	03.0 (next day)	Run off all hot water.
4.	09.0	Fresh water filled
	13.0	Run off 70 litres hot water
	03.0 (next day)	Run off all hot water
5.	03.0	Fresh water filled
	10.0	Run off 15 litres hot water
	12.0	Run off 15 litres hot water
	14.0	Run off 15 litres hot water
	16.0	Run off all hot water
6.	09.0	Fresh water filled
	03.0 (next day)	Run off 70 litres hot water
	11.0	Run off 15 litres hot water
	13.0	Run off 15 litres hot water
	15.0	Run off 10 litres hot water
	17.0	Run off 30 litres hot water
	03.0 (next day)	Run off all hot water.

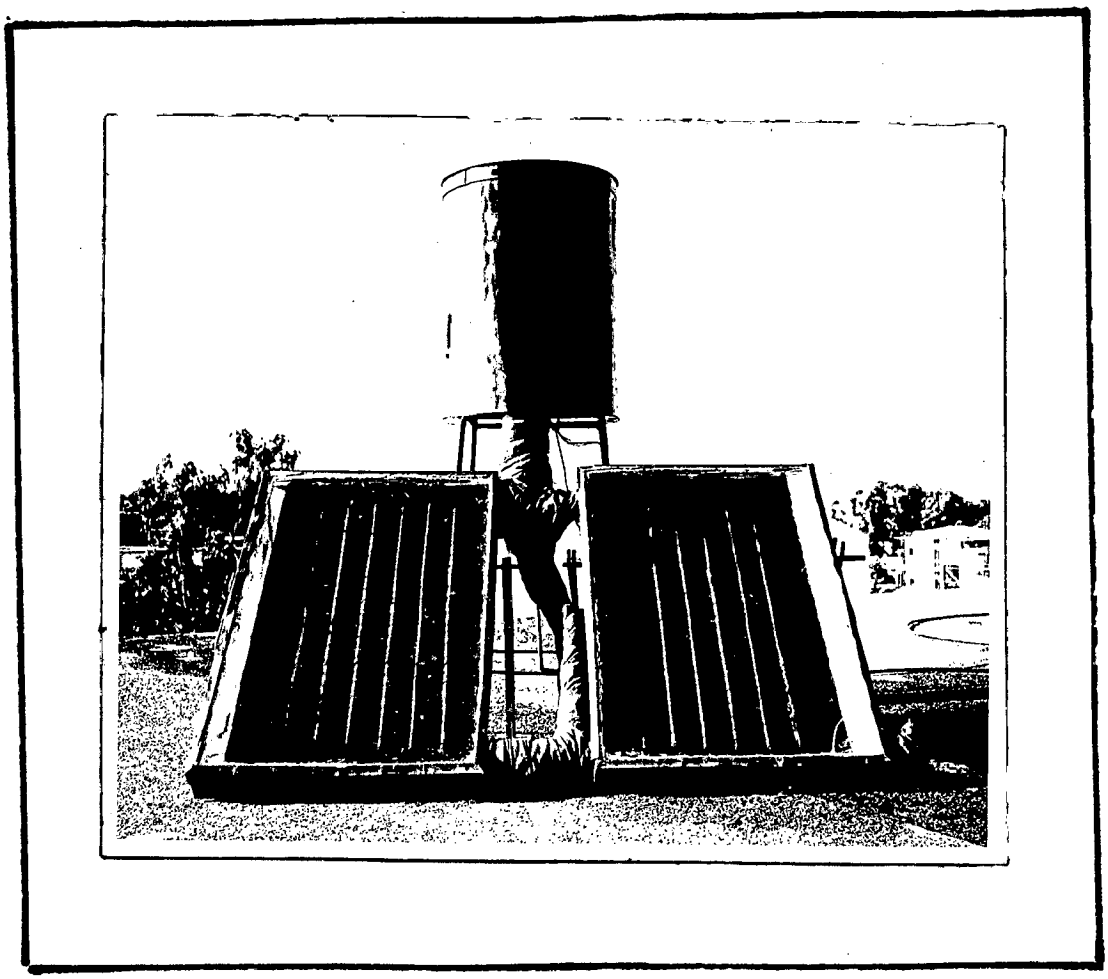

FIG.4.24: PHOTOGRAPH OF DOMESTIC SOLAR WATER HEATER (140 LITRES)

From measurements of water temperature drawn off and total solar radiation incident on the absorber face, the efficiency was calculated as the ratio of total heat content of water drawn-off to the total heat energy incident on the absorber face.

Typical results on a winter day are graphically represented in fig 4.23 for test No.2 where hot water was stored for an overnight period. Fig 4.23(a) shows the variation of mean water temperature in tank at various hours of the day. It is seen that maximum mean tank temp. is of the order of 65°C at about 16 hours and it is 40°C in the next day morning. Fig 4.23 (b) shows the temp. of drawn-off water quantities. We see that as the water is drawn from the tank, initially the temperature slightly increases and then slowly decreases upto 120 litres, beyond which there is a rapid fall in temperature.

A prototype unit was installed at a residence at Roorkee to study its performance under actual domestic use. The temperature data as reported by one of the user is shown in fig 4.20. From this figure it is clear that except for few days (cloudy) the heater gives satisfactory results. The values reported are without making use of the immersion heater. The reported values are at 6.0 pm on every day while the heater is designed for the maximum temperature which occurs at about 4.0 pm. From this it is evident that the solar water heater can provide hot water at

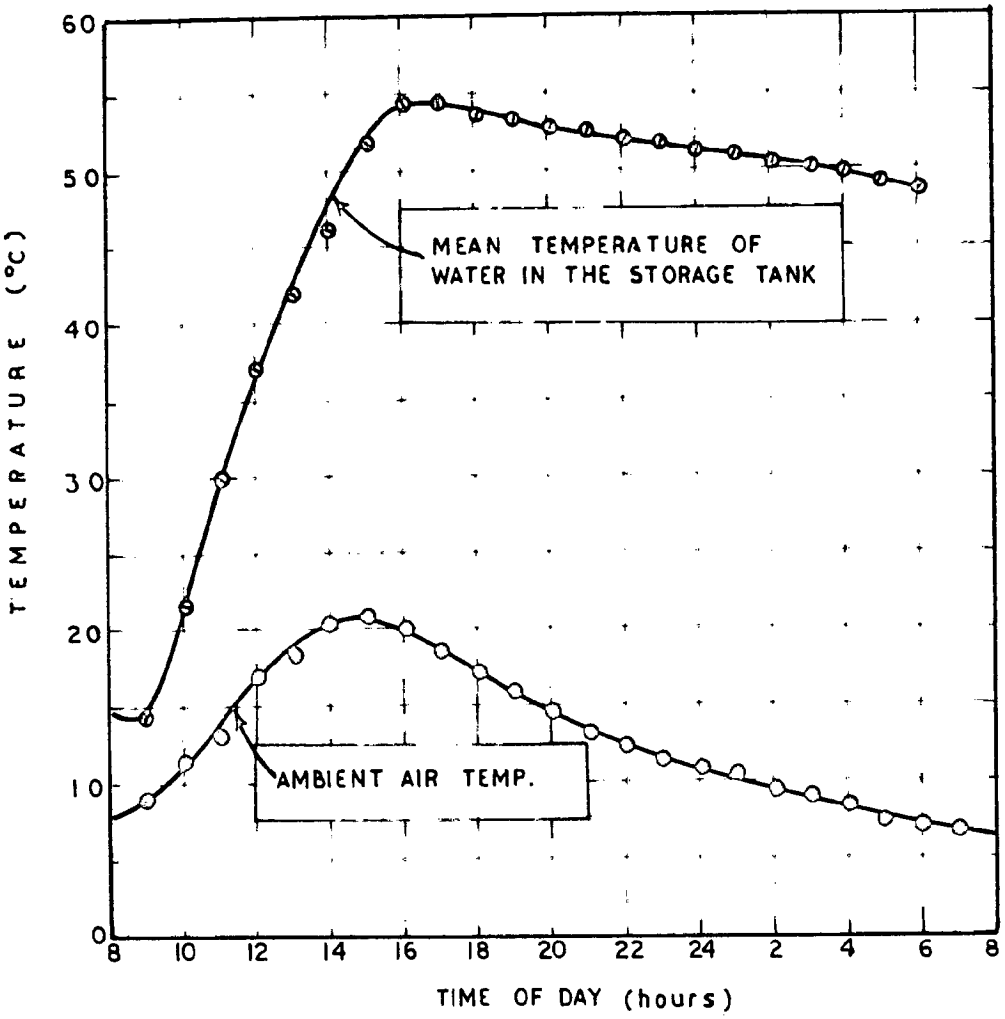

(A) Typical graph showing temperature with time at middle of tank.

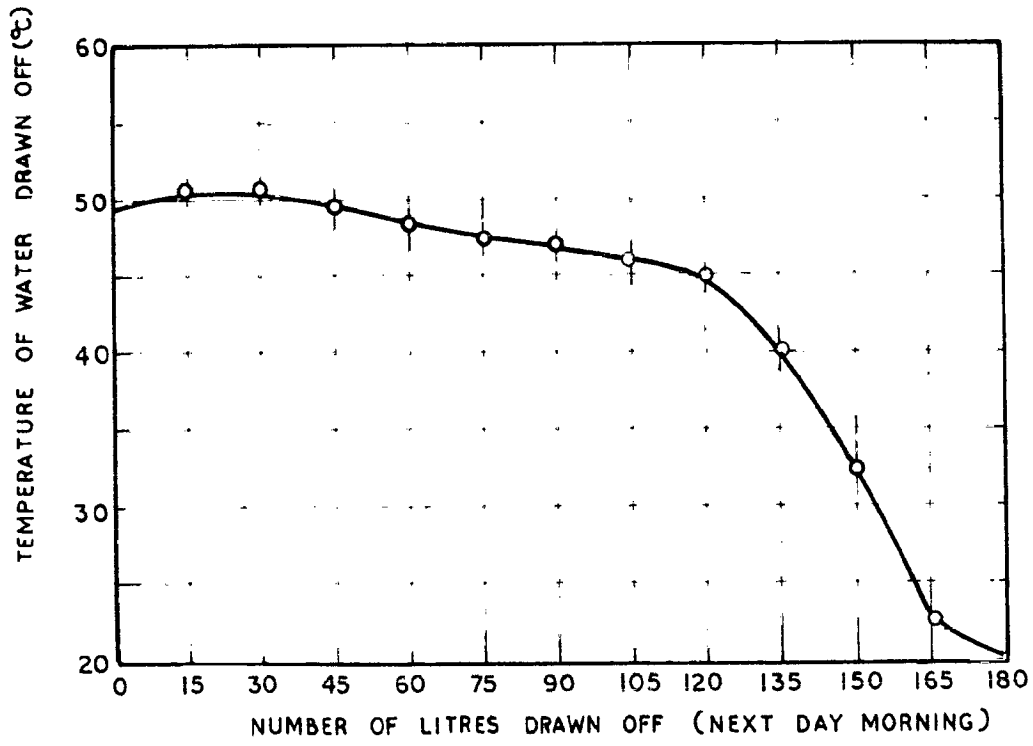

(B) Graph showing temperature variation of water with quantity drawn off.

FIG. 4·25 TYPICAL RESULTS FOR TEST No. 2.

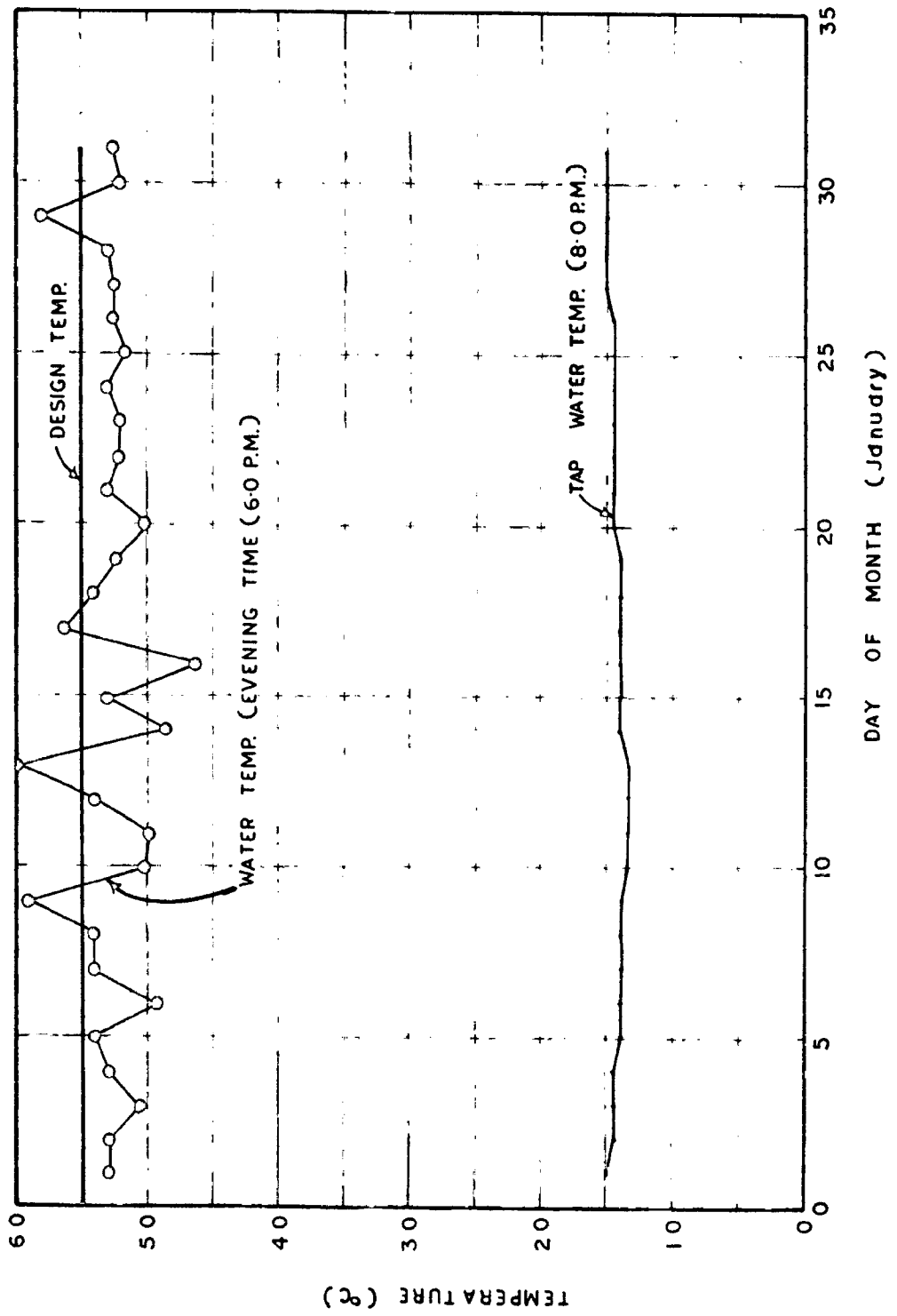

FIG. 4.26 MONTHLY PERFORMANCE OF DOMESTIC SOLAR WATER HEATER

temperature as per design. The over night heat losses from the storage tank result in drop in temperature of the order of 10 percent.

(a) Influence of the test :

It is quite obvious that the nature of test will have a significant effect on the efficiency of a solar water heating system. Maximum efficiency will be obtained if the water is drawn off at short intervals without allowing the temperature of the water to rise much in excess of outdoor air temperature, i.e. heat losses are restricted to a minimum. Typical results for various tests are depicted in Fig.4.27.

The influence of the type of test can be seen from the results obtained in two extreme cases in tests 2 and 6. A difference in efficiency of about 10 percent was obtained. In test 2 the water was allowed to heat up undisturbed throughout the day and was stored overnight before it was drawn off the following morning, this allowed substantial heat losses to take place in the late afternoon and overnight, and thereby reduced the efficiency. In test 6, on the other hand, water is drawn off at hourly intervals throughout the day, in such a way that the water temperature does not fall below 30°C and all the remaining hot water was drawn off at 4.0 pm. Heat losses from the absorber and water go tank during the day were therefore reduced considerably. Here though the efficiency was higher in

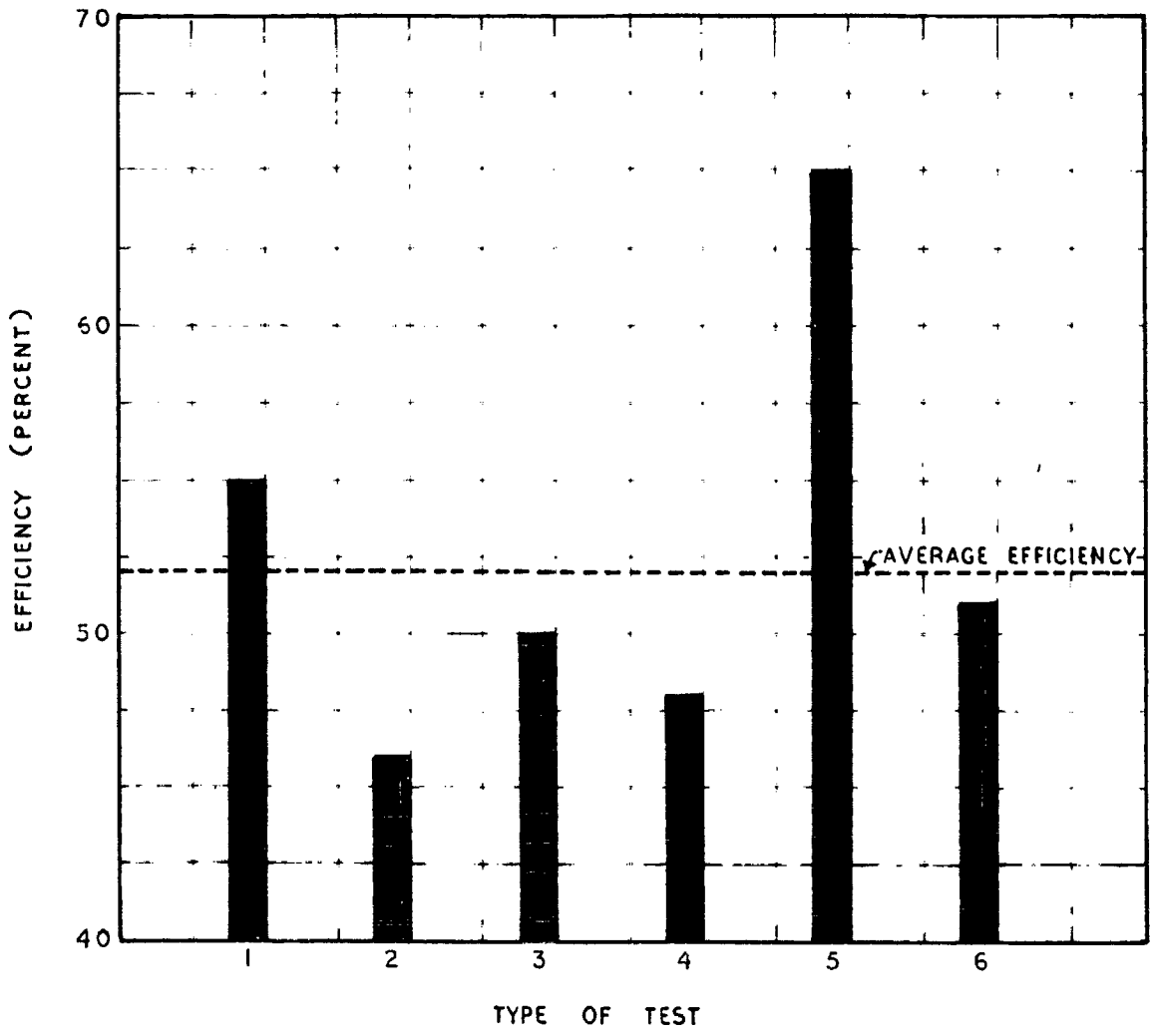

FIG. 4·27 VARIATION OF EFFICIENCY WITH TYPE OF TEST

comparison with the previous test, the rise in temperature of water was restricted.

(b) Influence of weather:

The solar water heater was studied in summer and in winter conditions. The results are summarised in Table(4.6). It can be seen that practically the efficiency does not change much throughout the year. Average difference of about 3 percent is observed. However, it was observed that the maximum storage temperature was higher in summer as compared to that in winter. It may be because of the initial water temperature (top) in summer is at higher level.

(c) Influence of type of insulation:

Saw dust and Fibre glass insulation, both about 5.0 cm thick, were tested in the absorber box to determine their relative insulating properties. It can be seen from table (4.6) that the efficiency is not significantly affected by the type insulation used.

Sawdust, however, has the disadvantage that it settles at the lower end of the absorber. Fibreglass, mat are available in various lengths, thickness and densities and can be easily cut to the required dimensions.

(d) Influence of transparent cover:

The use of double glazing on the absorber gives better performance where the outdoor temperatures are too low. As the double glass reduces the losses to the outside

it also reduces the solar heat input to some extent. A comparison of efficiency in case of single and double glazing is made in Table 4.0. It is seen that though the double glass gives better performance. It is not sufficiently high to justify the extra cost of additional glass sheet, under our climatic conditions.

4.0. LARGE SIZE SOLAR WATER HEATER:

There is an increasing demand for large size solar water heaters such as in hospitals, hostels and large kitchens. In such large systems it is impractical to mount the storage tank above the absorber level and a forced circulation system is to be used. Here a pump is required to circulate the water through the absorbers and the storage tank. Some sort of controls is also required for the operation of water pump.

The additional points pertaining to the forced circulation system as compared to natural circulation type of solar water heater are discussed below:

4.01 Collector area determination:

A simple way of estimating the absorber area is given below. Suppose that the cold water temperature is $10^{0}C$, and the water heater is to deliver 600 litres of water per day at $60^{0}C$, then the mean daily energy require-

TABLE 4.5:

Comparison of efficiencies of Domestic solar water heater (140 litres) with different nature of tests for various influencing parameters :

Nature of test	EFFICIENCY		EFFICIENCY		EFFICIENCY	
	Summer	Winter	Fibreglass insulation	Saw dust insulation	One glass cover	Two glass cover.
1	0.63	0.56	0.56	0.54	0.56	0.60
2	0.47	0.46	0.43	0.44	0.48	0.50
3	0.51	0.50	0.50	0.47	0.50	0.53
4	0.50	0.43	0.49	0.46	0.43	0.51
5	0.68	0.65	0.63	0.63	0.65	0.69
6	0.55	0.51	0.51	0.49	0.51	0.55
Average efficiency	0.59	0.52	0.52	0.50	0.52	0.58

ment will be

$$Q_L = 600\ (60-10)$$
$$= 24000\ \text{Kcal/day}.$$

Now the mean daily available insolation on a surface inclined at about 45^0 to the horizontal and facing south at Roorkee for the month of January is obtained as

Q_A = Daily total solar radiation on horizontal surface x average daily conversion factor.

$$= 360 \times 1.6\ \text{Cal/cm}^2\ \text{day}$$
$$= 5800\ \text{Kcal/m}^2\text{day}$$

If the collector efficiency is assumed to be 60 percent, then the useful energy will be

$$Q_u = 5800 \times 0.6$$
$$= 3200\ \text{Kcal/m}^2\text{day}$$

and thus the collector area (A) will be

$$A = \frac{\text{energy required}}{\text{energy available}} = \frac{Q_L}{Q_u}$$
$$= \frac{24000}{3200} = 8.6\ \text{m}^2$$

For simplicity it can be assumed that 1 m^2 of absorber area will heat 70 litres of water upto 65^0C.

4.03 <u>Interconnection of absorber banks</u>

In large size solar water heaters, a number of absorbers are used, which are mostly connected in parallel (cascade). In this arrangement cold water enters via the

lower header of the first absorber, flows through the absorbers and is discharged from the top header of the last absorber. However, it is doubtful whether efficient flow of water through the first few absorbers is ensured in this system. This may result in high plate temperatures and consequent higher heat losses and thereby lowering their heat collecting efficiency.

An experimental study has been carried out on different modes of arrangements of absorbers with a view to evolve a most efficient and economical system. The following factors are taken into consideration in evaluating the relative performance of the arrangements studied:

1. Uniformity of flow,
2. Frictional head losses,
3. Overall efficiency of the system,
and 4. Energy consumption by the pump.

Experimental arrangement:

Six absorbers each having dimensions 100x70 cms as optimised earlier were connected by transparent high density polyethlene pipe with gate valves in both upper and lower headers. Series, parallel or in mixed mode connecting arrangements can easily be made by suitable combinations of opening and closing of gate valves.

Temperatures were measured by Cu-Const thermocouples of 33 S.W.G. Six thermocouples one each at the centre of the absorber plate were fixed and their outputs were continuously recorded on a multipoint millivolt chart recorder. The pump used for water circulation was operated continuously during the period of observations in each case. The various modes of connecting the absorbers, studied are shown in fig 4.28.

The temperatures of all the six absorber plates in case of parallel (A), series (B), series parallel[27] (C) and true parallel (P) mode of arrangement are shown in fig 4.29, 4.30, 4.31 and 4.32 respectively. It can be seen that out of all these arrangements only in case of true parallel 4.32 (P), the plate temperatures are uniform. This confirms the uniformity of flow in all the absorbers which is further confirmed by visual observations.

Energy consumption by the pump:

The energy consumption by the pump forcing the same quantity of water in different types of arrangement has been recorded and is shown in fig 4.33. Here the flow rate varies for different types of arrangements depending upon the frictional losses. For example, for pumping 20,000 litres of water, the energy consumed in series arrangement(4.30C) is 5.5 KWH, in series parallel (4.29 C) is 5.0 KWH, in

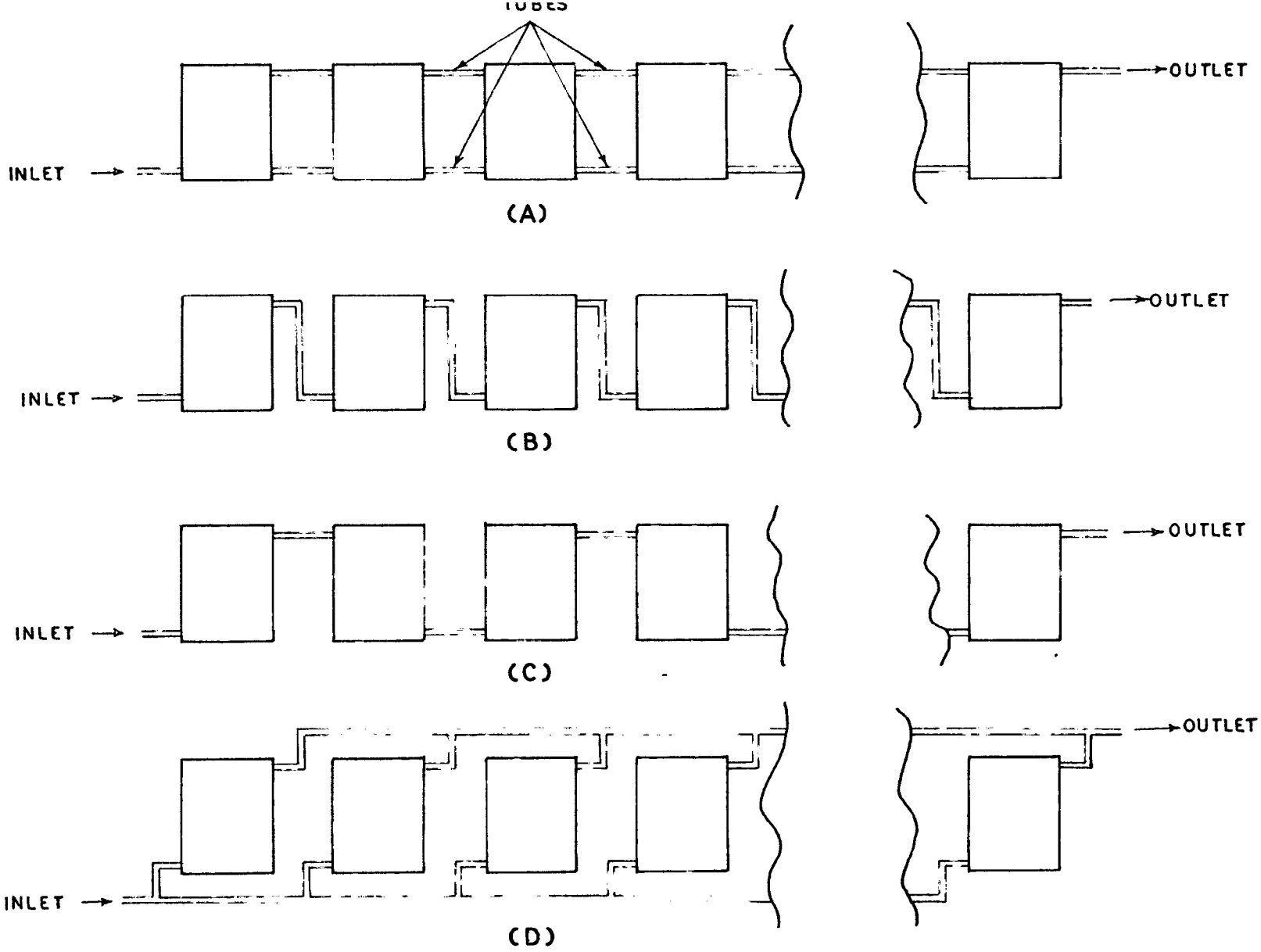

First sheet

FIG.4·28 VARIOUS MODES OF ABSORBERS ARRANGEMENT

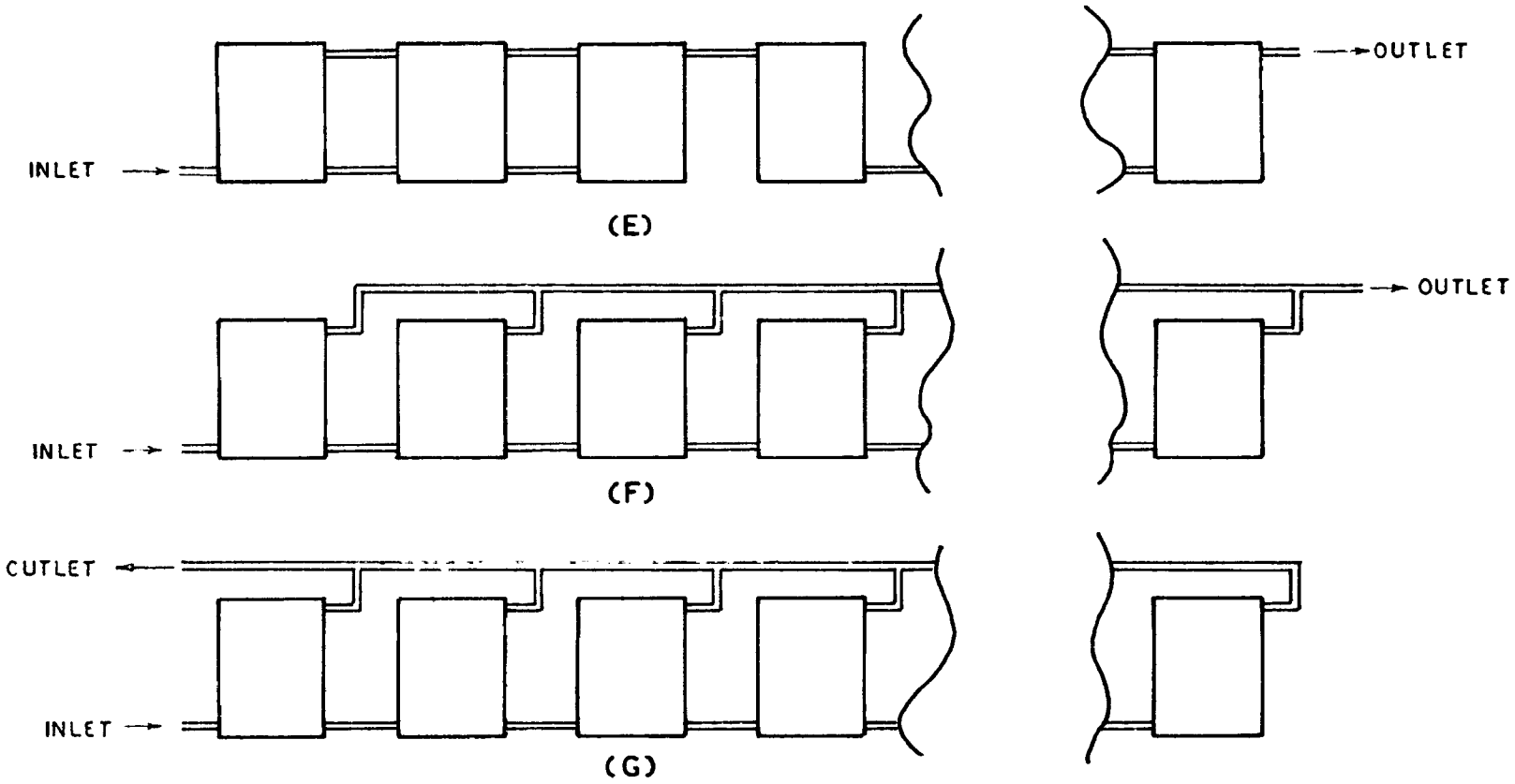

Second sheet

FIG. 4-28 VARIOUS MODES OF ABSORBERS ARRANGEMENT

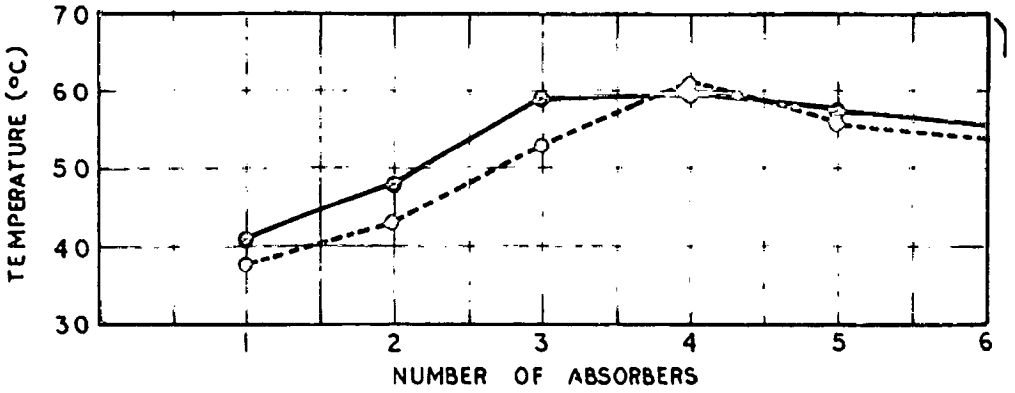

FIG.4·29 PLATE TEMPERATURES WHEN ALL ABSORBERS ARE IN PARALLEL (A)

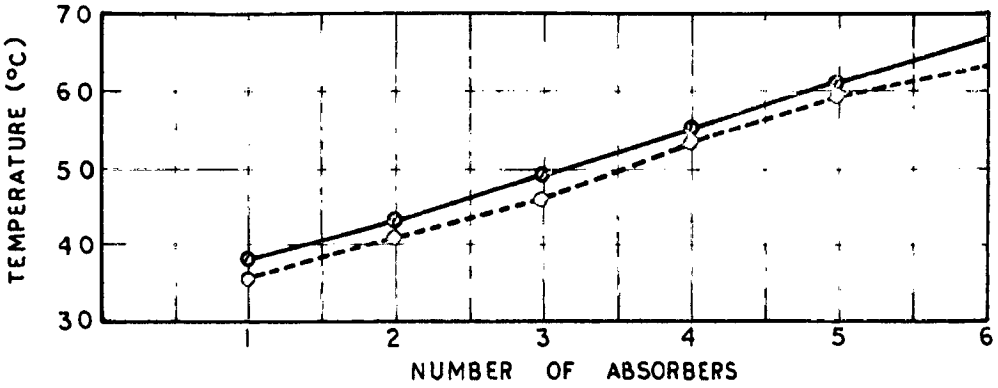

FIG.4·30 PLATE TEMPERATURES WHEN ALL ABSORBERS ARE IN SERIES (B)

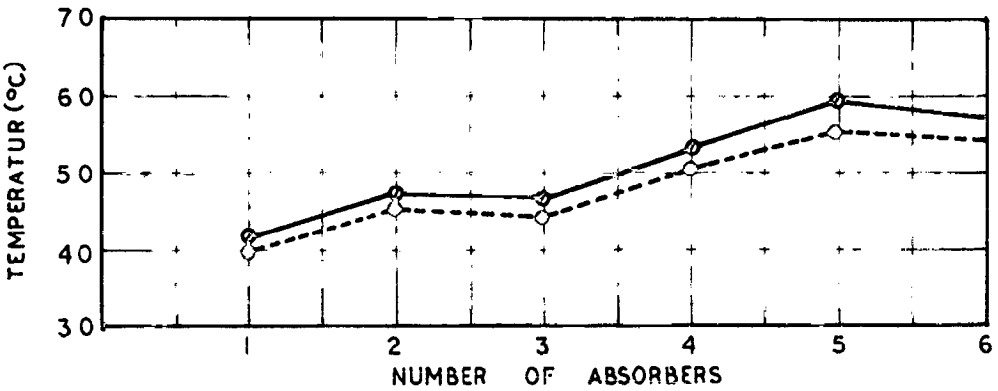

FIG.4·31 PLATE TEMPERATURES WHEN ABSORBERS ARE IN SERIES PARALLEL ARRANG-EMENT (E)

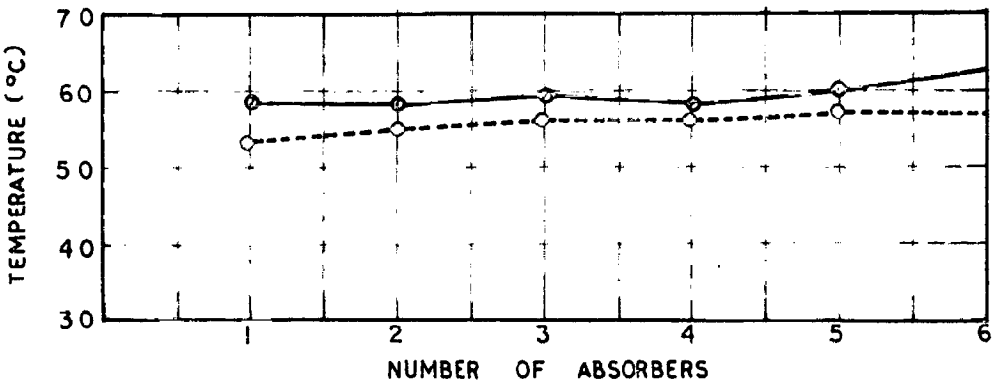

FIG.4·32 PLATE TEMPERATURES FOR RECOMMENDED ABSORBER ARRANGEMENT (F)

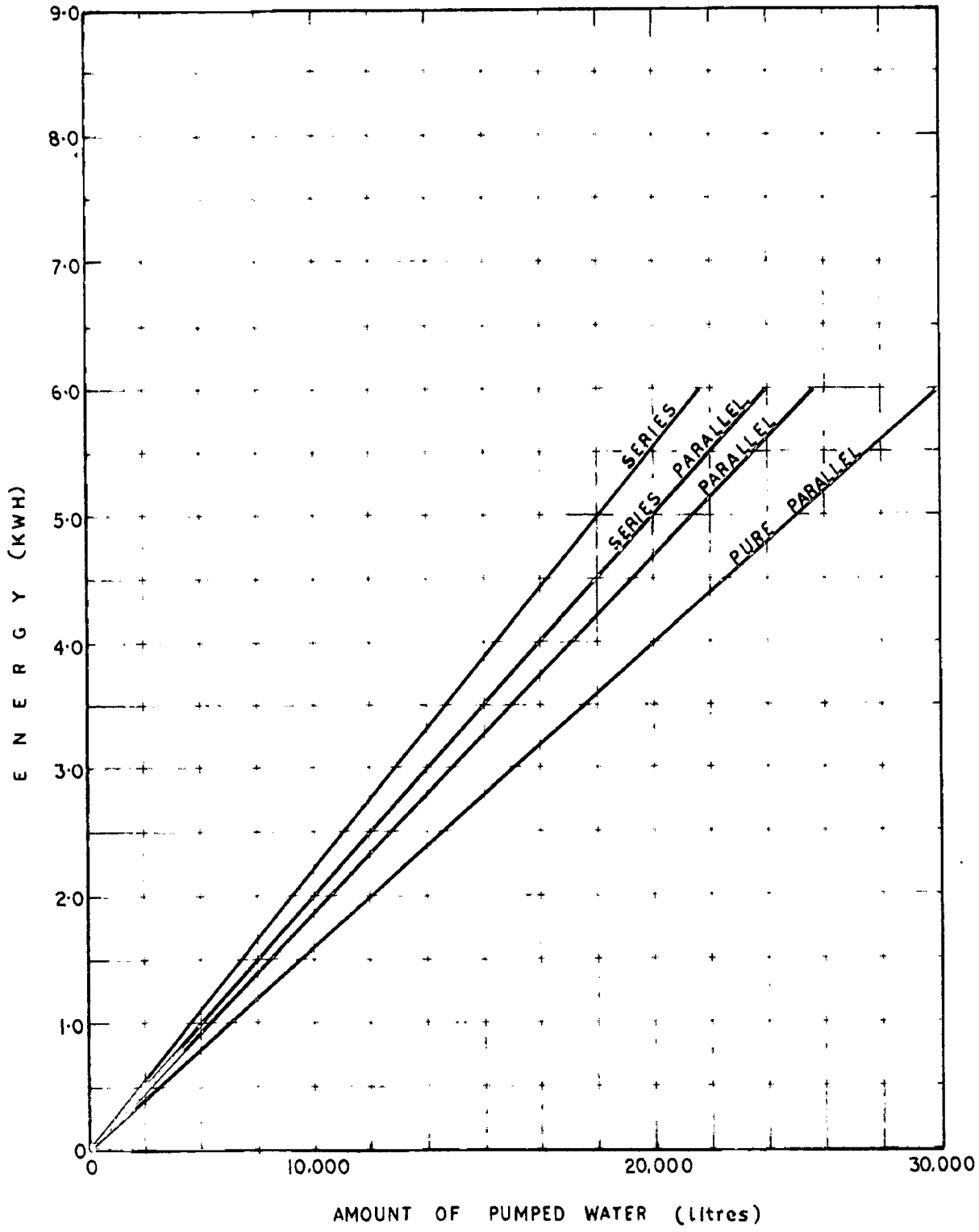

FIG. 4·33. ENERGY CONSUMPTION FOR VARIOUS MODES OF COMBINATION

cascade (4.20A) is 4.7 KWH, and in true parallel (4.20F) is 4.0 KWH. Thus on the basis of energy consumption as well, the true parallel arrangement proves to be the best.

Frictional head losses:

Frictionalhead losses offered by the absorbers will be a direct measure of the pumping cost and the capacity of the pump to be used. The head loss by friction was measured by means of a U-tube connected at the inlet and outlet of the collectors successively. Fig.4.34 illustrates the effect of connecting two absorbers in series on the frictional head loss for different flow rates. The head losses for various flow rates and for various modes of connecting six absorbers are shown in fig.4.35. The slope of the curves suggest that the flow in absorbers is turbulent even at low flow rates. It can also be seen from the curves given in fig.4.35, that the head losses are minimum in case of true parallel arrangement fig.4.23(F). So one could safely conclude that with this type of arrangement, for pumping the same amount of water, less energy will be consumed by the pump and also a pump of low capacity can be employed.

4.93 Flow rate optimization:

It is a well known fact that the heat transfer

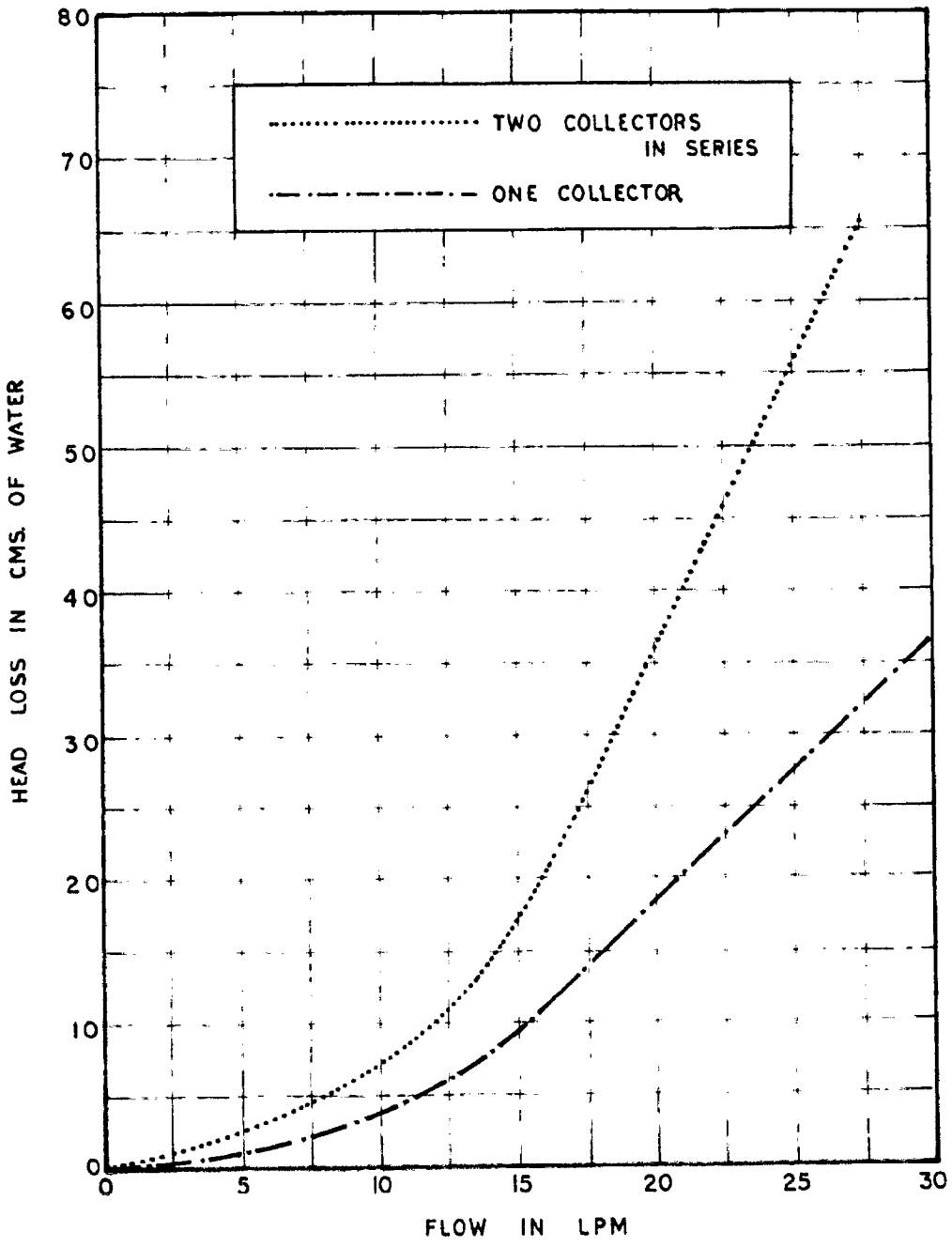

FIG. 4·34 HEAD LOSS DUE TO FRICTION WHEN COLLECTOR IN SERIES FOR VARIOUS FLOW RATES

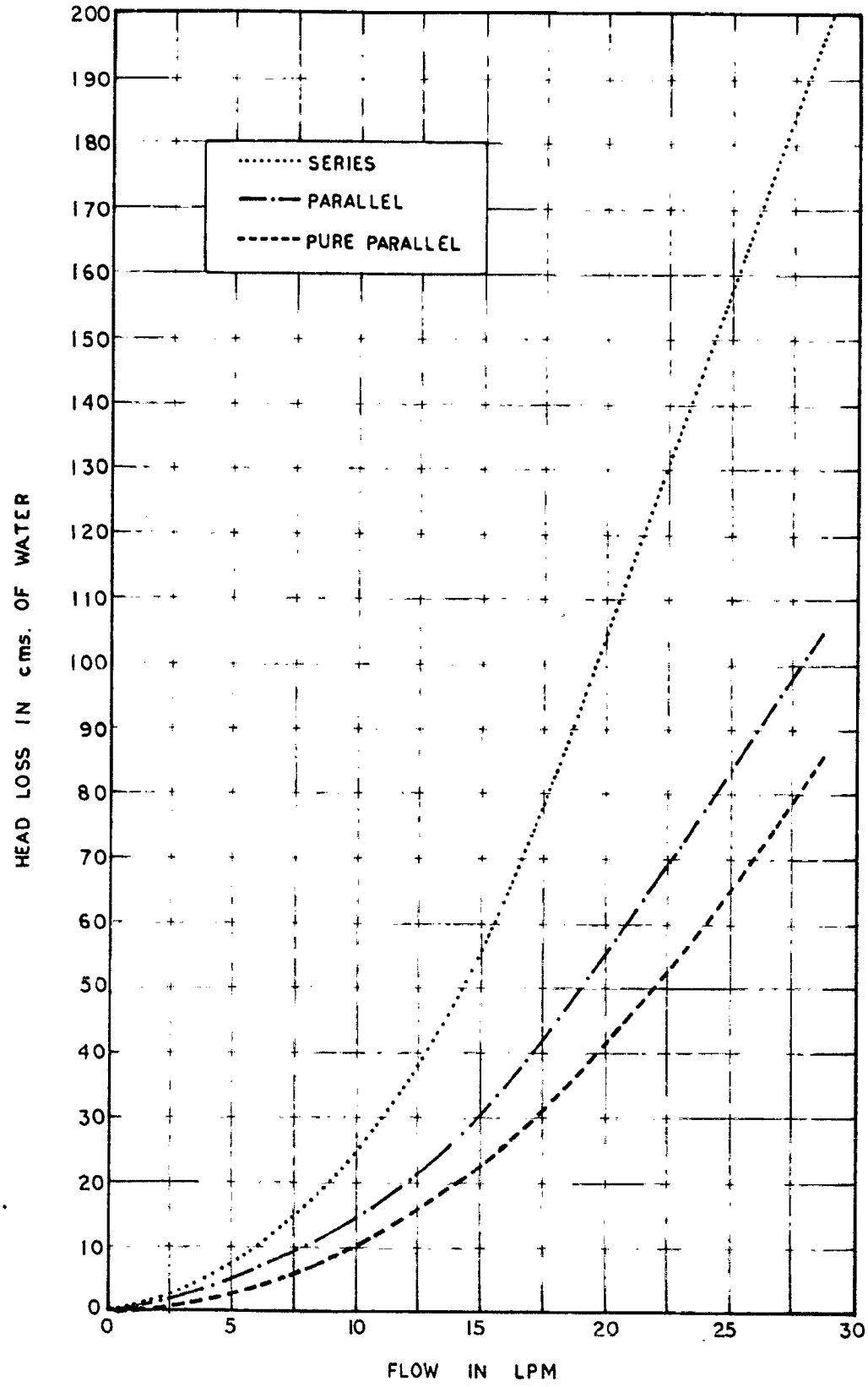

FIG. 4.35 HEAD LOSS DUE TO FRICTION FOR VARIOUS FLOW RATES

from the tube's inner wall to a fluid flowing within the tube can be considerably increased by increasing the flow rate of the fluid. Theoretically Bliss [28] has shown that the rate of useful energy collection can be increased three times if the flow changes from laminar to turbulent. But it has been shown by Sheridan[29] and Close[30] that the flow rate has negligible effect on the daily total heat collected in a closed system by using analog and digital computer methods respectively.

Experimental tests were carried out on clear days at various flow rates to verify these findings. The large size solar water heater used for this study had six absorbers of total area 8.4 m^2 and storage capacity of 600 litres. A pump of 0.75 H.P. was used to get the required flow rates. A water meter and a stop watch was used for the measurement of flow rates. The pump was kept in use from 8.0 A.M. to 4.0 p.m. This time is chosen since by experience it is observed that heating starts nearly at 8.0 AM and maximum temperature in the storage tank reaches at about 4.0 p.m. The summarised results for various flow rates i.e. 20, 40, 60, 80 litres/m^2hr are given in Table 4.6.

From this table it will be noted that the flow rate has got negligible effect on the overall performance of the system. One interesting point here is that when these results are compared with the natural circulation type solar water heater we find that efficiency is almost

TABLE 4.6: Effect of flow rate on the performance of forced circulation solar water heater (600 litres)

Flow rate litres/m^2hr	Time (hours)	Water temp. in the tank ^oC	Total heat collected Kcal/day	Total insol. on chamber, Kcal/day	Efficiency of collection percent.
20.0	8.0 A.M. 4.0 P.M.	16.0 58.0	24000	43510	55
40.0	8.0 A.M. 4.0 P.M.	16.0 60.0	25200	44010	57
60.0	8.0 A.M. 4.0 P.M.	17.0 58.0	24600	43330	56
80.0	8.0 A.M. 4.0 P.M.	17.0 59.0	25200	43920	57

the same. It appears that, from a performance point of view, there is no advantage to be gained by the use of forced circulation, in a closed system.

4.04 Comparison of control systems:

An automatic control for the pump is essential though it is an added expense in systems with forced circulation. The types of control systems that are applicable for the forced circulation water heating systems are : (1) time switch, (2) temperature set control, (3) radiation set control (4) differential control.

A simple control is a time switch which would switch the pump, and off at predetermined times in the morning and afternoon. Its setting could be altered for summer and winter conditions so that advantage could be taken of the longer summer days. Its main disadvantage is that it would operate irrespective of whether there is sufficient solar radiation for heating purposes or not.

In a temperature set control device a commercial bi-metallic, on-off thermostat of the type used in ovens, whose sensitive element is placed in the outlet of the heat absorber is used. The thermostat is set at the desired temperature. The pump switches on automatically when the outlet temperature equals or exceeds the set

temperature of the thermostat. The disadvantage of this arrangement is that the pump may continue running for some time in the evening without any heat gain to water in the tank.

In the radiation set control a radiation sensor fixed at certain level is used. The pump is switched on or off according to whether incoming radiation is greater or smaller than some predetermined minimum.

A more elaborate but costly is a differential control developed by Chinnery[31] in South Africa. Here the cost of control system is very high and the life of control is a function of a number of transistors and battery used in the circuit. A simple and of low cost differential circuit is developed by the author[37] and tested in the prototype unit. In the circuit a thermostat similar to the one in the temperature set control arrangement is fitted at the outlet of the last absorber and is connected in series with an another direct type thermostat which in turn is fitted in the bottom of storage tank. In this arrangement, the pump circulates water only when the outlet temperature equals or exceeds the water temperature in the tank, thereby always adds the energy to the system.

A detailed experimental study is made to study the effectiveness of various control devices. These

devices were tested at various flow rates such as 20, 40, 60 and 80 litres/m^2hr. The summerised results are shown in table 4.7. From this table it appears that from practical point of view the collection efficiency is independent of the type of control. But in case of time switch control the pump runs continuously throughout the day and thus increases the running cost. Similarly in case of set temperature and set radiation control the running cost was high as compared to differential control. So differential controler is expected to be more efficient.

4.05 Development of a computer model:

Here a rational approach to the system analysis using a digital computer has been developed and with its help the effect of insolation rate, absorber areas for a fixed storage capacity and storage capacities for a fixed absorber area on the overall performance was studied.

The basic models developed separately by Sheridan, Bullock and Duffie[29], and Close[30] have been further extended and simplified to suit the practical conditions.

As before a pump is used for the circulation of water through the absorber and storage tank. It is assumed that pump runs continuously throughout the day. The only condition being that it is switched only when the absorbed energy by the collector is equal to or more than the outward

TABLE 4.7:

Collection efficiency (percent) for various control systems in case of forced circulation solar water heater (600 litres).

Flow rate (litres/m^2) hr	Differential	Set temperature	Set radiation	Time switch
20	54	52	53	56
40	55	53	53	57
60	56	53	54	56
80	56	53	54	57

losses. This condition automatically takes place in natural convection type of solar water heater.

It is desired to find out the storage temperature as a function of time, and to compare the integrated values of various energy quantities.

Under steady state conditions the rate of useful energy collection from the collector is given as

$$\frac{d Q_u}{d\theta} = F_p A \left[H\tau\alpha - U_L (t_m - t_a) \right] - U_C \frac{dt_m}{d\theta} \qquad \text{-----(4.44)}$$

where t_m is the mean collector temperature and U_C is the thermal capacity of collector (Kcal/$^{\circ}$C).

This useful energy goes to the storage tank, part of this is used in increasing the enthalpy of water and part is lost to the outside, or

$$\frac{d Q_u}{d\theta} = m_s C_p \frac{dt_s}{d\theta} + U_T (t_s - t_a) \qquad \text{-----(4.45)}$$

where m_s is the storage capacity (Kgm), $dt/d\theta$ is the rate of rise of storage temperature and U_T is the tank overall heat loss coefficient (Kcal/$_{m^2}$hr$^{\circ}$C).

Here it has been assumed for simplicity that there is no absorption or loss of heat in the circulation pipes. Without much error it can also be assumed that the mean collector temperature is same as the mean storage temperature i.e. $t_m = t_s$.

By putting this value in equation (1.44) and rearranging equation 4.47 and 4.45, we got.

$$(m_s C_p + W_c)\frac{dt_s}{d\theta} = F_p A H (\tau\alpha) - (t_s - t_a)(F_p A U_L + U_T) \quad ----(4.46)$$

From equation (4.46) the value of storage temperature t_s can be predicted from the known climatic and design conditions.

The measured solar radiation H and ambient temperature t_a were expressed as fourier series and are as follows :

$$H = A_0 + \sum_{n=1}^{N} (A_n \cos n w\theta + B_n \sin n w\theta) \quad ---(4.47)$$

and $$t_a = C_0 + \sum_{n=1}^{N} (C_n \cos n w\theta + D_n \sin n w\theta) \quad ----(4.48)$$

Checking of model:

The system considered here was as follows: absorber area, 8.4 m^2; tank capacity (M_s), 600 litres ; no draw off water during experimentation. The collector loss coefficient and tank loss coefficient is assumed as 6.0 Kcal/m^2 hr ^oC and 2.0 Kcal/m^2hr^oC respectively. The thermal capacity of collector is found as 3.24 Kcal/$m^2{}^oC$. The value of plate efficiency factor (F_p) as described earlier is 0.95.

For a clear day Fig (4.36) shows the measured value of storage temperature alongwith the computed values. The measured solar radiation on the collector surface is shown in the upper curve of fig 4.36. It is seen that there is a very close agreement between the measured and computed values of storage temperature. As such the model is experimentally verified and now can be used for studying the effect of various design parameters.

The collection efficiency(η) which is defined as the ratio of useful energy collected to the total energy incident can be computed from the above observations as follows :

$$\eta = \frac{m_f C_p \, dt_a/d\theta}{HA} \qquad \text{-------(4.49)}$$

The efficiency so computed is shown in fig 4.37 alongwith the efficiency obtained from measured data. Again there is a very good agreement between the efficiencies obtained from measured and computed data.

Effect of absorber area :

Here the effect of varying absorber area for a fixed storage capacity m_s(600 litres) is studied. The flow rate was kept constant at 20 litres/m^2. It is also assumed that the overall heat loss coefficient from the collector plate to the outside air remains constant.

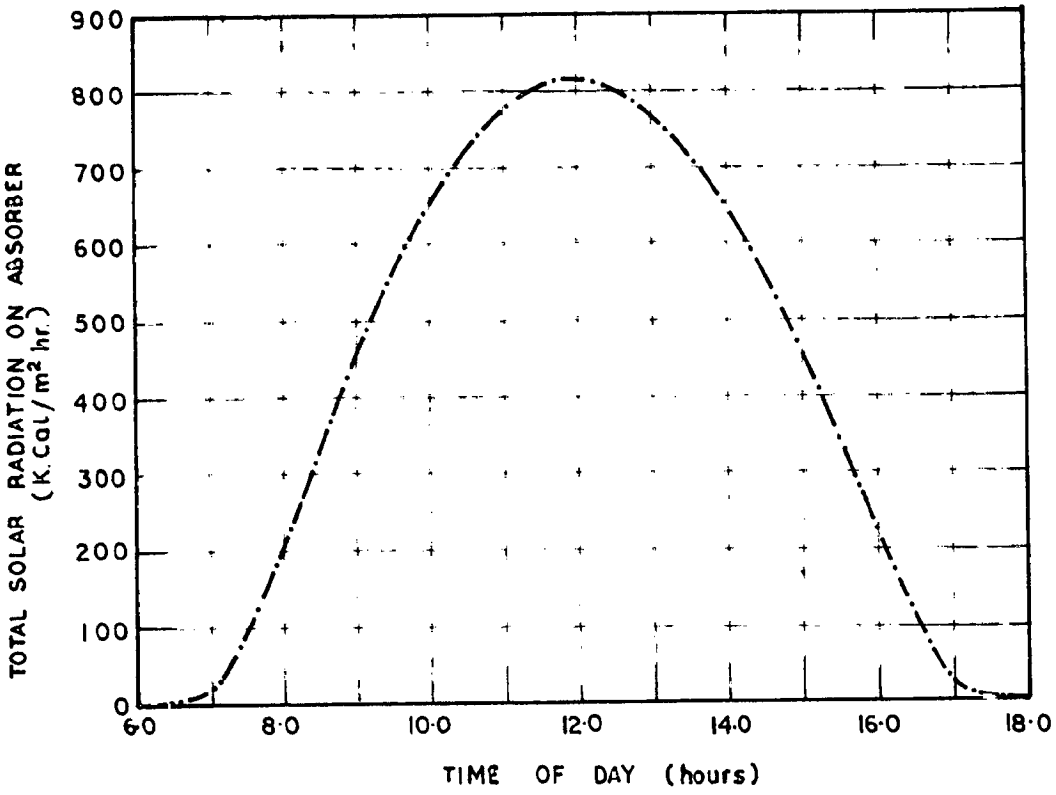

FIG. 4·36 (a) SOLAR INSOLATION ON OBSERBER SURFACE FOR TEST DAY

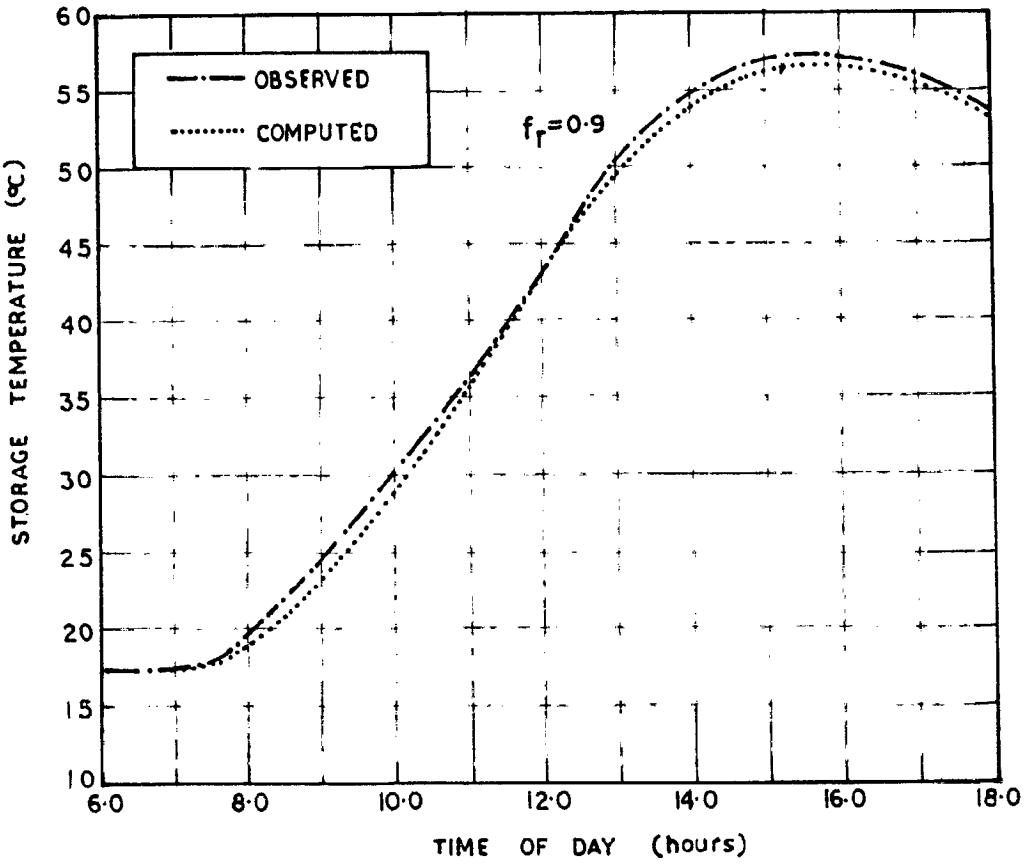

FIG. 4·36 (b) COMPARISON OF COMPUTED & OBSERVED STORAGE TEMPERATURES

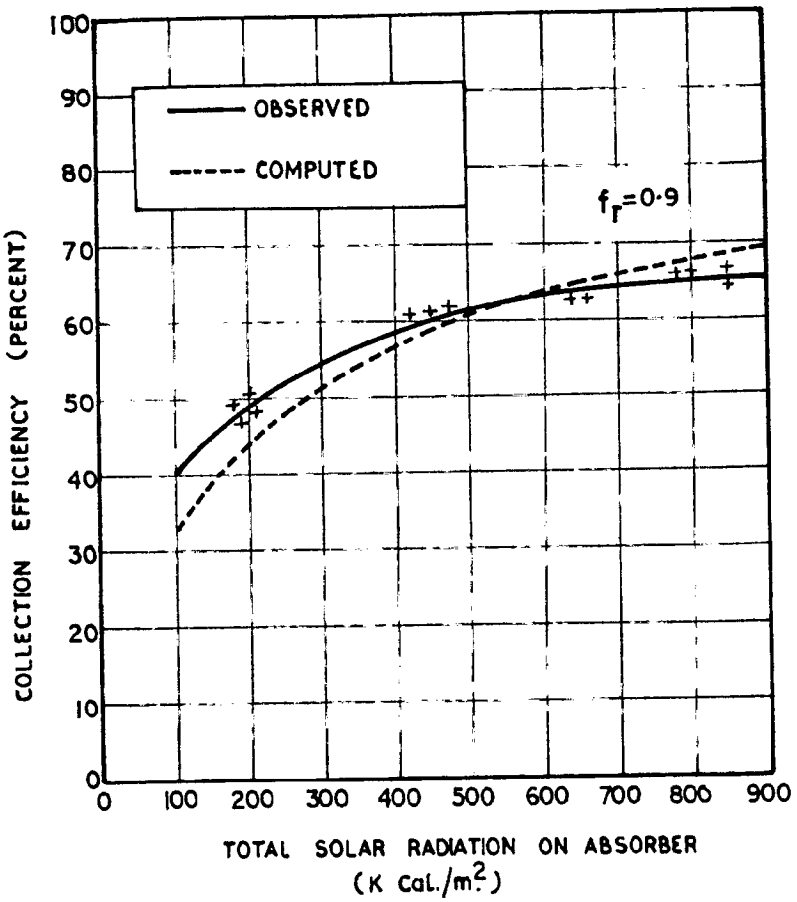

FIG. 4·37 COMPARISON OF COMPUTED AND OBSERVED COLLECTION EFFICIENCY

The hourly efficiencies computed with the help of equation(4.46) and (4.49) for various absorber area i.e. 4,8,12 and 16 m^2 are shown in fig 4.38(a). It is seen that for any fixed absorber area the collection efficiency first gradually increases reaches a maximum and then falls rapidly. It is also seen that as the absorber area increases the peak efficiency decreases and shifted towards the early hours.

The daily collection efficiency (η) is also determined as follows :

$$\eta = \frac{\text{daily useful energy into the system}}{\text{daily solar energy incident on the collector}}$$

$$= \frac{\int Q_u \, d\theta}{\int H \, d\theta} \qquad \text{----------(4.50)}$$

The daily collection efficiency so computed is shown in fig 4.38 (b) for various absorber areas. It is seen that for a fixed storage, the collection efficiency decreases as the absorber area increases. The reason for this is that the total outward loss from the collector increases because of increase in plate temperature as the absorber area increases.

Effect of storage size:

The effect of storage capacities for a fixed absorber area on the collection efficiency is also studied. The same equations can be employed for this study. The hourly collection efficiency for storage capacities of 300,400,600

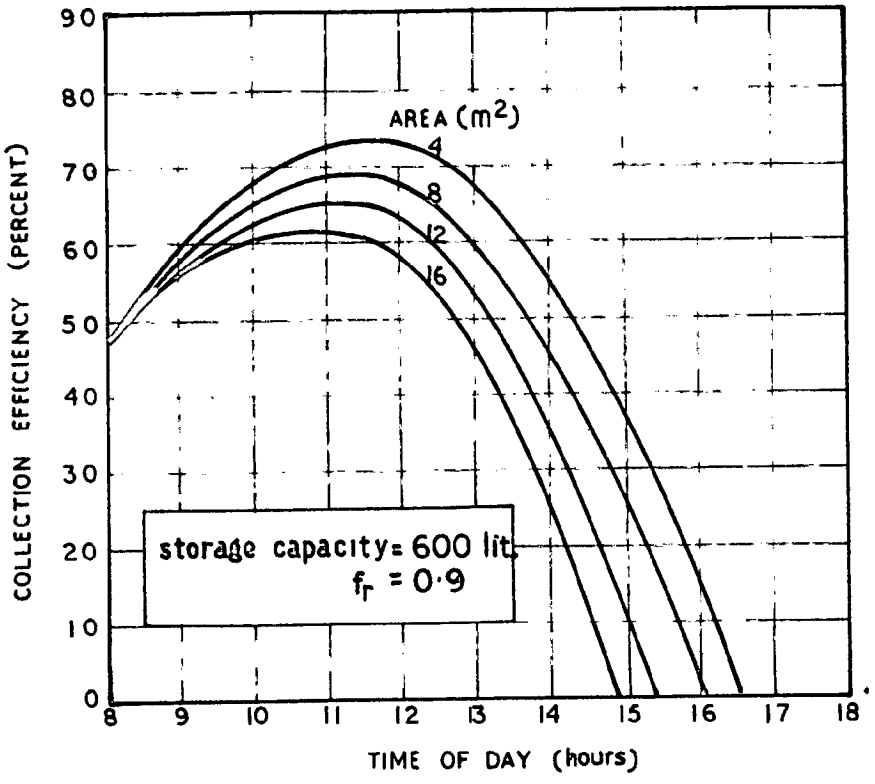

FIG. 4·38(a) EFFECT OF COLLECTOR AREA WITH TIME ON COLLECTION EFFICIENCY.

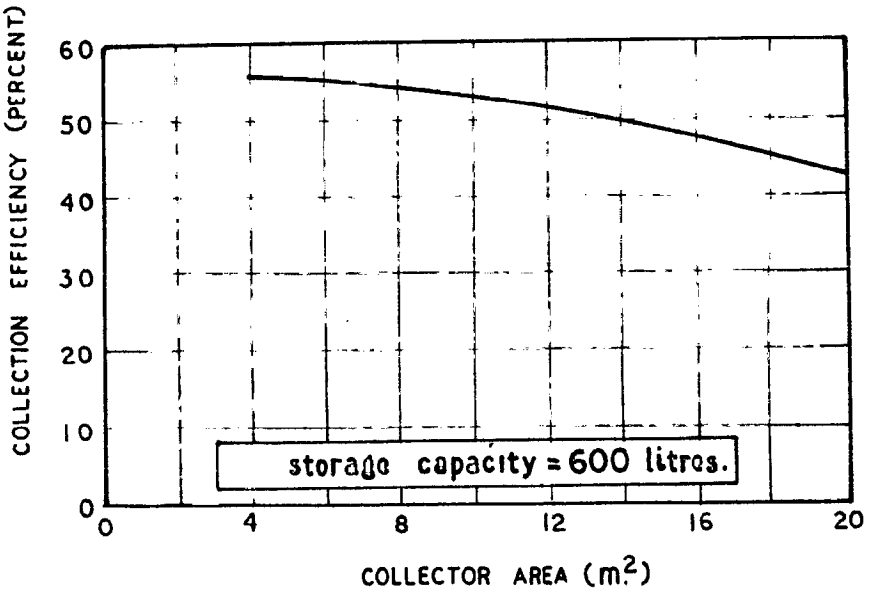

FIG. 4·38 (b) EFFECT OF ABSORBER AREA ON COLLECTION EFFICIENCY

end 300 litres for a fixed absorber area of 8.4m^2 is shown in fig 4.38(a). It can be seen from this figure that as the storage capacity increases the difference in efficiency goes on decreasing. It means that for a fixed absorber area there should be an optimum storage size. The integrated results are shown in fig 4.39 (b). From this it becomes clear that for a fixed absorber size, as the storage capacity increases, the efficiency increases but beyond 1000 litres, no significant advantage in efficiency can be expected.

4.9 Storage Tank Designs

The size of storage tank depends on the daily demand of hot water and also on the radiation intensity available at the place. Although a cylindrical tank having height equal to diameter will give minimum loss of heat from the tank for a given volume, a storage tank of height equal to twice its diameter is chosen since in the former case the stratification is poor and it is difficult to reduce mixing of the incoming cold water with the hot water.

The storage tanks may be either pressure type as is usually used in electric geysers or a non pressure type as shown in Figs 4.40 (a) and (b) respectively. Generally for similar installations non-pressure type, where the level in the tank is maintained with a float valve fitted in the tank recommended. In this type a tube fitted at the outlet of the float valve leaves the cold water at the bottom of the storage tank.

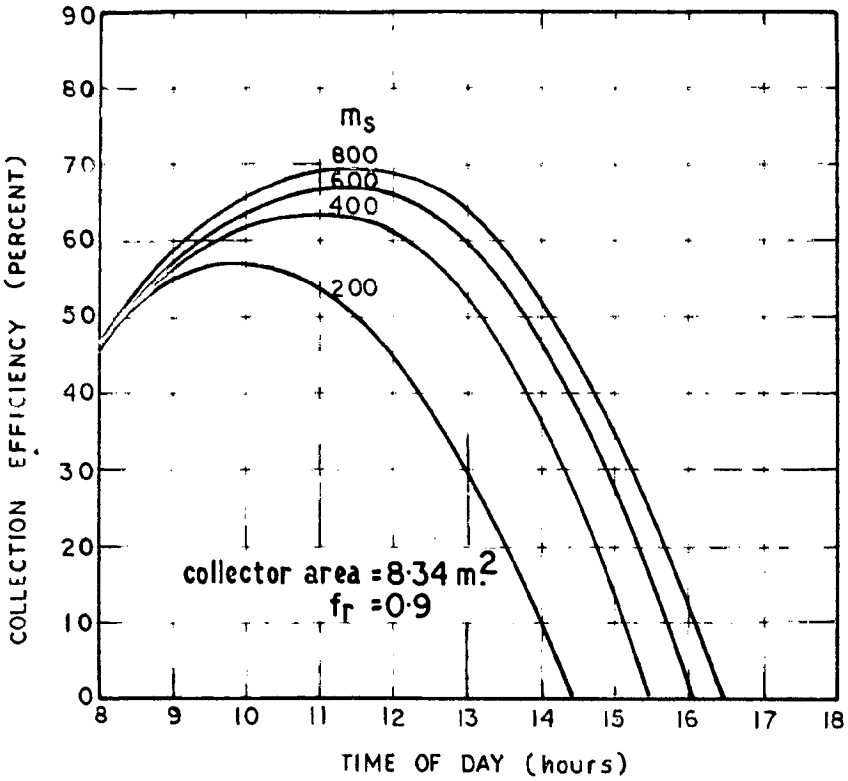

FIG. 4·39 (a) EFFECT OF STORAGE CAPACITY WITH TIME ON COLLECTION EFFICIENCY

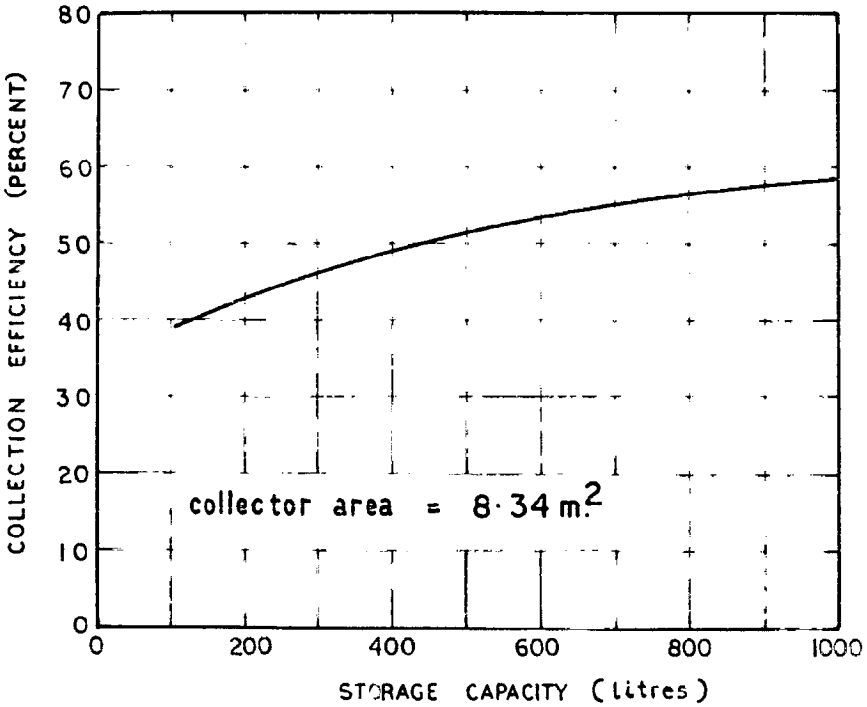

FIG. 4·39 (b) EFFECT OF STORAGE CAPACITY ON COLLECTION EFFICIENCY

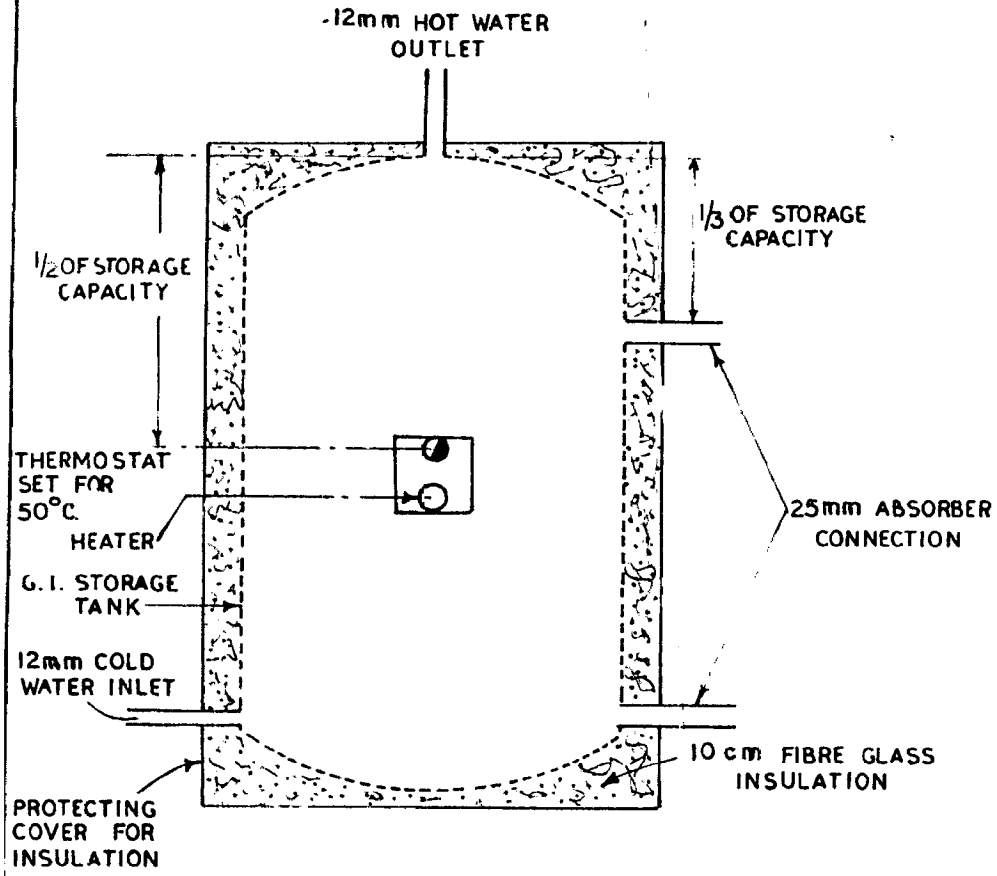

(a) Pressure type storage tank.

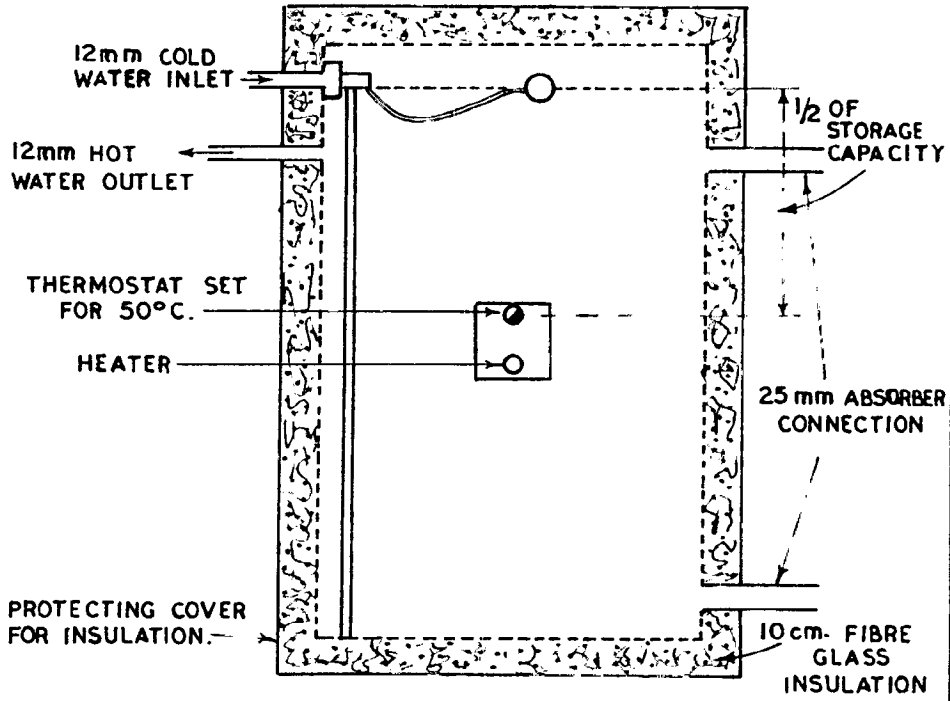

(b) Non pressure type storage tank

FIG. 4·40 STORAGE TANKS FOR SOLAR WATER HEATING

The location of the absorber flow and return pipes and also the suitable position for locating electric boosting elements which may be provided are shown in the above figures. The tank shown has a capacity of 600 litres. For a system requiring a very large storage, it is usually both more economical and convenient to install the required capacity in a number of smaller tanks and to connect these either in parallel or series, depending on the circumstances.

Of great importance to any solar water heating system is the insulation, which reduces heat losses from the storage tank. A number of insulating materials are available and their choice has been discussed earlier. If the tank is to be installed in the open it will, of course, be necessary to protect insulation by a suitable lining.

A cheap method for protecting the insulation around a large storage tank would be to build a wooden or angle iron frame-work around the tank, to which asbestos-cement sheeting or any other type of suitable sheeting could be attached.

4.07. Auxiliary heating.

The design of a solar water heater can be based on the availability of minimum radiation in winter months. By basing the design on minimum radiation received during winter months, the capital cost will be higher. The ideal thing would be to base the design on minimum radiation received so that it may give sufficient hot water throughout

the year and to make provision for auxiliary heating during cloudy days. An auxiliary heater is therefore suggested in the present case, though it raises the capital costs and operating nominally.

The electric immersion heater in the solar storage tank may be fitted either at half or one-third the height of storage tank depending on the way of use. The element must be automatically controlled by means of a safety thermostat fitted at the centre of the storage tank and adjusted to a suitable temperature, say 60°C. Suggested ratings for electric elements used in this way are given in Table 4.8.

For controlling the operation of the immersion heater time switches are usually employed. The time switch keeps the electric circuit disconnected during a preset time interval (which is generally from sunrise to sunset). It has been observed that such a fixed type of time switch will not respond when clouds appear and there is an intermittent demand of hot water during day time. To overcome this difficulty, a solar switch, similar to that designed by Robinson and Beckman[33] has been developed by the author and tested in a prototype unit. This solar switch is connected in series with the electric immersion heater and safety thermostat fitted in the tank. The solar switch is set at 45°C and acts as a master switch for the immersion heater. With this arrangement, the immersion heater will be on only when the solar switch temperature is

TABLE 4.8:

Loadings for auxiliary electric immersion heaters

Total capacity of storage tank (litres)	Loading (K W)
100	0.5
200	1.0
300	1.5
400	1.5
500	2.0
600	3.0

below 40° and simultaneously the tank water temperature is below the set point of the safety thermostat.

4.98. PROTOTYPE LARGE SIZE SOLAR WATER HEATER:

The heater was designed for 20 persons for taking bath in the early mornings. For twenty persons, the normal hot water requirement has been assessed as about 600 litres, at a temperature of 45°-60°C. As has been seen that the absorber area for Roorkee region for this requirement comes to 8.4 m^2. Six absorbers each having an area of 1.4 m^2, were, connected in true parallel arrangement as discussed earlier. A small pump (1/6 H.P.) was used for the circulation of water through the absorbers and storage tank. The complete schematic diagram of the set-up is shown in fig. 4.41. The photo of the prototype unit installed at the Institute is shown in fig.4.42.

4.99 Performance:

Performance tests on a prototype unit were conducted during the winter seasons. It was observed that maximum mean tank temperature was of the order of 65°C and the morning temperature was 48°-50°C. These values were obtained without resorting to the use of the immersion heater provided in the tank. The data given in Table 4.7 provide an idea of the performance of the heater. It is seen that the collection efficiency is of the order of 50 percent. The power consumed by the pump is only about 0.23 KWH/day.

TABLE 4.9: PERFORMANCE DATA OF SOLAR WATER HEATER(600 LITRES CAPACITY)

Date	Time (hours)	water temperature (^{o}C)	Total heat collected (K cal)	Total insolation absorb. (K cal)	Efficiency of collection in percent.	water temperature next day (^{o}C)	Electric energy consumed by pump per day (KWH)
20th Nov. 68	8.0 AM 4.0 PM	20.0 56.0	21600	43520	49.6	51.0	0.24
20th Dec. 68	8.0 AM 4.0 PM	18.0 56.0	22800	43346	52.0	50.0	0.22
16th Jan. 69	8.0 AM 4.0 PM	17.0 55.0	22800	43036	51.8	48.0	0.25
15th Feb. 69	8.0 AM 4.0 PM	18.0 54.0	21600	43722	49.4	48.0	0.21
24th Nov. 69	8.0 AM 4.0 PM	18.0 55.0	23300	43500	61.0	49.0	0.23
23rd Dec. 69	8.0 AM 4.0 PM	17.0 55.0	22800	43819	52.3	50.0	0.25
8th Jan. 70	8.0 AM 4.0 PM	15.0 55.0	24000	43960	54.4	49.0	0.25

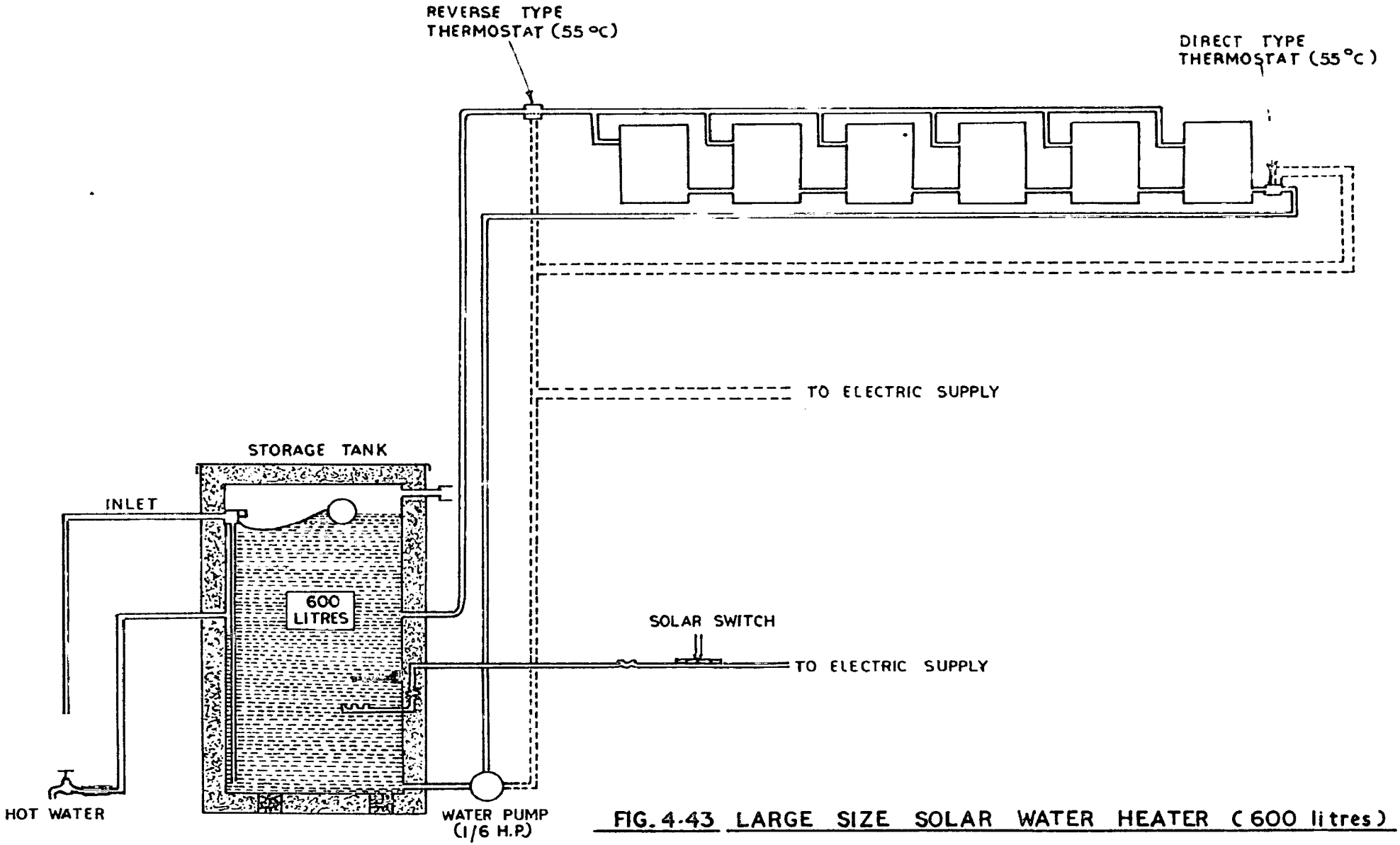

FIG. 4-43 LARGE SIZE SOLAR WATER HEATER (600 litres)

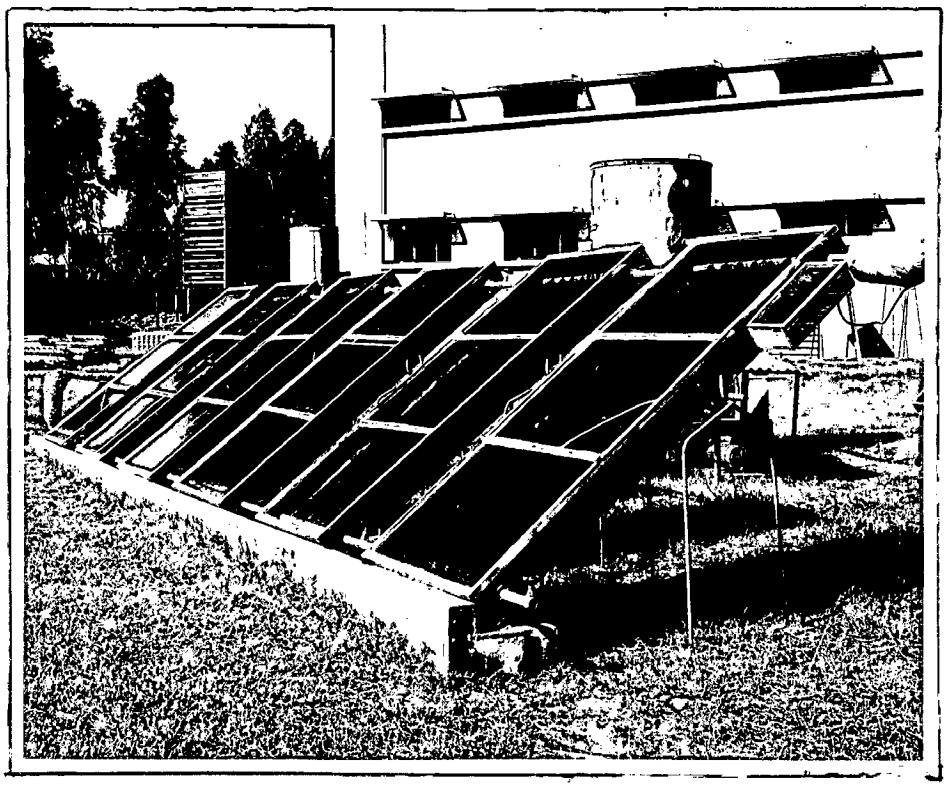

FIG.4.42: PHOTO OF LARGE SIZE SOLAR WATER HEATER (600 LITRES)

4.10. Low cost solar water heater:

The cost of conventional solar water heater i.e. with a separate absorber plate and storage tank is not low enough to be afforded by a common man in India. So a built in storage type solar water heater, where a flat, shallow tank which performs the dual function of absorbing heat and storing the heated water, is developed and tested for its performance. It is reported that a few types of low cost solar water heaters are in use in South Africa[34] and Japan[35]. However, no data is available regarding their performance[36,37]. The so called low cost of solar heater developed and tested by Chinnappa [38,39] will prove to be more expensive than the domestic type[40] solar water heater in this country.

The main disadvantage of combined collector and storage type solar water heater is that it does not provide hot water at the desired temperature for early morning use. For day time use it is ideal. Its advantages being of ease of installation and of low cost. The heater is designed and tested under various operating conditions. A theoretical model is also developed which can predict the storage temperature at various operating conditions.

4.10.1 Design of heater unit:

The unit consists of a G.I. rectangular tank of 20 gauge and of dimensions 110x60x10 cm with a capacity of 80

litres. It is placed on a 2.5 cm layer of insulating material such as fibreglass in a glass-fronted tray. A photograph of the prototype is shown in Fig.4.43. The main design feature of the heater are described below:

1. The heater works on the push through principle and hence is of a non pressure type. The flow of hot water in the outlet pipe is controlled by a gate valve provided at some convenient place in the inlet pipe.
2. The inlet and outlet pipes are provided along the length of heater, in order to minimise the mixing of cold water with the hot water in the tank.
3. A short vent pipe is provided at the outlet pipe just as a safety precaution.
4. The front face of the tank is blackened by lamp-black-paint.
5. To avoid condensation on the underside of the glass a number of breathing holes are drilled in the tray.
6. No sealing material is used with the glass and is fixed by means of clamps.

4.10.2 Performance of the heater:

A number of thermocouples were used for the measurement of temperature. Some of the thermocouples were soldered on the front and rear side of the tank. The readings were recorded on a 12 channel potentiometric recorder.

A programme was chalked out as shown in table 4.10 to simulate the test with the domestic conditions.

TABLE 4.10:

Performance test programme for low cost solar water heater (90 litres)

Test No.	Time	Nature of Test
1	08.0	Fresh water filled
	16.0	Run off all hot water
2	08.0	Fresh water filled
	08.0 (next day)	Run off all hot water.
3	08.0	Fresh water filled.
	14.0	Run off 30 litres hot water
4	08.0	Fresh water filled
	10.0	Run off 5 litres hot water
	12.0	Run off 10 litres hot water
	14.0	Run off 15 litres hot water
	16.0	Run off all remaining hot water.
5	08.0	Fresh water filled
	09.0	Run off all hot water above 30°C.
	10.0	
	11.0	
	12.0	
	13.0	
	14.0	
	15.0	
	18.0	Run off all remaining hot water.

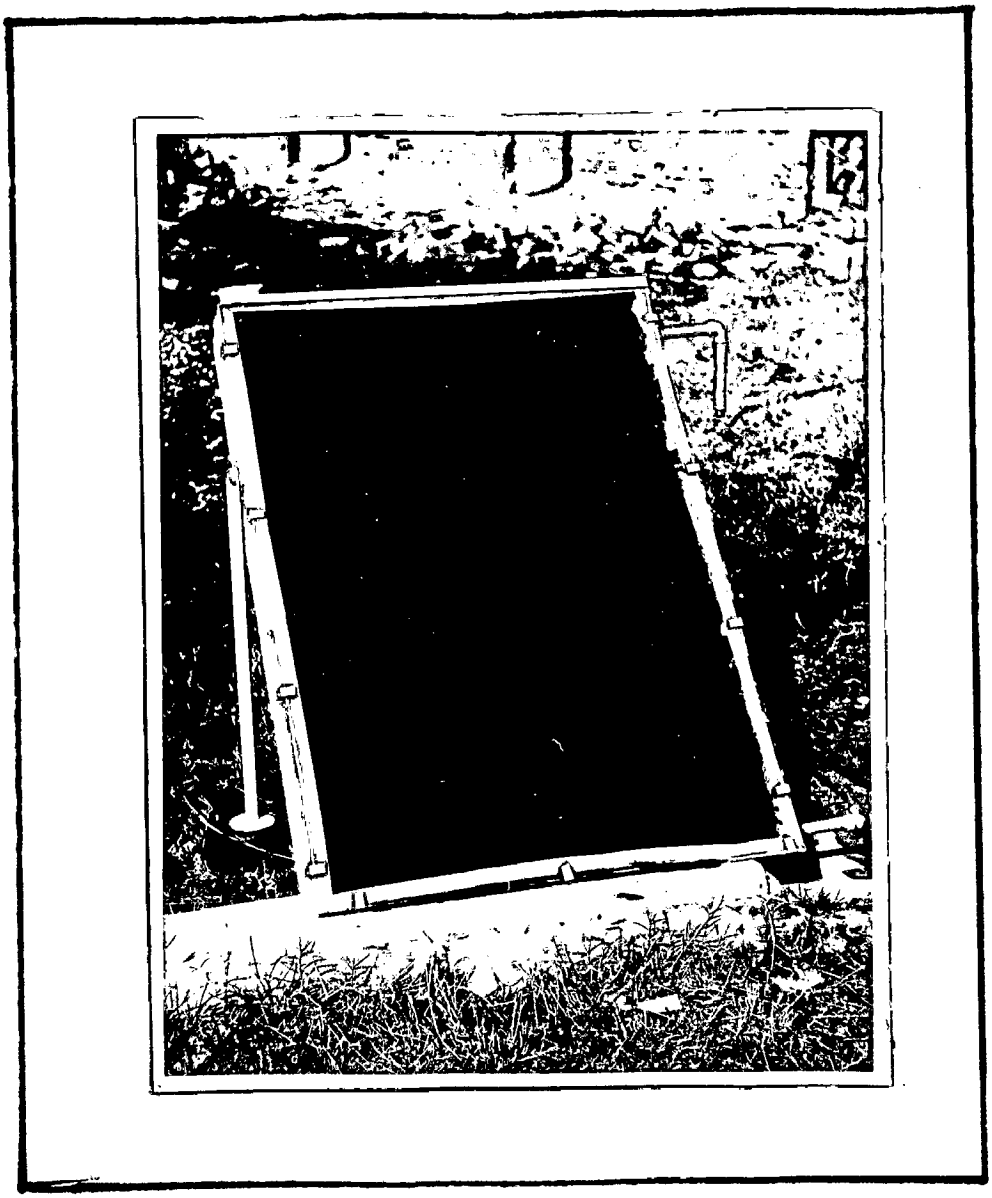

FIG.4.43 PHOTO OF LOW COST SOLAR WATER HEATER

Fig.4.43 (a) shows the variation of temperature at different levels of the tank alongwith the ambient air temperature for various hours on a typical winter day. It can be seen that the maximum temperature of water reaches at about 4.0 p.m. and the average temperature of water at this time is about 64°C. In Fig 4.44(b) the temperature of water with quantity drawn-off at 4.0 pm are shown. It can be seen that the average temperature of water drawn off is about 60°C.

The heater was not designed to store the hot water overnight, but the observations were recorded for 24 hours to see the storage efficiency when no water was drawn off during daytime. The observations are plotted in fig 4.45. It is seen that the temperature of the water in the tank falls considerably and as such it cannot be used for providing hot water in the early mornings. The most obvious method of improving on this would be to cover the glass overnight with an insulating material during night time. A test was carried out to indicate the possibilities of this method and the results are shown in fig 4.46. The water was allowed to heat up undisturbed during the day and at about 4.0 pm the glass was covered with a 6.0 cm layer of fibre-glass insulation mat. The water was then left undisturbed overnight and was found to be reasonably hot in the morning (see fig 4.43).

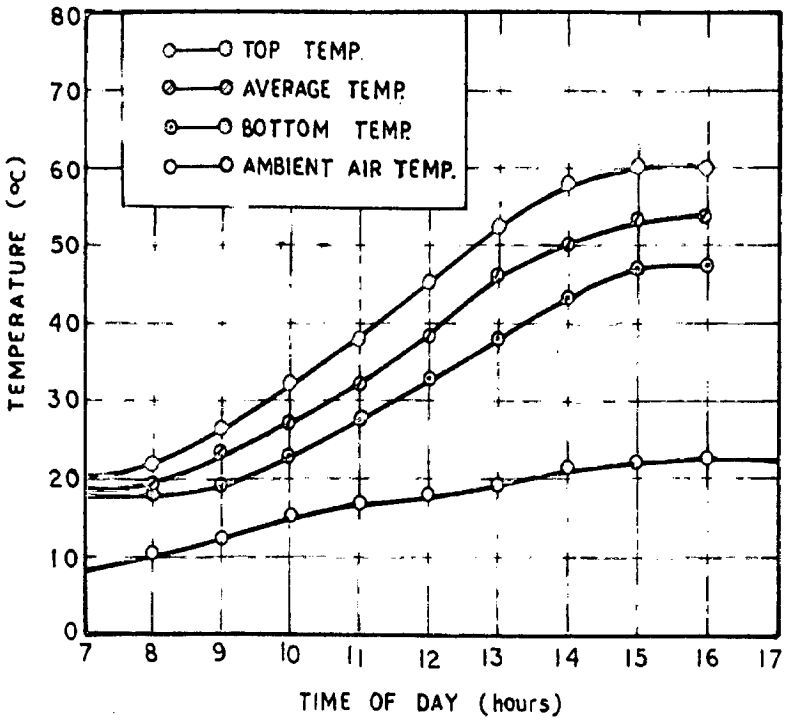

(a) Variation of water temperature in absorber tank at various hours of the day.

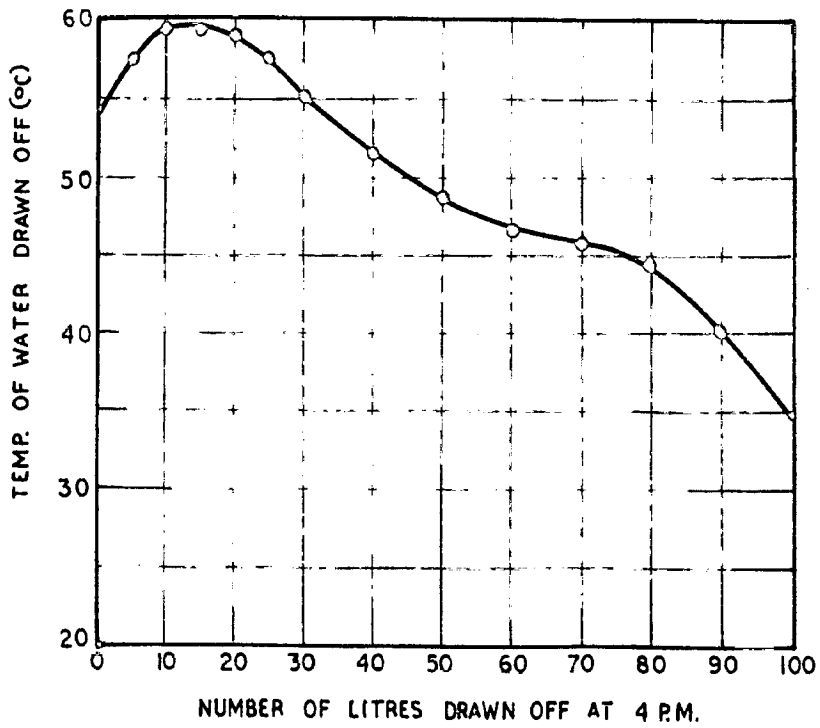

(b) Temperature variation of water with quantity drawn off at 4 P.M.

FIG. 4.44. RESULTS ON A LOW COST SOLAR WATER HEATER ON A TYPICAL WINTER DAY

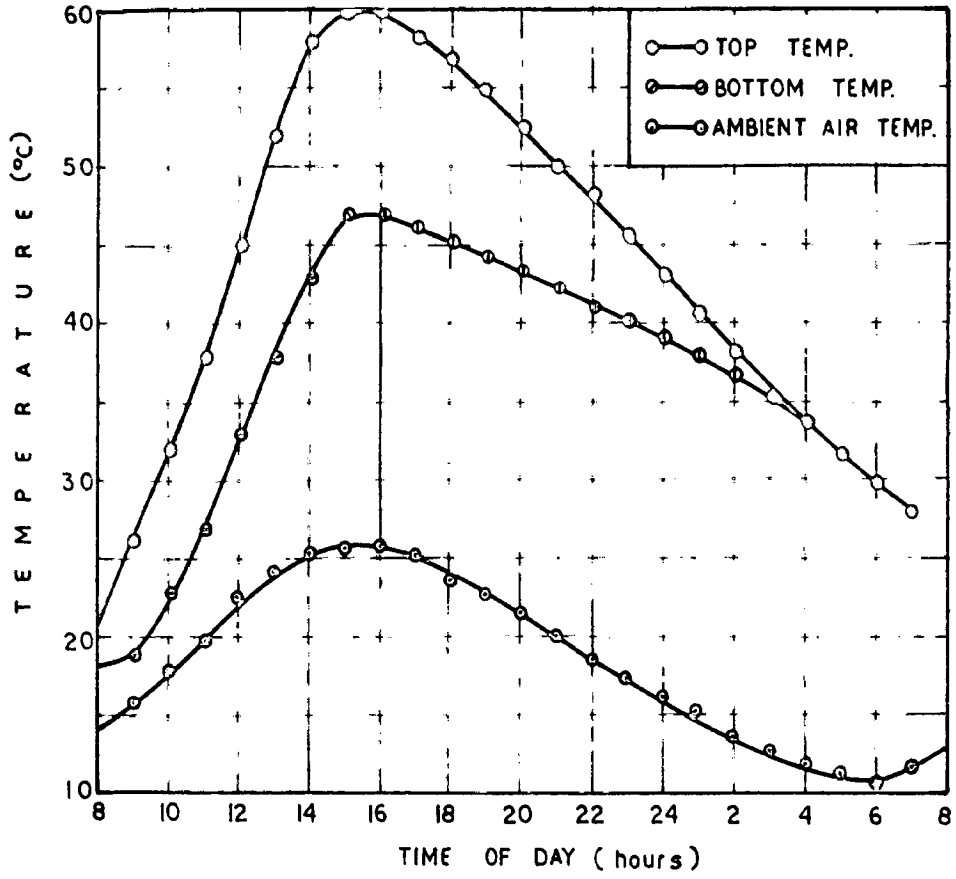

FIG. 4.45 GRAPH SHOWING TEMPERATURE VARIATION OF WATER IN TANK AT DIFFERENT HOURS ON A TYPICAL WINTER DAY

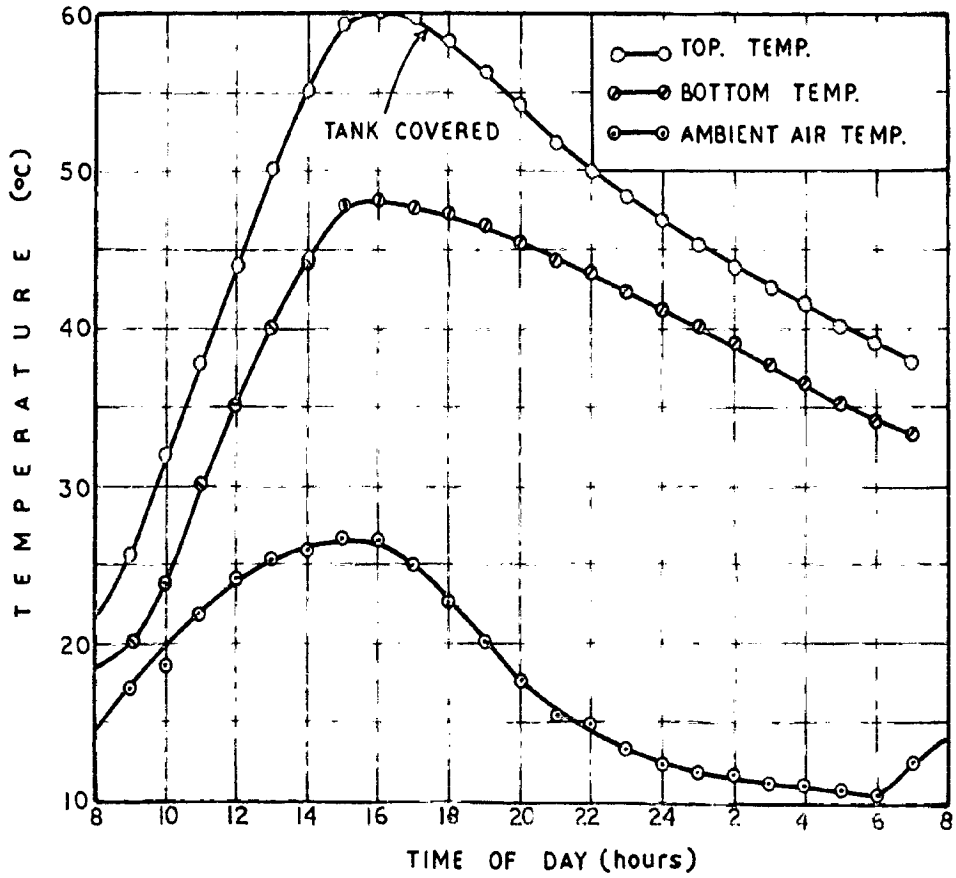

FIG. 4.46 TEMPERATURE VARIATION OF WATER IN TANK AT VARIOUS HOURS WHEN TANK COVERED OVERNIGHT WITH FIBRE GLASS INSULATION ON A TYPICAL WINTER DAY

A number of performance tests under different operating schedules as given in table 4.10 have been made. The results are summarised in table 4.11. The table also shows the effect of single and double glass, insulation, night insulation cover and drawing and filling water. It can be seen from the table that maximum efficiency is obtained in test 6 where all the water above 30°C is drawn off at each hour of the day. As expected the minimum efficiency is observed in Test No.8, where no water was drawn off during day time and only drawn off next day morning.

When compared the results of a single and double glass cover it is found that double glass does not show significant improvement. Similarly the type of insulation does not appear to play an important role and hence any cheap but durable insulation could be used. If the outlet pipe is taken from the lower side of the heater and the tank is not refilled after drawing the water, higher temperatures would result. However the efficiency will be lower in this set-up as can be seen from the table. By the provision of night insulation the performance efficiency is practically doubled as compared with the uncovered case.

4.10.3 Theoretical model:

Under steady state conditions, the instantaneous rate of incidence of total radiation on the absorber tank is equal to the sum of instantaneous rate of increase in heat content of water and the instantaneous rate of heat loss

TABLE 4.11: Results of performance of low cost solar water-heater.

Capacity for solar water heater = 30 litres
Area of absorber surface = 0.9 m^2
Angle of inclination of absorber = 45 degrees.

Type of test	Efficiency		Efficiency		Efficiency		Efficiency	
	one glass cover	two glass cover	Fibre glass insulation	Saw dust insulation	push through type	Box filled type	No cover at night	Cover at night.
1	61.2	64.8	61.2	60.0	-	-	-	-
2	12.1	12.3	12.1	11.1	-	-	13.1	25.6
3	63.4	66.0	63.4	61.5	-	-	-	-
4	65.0	67.1	65.6	64.1	65.6	63.5	-	-
5	70.7	70.8	70.7	69.8	70.7	68.5	-	-

from the tank. Mathematically it can be expressed as :

$$I_{St}(\tau\alpha)_o A_c = W_c\left(\frac{d\theta_{wm}}{d\theta}\right) + W_{co}\frac{d\theta_c}{d\theta} + (U_L + U_D) A_c\left[(\theta_c - \theta_a) + \frac{\frac{d\theta_c}{d\theta} - \frac{d\theta_a}{d\theta}}{2}\right]$$

----------(4.61)

where I_{St} = Instantaneous rate of total radiation (Kcal/m^2 hr).

$(\tau\alpha)_o$ = effective transmissivity absorptivity product.

A_c = area of absorber tank surface (m^2) = 0.806 m^2

W_c = weight of water in tank, Kgms = 80 Kgs.

W_{co} = water equivalent of tank, Kgms = 3.20 Kgs.

U_L = overall heat transfer coefficient from absorber tank surface upward through glass sheet to ambient air

= 6.0 Kcal/m^2 hr°C.

U_D = overall heat transfer coefficient from absorber tank surface rear wards through insulation to outside air

= $\frac{K}{d}$ = $\frac{0.028}{0.028}$ = 1.00 Kcal/m^2 hr°C. Here K is thermal conductivity of fibreglass insulation and d its thickness used on the rear of absorber tank.

$\frac{d\theta_{wm}}{d\theta}$ = rate of rise of average water temperature (°C/hr)

$\frac{d\theta_c}{d\theta}$ = rate of rise of average tank temperature (°C/hr)

$\frac{d\theta_a}{d\theta}$ = rate of rise of ambient air temperature(°C/hr)

For simplification, we can assume twc = tc or $\frac{dt_{wc}}{d\theta} = \frac{dt_c}{d\theta}$, Eq. (4.61) reduces to :

$$I_{Tt}(\tau\alpha)_e\, A_C = \left[W_{wc}+W_{co} + (U_L+U_B)\frac{A_C}{2}\right] \frac{dt_{wc}}{d\theta} + (U_L+U_B)\, A_C\, t_{wc} - (U_L+U_B)\frac{A_C}{2}\left[\frac{dt_a}{d\theta} + 2\, t_a\right] \qquad \text{------(4.62)}$$

This may be rewritten as

$$X \frac{dt_{wc}}{d\theta} + Y\, t_{wc} = Z \qquad \text{------(4.63)}$$

where
$$X = W_{wc} + W_{co} + (U_L+U_B)\frac{A_C}{2} \qquad \text{------(4.64)}$$

$$Y = (U_L+U_B)\, A_C \qquad \text{------(4.65)}$$

$$Z = I_{Tt}(\tau\alpha)_e\, A_C + (U_L+U_B)\frac{A_C}{2}\left[\frac{dt_a}{d\theta} + 2\, t_a\right] \qquad \text{------(4.66)}$$

The above equation is a first order inhomogeneous differential equation with constant coefficient. The solution of this equation becomes :

$$t_{wc} = \frac{Z}{Y} + \left(t_{wo} - \frac{Z}{Y}\right) e^{-Y/X\,(\theta - \theta_o)} \qquad \text{------(4.67)}$$

where two is the initial system temperature at time θo, when fresh water is filled in.

This equation can be used for the computation of mean water temperature when proper values of constants are taken.

The value of I_{gt} and ta i.e. the hourly total solar radiation and ambient air temperature were expressed as Fourier series and are obtained by harmonic analysis.

A comparison of the computed and measured values of the tank mean temperature alongwith the measured ambient air temperature is shown in fig 4.47(b). A close agreement is observed between the computed and measured tank mean temperatures. The total solar radiation in the plane of the heater is measured with the help of Eppley solarimeter and the values are shown in fig 4.47(a).

The ratio of the capacity of the tank to the area of the absorbing surface is important since this is responsible for the maximum temperature reached in the tank and also to the heat losses. The maximum stor ge temperature reaching in the absorber tank for various capacity to area ratios are computed with the help of equation 4.37 and the results are shown in fig 4.48. From this figure it is clear that for a fixed capacity to area ratio, the storage temperature is fixed. The efficiencies are computed for the same capacity to area ratios, and are shown in the same fig. 4.49. From this it is clear that as the capacity to area ratio decreases the efficiencies also decreases. This is due to higher heat losses from the unit, that would result because of increased temperatures.

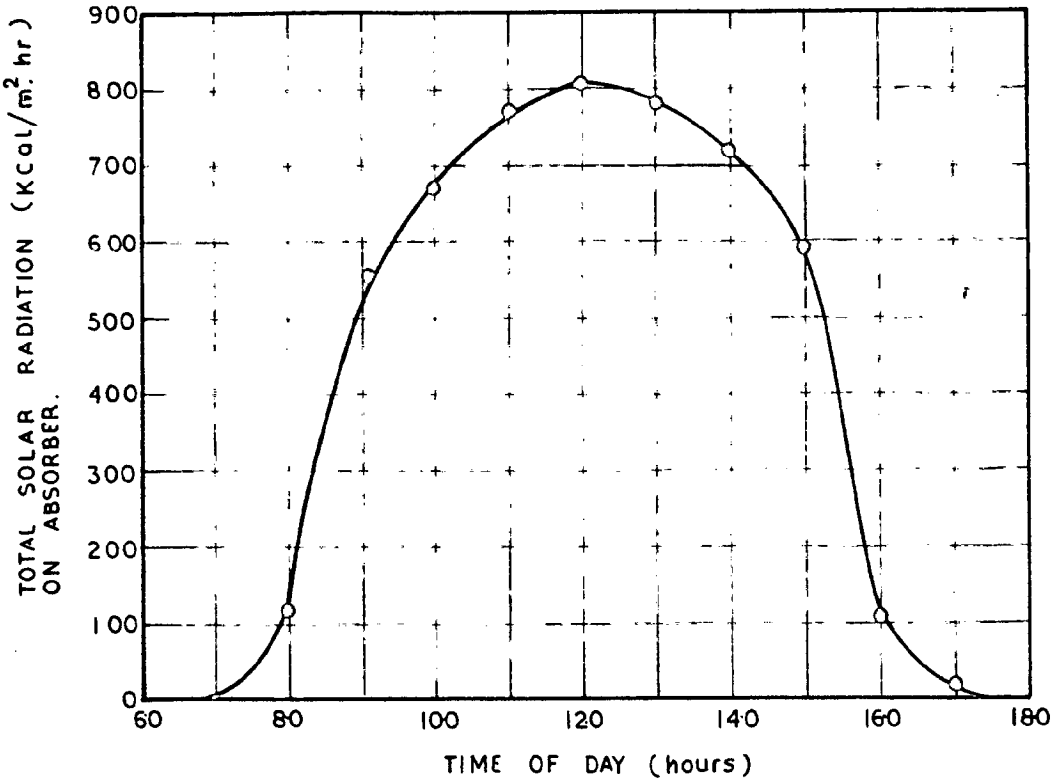

(a) MEASURED TOTAL SOLAR RADIATION ON ABSORBER SURFACE AT VARIOUS HOURS OF THE DAY

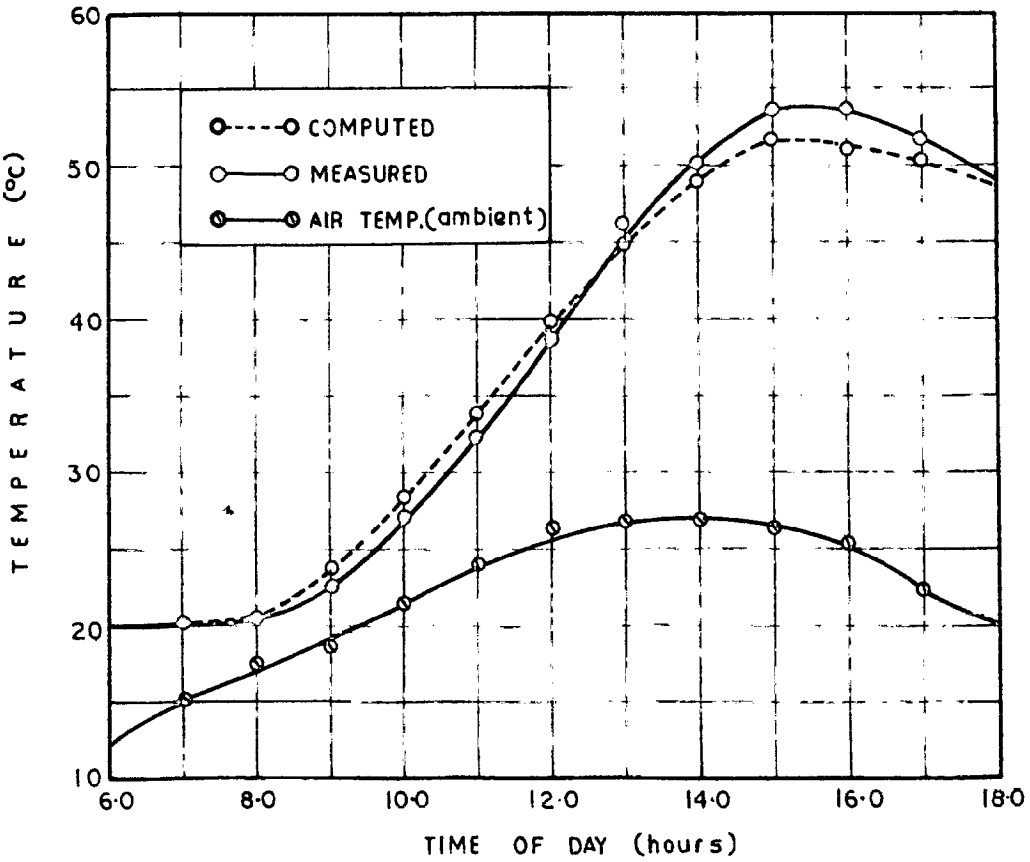

(b) Comparison of computed and measured tank mean temps. at various hrs. of the day.

FIG. 4·47 MEAN TANK TEMPERATURE ON A TYPICAL WINTER DAY

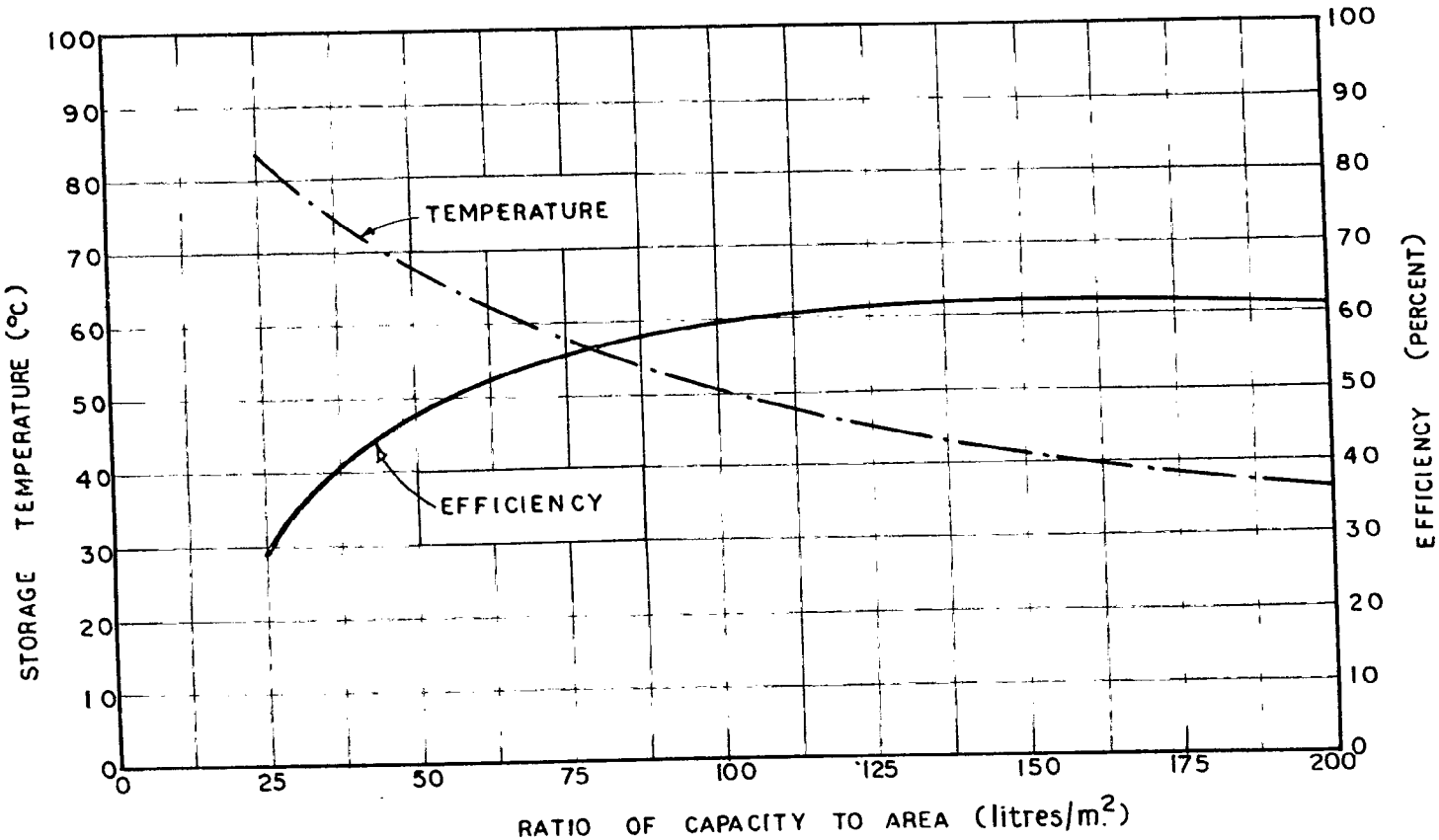

FIG. 4·48 EFFECT OF CAPACITY TO AREA RATIO ON THE STORAGE TEMPERATURE & EFFICIENCY

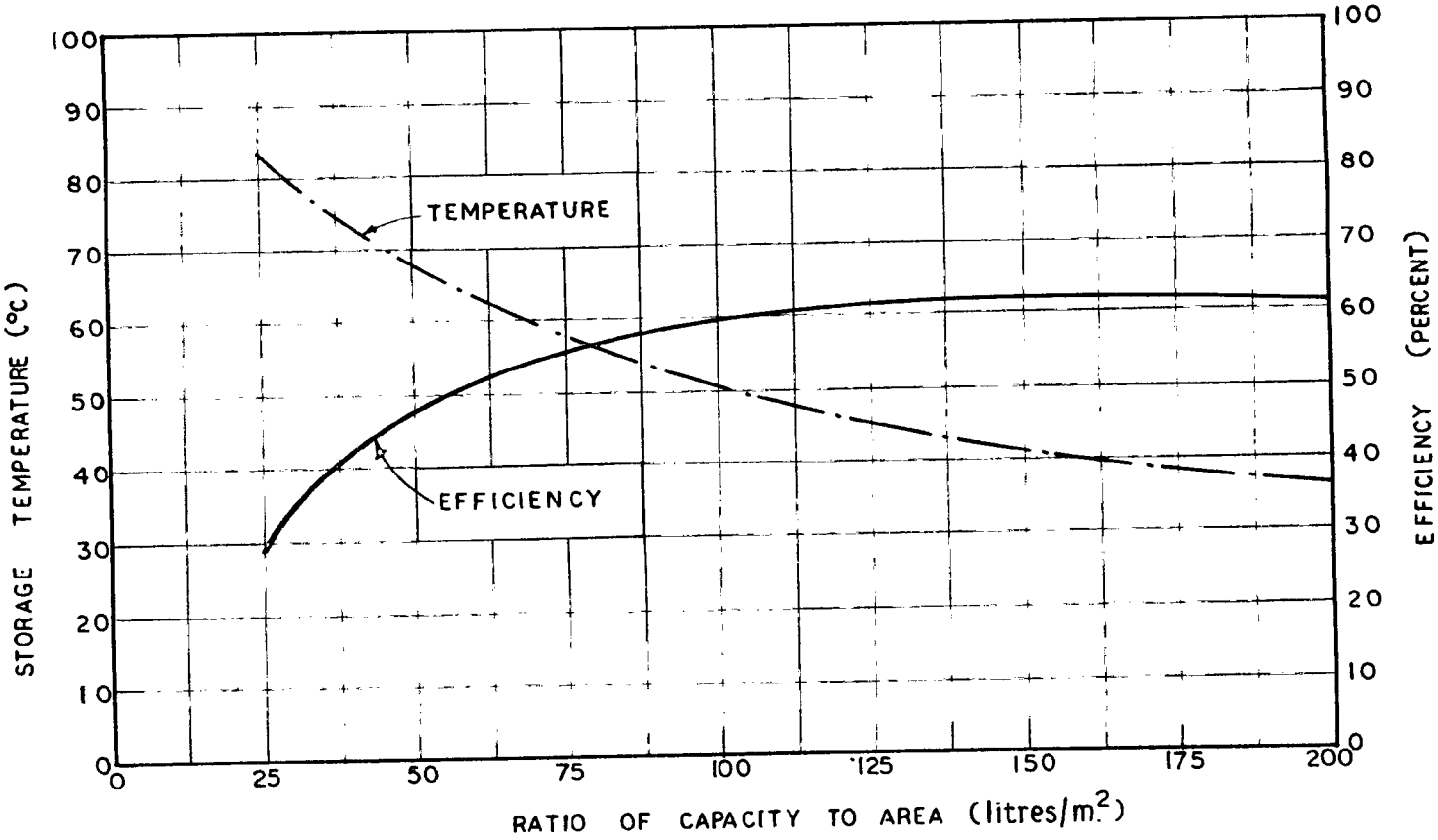

FIG. 4·48 EFFECT OF CAPACITY TO AREA RATIO ON THE STORAGE TEMPERATURE & EFFICIENCY

These the curves can be used for optimising the capacity to area ratio for any desired storage temperature.

4.11. Economics of solar water heating:

Since the solar energy is free, the yearly cost will be the sum of the interest on investment, the yearly maintenance of the installation, the yearly depreciation, and the cost of the auxiliary power, if used.

Of D is the cost of storage tank, circulation pipes and its insulation etc. The cost of absorber per m^2 is B. Rs. and A (m^2) absorber area used. Then the total capital investment (C) will be

$$C = D + B.A. \qquad \text{----------(4.60)}$$

If d is the depreciation factor which depends on the life ('n' years) of the equipment, and if b be the interest (percent) on the capital invested and if c is the yearly maintenance expressed in percent. Then the yearly distributed cost (C_1) not using any auxiliary power will be

$$C_1 = (d + b + c) \quad (D + BA) \qquad \text{-----(4.60)}$$

where $d = 1/n$

The value of C_1 i.e. annual distributed cost is computed for different absorber costs and for various life expectancies and is shown in fig 4.60. In this figure the cost of water heating by electric geyser with various power rates, is also included. It is assumed that electric geysers cost is Rs.600 and a life of 15 years. The economics of the present solar water heater comes where

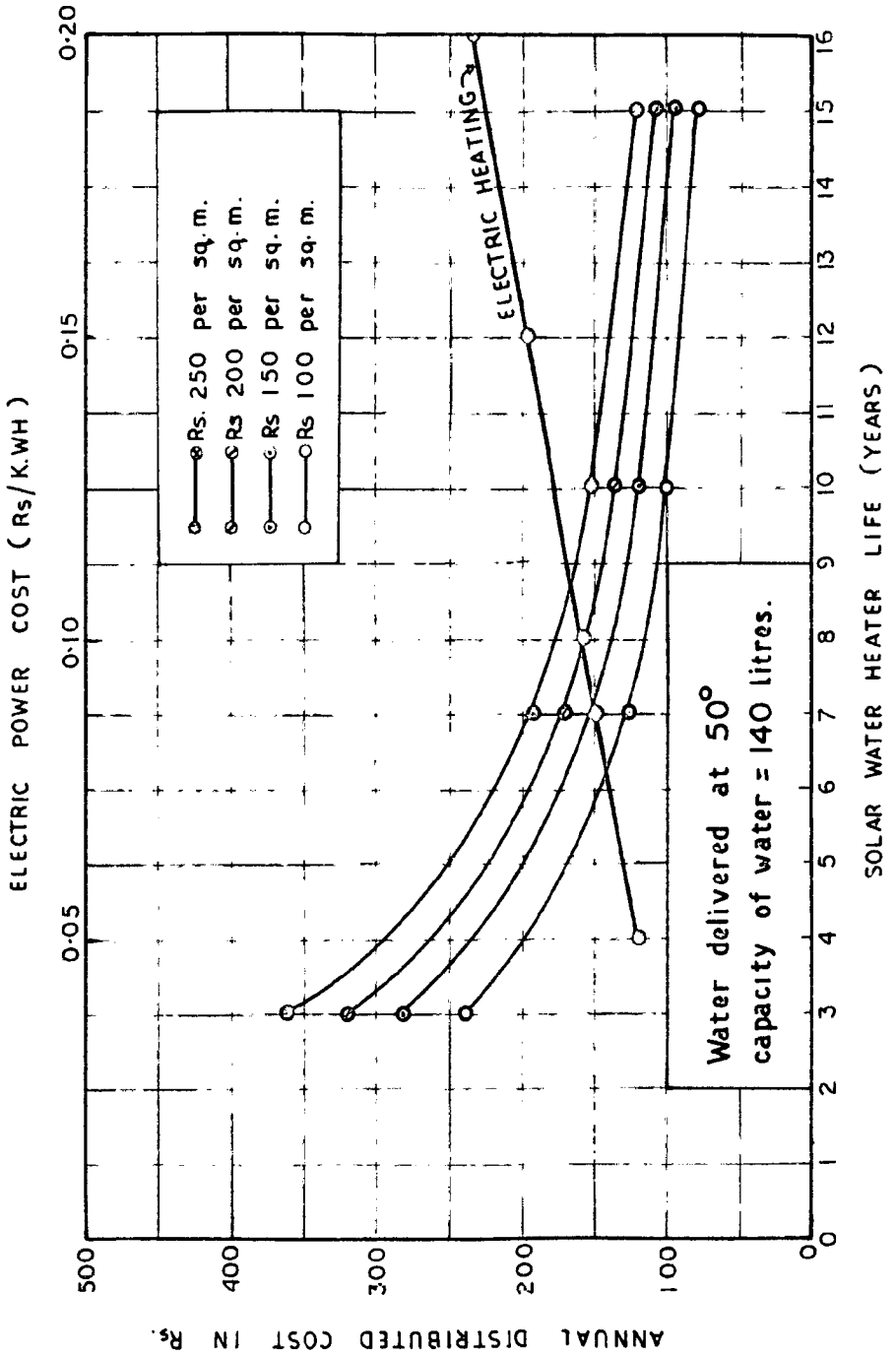

FIG. 4.49 ECONOMICS OF SOLAR WATER HEATER

β = Rs.400 and A = 3 m^2 and B = Rs.150 per m^2. is worked out and given in Table 4.12.

It can be seen from this table that even if the life of solar water heater is taken as 7 years and the electric power rate is Rs.0.10 solar water heater proves economical. If the life of solar water heater is longer than 7 years and or the electric power rate is higher the solar water heater will be much more economical.

In the above statement it is assumed that solar water heater gives hot water for all the heating days but this is not true because there are few cloudy or rainy days for which auxiliary power is needed. So one should also work out the cost of the auxiliary power needed. If the deficiency in energy (Kcal/season) increases then the absorber area required to give the same heating output increases and hence the capital cost of solar water heater and hence the annual distributed cost increases. This is shown by dotted line curve in Fig. 4.60. But if the area is fixed i.e (3 m^2 here) and the deficiency in energy is made up by electric booster provided in the storage tank the annual distributed cost varies linearly with the ~~difficulty~~ deficiency in energy as shown in fig 4.60 for various power costs. Thus if the deficiency in energy at a particular place is known, a comparison of the economics for solar water heater versus with electric geyser and with (solar + electric) heater can be found out from figs 4.60 and 4.60.

TABLE 4.12:

Comparison of annual distributed cost for solar water heating and electric geyser (it is assumed that solar water heater works for 120 days (winter season) with no rainy days in between).

Life (years)	Annual distributed cost (₹/year)				
	Solar heating	Electric heating by geyser			
		@ 0.05	@ 0.10	@ 0.15	@ 0.20 ₹/KWH
3	202.0	-	-	-	-
7	149.0	-	-	-	-
10	119.0	-	-	-	-
15	95.0	121	160	199	238

TABL 4.13:

Comparison of annual distributed cost for various heating devices.(life of electric geyser and solar water heater is assumed as 15 years).

Heating device		Annual distributed cost (Rs/year) @ 0.05	@ 0.10	@ 0.15	@ 0.20 Rs/ KWH
Electric geyser		121	160	199	238
Solar water heater (No electric heater)		95	95	95	95
Solar + electric booster.	DELHI	99	102	106	110
	POONA	97	98	100	102
	CALCUTTA	98	100	102	105
	MADRAS	100	104	108	113

* It is expected that 85 to 95 percent days the performance will be satisfactory and do not require any supplementary electrical energy.

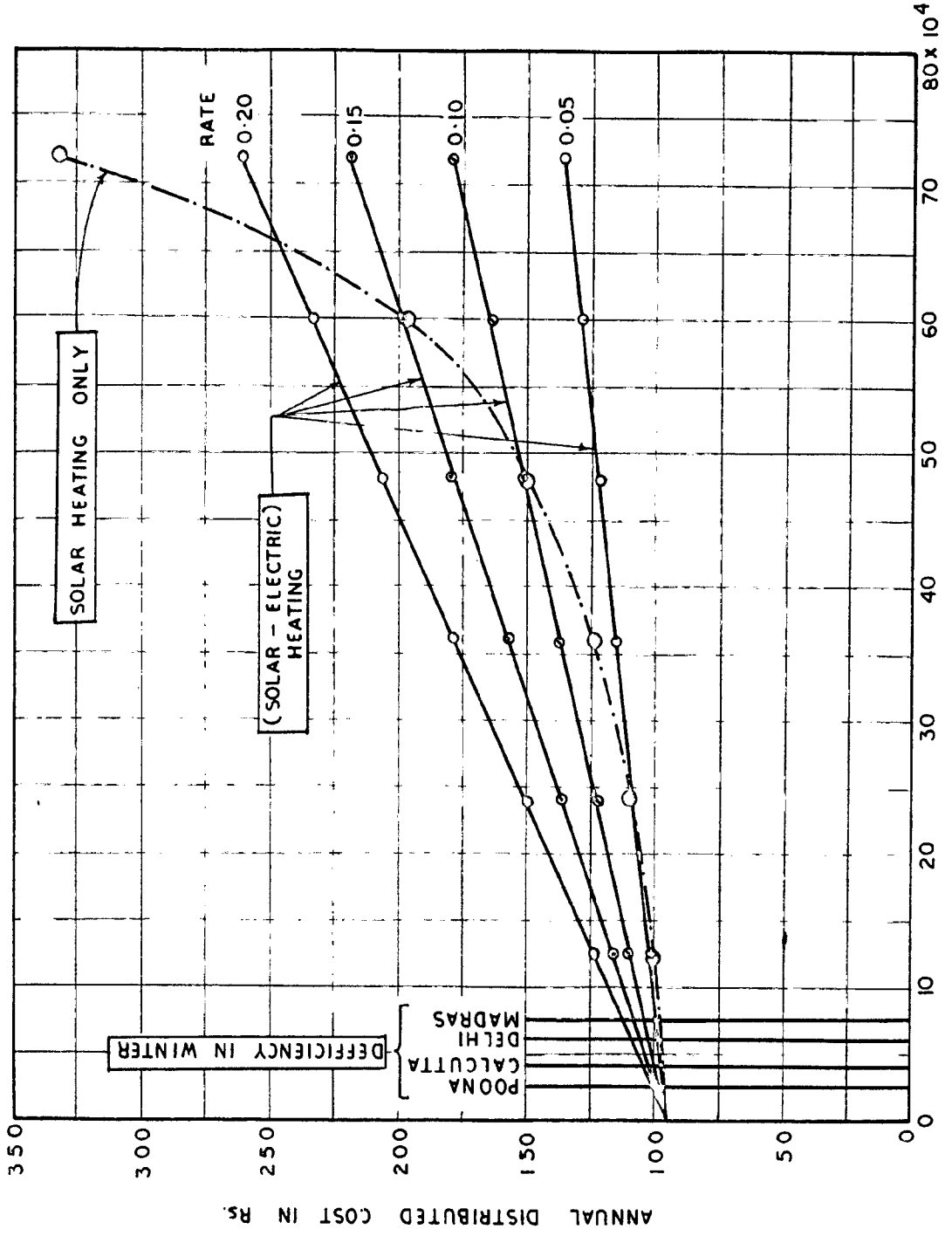

FIG. 4·50 ECONOMICS OF SOLAR WATER HEATER AT VARIOUS INDIAN CITIES

The difficulty in energy has been worked out for Delhi, Poona, Calcutta and Madras from the actual measured data of solar radiation for winter season. The annual distributed cost for all these four places for three methods i.e. by electric geyser, by solar water heater and by solar water heater with electric booster are compared in Table 8.13. It can be seen from this table that the solar water heater supplemented with electric booster which will provide hot water for all days is economical as compared to electric geyser for all the above places.

C H A P T E R-5.

ROOM HEATING BY SOLAR ENERGY

CHAPTER 5

ROOM HEATING BY SOLAR ENERGY

5.1 INTRODUCTION

For room heating also low-grade heat can be employed satisfac torily and hence flat-plate collectors can generally be used. The basic difference between the flat-plate collectors used for water heating and those for air heating is the mode of heat transfer between the absorber plate and the heated fluid. In case of water heating the collectors are usually of fin-tube type and heat absorbed is transfered to the water by conduction. So high conductinity of the plate and tube of high resistance to corrosion are the essential features. But in case of air heaters the conductinity of the plate does not play important role since all the air remains in touch of the whole absorbing plate. Corrosion of the absorber plate is also a secondary consideration in solar air heaters. Thus solar air heater appears to have been stringent requirements than a water heater.

A design study to determine the important factors influencing air heater performance has been made in this chapter. An equation for the conventional solar air heater is presented from which the rate of useful heat collection at any operating condition can be computed.

There are many designs of solar air heaters and a few popular designs are described in literature[1,2,3,4] and shown in Fig. 5.1.

5.2 THEORETICAL ANALYSIS OF HEAT TRANSFER IN AN AIR HEATER

In conventional air heaters the air passes through a gap between the absorbing plate and rear-plate as shown in Fig. 5.1(a). The important factors that effect the performance of the heater are:

i) Heater configuration i.e. aspect ratio of air-duct and its length.

ii) Heat transfer co-efficient between the absorber plate and air-stream.

iii) Transmittance properties of the transparent cover.

iv) Absorption and emission properties of the absorbing plate.

v) Air mass flow rate through the heater.

vi) Solar radiation intensity on the absorber surface.

vii) Amount of insulation provided on the rear side of the plate.

If B and L represent, width and length of the air heater respectively then the energy balance for the absorption plate and the fluid element can be given by

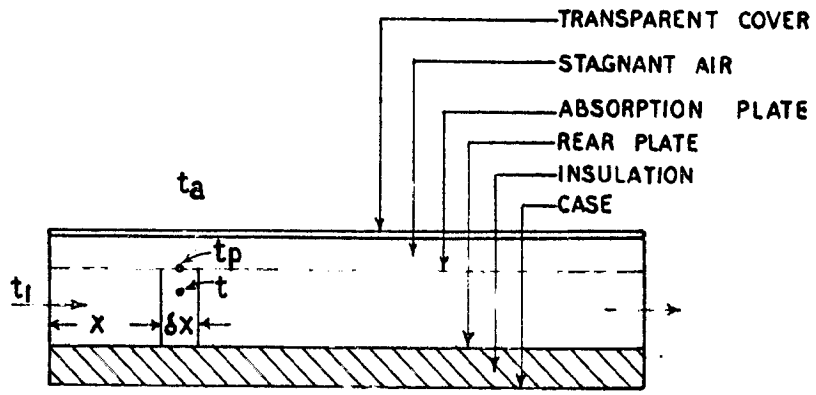

(a) Conventional solar air heater.

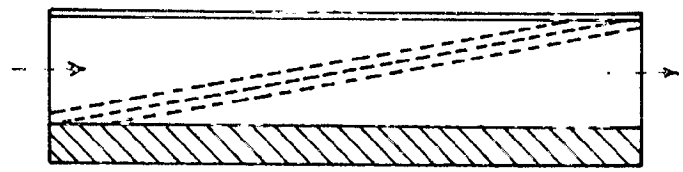

(b) Matrix type solar air heater.

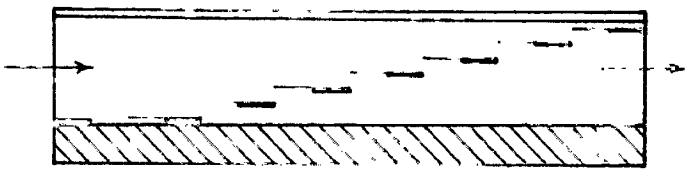

(c) Overlapped glass solar air heater.

FIG. 5·1 TYPICAL DESIGNS OF SOLAR AIR HEATER

equations 5(1) and 5(2) respectively:

$$Hf(B\,\delta_x) = U_L(B\,\delta_x)(t_p - t_a) + h_c(B\,\delta_x)(t_p - t) \quad \ldots(5.1)$$

$$WC_p \frac{dt}{dx}\delta_x = h_c(B\,\delta_x)(t_p - t) \quad \ldots(5.2)$$

where

H = solar radiation incident on collector (kcal/m^2hr)

f = effective transmissinity absorptivity product.

U_L = overall heat loss co-efficient from collector plate to outside air (kcal/m^2 hr °C)

t_p = collector plate temperature (°C)

t_a = ambient air temperature (°C)

h_c = film heat transfer co-efficient from absorber plate to fluid inside (kcal/m^2 hr°C)

t = temperature of air in the collector at dist ce x from inlet side (°C)

W = mass flow rate through absorber (kgm/hr)

C_p = specific heat of air (kcal/kgm °C)

On eliminating t_p from equations (5.1) and (5.2) we get the following differential equation:

$$\frac{dt}{dx} + C_1\, t = C_2 \quad \ldots(5.3)$$

where $C_1 = \dfrac{BF_p U_L}{WC_p}$ $\quad \ldots(5.4)$

& $C_2 = \dfrac{BF_p}{WC_p}(Hf + U_L\, t_a)$ $\quad \ldots(5.5)$

where $F_p = \dfrac{h_c}{(U_L + h_c)}$ $\quad \ldots(5.6)$

The solution of equation (5.3) for boundary conditions at $x = 0$, $t = t_1$ is given as

$$t = \frac{C_2}{C_1} + (t_1 - \frac{C_2}{C_1}) e^{-C_1 x} \qquad ...(5.7)$$

from the above equation temperature, t of fluid at any distance x from the inlet end can be computed. The temperature rise through the heater of length L will then be

$$(t_2 - t_1) = (\frac{Hf}{U_L} - t_1 + t_a) \left[1 - e^{-F_p U_L / GC_p}\right] \qquad ...(5.8)$$

Now if U_o is defined as the heat loss coefficient from the fluid inside the heater to the outside air, then it can be proved as

$$U_o = F_p U_L \qquad ...(5.9)$$

The useful energy (q_u) collected per unit of area will be

$$q_u = GC_p(t_2 - t_1) \qquad ...(5.10)$$

where G = mass flow rate per unit of collector area (kg/m^2 hr).

After putting the value of $(t_2 - t_1)$ as obtained from equation (5.8) in equation (5.10)

$$q_u = F_p F_f (Hf - U_L(t_1 - t_a)) \qquad ...(5.11)$$

where F_f is flow factor and is given by

$$\frac{1 - e^{-U_o/GC_p}}{U_o/GC_p} \qquad \ldots(5.12)$$

Thus we get an expression for useful energy (q_u) as

$$q_u = F_R \left| Hf - U_L(t_1 - t_a) \right| \qquad \ldots(5.13)$$

where $F_R = F_p . F_f$ = heat removal efficiency factor.

The collection efficiency (η) of the heater which is defined as the ratio of useful heat collected to the solar radiation intensity incident on it, will be

$$\eta = \frac{GC_p(t_2 - t_1)}{H} \qquad \ldots(5.15)$$

From equation (5.13) the useful energy collected can be computed provided the film heat transfer coefficient h_c, overall heat loss coefficient U_L, mass flow rate per unit permit area G, solar insolation H, effective transmissivity absorptivity product f, inlet air temperature t_1 and ambient air temperature t_a are known. Integration of this equation for all hours of the day would give the daily useful heat collected.

5.2.1 Solar Air Heater Design Curves

Simple design curves are drawn for getting the temperature rise through the solar air heater of conventional type based on performance equations developed in section (5.2). The plate efficiency factor (F_p) which is directly proportional to the useful energy collect 1 is a function of film heat transfer coefficient h_c as can be seen from equation (5.6). The

values of F_p for various values of h_c and for possible values of U_L is computed by using equation (5.6) and are plotted in Fig. (5.2). The figure indicates that increasing the value of h_c increases the efficiency factor F_p and thereby increases the value of collection coefficiency. Thus for getting higher efficiencies it is desirable to design the air flow passages so as to ensure that the numerical value of film heat transfer coefficient h_c exceeds 30 kcal/m^2 hr °C. There are several ways of increasing the values of h_c such as:

i) using extended surfaces (fins) beneath the collector-plate.

ii) using roughned plates.

iii) using over-lapped glass-plates.

iv) using matrix of various types.

Higher values of h would be better, provided that the frictional losses which the air would increase pumping cost, excessively high.

For a conventional air heater with one glass cover, the values of heat removal efficiency factor F_R which is directly proportional to the collection efficiency are computed and plotted in Fig. (5.3) using equation (5.14) for various values of air mass flow rates G and plate efficiency factors F_p for a fixed value of overall heat loss coefficient U_L equal to 6.0 Kcal/m^2 hr °C.

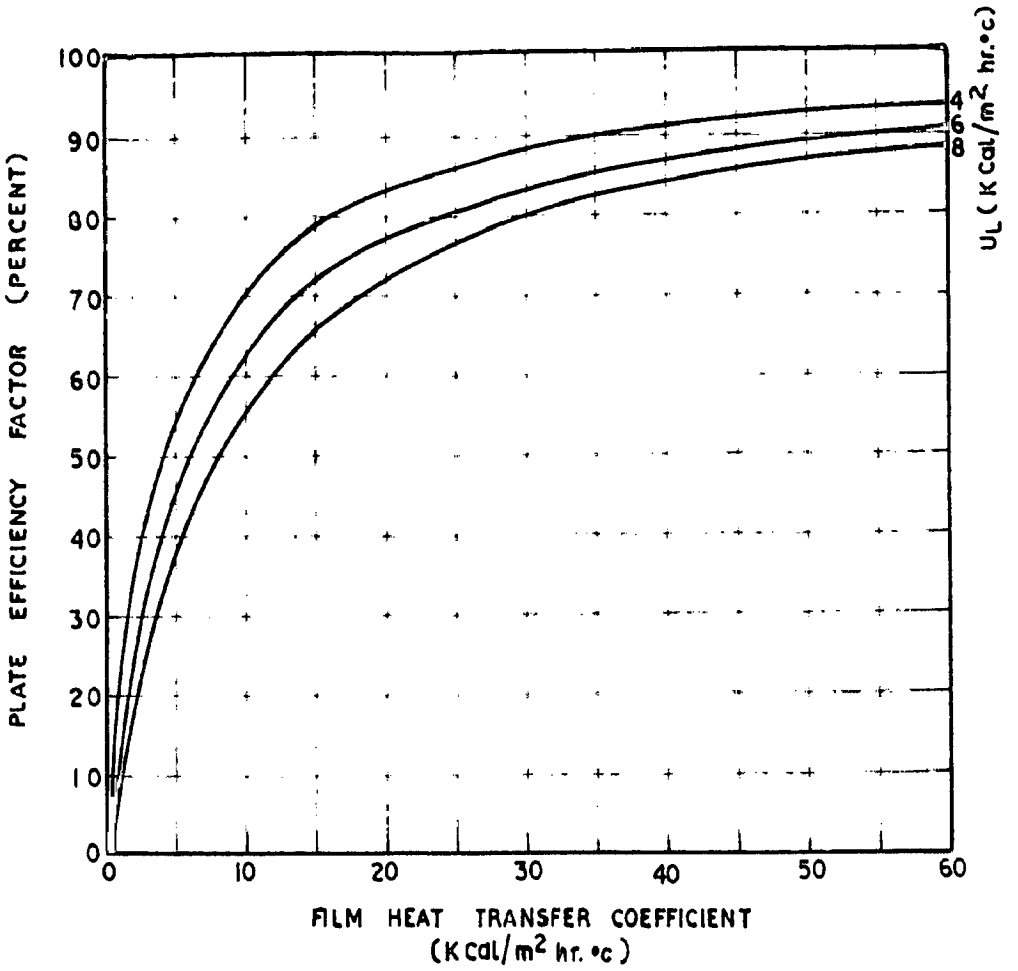

FIG. 5·2 EFFECT OF HEAT TRANSFER COEFFICIENT ON PLATE EFFICIENCY FACTOR

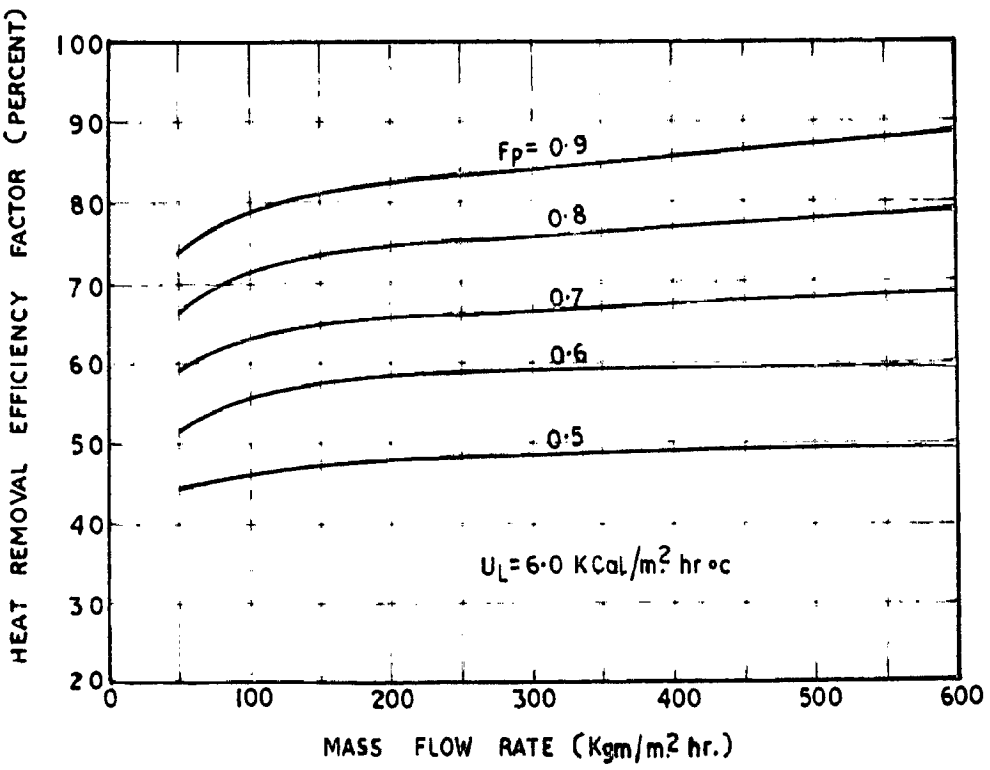

FIG. 5·3 EFFECT OF MASS FLOW RATE ON HEAT REMOVAL EFFICIENCY FACTOR

The ratio of collection efficiency to heat removal efficiency factor (η/F_R) for different solar radiation intensities (H) and different inlet temperature rises of intel air over ambient air temperature (t_1-t_a) are computed from equation (5.15) and plotted in Fig.(5.4).

Fig. 5.2, 5.3 and 5.4 now can be used for predicting outlet temperature of air heaters for a given climate and heater configuration. Air temperature rise through the heater (t_2-t_1) of 1 m^2 for various mass flow rates and solar insolation rates for heater having F_p = 0.9 are computed and plotted in Fig.(5.5).

The use of Figs. 5.2, 5.3 and 5.4 are further illustrated by the following practical example.

Example: Calculate the temperature rise of air steam through a conventional type solar air heater with one glass cover having heat transfer coefficient h_c as 25 Kcal/m^2 hr °C and mass flow rate of air is 200 kgm/m^2 hr and ~~mass flow rate of air is 200 kgm/m^2 hr and~~ solar insolation rate H is 600 Kcal/m^2 hr. Air enters in the heater at a temperature 10°C above ambient air temperature.

Solution: From Fig.(5.2) with h_c = 25 and U_L = 6.0, the plate efficiency factor F_p = 0.80.

From Fig. (5.3) with G = 200 and F_p = 0.80, the heat removal efficiency factor F_R = 0.74.

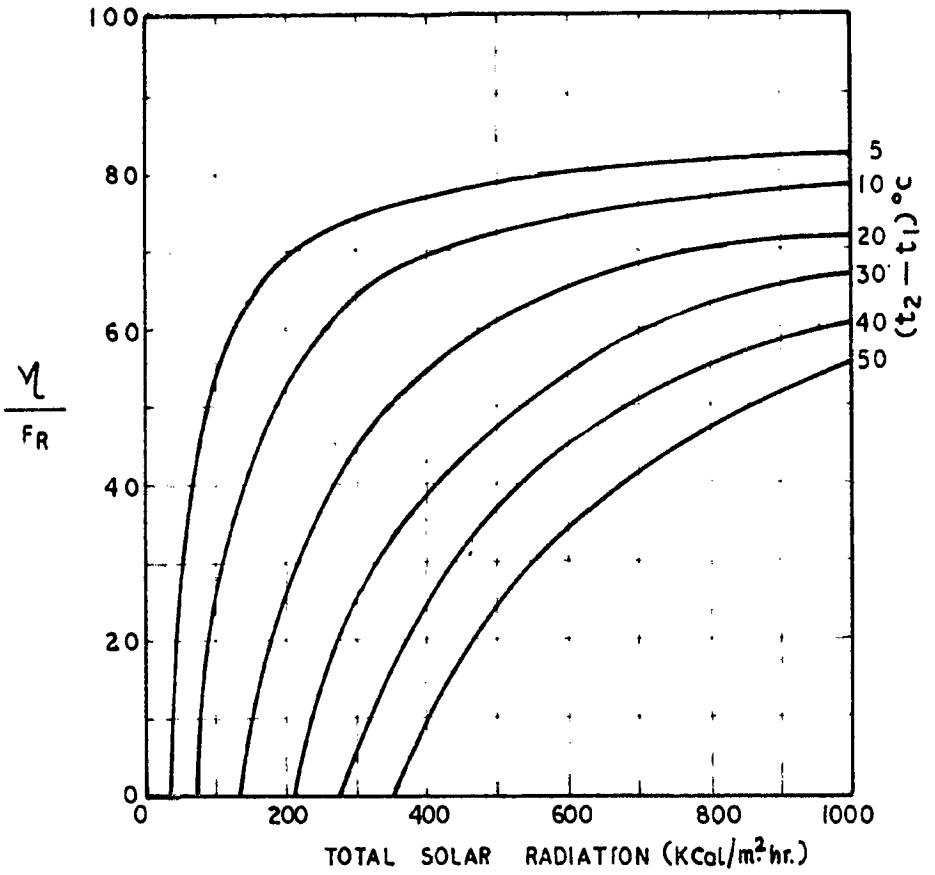

FIG. 5·4 EFFECT OF SOLAR INSOLATION ON EFFICIENCY

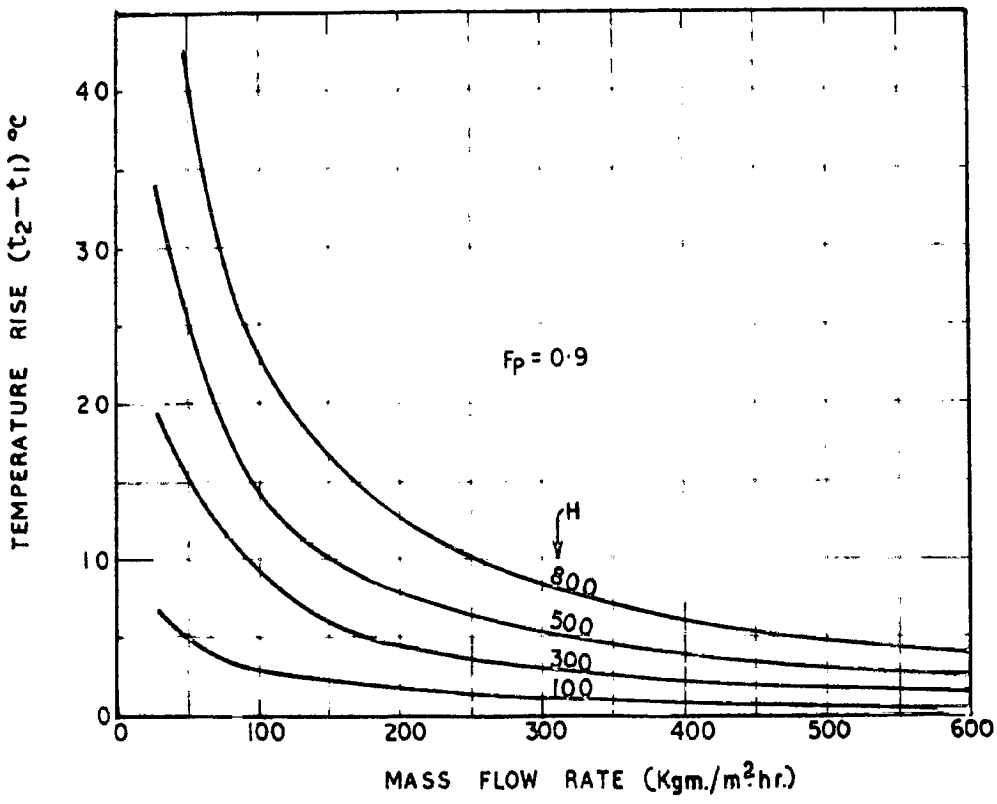

FIG. 5·5 TEMPERATURE RISE THROUGH THE HEATER FOR VARIOUS Mass Flow Rates.

From Fig. (5.4), with H = 600 and (t_1-t_a) = 10°C, the ratio of collection efficiency to F_R is 0.75

This collection efficiency = 0.75 x 0.74 = 0.555

or useful energy per unit area = q_u = 0.555 x 600

= 333 Kcal/m^2hr.

The rise of temperature through the heater (t_2-t_1) will be; $(t_2-t_1) = \frac{q_u}{GC_p} = \frac{333}{200 \times 0.24} = 6.9°C$

5.2.2 Optimisation of duct depth in Solar Air Heater

It is now clear that increasing the air velocity through a heater, results in higher collection efficiencies. However, this will also increase fan running costs. So the duct depth of the heater is to be optimised to give maximum efficiency and minimum fan running cost.

The pressure drop for a fully developed turbulant flow of air is given by the normal D' Arcy formula

$$\Delta p = \frac{4fLv^2}{2gd_e} \qquad \ldots(5.16)$$

where $f = (0.079/R_e^{0.25})$ ...(5.17)

L = length of heater

v = velocity of air (m/sec)

g = acc. due to gravity (m/sec²)

d_e = equivalent diameter of duct

= $\frac{4 \times \text{area of cross section of duct, (m)}}{\text{perimeter of duct}}$

R_e = Reynolds number $(\frac{d_e v \rho}{\mu})$

ρ = density of air (kgm/m^3)

μ = uncosity of air (kgm/m sec)

The pumping power P required will be

$$P = W.\triangle P \qquad \ldots(5.18)$$

This pumping power required for straight flow even at high flow rates is not much high. The main head loss would be due to resistance offered by bends, tees and elbows etc.

Experimental corelations[5,6,7,8] are now available for the case of asymmetrically heated rectangular ducts, from which the prediction of heat transfer is possible. The general correlation for forced convective heat transfer found in literature is of the type:

$$N_u = a\,(R_e)^x\,(P_r)^y \qquad \ldots(5.19)$$

where $N_u = \frac{h_c d_e}{K}$ = Nusselt number.

$P_r = \frac{C_p \mu}{K}$ = Prandtl number.

K = thermal conductivity of air (Kcal/m hr °C)

ν = Kinematic viscosity.

C_p = specific heat of air.

a, x and y are constants.

For rectangular duct the h_c is given as:

$$h_c = 0.\text{mg}2\left(\frac{K}{d_e}\right)\left(\frac{d_e v}{\nu}\right)^{0.8}\left(\frac{C_p \mu}{K}\right) \qquad \ldots(20)$$

From equation, (5.18) and (5.19) it appears that it is not possible to optimise in a direct way since with the increase the duct depth, both the velocity of air through duct and so the heat transfer coefficient will increase along with

the pumping cost. On the other hand for a fixed mass flow rate, both the heat transfer coefficient and pumping power decreases as the duct depth increases.

Sample calculations show that for a duct depth of 4.0 cm and mass flow rate 500 kgm/hr and film heat transfer coefficient as 9.0 Kcal/m^2 hr °C, the fan running costs are negligible compared to the capital cost of the heater.

Based on equation (5.20) film heat transfer coefficient h_c for various mass flow rates and duct depths are computed and plotted in Figs. (5.6) and (5.7). These figures now could be used to find the value of h_c for any duct depth and mass flow rate.

The mass flow rate has also been optimized for various duct depths as can be seen from Fig.(5.8). It can be seen that for a fixed duct depth as the mass flow rate increases the collection efficiency also increases, initially at a faster rate and then at a slower rate.

It is seen above that for a fixed mass flow rat through the solar air heater, the heat transfer coefficient decreases as the duct depth increases and hence the collection efficiency decreases. In other words, the collection plate area required to give a constant heat output increases. This effect can clearly be seen from Fig.(5.9). From this it can be said that if the duct depth increases from 1.0 cm to 4.0 cm the collector plate area required

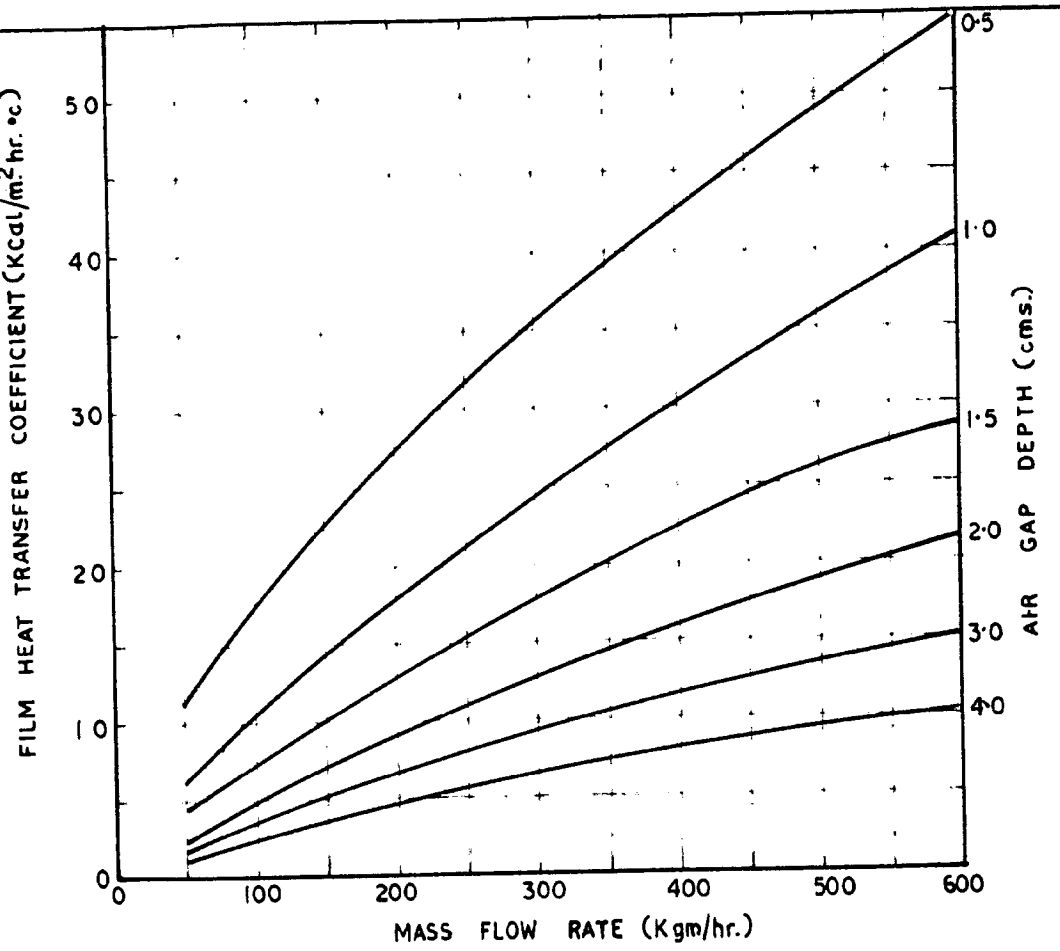

FIG. 5·6 EFFECT OF MASS FLOW RATE ON HEAT TRANSFER COEFFICIENT

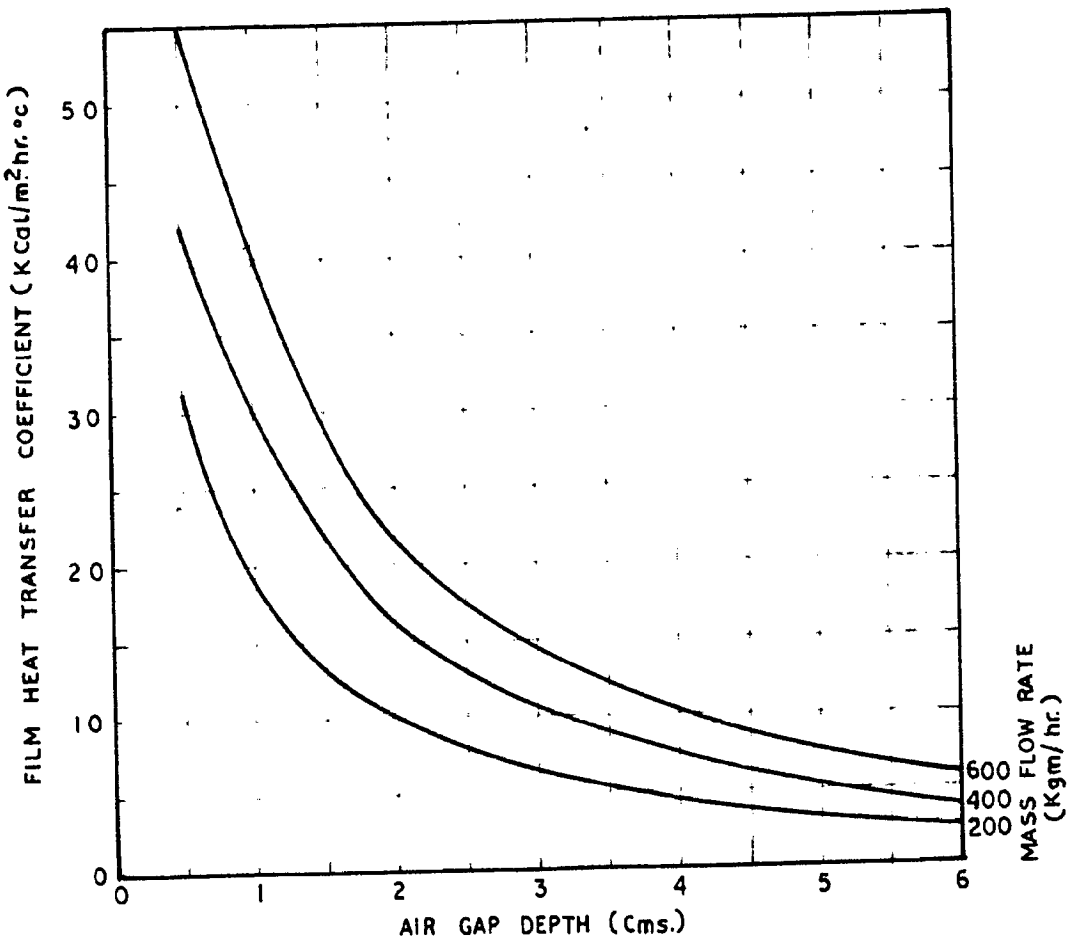

FIG. 5·7 EFFECT OF AIR GAP DEPTH ON HEAT TRANSFER COEFFICIENT

to give the same heat output increases from 1.0 m^2 to 1.4 m^2 while the increase in pumping cost is negligible. It can be concluded on the basis of above findings, that lower duct depths will give higher efficiencies with negligible increase in operating cost.

5.3 PERFORMANCE STUDIES ON SOLAR AIR HEATERS

Some experimental study on overlapped glass plate air heater by Loff[2] and Selcuk[9] corrugated sheet air heaters by Buelow[4], Matrix type by Chiou[10] and finned type by Bevill and Brandt[11] has been made.Buelow[12], Whillin[1] Close[13] and Selcuk[9] have analytically determined the performance equations and discussed the role of different variable of design and operation on the performance characteristics of air heaters. The wa present study is made to experimentally determine the value of design constants under Indian climates for air heaters developed by the author.

5.3.1 Types of Air Heaters Tested

Two of the air heaters (types I and II) use two corrugated sheets and the other two types (III and IV) employ one corrugated sheet and a wire mesh matrix.Type I air heater consisted of two corrugated galvanized iron sheets (24 gauge) placed transversely over each other and welded along the length. The exposed side was painted black. Type II air heater was similar to type I except that two aluminium corrugated sheets (28 gauge) were used. This is shown along with the test set-up in

Fig. (5.10). Type III air heater consisted of a single G.I. wire mesh screen held inclined between the glass cover and a corrugated G.I. sheet (24 gauge) below. The open space of the wire screen was 44 per cent and the hydraulic radius was 0.24 mm so that nearly half the radiation was absorbed at the bottom plate. Type IV air heater was similar to the type III except that double layer of aluminium expanded metal screen was employed in place of G.I. wire mesh. Each of the aluminium screen was 1.27 mm thick with open space 69 per cent of the total for single layer. The unit is shown in Fig.(5.11).

The size of the absorber plate of all the units was 123 cm by 76 cm. Each of them was housed in a G.I. box 15 cm deep and having 15 cm insulation of loose glass wool around the perimeter and 5 cm in the back. The box was covered at the top with a 3mm thick single sheet of clear window glass. The orientation was kept due south at an inclination of 45 deg, which happen to be an optimum tilt for the latitude of 30 deg N. (Roorkee). The inlet and outlet headers were of uniformly converging type so as to ensure uniform mass flow rate along the entire width of the collector. An available 80 watt. electric fan was used to force in the air.

5.3.2 <u>Equipment and Test Procedure</u>

It is clear from the following performance equations;

$$q_u = F_r \left| Hf - U_L(t_1 - t_a) \right| \qquad \ldots(5.21)$$

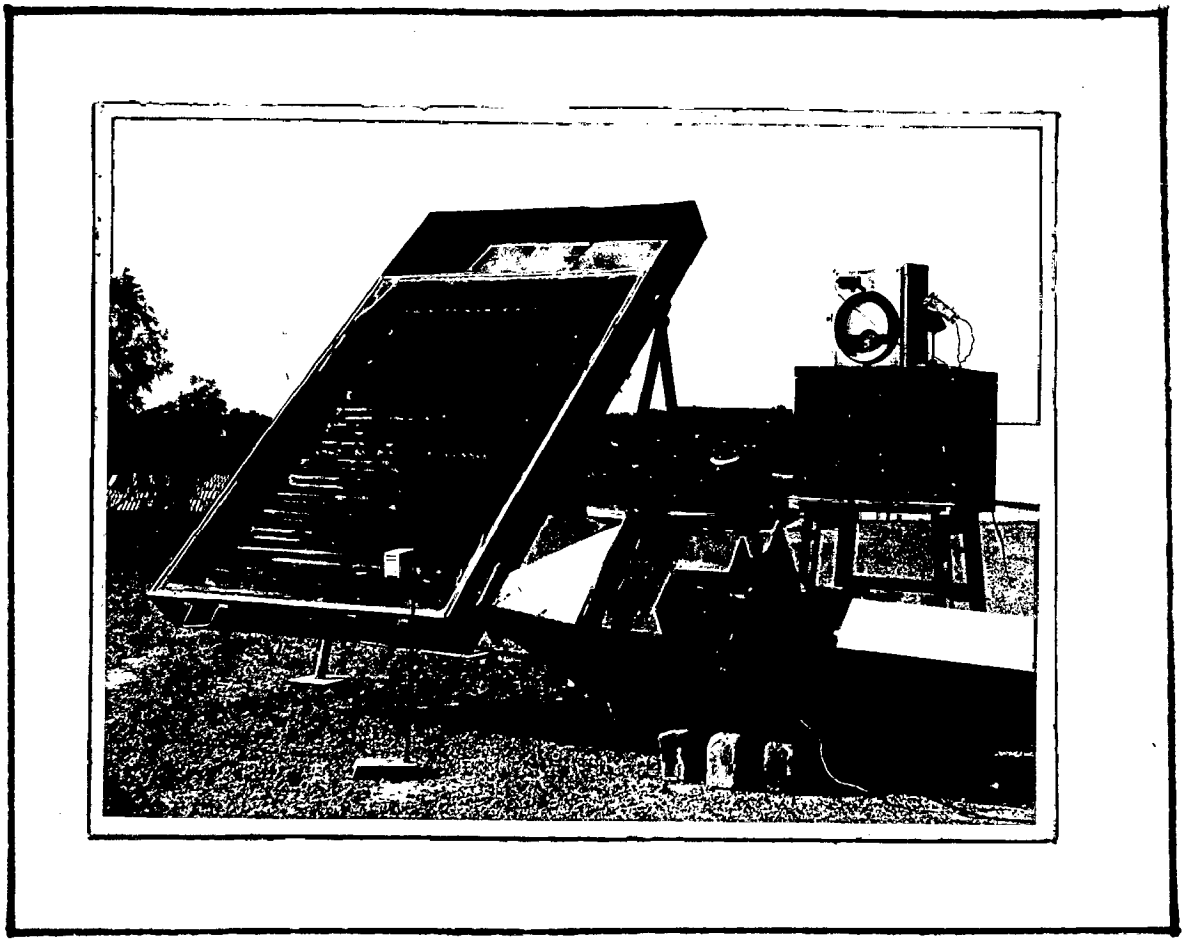

FIG.5.10 CORRUGATED AIR HEATER

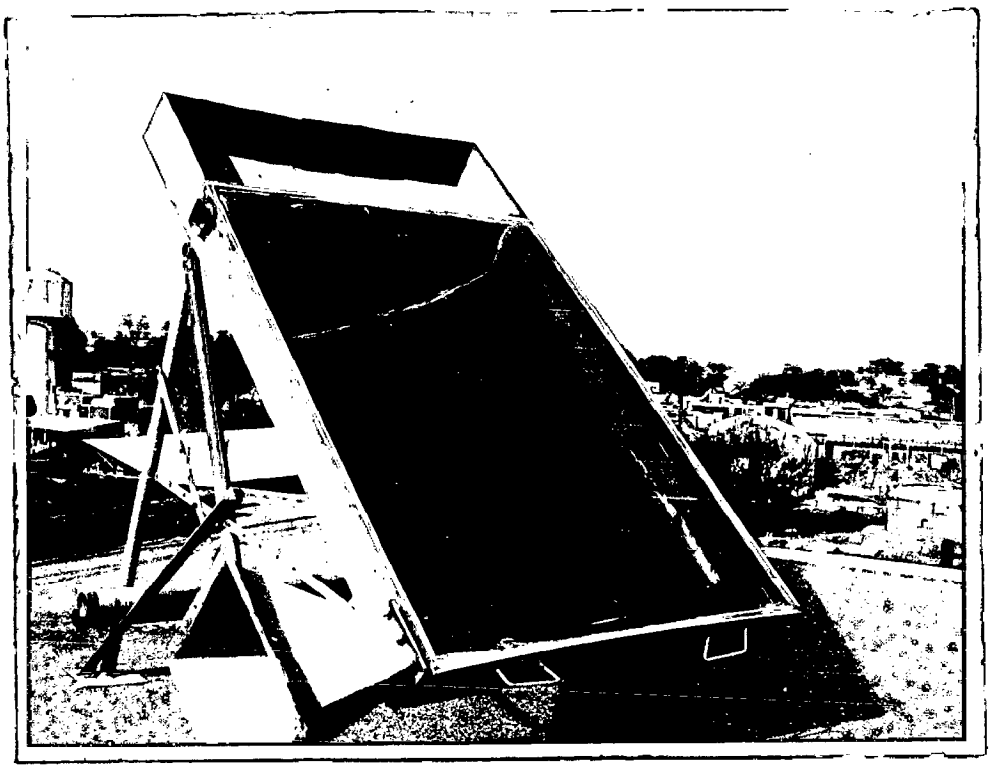

FIG.5.11 MESH AIR HEATER

$$q_u = F_p \left[\overline{Hf} - U_L (t_{av}-t_a)\right], \quad t_{av} = \frac{t_1+t_2}{2} \quad \ldots(5.22)$$

$$\eta = \frac{GC_p(t_2-t_1)}{H} \quad \ldots(23)$$

derived in section 5.2 that if it is possible to measure simultaneously at any instant the temperatures t_a, t_1 and t_2, the solar intensity incident on the collector H, and the mass flow rate G, the instantaneous efficiency of the air heater can be determined. Further, if these experiments are repeated at different values of t_1 and H, it is possible to calculate the values of groups of terms $(F_R f)$, $(F_p f)$ and f/U_L using the equations 5.21 to 5.23. Once quantitative values of these groups are known it is easy to obtain the values of the rating parameters F_p, F_R, U_L and f separately.

To realize the above objectives, four sets of measurements were taken for each heater.

(a) Physical dimensions of the heater: The absorber area and cross-sectional area of outlet header is measured, the ratio of corrugated area to the nominal area (ρ) was computed.

(b) Solar transmittance of the glass cover: This factor was measured as described in detail, in chapter 2.

(c) Solar absorptance of the absorber plate: This is measured by an instrument developed by the author[14].

(d) Outdoor colorimetric tests: The equipment for these colorimetric tests, is similar to, one suggested by Whillier[15] for water heaters and is shown in Fig.(5.10). In this case instead of a feed tank, a fan with thermostatic arrangement has been used to force the air through a finned air heater. With this arrangement any desired inlet temperatures could be maintained. The shade temperatures were recorded in a small stenvenson screen mounted nearby. Thirty two gauge copper constant thermocouples were used as temperature sensors and the corresponding thermal emf's were recorded every half hour with a potentiometer having a minimum count of ten microvolts. Casella air meter was used to measure the mean flow velocity at the outlet. Data on instantaneous total and diffused solar radiation on a horizontal surface were available from the solarimeters.

5.3.3 Results and Discussions

A computer programme was developed, to take the recorded observations as input data, to process them and obtain the temperature rise, the mass and discharge flow rates per unit area, the intensity of solar radiation on the collector (H) and the transmissivity, absorbtivity products (f). The same programme computes the value of $(t_1-t_a)/H$ and $(t_{av}-t_a)/H$ and the corresponding efficiency values. The measured results are shown in table (5.1) for all the four types of heaters tested at a fixed mass flow rate. The overall efficiency has been found to vary with the time of day and th diurnal variation

Table 8.

Results of tests on solar air heaters.

Heater type	Time (hours)	Solar radiation incident on surface cal/cm² hr	Temperature °C Shade air	Temperature °C Inlet air	Temperature °C Outlet air	Collection efficiency
I	10	64.4	29.2	43.8	76.0	0.66
	11	71.2	33.7	44.7	80.1	0.62
	12	67.2	33.0	42.4	71.0	0.61
	13	68.0	29.8	40.2	64.8	0.64
	14	70.4	33.0	44.0	64.2	0.65
	15	66.0	33.7	43.2	77.4	0.63
	16	58.8	31.6	41.0	61.9	0.63
II	10	67.0	32.6	43.3	68.9	0.60
	11	74.4	30.1	42.6	72.4	0.61
	12	74.4	30.9	46.6	75.7	0.63
	13	67.2	26.7	42.1	76.3	0.70
	14	67.2	29.1	44.0	73.0	0.66
	15	64.4	29.6	43.3	67.8	0.64
	16	59.6	30.1	43.2	64.8	0.63
III	10	63.1	31.0	43.4	60.6	0.40
	11	69.4	33.5	41.6	63.8	0.61
	12	76.8	37.9	42.1	74.3	0.60
	13	73.2	37.9	45.1	70.8	0.53
	14	61.8	37.6	44.0	70.5	0.56
	15	53.4	37.5	43.8	65.2	0.55
	16	49.4	37.5	41.2	56.9	0.56
IV	10	60.2	23.6	43.1	60.2	0.34
	11	70.0	27.6	46.7	75.8	0.36
	12	75.6	27.5	44.5	73.6	0.41
	13	76.0	30.4	46.5	78.6	0.33
	14	46.6	32.1	43.2	73.1	0.62
	15	31.2	30.2	42.6	59.1	0.52
	16	20.8	29.4	39.8	44.6	0.33

for a constant inlet temperature is given in Fig.5.12. From these observations the values of F_p, F_R, U_L etc. can be determined graphically as per the procedure described in an earlier publication[16]. The results are shown in Table (5.2). The required numerical values of all the parameters that appear in the generalised performance equations for each of the heater are now known and the efficiency and outlet temperatures can be computed for any set of operating conditions.

It can be seen from Table (5.2) that though the air heater type I has the highest plate efficiency factor (ξ_p) the heater type II is marginally better from performance point of صفلا because of lesser friction and greater discharge for the same pumping cost.

In case of matrix heaters, the type III is not very inferior to types I and II and in view of its ease of fabrication and possibly lower cost, it is likely to find a wide acceptance. Type IV is practically ruled out be cause of its low efficiency and high cost. Lowand[17] reported that the matrix type air heater has a better efficiency than a parallel plate type air heater. The present studies indicate that a corrugated pulsating type air heater (types I or II) will have still higher efficiencies than those of matrix types.

5.4.1 Room Heating Using Solar Air Heaters:

Heating studies for office rooms which are occupied during day time (sun-up hours) have been carried out at

TABLE 5.2: Rating parameters of the collectors tested for performance.

Collector type	Plate efficiency factor (F_p)	Heat removal efficiency factor (F_R)	Overall heat loss coeff. U_L (Kcal/m^2 hr°C)	Average efficiency	Shape factor (β)	$F_p U_L / C_p$	Total rate of discharge Q (litres/sec)	Rate of discharge per unit area V (cm/sec.)	Air mass flow rate G. (Kgs/m^2 hr)
I	0.86	0.76	8.67	0.61	1.166	0.39	14.66	1.57	58.16
II	0.84	0.77	8.71	0.62	1.166	0.47	10.20	1.95	78.00
III	0.89	0.73	8.70	0.64	1.0	0.49	17.43	1.87	69.43
IV	0.69	0.62	11.43	0.36	1.0	0.72	11.03	1.19	43.02

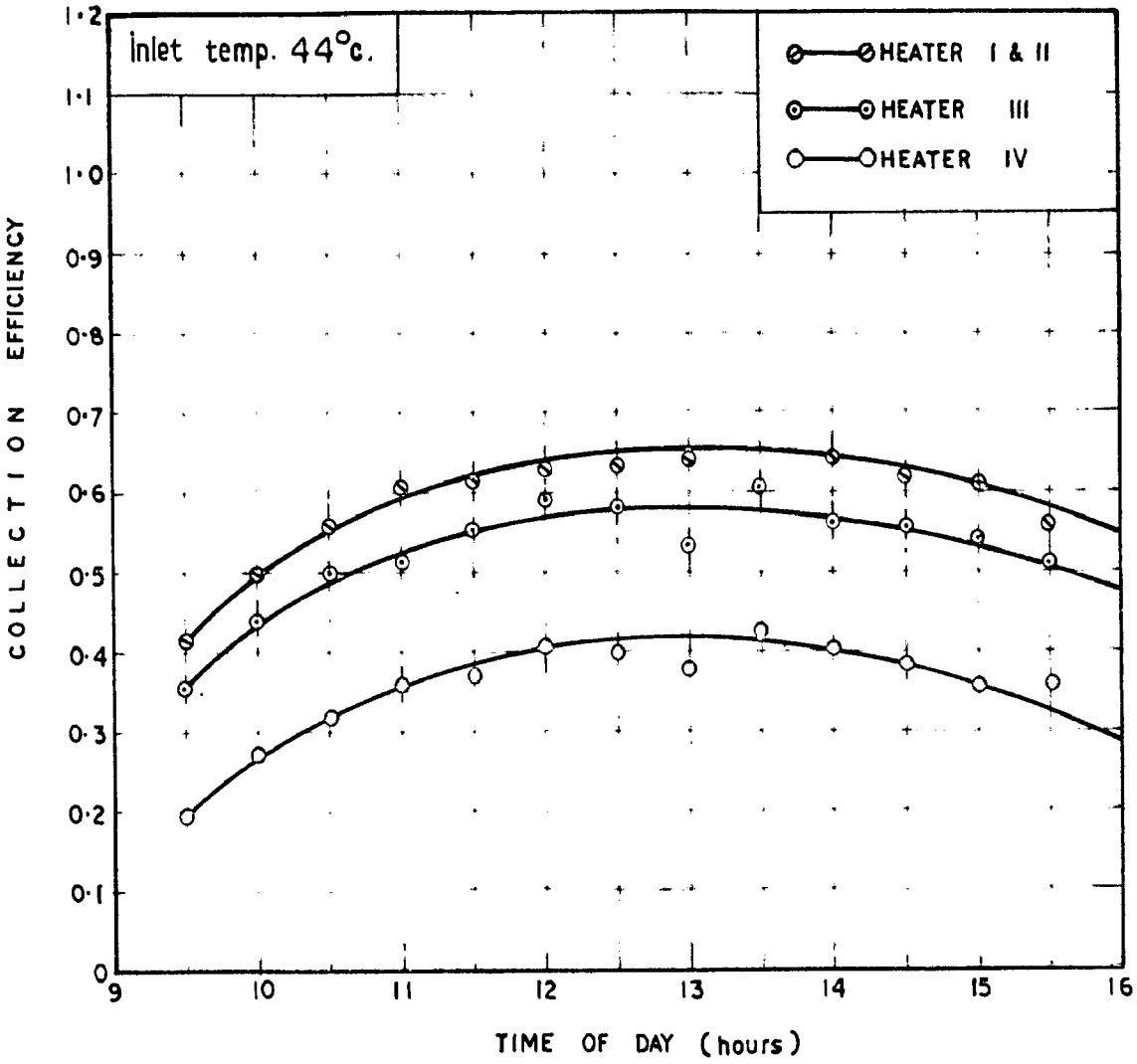

FIG. 5·12 DIURNAL VARIATION OF COLLECTOR EFFICIENCY

Roorkee (29° 51' N latitude). No provision of storing heat has been made in these studies, but an ausuliary electric heating arrangement was provided as a stand by to cope with the demands on cloudy or rainy days. The analysis of sun-shine hours and solar radiation intensity at Roorkee shows that there are hardly ten days for which extra electrical energy is required for heating purposes.

5.4.2 Experimental Room

The experimental room has the inner dimensions of 3.50 x 2.89 x 3.19 metres. It has unobstructed wind and solar exposure. Entrance to the room is through a door on the north partition wall and a 1.22 metres wide anteroom. The anteroom serves to minimize air infiltration. Three walls of the room facing east, south and west consists of 20 cm solid brick masonary with 1.0 cm plaster on either side. The roof consists of 16.5 cm R.C.C. over which 10.0 cm mudphuska, 5.0 cm brickTile and tarfelt at the top are laid. The room is without any window or ventilator, except the door which opens into the anteroom on the north partition wall of a 22.8 cm solid brick wall plastered on both sides. The structural specifications of the room are given in Table (5.3) and the thermo-physical properties[18] of the materials used for computations of heating load are given in Table (5.4). The plan of the test room is shown in Fig. 5.15.

5.4.3 Heating Load Estimation

q_s represents the total rate of heat loss

TABLE 5.2: Structural specifications of the experimental room.

Test unit components	Specifications (outer-inner layers)	Thickness (cms)	Interior surface area (m^2)	U (Kcal/m^2 hr^{0}C)
1. East wall	Cement plaster	1.0	11.165	1.94
2. South wall	Brick work	20.0	9.219	
3. West wall	Cement plaster	1.0	11.165	
4. North wall	Cement plaster	1.0	9.219	1.20
	Brick work	22.8		
	Cement plaster	1.0		
5. Roof	Tarfelt	0.04	10.126	1.42
	Brickfilo	5.0		
	Mud phuska	10.0		
	Cement concrete	10.0		
	Cement plaster	1.0		
6. Floor	Soil (compacted)	60.0	10.126	1.07
	Brick concrete	15.0		
	Cement concrete	5.0		

TABLE 5.4: Thermophysical properties of materials used

Material	Thermal Conductivity (Kcal/m hr^{0}C)	Density Kg/m^{3}	Specific heat Kcal/Kgm^{0}C
1.Brick work	0.697	1820	0.19
2.Cement concrete	1.360	2288	0.21
3.Cement plaster	0.620	1768	0.21
4.Mud phuska	0.446	1922	0.30
5.Soil (compacted)	1.000	1760	0.20
6.Brick tile	0.586	1892	0.19

(Kcal/hr), we know

$$Q_L = Q_{L,w} + Q_{L,R} + Q_{L,F} + Q_{L,G} + Q_{L,I} \quad \ldots(5.24)$$

where $Q_{L,w}$ is through walls, $Q_{L,R}$ roof, $Q_{L,F}$ floor, $Q_{L,G}$ glass and $Q_{L,I}$ air infiltration. The climatic data required for the estimation of heating load are dry and wet bulb temperature and solar radiation intensity. Based on the recommendations made in ASHRAE Guide[19], design dry-bulb and wet bulb temperatures are computed based on 10 years data for Roorkee and are, given in Table 5. Design solar radiation for all the orientations and for horizontal and vertical surfaces are also shown in Table (5.5).

The calculation of heating load is based on the following usual assumptions:

(1) Unidirectional heat flow.
(2) the material properties are constant.
(3) outside and inside surface coefficients i.e. h_o and h_i are constant.

The heat flow equation can be written as,

$$\frac{\partial t}{\partial \theta} = \alpha \frac{\partial^2 t}{\partial x^2} \quad \ldots(5.25)$$

where $\alpha = K/\rho C$ is the thermal diffusivity of the roof or wall.

The solution of equation (5.25) for various boundary conditions are given by Alford, Ryan and Urban[20]. The

TABLE 5.5: Design DryBulb and WetBulb temperatures (°C) and total solar radiation on horizontal and vertical surfaces (Kcal/m² hr) for Roorkee for winter season.

Time (hrs)	Temperature (°C)		Total solar radiation (Kcal/m² hr)								
	Dry bulb	Wet bulb	N	NE	E	SE	S	SW	W	NW	Hor.
1	7.3	6.5	-	-	-	-	-	-	-	-	-
2	6.8	5.9	-	-	-	-	-	-	-	-	-
3	5.6	5.2	-	-	-	-	-	-	-	-	-
4	5.6	4.0	-	-	-	-	-	-	-	-	-
5	5.0	4.3	-	-	-	-	-	-	-	-	-
6	4.8	4.0	-	-	-	-	-	-	-	-	-
7	3.9	3.2	-	-	-	-	-	-	-	-	-
8	4.5	3.2	32	70	320	370	230	32	32	32	130
9	6.2	3.6	33	38	330	470	340	33	33	33	260
10	9.8	5.3	50	50	330	500	440	160	50	50	300
11	12.3	8.5	57	57	200	470	500	270	57	57	430
12	14.6	10.4	69	69	69	390	625	300	69	69	470
13	16.2	11.3	67	67	67	330	500	470	200	67	430
14	16.7	11.0	60	60	60	160	440	600	360	60	360
15	16.7	11.8	33	50	33	33	340	470	360	33	260
16	16.2	11.3	22	22	22	22	220	350	320	76	130
17	15.0	11.6	-	-	-	-	-	-	-	-	-
18	14.5	11.6	-	-	-	-	-	-	-	-	-
19	12.8	11.4	-	-	-	-	-	-	-	-	-
20	11.7	11.3	-	-	-	-	-	-	-	-	-
21	10.6	7.3	-	-	-	-	-	-	-	-	-
22	9.5	6.8	-	-	-	-	-	-	-	-	-
23	8.4	6.4	-	-	-	-	-	-	-	-	-
24	8.4	6.7	-	-	-	-	-	-	-	-	-

hourly heat flow through any building section is given as:

$$Q = U(t_{sm}-t_i) + h_i \sum_{n=1}^{N} \lambda_n t_{en} \cos(w_n\theta - \psi_n - \phi_n) \quad \ldots(5.26)$$

where U = overall heat transfer coefficient (Kcal/m^2hr°C)

t_{sm} = mean solar air temperature (°C).

t_i = room air temperature which is to be maintained (°C).

h_i = inside surface coefficient (Kcal/m^2hr°C)

t_{en}, ψ = anaplitude and phase of the sol-air temperature harmonic components.

$\lambda n, \phi$ = decrement factor and phase lag angles.

The sol-air temperature(t_e) has been expressed as fourier series as follows,

$$t_e = t_{sm} + \sum_{n=1}^{N} t_{e,n} \cos(w_n\theta - \psi_n) \quad \ldots(5.27)$$

In the computation of sol-air temperature the low temperature radiation exchange between the outside surface and sky as suggested by Rao[21] has been included.

The inside and outside surface coefficients are taken as 7.32 and 17.08 Kcal/m^2hr°C. The values of absorptivity of solar radiation for roof and walls are 0.7 and 0.5 respectively. The infiltration of air has been assumed to be negligible in the computation. In winter, the indoor conditions for comfort are assumed as 21°C air temperature and 50 per cent relative humidity

as recommended in ASHRAE guide.

The equations for design sol-air temperatures computed as above for Roorkee are given below:

For Horizontal Surface (Roof):

$$t_e = 13.76 + 10.90 \cos (150-207.56) + 5.25 \cos (300-15.35) + 1.75 \cos (450-184.35) + 0.15 \cos (600-253.48)$$

For East Wall:

$$t_e = 9.86 + 3.89 \cos (150-230.47) + 1.89 \cos (300-249.00) + 3.63 \cos (450-54.91) + 3.41 \cos (600-231.91)$$

For South Wall:

$$t_e = 13.45 + 10.35 \cos (150-209.17) + 4.60 \cos (300-17.50) + 1.16 \cos (450-186.91) + 0.41 \cos (600-202.41)$$

For West Wall:

$$t_e = 11.20 + 8.12 \cos (150-231.80) + 3.54 \cos (300-63.52) + 1.34 \cos (450-281.37) + 0.86 \cos (600-180.26)$$

For North Wall:

$$t_e = 10.07 + 6.09 \cos (150-231.80) + 1.92 \cos (300-5025) + 0.55 \cos (450-209.51) + 0.11 \cos (600-0.00)$$

Using IBM 1620 computer the hourly heat losses through roof, walls and floor, ($Q_{L,R}$; $Q_{L,w}$; $Q_{L,G}$ & $Q_{L,F}$) have been computed as described above. The total estimated hourly heat loss for the experimental room are shown in Fig.13.

5.4.4 Experimental Arrangement:

It is seen that the integrated heating load for the experimental room is 23690 Kcal/day. But as the room is required to be heated during day time (office hours) only i.e. from 9.00 A.M. to 5.00 P.M., we are interested in the heating load for this period which comes to 9,608 Kcal.

As has been seen in Chapter (2) the total solar radiation on the air heater surface is given as:

$$H = 350 \times 10 \times 1.6$$
$$= 5600 \text{ Kcal/day.}$$

If air heater of corrugated type is used for this study which has an overall efficiency equal to 60 per cent then the total heat supplied to the room by a air heater of 1 m^2 collector area will be

$$= 5600 \times 0.6 \times 0.9$$
$$= 3024 \text{ Kcal/day } m^2$$

Thus the total area (A) of solar air heater required to match the demand will be

$$A = \frac{\text{Heat required}}{\text{Heat delivered}}$$

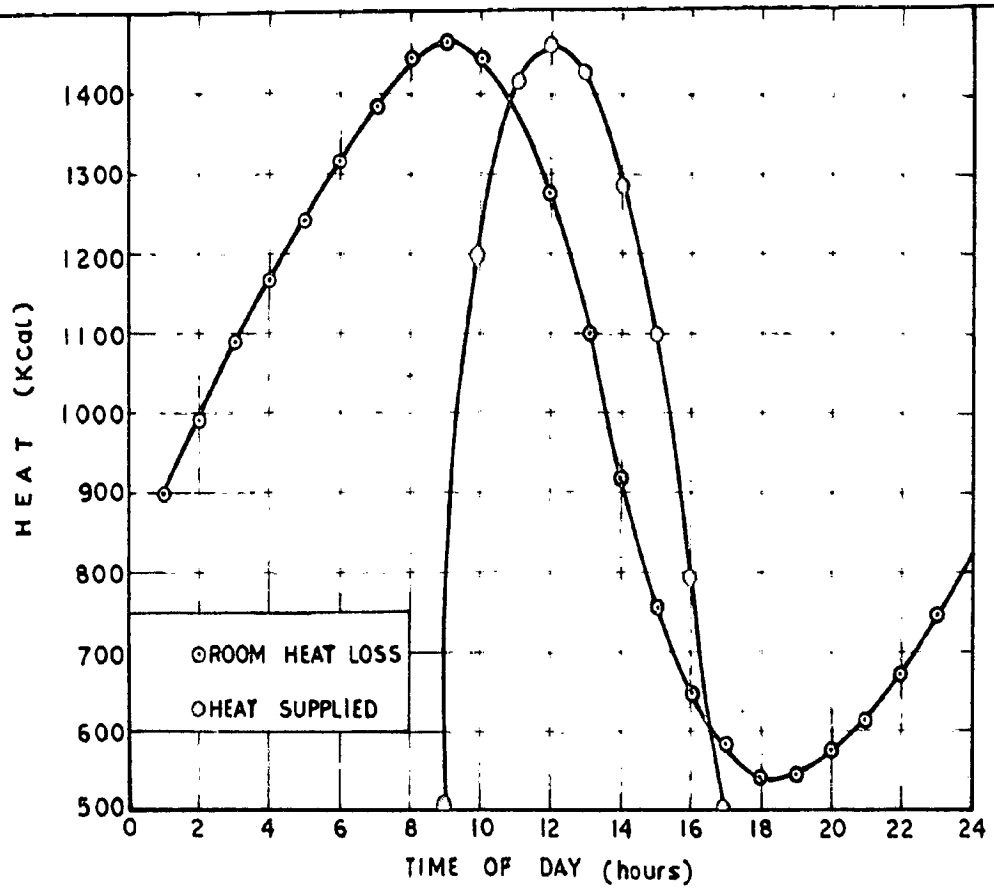

FIG.5·13 VARIATION OF HEAT LOSS AND HEAT SUPPLIED TO THE ROOM

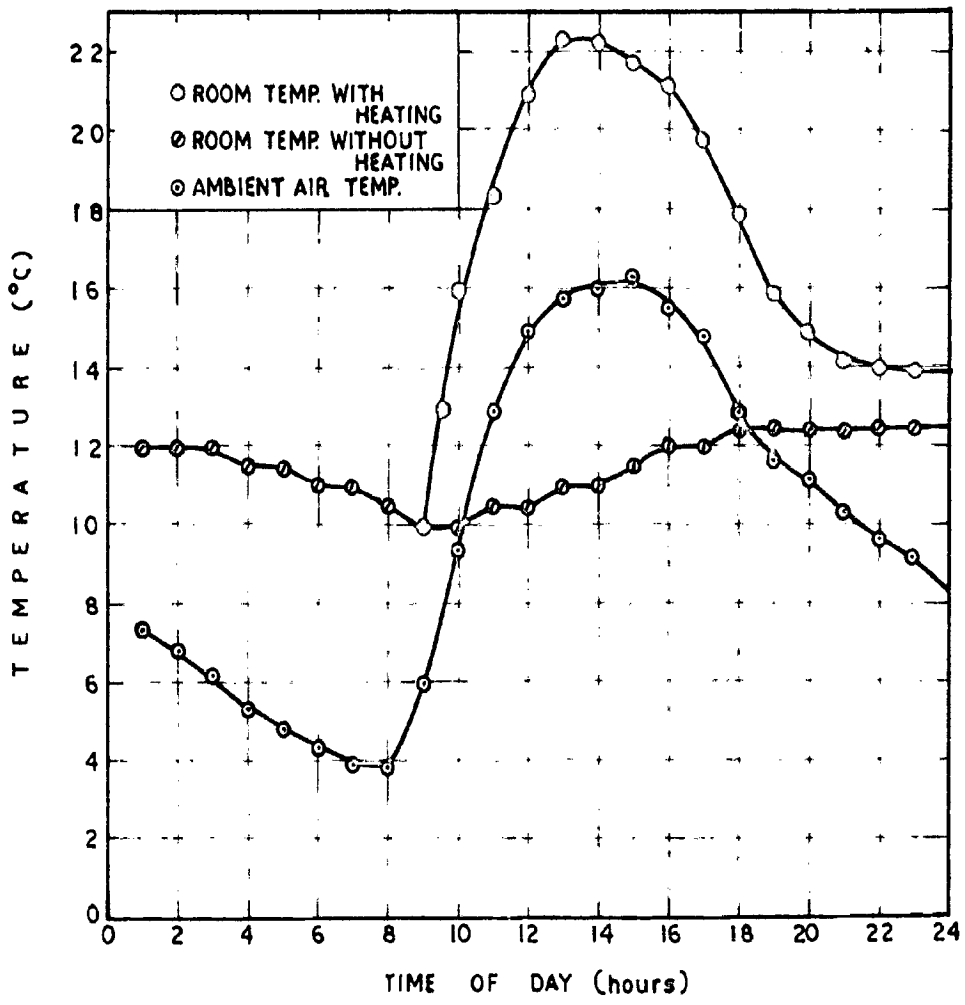

FIG.5·14 HOURLY VARIATION OF ROOM AIR TEMP. AND SHADE AIR TEMPERATURE

$= \frac{9608}{3024} = 3.17\ m^2$

So three collectors each having an area of 1.0 m^2 of type I described earlier are used. These absorbers inclined at 45° from horizontal, the optimum angle for Roorkee, are connected in cascade and then to the room as shown in Fig.(5.15). Hot air from the solar air heaters enter the room near the floor and is distributed in the room along its entire length by a perforated duct. The outlet is taken from the room near its ceiling forming a closed cycle of air circulation. If more air heaters are to be used on the roof then they should be mounted as shown in Fig.(5.16) so that there may not be any shadow cost by any unit on other collectors during the sunup hours.

A centrifugal fan of 0.5 H.P. is used for the circulation of air through the collectors and room. The fan was in operation from 9.0 A.M. to 5.00 P.M. daily and was controlled with the help of time switch. A number of 32 gauge copper constantan thermocouples are used for the measurement of air temperature at various levels in the room and inlet and outlet of the air heaters and ambient air temperature.

The hourly heat supplied to the room for a typical winter day is shown in Fig.(5.13) along with the hourly heat loss from the room. The resulting rise in room air temperatures with and without heating along with the ambient air temperature are shown in Fig.(5.14). It can be seen here that when the room was not heated the

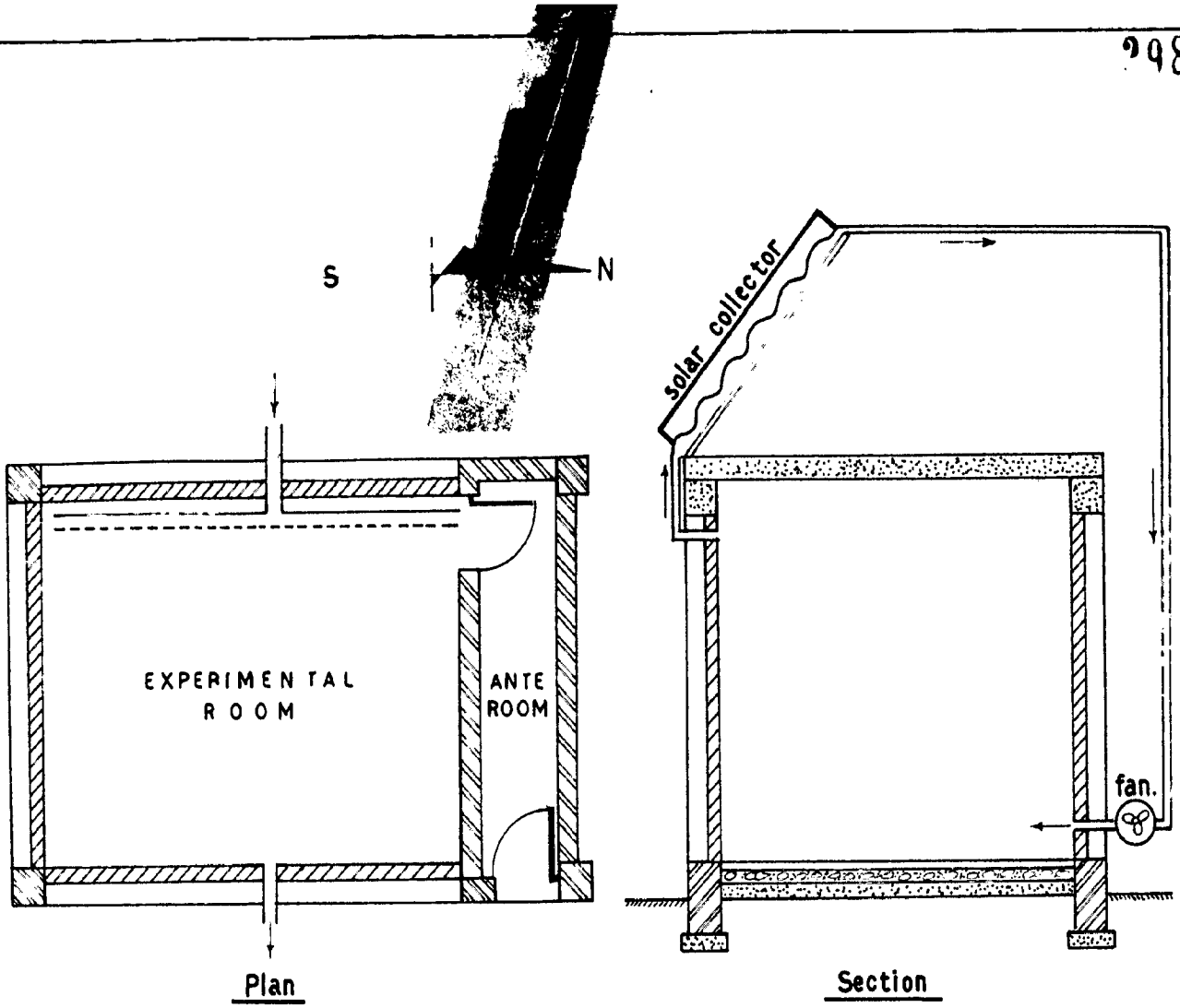

FIG.5·15 EXPERIMENTAL TEST ROOM SHOWING THE POSITION OF COLLECTOR. FAN, INLET AND OUTLET POSITION OF DUCT

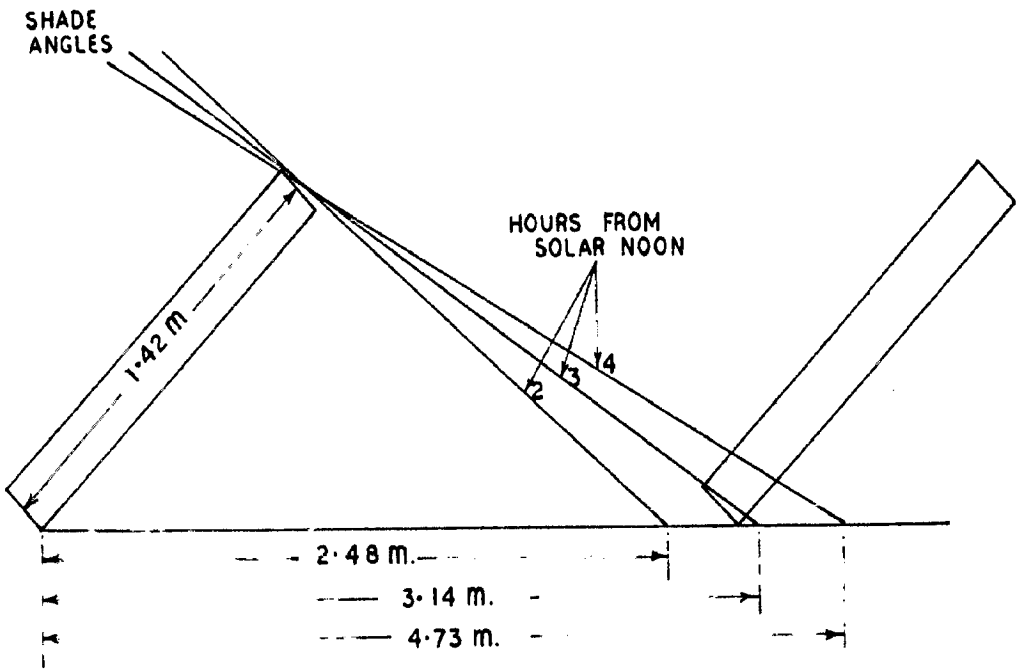

FIG.5·16 POSITION OF ROOF MOUNTED SOLAR AIR HEATERS

temperature varies from 10 to 12.5°C, and where as with the heating system in operation the room air temperature rises, from 9.00 A.M. onwards reaching maximum of 22.4°C at 13 hours. The temperature then fall slowly and even after the sun set the indoor air temperatures are maintained at about 1.5 to 2°C as compared to that of unheated case. The performance data of the system is given below:

1. Heating load (9.0 A.M. to 5.0 P.M.)	=9608 Kcal.
2. Solar radiation incident on absorber surface.	=5188 Kcal/m^2 day.
3. Collector area.	=3.0 m^2
4. Total heat supplied to room (Including duct losses).	=9460 Kcal/day.
5. Efficiency of the system.	=0.60
6. Average mass flow rate.	=100 kgm/hr.
7. Power consumed by fan.	=3.2 KWH.
8. Booster energy supplied.	= Nil.

5.4.5 Conclusions

From the foregoing the following conclusions can be drawn with regard to the performance and characteristics of air heaters.

1. The solar air heaters described, can be conveniently used for heating office rooms without any provision for the storage of energy.

2. Auxiliary heating arrangement for cloudy or rainy days would be more economical then to

store the solar heat for such buildings.

3. The power consumed by the fan meant for circulation of air would be common to any other type of ducted air heating system and hence is not a special requirement for the solar air heaters.

4. The fan operating cost can be reduced by using an on-off control type thermostat instead of a continuous operation. The thermostat may be set at a suitable temperature so that it would ensure the most efficient room heating.

5. The method presented and the climatic data analysed can be confidently be used for the accurate estimation of heating loads for any type of building at a given place.

6. The collector area can be considerably reduced by providing an insulation layer on the inner side of the room as this will reduce the ~~effect~~ heating load. The effect of insulation will be presented in the next section.

5.5 ROOM HEATING USING HOT WATER PANELS:

A solar room heater capable of heating single rooms to compertable level has been designed and tested for two winter seasons at Roorkee. Water is used as a heat storage media and hot water is stored in a number of storage panels placed inside the room near the wall. Radiative and connective heat losses from the surface of panels

heat the room and thus the principle of panel heating is utilized. Storage panel heating is prefered since it has a number of advantages over the connective type of heating, such as

1. It is very suitable for small sized rooms and does not require any extra heat storage tanks.
2. The heat dissipating elements can be integrated with the interior surfaces.
3. Air currents within a room heated by panels have lower velocities eliminating the problems of draught.
4. The same heating panels may also be used for radiant cooling panels in climates where summer cooling is also a major requirement.
5. It cannot be easily tampered.

5.5.1 Experimental Room:

This study is divided into the following heads:-

1. Heating load estimation.
2. Collector area estimation.
3. Panel size estimation.
4. Experimental test set-up
5. Observations.

1. Heating Load Estimation:

Heating load for various roof and wall sections,

insulative and non-insulative type which are commonly used are computed and are given in Table (5.6) and (5.7). The method used is the same as discussed in section 5.4 of this Chapter and is discussed in detail by Rao[29]. The inside and outside surface co-efficient are taken as 7.32 and 17.08 Kcal/m^2 hr °C. The values of absorptivity to solar radiation have been taken 0.5 for walls and 0.7 for roofs, in view of the relatively darker shades of roofs. The source for thermal properties of building materials is the C.B.R.I. Building Digest No. 52 and Dr. Rao's[18] thesis. The heat gain or loss through glazing and due to infiltration of air can be estimated according to the procedures given in H.V.A.Guide[30], and be finally added to the structural heat losses. The U values and heat loss for various constructions are presented in table (5.7) for four cardinal orientations. For economy of space, maximum, total and average heat losses only are tabulated. In all these calculations it has been assumed that the inside air temperature is maintained at 21°C.

2. Collector Area Estimations

Tube in plate type collector as discussed in Chapter 4 is used here for heating water. For a given load and under specific climatic conditions the collector area can be fixed. Design curves, for estimating the collector areas for few cities representing wide climatic conditions and for various heating load requirements, are developed for a collector having an efficiency of 50 per cent. These design curves are shown in Fig.(5.17).

S.No.	Specifications	U (Kcal/m^{2}hr °C)	HEAT GAIN MAXIMUM (Kcal/m^{2}hr)	HEAT GAIN TOTAL (Kcal/m^{2}day)	HEAT GAIN AVERAGE (Kcal/m^{2}hr.)
1.	G.I.sheet +7.62 cm air space +2.5 cm mineral wool+0.61 cm plywood.	1.23	24.45	365.40	15.22
2.	G.I.sheet + 5.0 cm air space + 5.0 cm mineral wool + 0.61 cm plywood.	0.81	18.30	231.47	9.64
3.	A.C.sheet + 7.62 cm air space + 2.5 cm mineral wool + 0.61 cm plywood.	1.20	27.64	343.19	14.30
4.	A.C.sheet + 7.62 cm air space + 2.5 cm Thermocole + 0.61 plywood	0.69	16.01	206.93	8.62
5.	7.62 cm lime concrete + 11.43 cm B.B. +1.0 cm plaster	2.17	42.71	647.34	26.97
6.	7.62 cm lime concrete + 15.0 cm B.B. +1.0 cm plaster	2.04	37.20	617.91	25.74
7.	7.62 cm lime concrete + 10.cm R.C.C. + 1.0 cm plaster	2.45	49.61	730.63	30.69
8.	7.62 cm Brick flats + 7.62 cm mud phuska + 10 cm RCC + 1.0 cm plaster	1.99	42.20	604.22	25.17
9.	Terfolt + 10 cm foam concrete + 7.62 cm RCC + 1.0 cm plaster	0.73	12.20	212.68	8.86
10.	15 cm RCC + 1.0 cm plaster	2.86	62.33	941.77	39.24
11.	10 cm dense concrete + 5 cm Thermocole	0.49	8.31	112.5	4.69

TABLE 3.7: Heat loss factors for various commonly used wall sections.

Sr. No.	Specifications	U (Kcal/m^2 hr^{0}C)	Orientation	HEAT FLOW MAXIMUM Kcal/m^2 hr	HEAT FLOW TOTAL Kcal/m^2 day.	HEAT FLOW AVERAGE Kcal/m^2 hr.
1	1.0 cm plaster + 22.5 cm brick + 1.0 cm plaster	1.00	S	30.51	603.61	20.90
			SW	30.11	336.66	16.11
			W	31.36	506.00	21.00
			NW	32.24	270.01	20.25
			N	20.81	300.64	10.28
			NE	19.04	296.80	12.33
			E	21.67	400.07	16.69
			SE	21.56	420.64	17.80
2	1.0 cm plaster + 30.75 cm Brick + 1.0 cm plaster	1.46	S	22.61	331.04	16.32
			SW	22.12	307.55	12.81
			W	23.77	399.76	16.65
			NW	23.73	426.08	17.79
			N	20.93	488.96	20.37
			NE	20.30	380.70	16.03
			E	21.10	450.31	19.76
			SE	21.18	510.03	21.25
3	1.0 cm plaster + 11.25 cm Brick + 5.0 cm air space +11.25 cm Brick +1.0 cm plaster	1.46	S	19.91	368.46	15.35
			SW	19.06	291.14	12.13
			W	20.55	370.03	15.44
			NW	21.03	403.0	17.00
			N	11.19	199.43	8.31
			NE	11.33	156.03	6.52
			E	11.73	199.21	8.20
			SE	11.03	219.36	9.14
4	1.0 cm plaster + 7.0 cm Brick + 5.0 cm air space + 7.5 cms Brick + 1.0 cm plaster	1.72				
5	20.0 cm expanded clay aggregate concrete	1.27				
6	1.0 cm plaster + 11.25 cm Brick + 2.5 cm Thermocole + 1.0 cm plaster	0.717				

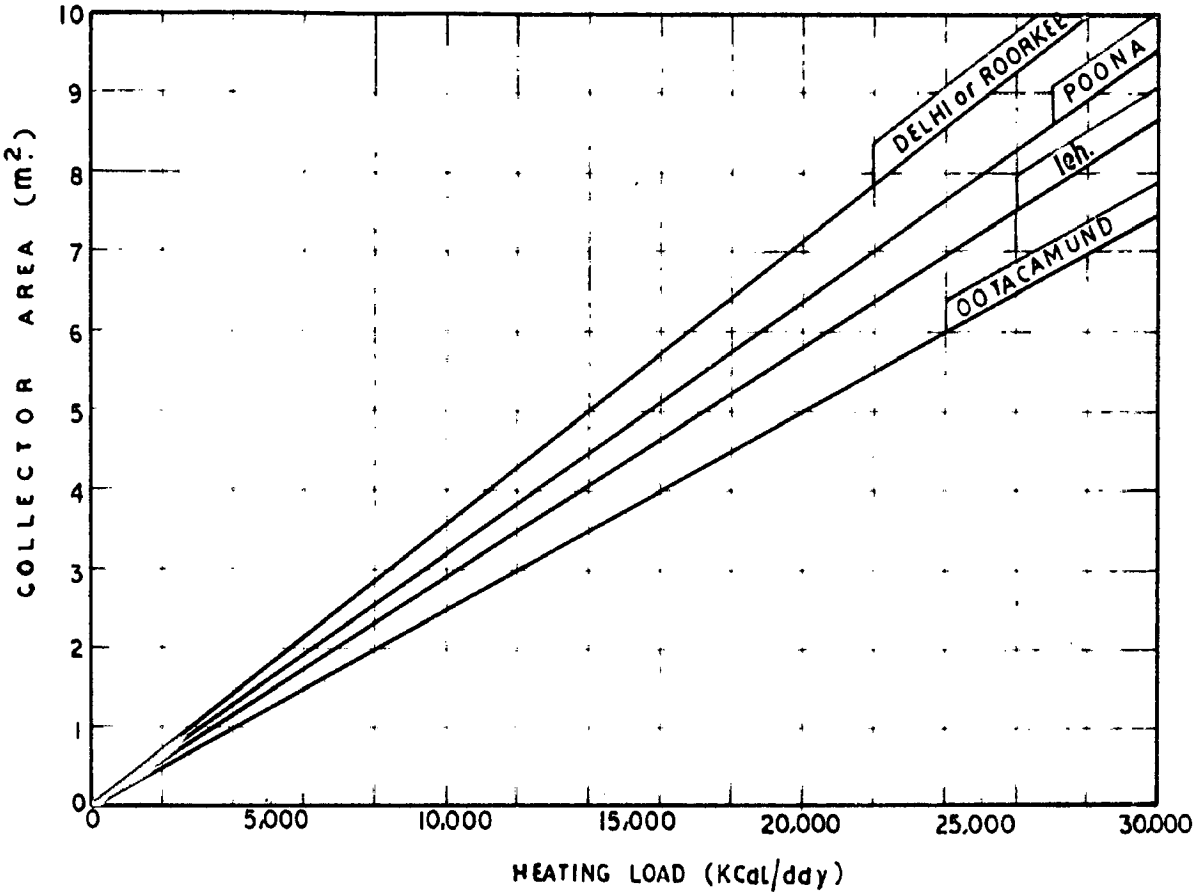

FIG.5·17 VARIATION OF COLLECTOR AREA WITH HEATING LOAD FOR VARIOUS PLACES

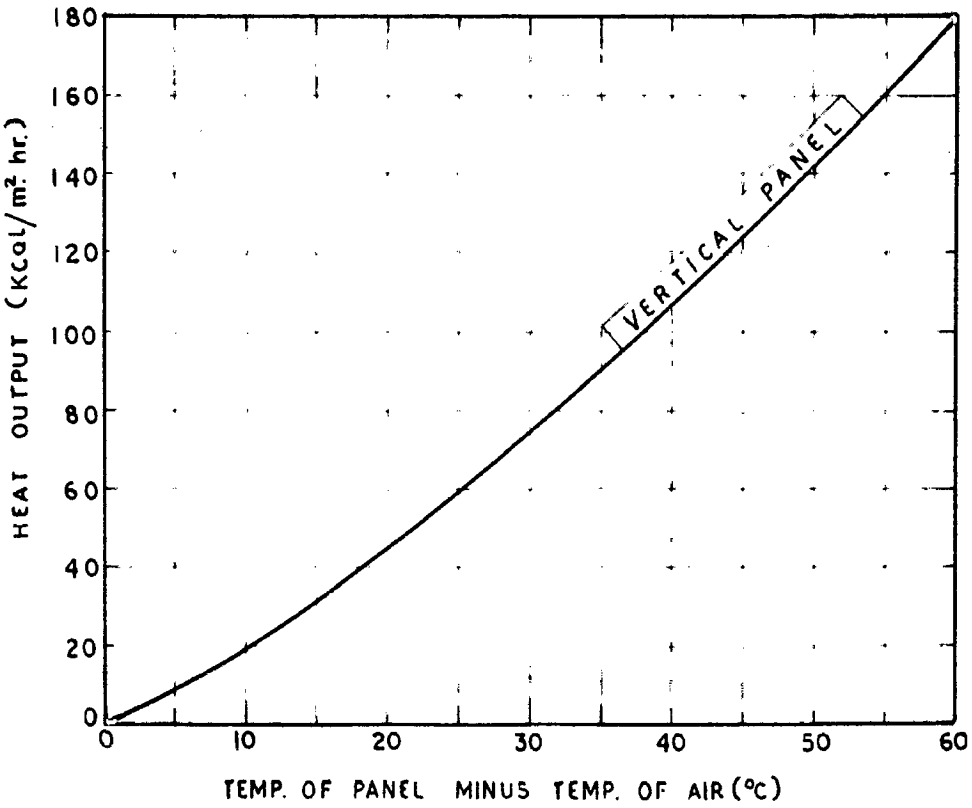

FIG.5-18. HEAT OUTPUT BY CONVECTION FROM VERTICAL PANEL

These estimates will hold good for collectors, oriented towards south and inclined at an angle of (L + 15°) from horizontal which is an optimum tilt for winter use. For example, if the heating load for any room at Roorkee is 20000 Kcal/day then the collector area to give this much of heat evaluated from Fig. 5.17, as 7.1 m^2. Suppose the each collector area is 1.0 m^2, then the number of collectors required to give 20,000 Kcal/day will be:

$$N = \frac{7.1}{1} \text{ i.e. } 7 \text{ numbers.}$$

3. Panel Size Estimation:

A heated panel transfers heat to a room by connection and radiation. The heat loss by convection and radiation are dealt seperately and then combined to get the overall effect.

Convective Heat Transfer: Since it is always convenient to put the storage hot water panels in a vertical position near the wall heat transfer calculation are made only for this special case. Here the heat transfer is basically by natural or free convection. It has been shown by M.C. Adams[7] on the basis of experimental data that heat loss by free convection for vertical plates or cylinders can be computed from the following dimensionless equation.

$$N_u = 0.53 \, (G_r \cdot P_r)^{1/4} \qquad \ldots(5.28)$$

where N_u = Nusselt number = $\frac{h_c \, d}{K}$

G_r = Grashaf number = $\frac{l^3 \rho^2 g \beta \Delta t}{\mu^2}$

If A_1 and A_2 are in the ratio of 1 to 10 then

$$F_c = 0.89$$

So

$$q_r = 0.89 \times 4.9 \times 10^{-8} \times 1 \left[(T_1^4) - (T_2^4)\right]$$

or

$$Q_R = 4.36 \left[\left(\frac{T_1}{100}\right)^4 - \left(\frac{T_2}{100}\right)^4\right] \qquad \ldots(5.31)$$

Here T_2 is the area waighted average t emperature of unheated surfaces in room i.e. mean radiant temperature (MRT) of the room, which is given as

$$MRT = \frac{\Sigma A t_s}{\Sigma A} = t_2 \qquad \ldots(5.32)$$

where t_s = surface temperature.

The heat output by radiation is computed with the help of equation (5.31) for various values of panel surface temperatures and mean radiant temperature and is shown in Fig.(5.19).

Combined Heat Transfer:

The heat transfer from a panel to a room can be determined by adding the convective heat transfer obtained from Fig.(5.18) to the radient heat transfer obtained from Fig.(5.19). For simplicity it can be assumed that the mean radiant temperature (MRT) of the room is equal to the air temperature which is to be mantained in the room. Here this temperature has been fixed as 20°C. Now for various values of temperatures difference the convective heat loss and radiant heat loss are computed and then the combined surface heat

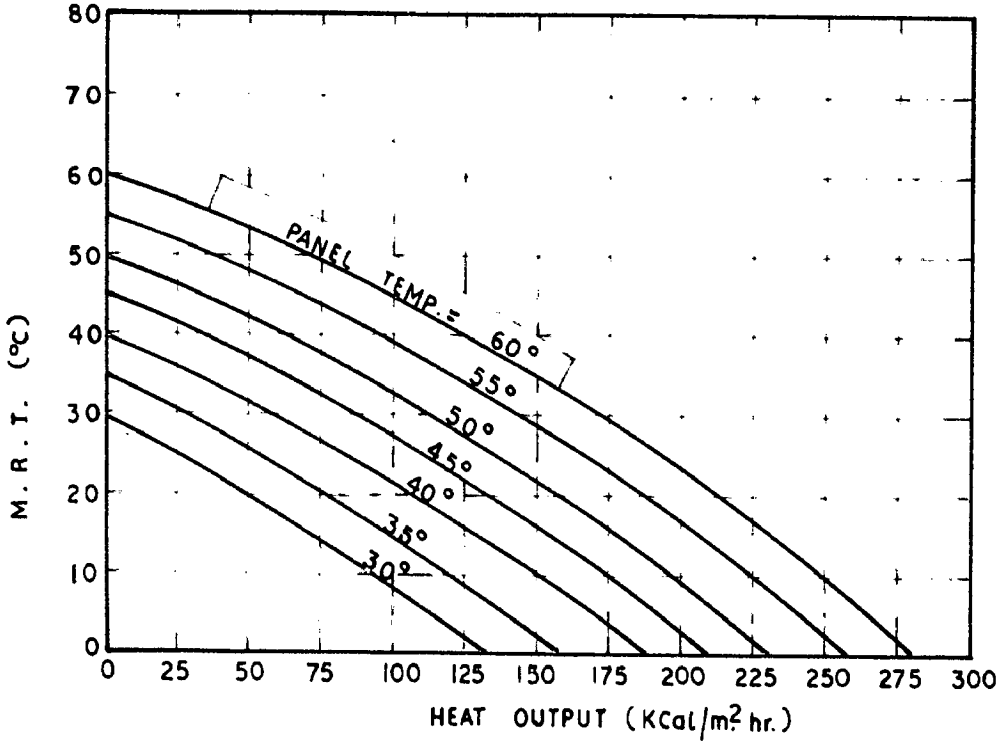

FIG. 5·19 HEAT OUTPUT BY RADIATION

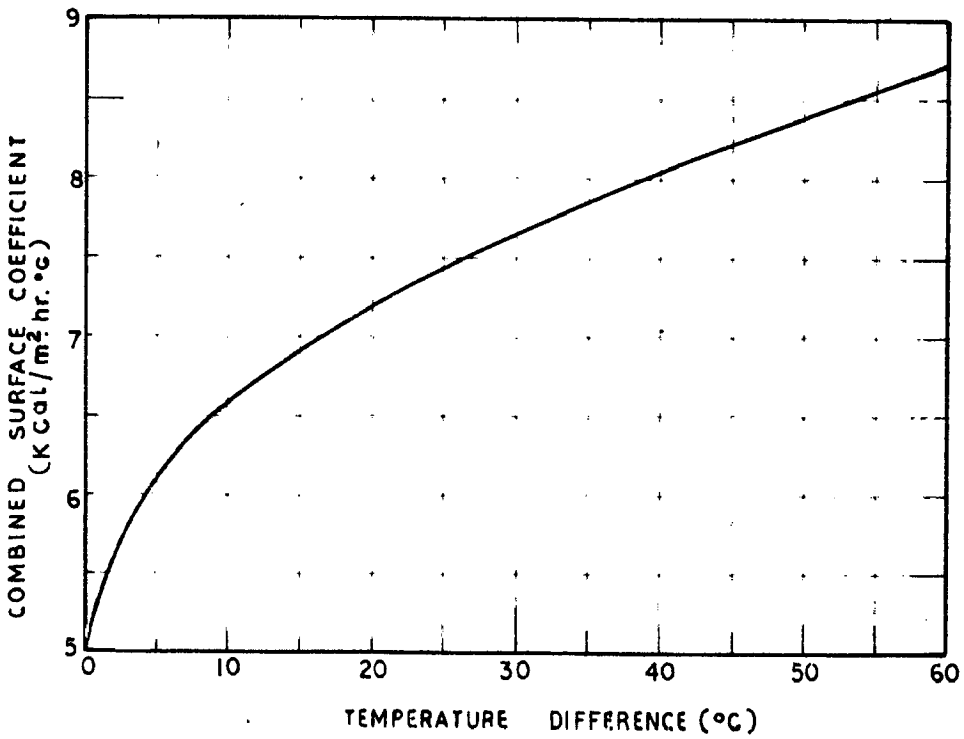

FIG. 5·20 VARIATION OF SURFACE COEFFICIENT WITH TEMPERATURE DIFFERENCE

transfer coefficient was determined by dividing the total heat loss by the temperature difference. The variation of the combined surface co-efficient with temperature difference shown in Fig.(5.20). It is seen here that after a temperature difference of 10°C the variation in film heat transfer with temperature difference is almost linear, and can be expressed by following linear equation.

$$h = 6.1 + 0.05 \Delta t \qquad \ldots(5.33)$$

This equation may be used for computing the surface coefficients for temperature differences above 10°C for a quick assessment.

AS has been seen in Chapter (4) that the efficiency of water heater depends on ~~the~~ its operating temperature so it has been assumed here that the system is capable of heating water upto 60°C. If the water in the storage panels cool from 60°C to 30°C in 24 hours, then

Mean temperature of operation of panel = $\frac{60+30}{2}$ = 45°C

The room is maintained at 20°C so the mean temperature difference is (45-20) = 25°C

$\therefore$ h = 7.35 (from equation 5.33)

$\therefore$ Total heat flow = 7.35 x 25

= 183.75 Kcal/m^2 hr.

Based on these computations a curve for arriving at panel area for various heating loads (panel output) is plotted and shown in Fig.(5.21). The amount of water required for various heating loads as a function of room

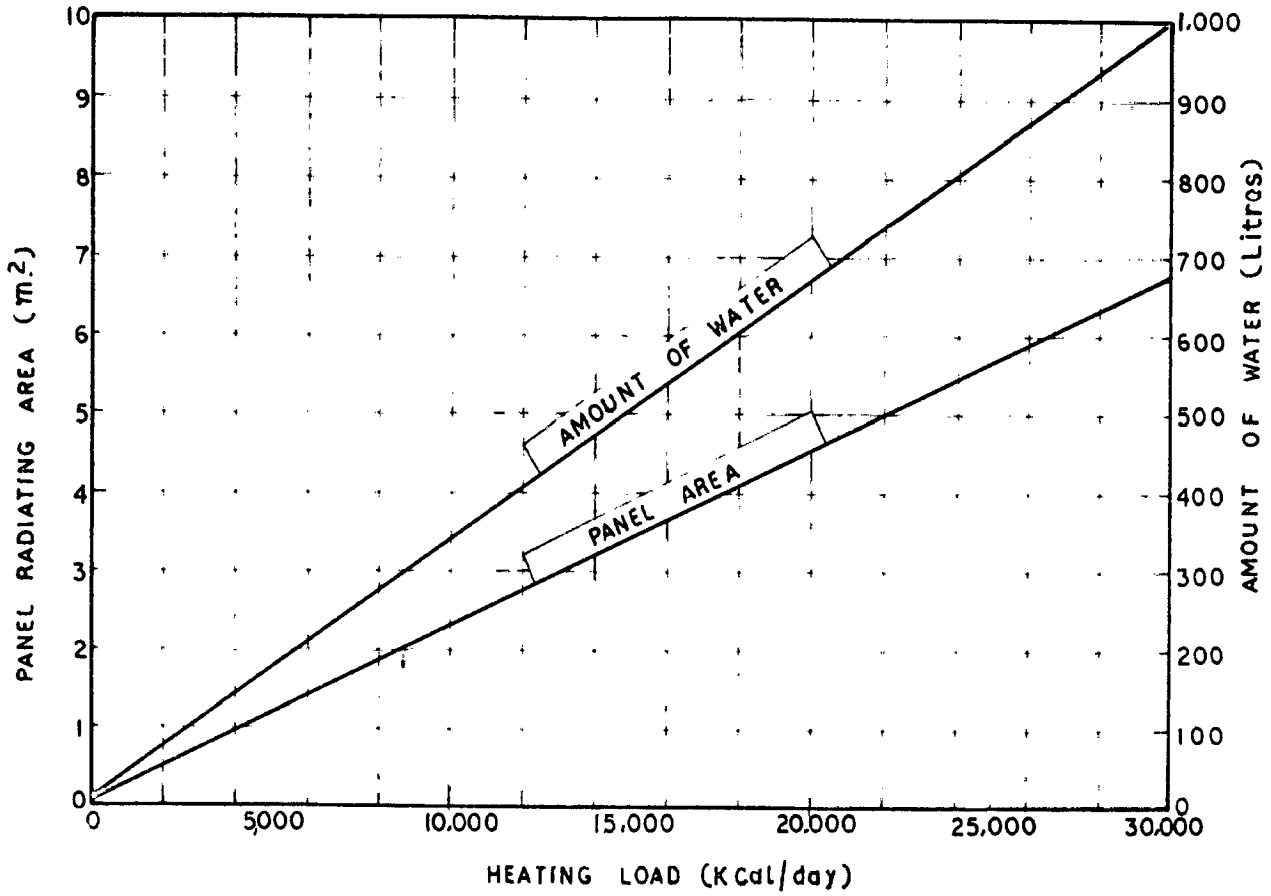

FIG.5.21 CURVE FOR PANEL AREA & WATER CAPACITY FOR VARIOUS HEATING Loads.

heat load is also shown in the same Fig. (5.21).

4. Experimental Test Set-up:

The room selected for this study is the same experimental room used in section (5.4) for heating with solar air heaters. It has been seen that the heating load for this room is 23690 Kcal/day. The collector area required to collect 23,690 Kcal/day heat from Fig.(5.17) is 8.46 m^2. The panel radiating area required to loose 23,690 Kcal/day from Fig.(5.21) is 5.36 m^2 and amount of water required to store this heat is 790 litres.

The absorber used has the dimension of 1.83 x 0.75m or an area of 1.37 m^2. Thus the number of absorbers are:

$$N = \frac{8.46}{1.37} \text{ ; i.e. 6 numbers}$$

A cylindrical tank of capacity 700 litres and surface area 4.67 m^2 was used for this study its dimensions and capacity is nearly the same as required here. This storage tank which acts as a heating panel is placed on the floor on wooden battens near the south wall of the room as shown in Fig.(5.22).

Here all the six absorbers were placed on the roof facing south having a tilt of 45°C from the horizontal which is the optimum tilt for Roorkee. The circulation of water through the absorbers and storage panel is made by a 1/6 H.P. booster pump. A reverse type thermostat set at 55°C is fitted at the outlet of the absorbers which is then connected in series with the pump. The

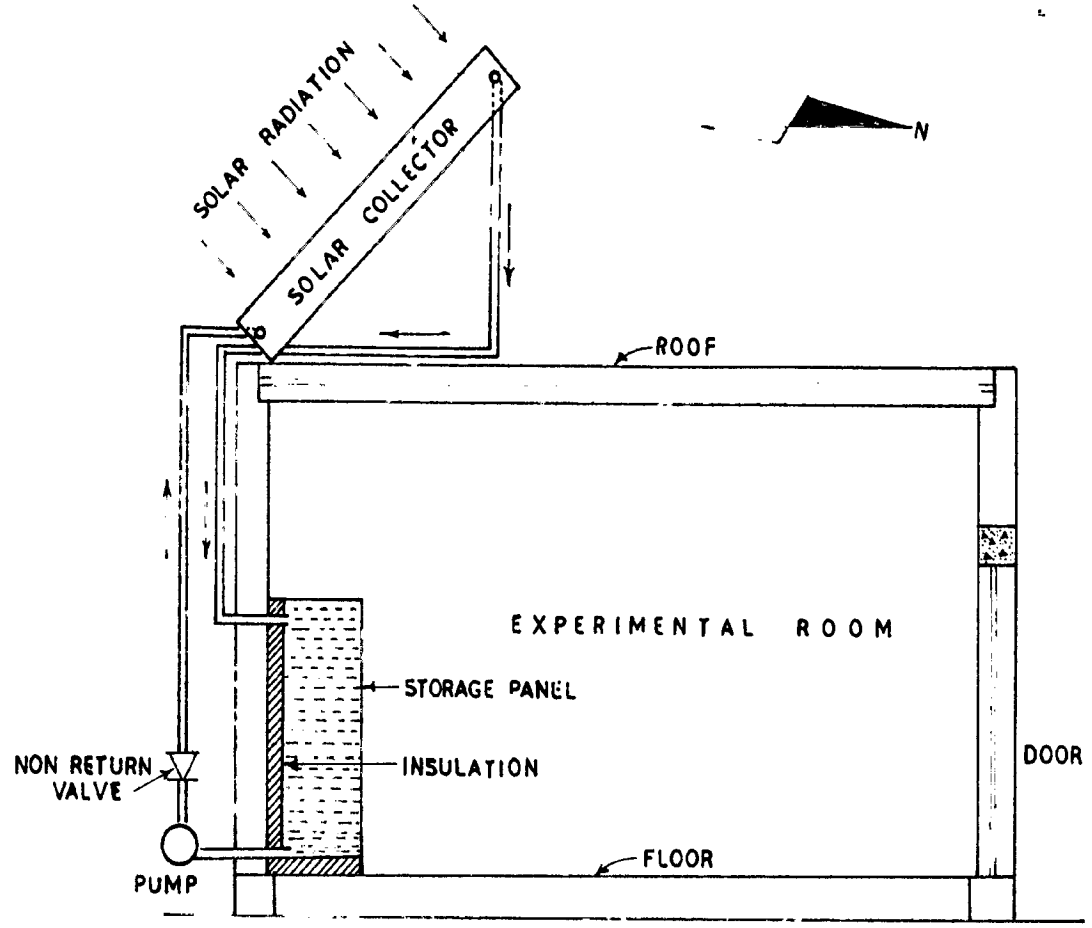

FIG.5·22 EXPERIMENTAL TEST SETUP WITH ROOF MOUNTED SOLAR COLLECTORS

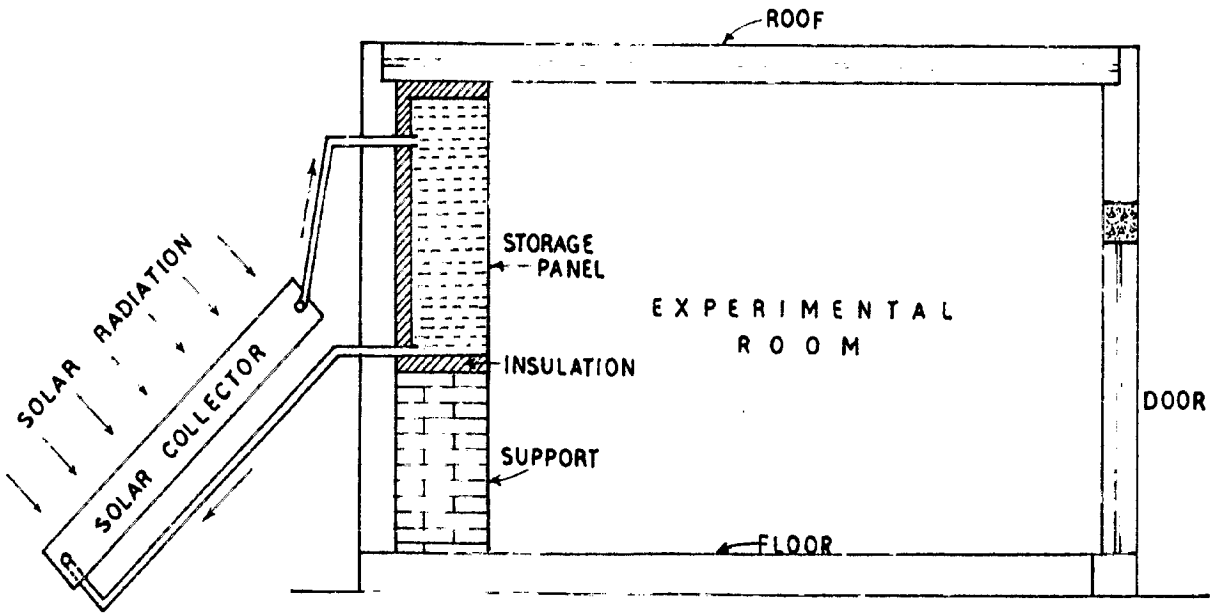

FIG.5·23. EXPERIMENTAL TEST SETUP WITH GROUND MOUNTED SOLAR COLLECTORS

power consumption by the pump is around 0.30 KWH per day.

Where there is no electricity, the principle of thermosyphon action may be used for the circulation of water. In this case, the storage panels should be placed at a higher level than the absorber for maintaining the pressure head necessary for natural circulation of water. This means that the absorbers are to be located on the ground. This arrangement is shown in Fig.5.23.

5. Observations:

A number of copper constantan thermocouples (32 SWG) are used in conjunction with an automatic multipoint millivolt recorder for the measurement of temperature. These thermocouples are used for measuring the inside wall, ceiling and floor temperatures, storage panel water and surface temperatures. Three thermocouples are used for measuring the room air temperature. One was fixed in the centre of the room at 30 cm. above the floor, another at 100 cm above the floor and the third at 30 cms below the ceiling. These were fixed to see the temperaturegradient along the height of the room. Observations are made for 10 continuous winter days during January 1971 (coldest month) with and without heating the room. The outside ambient temperature and total solar radiation on horisontal surface are also recorded to see the similarity of the days for intercomparison of data. The total solar radiation on horizontal surface for all the days of observations are

given in Table (5.8). It is seen that there is practically no variation in the solar radiation intensity in all the days.

From the temperature measurement in the absende of solar heating of the room it is observed that there is no gradient of air temperature from floor to ceiling. Table (5.9) gives the room air temperature (°C) without heating for a period of four days. It is seen from this table that room air temperature varies from 11.0°C to 13.6°C.

The hourly room air temperatures (centre of room) with heating for five continuous days as recorded are given in Table (5.10). The table shows that at any hour the air temperature in the room is at a higher temperature than that at the corresponding hour on the previous day. This is because of the storage effect of the structure. The maximum temperature reached in the room on the fifth day was 22°C which may further rise if heating is continued for more days till equilibrium conditions are reached. The diurnal variation of air temperature in the room without heating (one representative day) and with heating for five days is shown in Fig.(5.24). It can be seen clearly that there is a build up of temperature in the room with days.

The temperature distribution in the room has also been studied. It is observed that there is no variation of temperature along the width of the room. The variation of temperature along the length of the room (i.e. away from the panel) is shown in Fig.(5.25). It is seen that

TABLE 5.8: Hourly total solar radiation on horizontal surface at Aberdeen (Cal/cm^2 hr).

HOURS (I.S.T)	DAY : 13th Jan. 1971	14th Jan. 1971	15th Jan. 1971	16th Jan. 1971	18th Jan. 1971	19th Jan. 1971	20th Jan. 1971	21st Jan. 1971	22nd Jan. 1971.
07	0.0	0.0	0.0	0.0	0.0	0.0	0.0	0.0	0.0
08	6.8	8.2	7.6	8.2	7.2	6.8	6.4	10.2	10.2
09	20.6	21.8	21.5	20.0	23.6	23.2	24.2	20.6	23.7
10	36.3	35.5	33.4	32.2	41.5	40.9	43.4	40.4	41.6
11	46.4	51.9	50.6	47.0	56.6	54.6	55.9	50.9	55.3
12	54.6	54.6	54.5	53.5	57.5	57.3	57.3	57.3	57.3
13	53.2	51.9	52.5	50.8	54.5	54.6	56.6	54.6	53.2
14	47.8	43.7	46.5	43.9	45.9	43.4	43.7	43.6	42.3
15	36.3	33.4	32.6	30.0	30.3	31.4	30.0	27.3	27.8
16	20.5	18.4	18.5	18.6	17.5	16.8	18.8	18.1	20.1
17	2.7	1.8	1.7	1.2	0.3	0.8	1.0	1.6	1.5
18	0.0	0.0	0.0	0.0	0.0	0.0	0.0	0.0	0.0

TABLE 5.9 : Hourly room air temperature(°C) without heating in winter, at Roorkee.

Hours (IST)	Day : 13th Jan. 1971	14th Jan. 1971	15th Jan. 1971	16th Jan. 1971.
09	11.0	11.0	11.0	11.1
10	11.0	11.0	11.1	11.1
11	11.0	11.0	11.2	11.3
12	11.0	11.1	11.3	11.3
13	11.0	11.1	11.3	11.3
14	11.0	11.1	11.3	11.3
15	11.2	11.2	11.5	11.5
16	11.5	11.6	11.6	11.6
17	12.0	12.2	12.3	12.3
18	12.5	12.5	12.6	12.6
19	13.1	13.2	13.3	13.4
20	13.1	13.3	13.3	13.4
21	13.3	13.5	13.6	13.6
22	13.3	13.5	13.6	13.6
23	13.1	13.3	13.5	13.6
24	12.5	12.7	12.8	13.0
01	12.5	12.6	12.6	13.0
02	12.2	12.0	12.2	12.5
03	12.0	12.0	12.2	12.5
04	11.7	11.8	11.8	12.0
05	11.5	11.5	11.5	11.8
06	11.5	11.5	11.3	11.5
07	11.2	11.2	11.1	11.3
08	11.0	11.0	11.1	11.1
09	11.0	11.0	11.1	11.1

TABLE 5.10: Hourly room air temperature (^{o}C) with heating in winter at Roorkee.

Hours (I.S.T.)	Day: 19th Jan. 1971	19th Jan. 1971	20th Jan. 1971	21st Jan. 1971	22nd Jan. 1971.
09	13.6	14.7	16.5	16.2	18.8
10	12.8	14.9	16.4	18.0	18.6
11	12.6	15.0	16.3	18.0	18.0
12	13.4	15.3	17.4	18.7	19.3
13	14.0	16.4	19.4	20.0	20.0
14	15.0	17.6	20.0	20.6	20.5
15	15.0	18.0	20.3	20.8	21.0
16	15.5	18.2	20.5	21.0	21.3
17	16.7	18.5	20.7	21.1	21.5
18	17.0	18.9	20.7	21.4	21.5
19	17.6	19.0	20.5	21.6	21.7
20	17.9	19.0	20.3	21.7	21.8
21	18.0	19.0	20.2	21.7	22.0
22	18.0	18.0	20.0	21.6	22.0
23	18.0	18.0	20.0	21.5	21.8
24	17.0	18.8	20.0	21.3	21.6
01	17.7	18.0	19.8	21.1	21.4
02	17.3	17.8	19.6	20.8	21.2
03	17.0	17.6	19.3	20.5	21.0
04	16.6	17.0	19.0	20.1	20.2
05	16.0	17.0	19.0	20.1	20.2
06	15.7	16.8	18.9	19.7	19.8
07	15.3	16.8	18.7	19.6	19.6
08	14.8	16.6	18.5	19.0	19.2
09	14.7	16.6	18.2	18.8	19.0

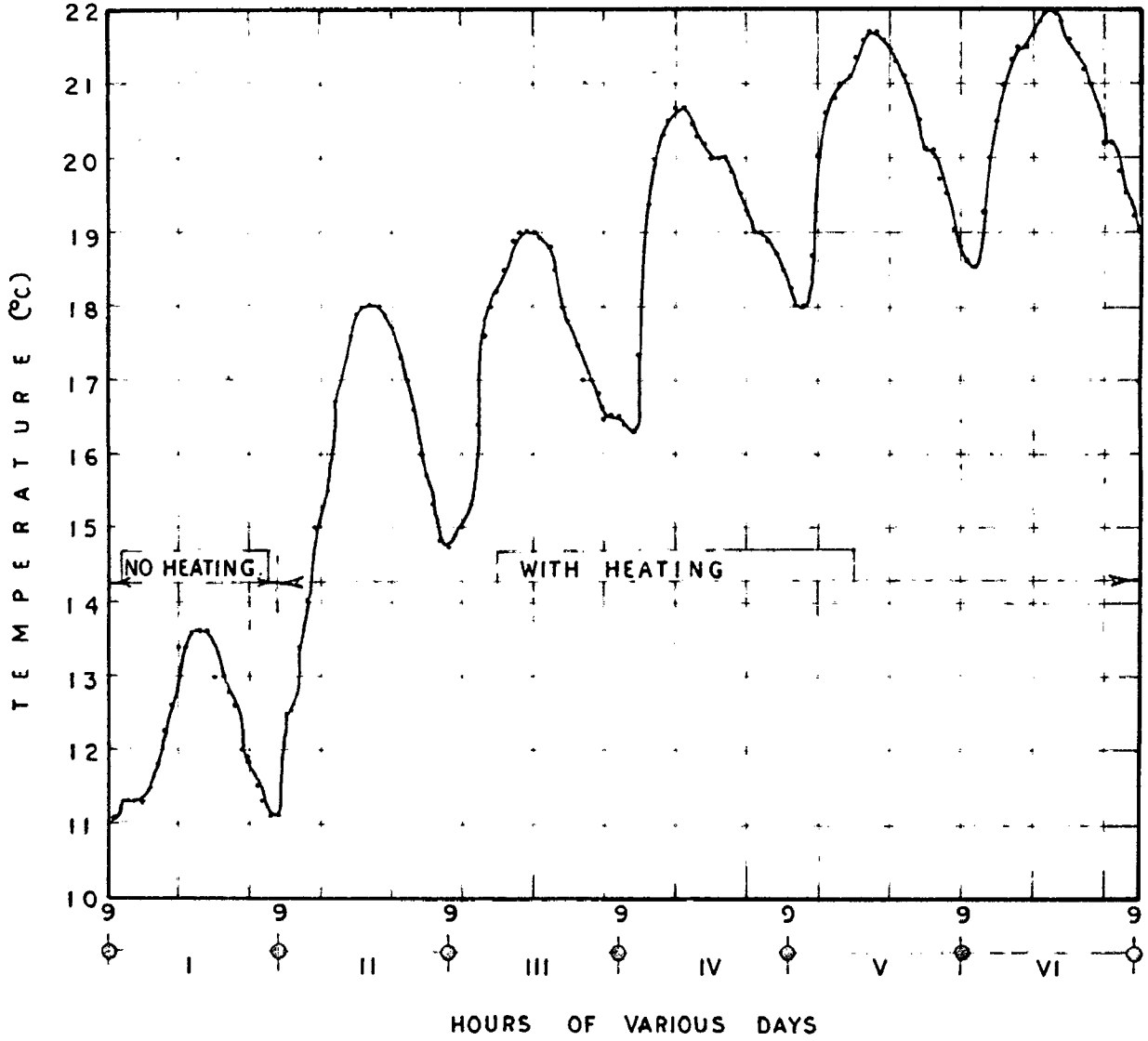

FIG.5·24 VARIATION OF ROOM AIR TEMPERATURE WITH & WITHOUT HEATING FOR DIFFERENT DAYS

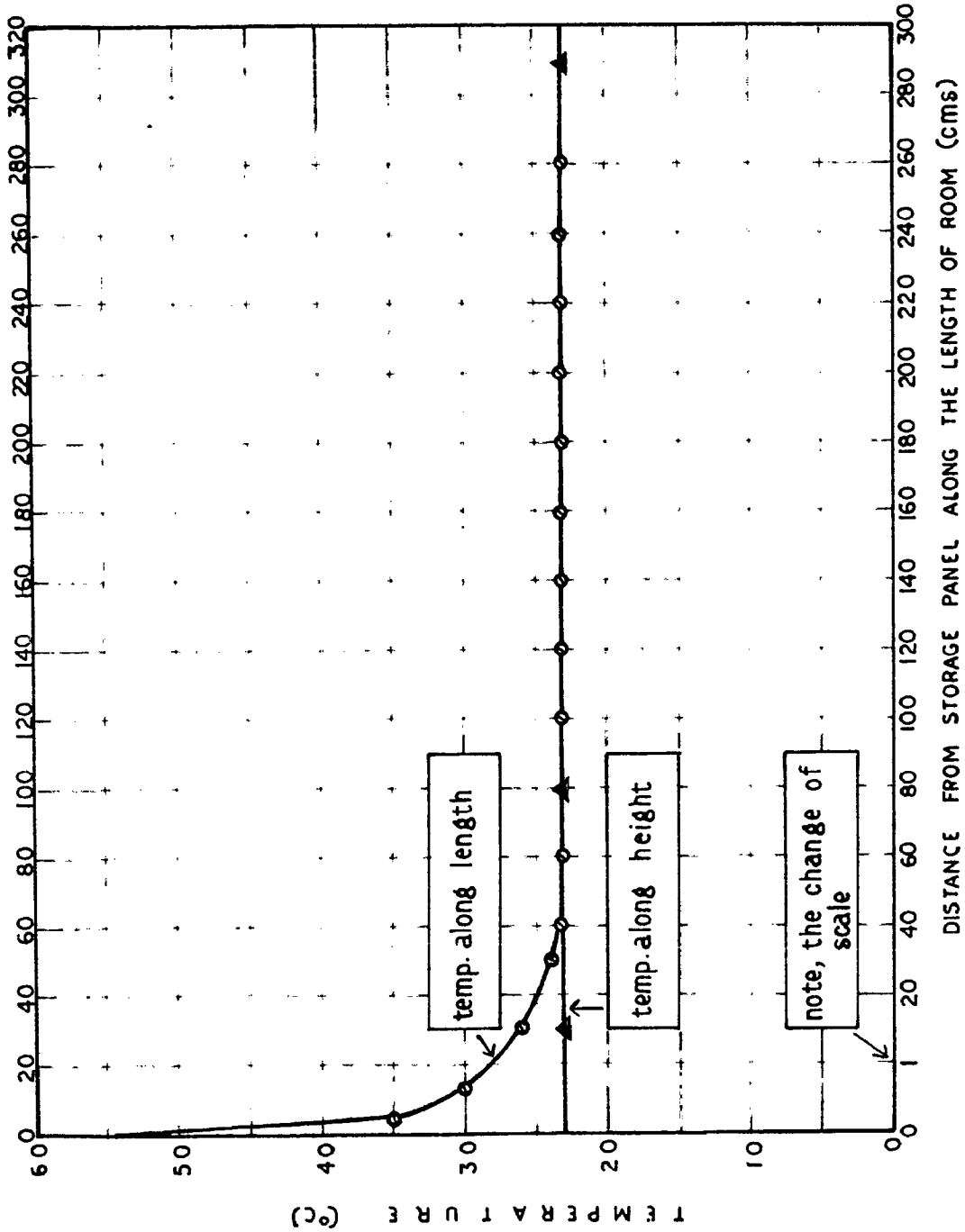

FIG. 5·25 VARIATION OF TEMPERATURE ALONG THE LENGTH AND HEIGHT OF THE ROOM.

the air temperature near the tank falls very rapidly i.e. 53.5°C to 28°C in 1 cm distance only. After 40 cm of distance from the tank there is no variation of temperature along the whole length of room. The temperatures along the height was also measured and are shown in Fig.(5.25). It is seen here that there is no gradient of room air temperature from floor to ceiling in this case too.

5.5.2 Office Room:

Further studies were made in a typical occupied office room in order to obtain factual performance data under actual usage conditions. For this purpose an office room having dimensions (6.7 x 3.5 x 3.5) is selected. This room is on the ground floor of a two storeyed building. The plan of the room, is shown in Fig. 5.26. The specifications along with the thermophysical properties are given in Table 5.11. In this case only one wall (NW) is exposed to outside, that too shaded by adjacent wings of the building. All the other three walls are partition walls.

Design of the System:

To maintain this room at 20°C in the month of January, the total heating load comes out to be 28000 Kcal/day. For this load the following design figures are obtained:

Room air temperature to be maintained = 20.0°C

Total heating load = 28000 Kcal/day

Table 6.11: Structural specifications of the office room used for solar heating.

Component	Orientation	Shaded or Unshaded	Specifications (outer- inner layers)	Interior surface area (m^2)	U ($Kcal/m^2 hr^0C$)
1. Wall	SW	Shaded	1 cm plaster + 11.4 cm Brick + 1 cm plaster	9.66	2.17
2. Wall	NE	Shaded	1 cm plaster + 11.4 cm Brick + 1 cm plaster	20.83	2.17
3. Wall	NW	Shaded	1 cm plaster + 45.7 brick + 1 cm plaster	8.8	1.14
4. Wall	SW	Shaded	1 cm plaster + 33.7 cm Brick + 1 cm plaster	23.45	1.24
5. Roof	Horizontal	Shaded	1 cm plaster + 11.25 cm RCC + 1 cm plaster	23.45	2.63
6. Floor	"	Basement	1 cm plaster + 11.25 cm RCC + 1 cm plaster	23.46	2.63
7. Window	NW	Shaded	3 cm window glass	3.45	4.83
8. Door	SE	Shaded	3.75 cm teak wood	3.50	2.44
9. Door	NE	Shaded	3.75 cm teak wood	2.09	2.44

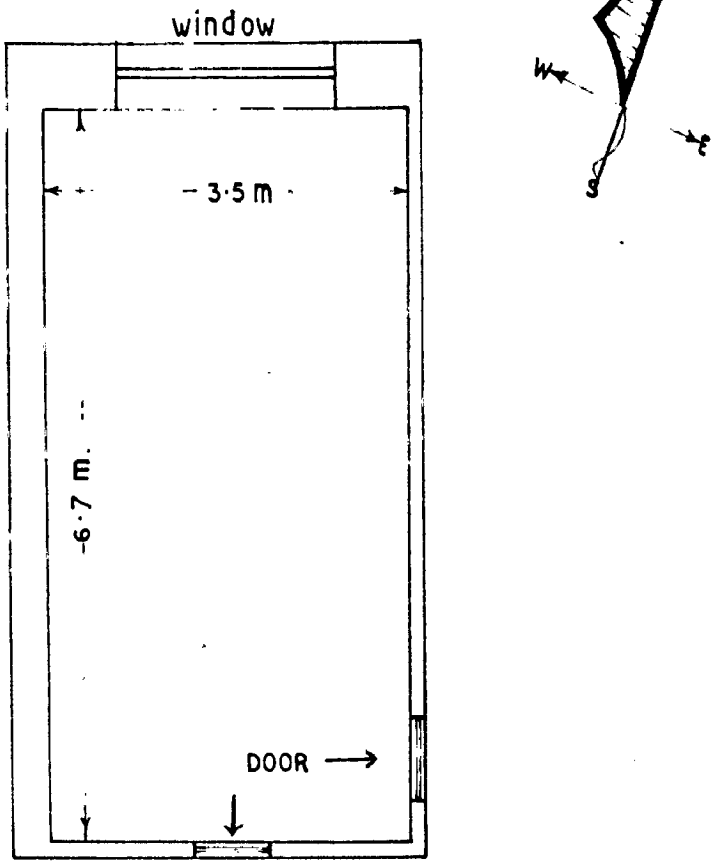

FIG.5·26 PLAN OF OFFICE ROOM USED FOR SOLAR HEATING

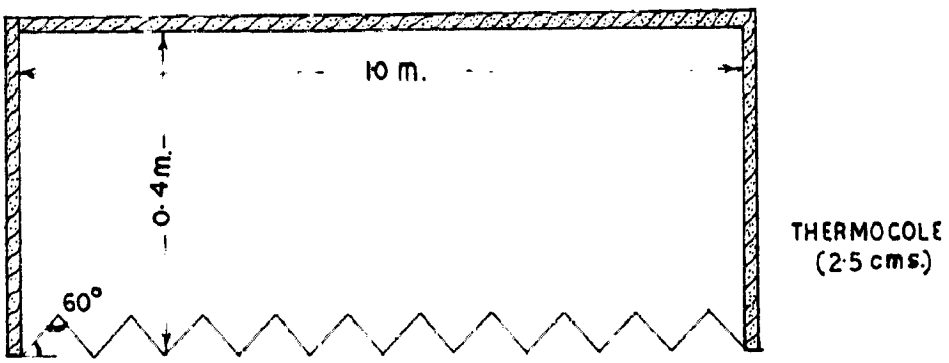

FIG. 5·27 STANDARD STORAGE PANEL

Collector area required (from Fig.5.17)	= 10 m^2
Panel area required (from Fig.5.21)	= 6.3 m^2
Amount of water required (from Fig.5.21)	= 940 litres.

Ten solar collectors each having an absorbing area of 1.0 m^2 were used and inter-connected in true parallel arrangement on the roof of the building parallel to the parapet wall. The collectors were not facing true south but were 30 degrees from the south towards east. The roof mounted collectors used are shown in Fig.(5.28). The observations of total solar radiation on the absorber surface show that the ratio of total solar radiation on a south facing collector to 30 degrees from south towards east is roughly 1.25 i.e. eight collectors facing true south will receive the same radiation as ten collectors facing 30 degrees from south towards east.

Three storage panels each having dimensions (1 x 1 x 0.4 m) are used and are kept near N.W. wall below the window as can be seen from Fig. 5.29. These panels are specially designed for this purpose and the radiating area is effectively increased by v-grooving the front side as shown in Fig.(5.27). These panels are inter-connected in parallel and are shown in photo Fig.(5.29) in the room used for solar heating. The rear bottom and sides of each panel was insulated with 2.5 cm w thick thermocole slabs. Thus the total exposed area of 3 panels is 7.2 m^2. The amount of water in the panels was about 1000litres.

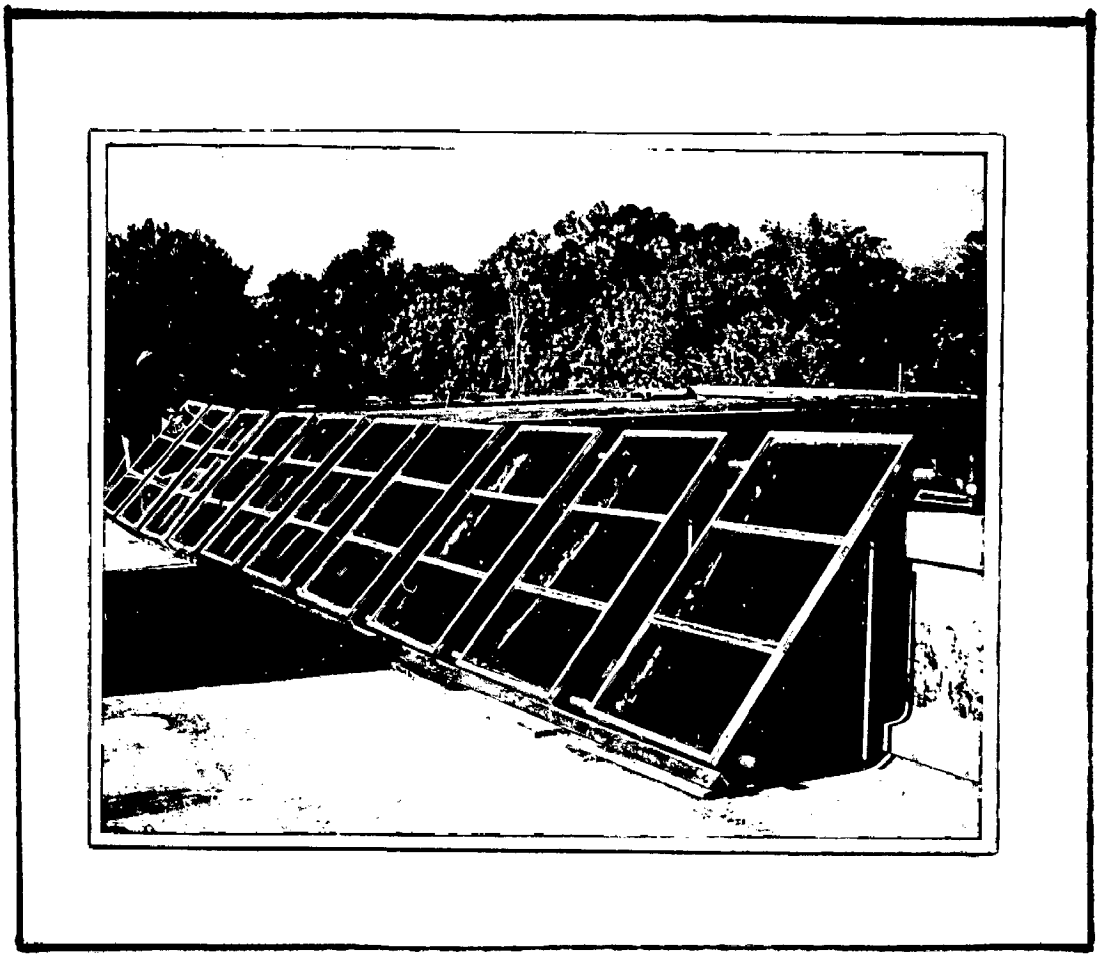

FIG.5.28 SOLAR COLLECTORS MOUNTED ON THE ROOF.

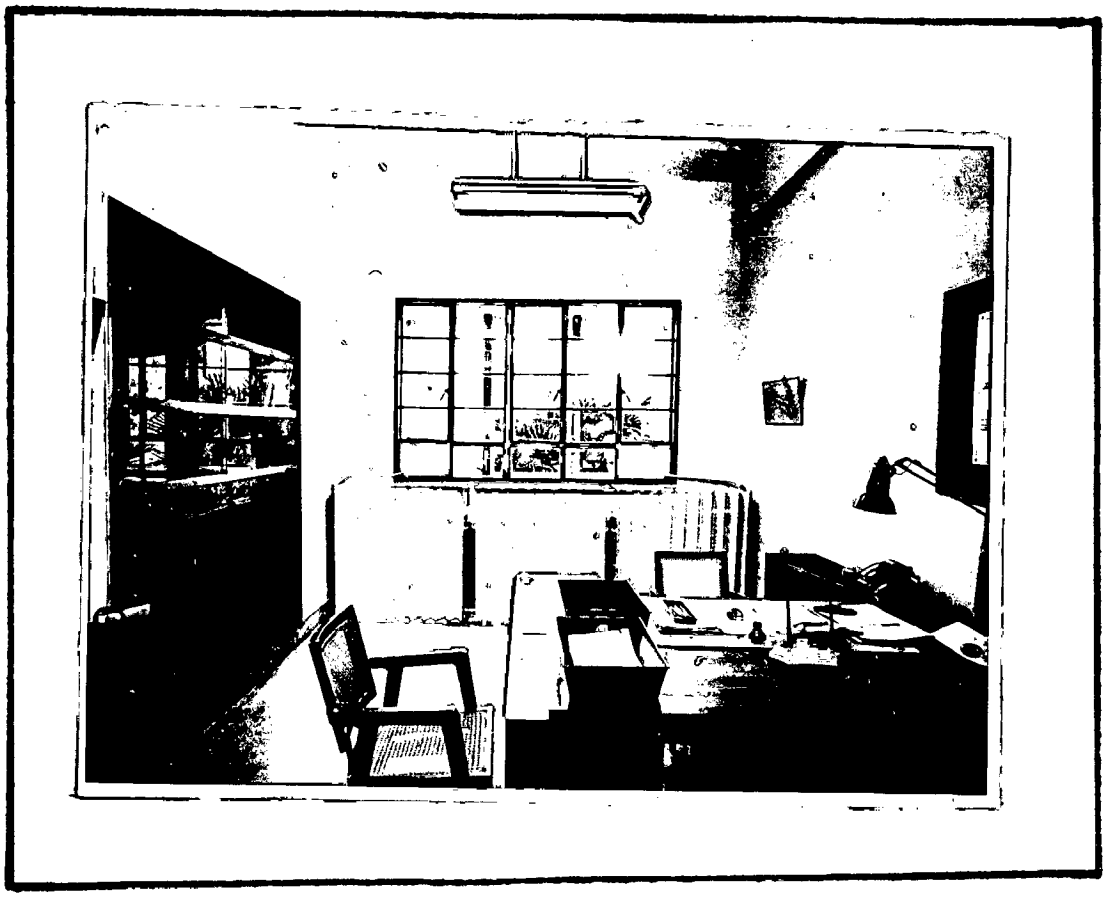

FIG.5.29 PHOTOGRAPH OF SOLAR HEATED OFFICE ROOM

A pump of 1/4 H.P. was used for the circulation of water through the absorbers and the storage panels and is controlled by a time switch which keeps the electric circuit on from 9.0 A.M. to 4.0 P.M.

Observations:

Continuous observations of room air temperature with and without heating the room, ambient air temperature and total solar radiation on absorber surface is made for two months i.e. from middle of December 1971 to middle of February 1972. The general feeling of the scientist sitting in the room and of the visitors was also recorded daily. This room which was reported to be the coldest room in the whole of the building was made effectively comfortable ~~comparable~~ through out the winter season. The mean room air temperature measured in the middle of the room for a number of days with and without heating is shown in Table (5.12). It is observed here that when no heating is used the mean room air temperature is about 14.0°C. In the month of January which is the coldest month of the year, it can be expected the mean room air temperature to further drop by 2°C. When solar heating is used was between 19°C to 22°C over a period of one month. It the mean room air temperature was observed that the diurnal variation of the room air temperature is only of the order of 2°C. Fig. 5.30 shows the hourly variation of room air temperature on a typical day.

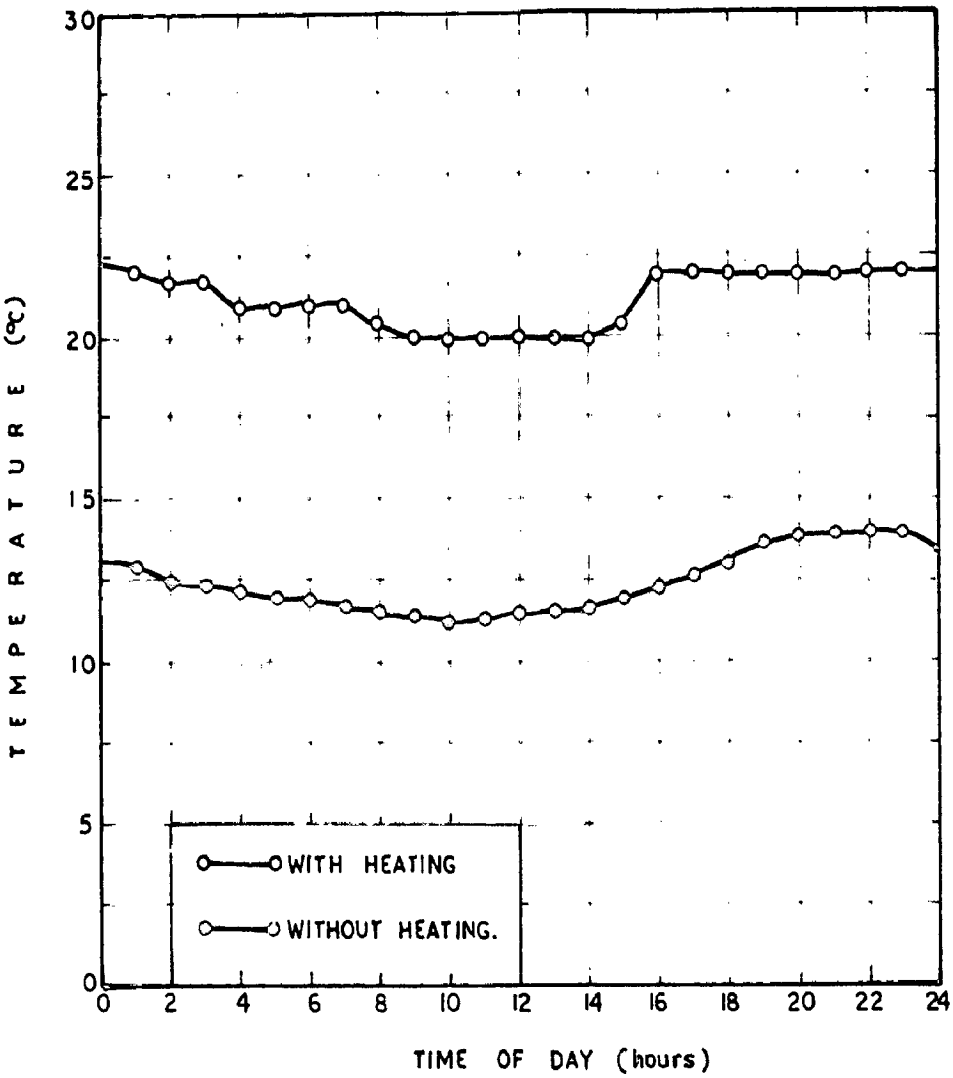

FIG.5·30 HOURLY VARIATION OF ROOM AIR TEMPERATURE WITH & WITHOUT HEATING ON A TYPICAL WINTER DAY

5.6 COST COMPARISON OF SOLAR HEATING SYSTEM FOR INSULATED AND UNINSULATED STRUCTURES.

Solar heating system will be economical for those places where number of heating days are more and the structure is of insulated. Two structures one of conventional construction i.e. 22.5 cm Brick work and other of insulated type i.e. 11.25 cm Brick + 2.5 cm thermocole, are selected for this study. The estimated heating load for these construction are given in Table 5.6 and 5.7. The dimensions of the room are the same as given in section (5.4). The design features and initial and operating costs are compared in Table 5.13 for the two cases. It is interesting to note that while the constructional cost of insulated and uninsulated structure may not differ much, the cost of solar heating system in case of uninsulated structure is practically double than that of insulated structure. Further, the temperature rise in the case of insulated structure will be rapid as compared to that of the uninsulated structure.

-*- *-*-

CONCLUSIONS

CONCLUSIONS

The data and methods provided for solar radiation estimations and the design and development details of solar energy collecting devices for water and space heating given in this thesis fills the gap existing in the field of solar energy utilisation. It has been shown that the solar water and space heating system can become an economical proposition for our country and should be adopted on a much wider scale specially in the present day of power shortage in the country.

Based upon the results of the present investigations, the following broad conclusions are made chapter wise:

1: (a) solar energy could make a significant contribution to the energy systems of the tropical arid and semi arid regions of the world.

(b) the success of a solar energy innovation in meeting a need of an energy user is dependent on a combination of technological, economic, social and political factors which are interdependent.

2: (a) for the rational design of solar energy utilisation devices for any location, the hourly values of total and diffuse radiation is needed. This can be predicted within 5 to 10 percent accuracy by the methods developed here.

(b) in the computation of conversion factors for converting solar radiation incident on a horizontal surface to that on an inclined surface, diffused radiation should not be considered as a beam radiation and the ground reflected radiations should also be included.

(c) even for overcast sky conditions the assumption of isotropic sky is not strictly valid in the estimation of total radiation on inclined and vertical surfaces.

3. (a) the choice of multiple transparent cover depends on the temperature of use. For low temperature applications such as water heating and space heating in tropics, one glass cover is adequate.

(b) the dirt correction factor for finding out the overall transmittance of glass cover inclined at 45° is 0.98.

(c) overall heat loss coefficient from the absorber plate to the outside air, can easily be found from the graphical data presented here.

(d) the following expression can be used for computing the plate-efficiency factor (F_p) which is a design constant:

$$F_p = \frac{1}{\frac{1}{\pi d_i h} + \frac{1}{\pi d_i h_r} + \frac{1}{C} + \frac{1}{(B + 2\,LF)\,U_L}}$$

(c) for the average winter, summer and year round performance the optimum tilts for flat-plate collectors are (latitude angle + 15°), (latitude angle-15 degrees) and 0.9 X latitude angle, respectively.

4. (a) The following collector configuration gives maximum efficiency and economy :

G.I. tube diameter	= 19.0 mm
plate material	= Aluminium
plate thickness	= 0.37 mm
tube spacing	= 10.0 cms.

(b) honeycomb does not increase the efficiency markedly and hence its addition involving extra cost, is not fully justified.

(c) the mathematical model developed for the prediction performance of natural circulation type solar water heaters has been found valid for clear as well as for cloudy days.

(d) the economic thickness of fibre glass insulation around the storage tank comes to 7.5 cms.

(e) the inferences drawn from the performance tests carried out on a domestic solar water heater of 100 litres capacity, shows a good agreement with the design values.

(f) the true parallel arrangement of interconnecting the large absorber banks ensures uniform flow and gives maximum efficiency with minimum operating costs.

(g) In a closed system, the flow rate of water through the collectors has no effect of any practical significance on the overall performance of the heater.

(h) The differential control developed for use with large size solar water heater for the operation of pump, provides higher efficiencies as compared with other types of controls.

(i) It has been shown that for a fixed absorber area there is an optimum storage capacity.

(j) The built in storage type solar water heater which is of low cost is ideally suited for daytime use.

(k) The mathematical model developed provides a basis for predicting the mean water temperature (t_{wo}) and the final form of the equation is :

$$t_{wc} = \frac{Z}{Y} + (t_{wo} - \frac{Z}{Y})\, e^{-\frac{Y}{B}(\theta - \theta_o)}$$

(l) A ratio of capacity to area of 100 litres/m^2 gives optimum performance in the case of built in storage type solar water heater.

5. (a) Based on the following equation :

$$t = \frac{C_2}{C_1} + (t_1 - \frac{C_2}{C_1})\, e^{-C_1 x}$$

derived for performance prediction of solar air heater, simple design curves are drawn from which the collection efficiency and outlet temperature can be determined in terms of airmass flow rate and solar insolation rate.

(b) lowering the duct depths in solar air heaters increases the efficiency without much increase in pumping cost.

(c) it has been shown experimentally that the solar air heaters can be used for heating rooms of daytime occupancy (office) on clear days, even without the provision of storage of energy.

(d) small rooms can easily and profitably be heated to comfortable levels, using storage cum radiant panels and flat-plate solar energy collectors with water as a medium.

(e) the following empirical equation, provides a quick estimate of the heat loss from the storage panel placed inside the room

$$h = 0.1 + 0.05\Delta t.$$

(f) if the heating load of a room is reduced by providing proper insulation on the inside surfaces of the room, the cost of solar heating system will also be reduced proportionately.

APPENDIX

PROGRAMME NO.1

```
C  EXTRATERRESTRIAL SOLAR RAD. ON HOR.AND INC. SURFACE  H P GARG Z
   DIMENSION DELTA(12),HOT(3),HOTH(3),SPT(3),B(5)
   FAC=3.14159265/180.
   READ6,NT
   FORMAT(I2)
   READ1,(DELTA(I),I=1,NT)
   FORMAT(6F10.4)
   DO3I=1,NT
   CIN=DELTA(I)*FAC
   CD=COSF(CIN)
   SD=SINF(CIN)
   TD=SD/CD
   DO 3 L=8,40
   C1=L
   C2=C1*FAC
   SL=SINF(C2)
   CL=COSF(C2)
   TL=SL/CL
   CWS=-TL*TD
   SWS=SQRTF(1.-CWS*CWS)
   TWS=SWS/CWS
   WS=ATANF(TWS)
   IF(WS)22,23,23
   WS=WS+3.14159265
   HO=2793.6*SL*SD*(WS-TWS)/3.14159265
   SP=2.*WS/(15.*FAC)
   B(1)=(C1+15.)*FAC
   IF(L-15)90,91,91
   B(2)=0.
   GO TO 92
   B(2)=(C1-15.)*FAC
   B(3)=(0.9*C1)*FAC
   DO4J=1,3
   SLB=SINF(C2-B(J))
   CLB=COSF(C2-B(J))
   CWST=-SLB*TD/CLB
   SWST=SQRTF(1.-CWST*CWST)
   TWST=SWST/CWST
   WST=ATANF(TWST)
   IF(WST)20,21,21
   WST=3.14159265+WST
   CONTINUE
   IF(WST-WS)101,101,102
   WST=WS
   CONTINUE
   HOT(J)=2793.6*(CLB*CD*SWS+WST*SLB*SD)/3.141569265
   HOTH(J)=HOT(J)/HO
   SPT(J)=2.*WST/(15.*FAC)
   PUNCH5,C1,DELTA(I),SP,HO,(SPT(N),HOT(N),HOTH(N),N=1,3)
   FORMAT(10F7.2)
   CONTINUE
   END
```

PROGRAMME NO.2

```
C  SOLAR RADIATION ON INCLINED SURFACES FOR ANY ORIENTATION H P GARG
   DIMENSIONTIM(13),TH(13),DFH(13)
   READ100,ALT,DEC,ALN,ENT,RHO
   READ100,(TIM(N),N=1,13),(TH(N),N=1,13),(DFH(N),N=1,13)
   FORMAT (9F7.2)
   R=3.141592654/180.
   ALT=ALT*R
   CL=COSF(ALT)
   SL=SINF(ALT)
   DEC=DEC*R
   CD=COSF(DEC)
   SD=SINF(DEC)
   PHI=0.
   DO 10 I=1,8
   BET=0.
   CF=COSF(PHI)
   SF=SINF(PHI)
   DO20J=1,7
   CB=COSF(BET)
   SB=SINF(BET)
   DO30N=1,13
   SN=12.0-ENT-(ALN-82.5)/15.
   W=(SN-TIM(N))*15.*R
   CW=COSF(W)
   SW=SINF(W)
   CTT=(CB*SL-SB*CL*CF)*SD+(CB*CL+SB*SL*CF)*CD*CW+SB*SF*CD*SW
   CTH=CL*CD*CW+SL*SD
   TTT=ATANF((1.-CTT*CTT)**.5/CTT)/R
   THH=ATANF((1.-CTH*CTH)**.5/CTH)/R
   DRT=CTT*(TH(N)-DFH(N))/CTH
   IF (DRT) 25,26,26
   DRT=0.0
   DFT=0.5*DFH(N)*(1.+CB)
   TRT=0.5*RHO*TH(N)*(1.-CB)
   TT=DRT+DFT+TRT
   PHR=PHI/R
   BER=BET/R
   PUNCH 100,TTT,THH,PHR,BER,TIM(N),TT,DRT,DFT,TRT
   BET=BET+15.*R
   PHI=PHI+45.*R
   STOP
   END
```

PROGRAMME NO.3

```
C  SOLAR COLLECTOR SYSTEM DESIGN H P GARG
   DIMENSION  TA(24),TG(24),HA(24),HB(24),T(64),H(64)
   DIMENSION TM(48),TD(48),TMC(48)
   READ  4,NH,NR
 4 FORMAT(2I2)
04 READ  11,K,L,M
11 FORMAT(3I2)
   READ 3,TC,(TA(I),TG(I),I=1,NH) $ READ 3,HC,(HA(I),HB(I),I=1,NH)
 3 FORMAT(F10.4,6F10.4)
   READ 2,TR,A,UUP,ECZY,DEW
13 READ 2,A0,H0,VT,HTT,R
   READ 2,DEI,SHI,AKI,CI,PII,TI
   READ 2,DEB,SHB,AK3,CB,PB,TB
   READ 2,DET,SHT,AKT,TT,ZETA,AKW
01 READ 2,DEP,SHP,AKP,DIP,PT
02 READ 2,F,DIC,DIH,S,SHC,WCE
   PI=3.1415926
   ECZY=ECZY*PI/180.
   SINEC=SINF(ECZY)
   BC=A0/H0          $ HOBC=H0/BC
   ANT=BC/S          $ BC=BC+0.5
   WWC=(DEW*PI/4.)*(A0*DIC*DIC/S+BC*DIH*DIH)
03 READ 2,BETA,GAMA,DELT,TCK
 2 FORMAT(6F12.4)
   HP=H0+HTT-GAMA+BETA*(1.+(1./SINEC))
   HPE=H0*((DIP/DIC)**5 )/ANT+BC*((DIP/DIH)**5 )
   HPP=HP+HPE
   FHP=H0*SINEC+2.*BETA+(HTT-GAMA)*(1.+GAMA/HTT)
   CONS=HPP*0.035*5.65*5.65/(64.*DIP)+(5.02*3.96)
   PROD=(DIP**4 )*(10.**12)/CONS
   HTD=HTT+DELT+ZETA
   DSI=DEI*SHI$ DSB=DEB*SHB$ DST=DET*SHT
   DSP=DEP*SHP$ WC=SHC*WCE+R*A0*(DSI*CI+DSB*CB)
   UC=1./(CI/AKI+CB/AKB+0.25)+UUP
   RIP=0.5*DIP$ REP=RIP+PT+PII+PB
   WPD1=DSP*(2.*RIP*PT+PT*PT)
   WPD2=DSI*(2.*(RIP+PT)*PII+PII*PII)
   WPD3=DSB*(2.*(REP-PB)*PB+PB*PB)
   WPD=HP*PI*(WPD1+WPD2+WPD3)
   ARGP=(RIP+PT+PII)/(RIP+PT)$ UPI=(LOGF(ARGP))/AKI
   UPD=(2.*PI)/((0.025+(PT/AKP))/RIP+UPI+((PB/AKB)+0.25)/REP)
   RIT2=VT/(HTT*PI)$ RIT=SQRTF(RIT2) $ RET=RIT+(TT+TI+TB)
   THDR=HTT/(2.*RIT)
   WTD1=HTD*DST*(2.*RIT*TT+TT*TT)
   WTD2=HTD+2.*(TT+TI)
   WTD3=DSI*(2.*(RIT+TT)*TI+TI*TI)
   WTD4=DSB*(2.*(RET-TB)*TB+TB*TB)
   WTD=PI*(WTD1+WTD2*(WTD3+WTD4))
   WT=2.*PI*(RIT2*(TT*DST+TI*DSI )+RET*RET*TB*DSB+RIT2*ZETA*DEW*0.5)
   WTT=WT+WTD
   WWT=VT*DEW$ WS=WC+WTT+WPD+WWT
   ARGT=(RIT+TT+TI)/(RIT+TT) $ UTI=(LOGF(ARGT))/AKI
   UTD=(2.*PI)/((0.025+(TT/AKT))/RIT+UTI+((TB/AKB)+0.25)/RET)
   UT=1./(0.025+TT/AKT+TI/AKI+TB/AKB+0.25+0.5*ZETA/AKW)
```

```
   UTT=UT*2.*PI*RIT2+UTD*HTD$ US=UTT+R*A0*UC+UPD*HP
   PUNCH 2,UC,UT,UTT,UPD,US,HP $ PUNCH 2,WC,WT,WTD,WPD,WWT,WWC
   PUNCH  2,HPE,FHP,PROD,CONS,THDR ,HOBC
   FNR=NR$ W=2.*PI/FNR$ NRN=NR+K
   TK=K        $ J=K          $ TCI=TCK    $ GO TO 15
16 TCI=TM(J)   $ TK=J   $ J=J+1
15 UWS=US/WS          $ LLK=1          $ LLM=1
   FWS=F*A0*TR*A/WS
17 THC=UWS*TC+FWS*HC
   IF (J-NRN) 24,24,19
24 TQ=J   $ TE=UWS*(TQ-TK)$ EX=1./EXPF(TE)
10 SOM=(THC/UWS)*(1.-EX)+TCI*EX
   SAM=HC$ SIM=TC$ DO 7 I=1,NH
   FNH=I$ WH=W*FNH$ ARG=WH*TQ
   THA=UWS*TA(I)+FWS*HA(I)
   THB=UWS*TG(I)+FWS*HB(I)$ ARGI=WH*TK
   COST=COSF(ARG)
   COSI=COSF(ARGI)*EX
   SINT=SINF(ARG)$ SINI=SINF(ARGI)*EX
   FMULT=1./(UWS*UWS+WH*WH)
   SIM=SIM+TA(I)*COST+TG(I)*SINT
   SAM=SAM+HA(I)*COST+HB(I)*SINT
   HX=(THA*UWS-THB*WH)*FMULT
   HY=(THB*UWS+THA*WH)*FMULT
 7 SOM=SOM+HX*(COST-COSI)+HY*(SINT-SINI)
   GO TO (49,50,48),LLK
49 TMC(J)=SOM
48 H(J)=SAM$ T(J)=SIM
   TM(J)=SOM   $ TD(J)=UWS*T(J)+FWS*H(J)-UWS*TM(J)
   EFD=TD(J)*(WWT+WTT)+(TM(J)-T(J))*UTT
   EFT=-TD(J)/(TM(J)-T(J))
   HX=10.
   IF (H(J)-HX) 21,9,9
21 PUNCH 6,TQ,TM(J),TD(J),TMC(J),EFT
   LLK=1
   GO  TO (54,59),LLM
54 TK=J   $ TCI=TM(J)   $ LLM=2
59 UWS=(US-UTT)/(WS-WWT-WTT+WWC)$ FWS=0.$ J=J+1   $ GO TO 18
50 TMC(J)=SOM
   UWS=UTT/(WWT+WTT)   $ FWS=0.
18 LLK=LLK+1    $ GO TO 17
 9 EFM=2.*.00000125*TM(J)-0.0000583
   EFC=EFD/(A0*H(J))    $ EFS=(TD(J)*WWT)/(A0*H(J))
   WFLX=0.5*PROD*FHP*EFD*EFM        $ AWFLX=ABSF(WFLX)
   WFL=AWFLX**0.3333333
   IF (WFLX)  31,32,32
31 WFL=-WFL    $ GO  TO  32
32 TFTS=EFD/WFL   $ TF=0.5*TFTS+TM(J)   $ TS=TF-TFTS
 5 PUNCH 6,TQ,TM(J),TD(J),TS,TF,WFL,EFC,EFS
   GO  TO  16
19 PUNCH 6,(T(J),J=K,NRN)
   PUNCH 6,(H(J),J=K,NRN)
 6 FORMAT(8F9.2)
   STOP
   END
```

LIST OF PUBLICATIONS

LIST OF AUTHOR'S PUBLICATIONS

1. Performance studies on solar air heaters' Solar energy (USA) Vol 11, No.1, 1967.
2. 'Design of flat-plate solar collectors for India'. J. of Inst. of Engrs.(India), Vol 47, No.9, pt.MS6, May 1967.
3. 'System design in solar water heaters with natural circulation'. Solar energy (USA), Vol 12, No.2, 1968.
4. 'Optimising the tilt of flat-plate solar collectors for India'. J.of Inst. of Engr.(India), Vol 48, No.1, pt. CE1, Sept. 1967.
6. 'Solar water heater'. Special publication of Central Building Research Institute, Roorkee, 1967.
8. 'Computation of average hourly global and diffuse solar radiation intensity from sunshine hours data'. Presented at conference on 'water desalination' held at Bhavnagar, 1967.
7. 'Solar-cum-electric water heater'. Indian and Eastern Engrs (India), Jan. 1969.
8. 'Design data for direct solar utilisation devices, part I- system data'., J.of Inst. of Engrs.(India), Vol 48, No.9, pt CH3, May 1968 (Special issue).
9. 'Design data for direct solar utilisation devices, part II solar radiation data'. Indian J.of Met.&Geophysics, Vol 20, No.3, July 1969.
10. 'Solar energy and its uses'. J.of Inst. of Engrs.(India) Hindi edition, Aug. 1968.

11. 'Solar water heater' Building digest No.61, Central Building Research Institute, Roorkee.

12. 'Solar water heater'. J.of Inst. of Engrs.(India) Vol.50, Jan. 1970.

13. 'An automatic control circuit for large size solar water heater'. Research and Industry, Vol 14, No.3, 1969.

14. 'Present status of solar water heaters in India. Presented at the International solar energy society conference, Melbourne, Australia, 2nd-6th March, 1970.

15. 'International solar energy society conference'. Journal of scientific and Industrial Research, Vol 29, No.9, 1970.

16. 'Measurement of solar absorptivity o black paints'. J.of Inst. of Engrs.(India), Oct. 1970.

17. 'Forced convection solar hot water heating system'. Research and Industry, Vol.16, No.1, 1971.

18. 'Optimization of flow in large solar absorber bankst Solar energy (USA), under publication.

19. 'Design and performance of large size solar water heater'. Presented in the 1971 International solar energy society conference, Washington, U.S.A.,10th-15th May, 1971. Solar energy (USA), V.16, No.2, 1972.

20. 'Design and performance studies on combined collector and storage type solar water heater'. Presented in the 1972 U.S.section meeting of International solar energy society, Washington, April, 1972.

21. 'Package type solar water heater' Research and Industry. (under publication).

22. 'Solar room heater'. Research and Industry,(under publication).

23. 'Measurement of global solar radiation on inclined surfaces of any orientation under overcast sky conditions'. Indian J.of Met.&Geophysics,(under publication).

24. ' esign approach to solar water heating'. Presented in the fourth meeting of all India solar energy working group, 5-6th July, 1972.

25. 'Performance prediction of solar room heater' Presented in the fourth meeting of all India solar energy working group, 5-6th July, 1972.

26. 'Design and performance studies on solar room heater'. Sent for presentation in 1973 International solar energy society conference, July 1973, Paris, France.

REFERENCES

BIBLIOGRAPHY

CHAPTER 1

1. 'Space heating with solar energy'. Proceedings of a course symposium held at the M.I.T. Cambridge, 1950.

2. 'Sun in the service of man'. American academy of arts and sciences, 79, 1951, 181-320.

3. Mac Mavin, W.C., 'The trapping of solar energy'. Ohio journal of science, 53(6), 1953, p.287-310.

4. 'Solar energy research' edited by F.Daniels and J.A.Duffie, Madison, University of Wisconsin Press, 1955.

5. 'Wind power and solar energy'. Proceedings of the New Delhi symposium, Paris, UNESCO, 1960.

6. 'Transactions of the conference on the use of solar energy: The scientific basis', Tucson, University of Arizona Press, 1958.

7. 'Proceedings of the world symposium on applied solar energy'. Phoenix, Arizona, 1956, Menlopark, Calif., Stanford Research Institute, 1963.

8. 'Applications Thermiques del' Energie Solaire dans le Domains de la Recherche et del' Industrie: symposium at Mont-Louis, France, Paris, Centre National de la Recherche Scientifique, 1961.

9. Research frontors in the utilisation of solar energy in proceedings of national Academy of sciences, 47, 1961, 1395-1396.

10. ' New sources of energy'. Proceedings of the conference Rome, 21-31 August 1961.

11. The U.N.S.C.O. seminar proceedings on solar and aeolian energy. Greece, September 6-16, 1961.

12. 1970 International solar energy society conference, Melbourne, Australia, March 3-6, 1970.

13. 1971 International solar energy society conference, Washington, U.S.A., May 10-16, 1971.

14. Bucley, F.H.'Heating air by solar energy'. Agricultural engineering, 38, No.1, Jan.1957, p.33-35.

15. Bu Low, F.E., 'corru ated solar heat collectors for crop drying'. Sun at work 4th quarter, 1961, p.8.

16. Miller, .'Performance of black painted solar air heaters of conventional design'. Solar energy, Vol.8, No.1, Jan. p.31-37.

17. Chiou, J.P., 'Heat transfer and flow friction characteristics of metallic foil n trices using radiation as the heat source'. Ph.D.thesis, University of Marquette Wisconsin, 1964.

18. Ward, C.T., 'Possibilities for the utilisation of solar energy in under-developed rural areas'. Farm power and machinery, Informal working bulletin No.16. Food and agriculture organisation of the United Nations, Rome, 66 p.

10. Whillier, A. 'Solar energy collection and its utilization for house heating'. Sc.D.Thesis. Cambridge, MIT, 1953. 203 p.

CHAPTER-3.

1. Kimball, H.H. 'Variation in the total and luminous solar radiation with geographical position in the united states'. Monthly weather Review, Washington, US Weather Bureau, 47, p.769-793, 1919.

2. Angstrom, A., ' Recording solar radiation'. Meddel. Stat. Met. Hydr., Anst. Stockholm ovelon, 4, p 1-37, 1923.

3. London, A.C. ' The influence of cloud on hourly total solar radiation at the sea level'. Duke Building Research station Note No.E H 29, 1954.

4. Kumura, K. and Stephenson, D.G., 'Solar radiation on Cloudy days'. Trans. ASHRAE, V.76, pt I, 1969.

5. Norris, D.J., 'Correlation of solar radiation with Clouds'. Solar energy, 12, p.107-112, 1968.

6. Moon, P., 'Proposed standard solar radiation curves for engineering use'. J. Franklin Inst., 230, p.583-617, 1940.

7. Klein, W.H., 'Calculation of solar radiation and the solar heat load on men'. J.Met., 5 (4), p.119-30, 1948.

8. Pleijel, G., 'The computation of natural radiation in architecture and town planning'. (Victor pettersons Bokindustri Aktiebolag: Stockholm).

9. Threlkeld, J.L., and Jordan, R.C., 'Direct solar radiation available on clear days'. Heat. pip, Air Condit.29 (12), p.133-45, 1957.

10. Rao, K.R. and Sadhadri, T.N., 'Solar insolation Curves'. Indian J. of Met. &Geophysics., 12 (2), 267-72, 1961.

11. Choudhury, H.K.D., 'Solar radiation at New Delhi'. Solar energy, 7(2), p.44, 1963.

12. Liu, Y.H. and Jordan, R.C., 'The inter-relationship and characteristic distribution of direct, diffuse and total solar radiation'. Solar energy, 4(3), 1960.

13. Sharma, M.R. and Pal, R.C., 'Inter-relationship between total, direct and diffuse solar radiation in the tropics" Solar energy, 9(4), p.183, 1965.

14. Parmelee, G.V., 'Irradiation of Vertical and horizontal surfaces by diffuse solar radiation from cloudless skies' ASHVE Transactions, 60, p.341, 1954.

15. Johnson, F.S., 'The solar constant'. Journal of Meteorology. 11, p.431-439, Dec. 1954.

16. Albon, C.V., Quart. J.Roy. Meteorol.Soc., 94,p.362, 307, 1963.

17. Thekaekara, M.P., 'Proposed standard values of the solar constant and the solar spectrum'. J. of Environmental Sc., 13(4), p.6-9, 1970.

18. The Nautical Almanac and astronomical ephemeris for the year 1961.

19. Angstrom, A.,'On the atmospheric transmission of sun radiation and on dust in the atmosphere'. Geogr. Ann. Stockholm, 11, p.160-163, 1929.

30. Angstrom, A., 'On the atmospheric transmission of sun radiation, II, 12, p.130-159, 1930.

31. Linke, F., 'Handbuch der Geophysik' Band VIII (in German) Gebruder Borntraeger, Berlin-Zehlendorf p.721.

32. Kimball, H.H., 'Measurement of solar radiation intensity and determination of the depletion by the atmosphere, with bibliography of pyrheliometric observations'. Monthly weather Review, Washington, U.S.Weather Bureau, 55, p.159, 1927.

33. Kimball, H.H., 'Amount of solar radiation that reaches the surface of the earth on land and sea and methods by which it is measured'. Monthly weather Review, Washington, U.S.Weather Bureau, 56, p.393, 1928.

34. Kimball, H.H., 'Measurements of solar radiation intensity and determinations of its depletion by the atmosphere'. Monthly Weather Review, Washington, U.S. Weather Bureau, 59, p.43, 1930.

36. Kimball, H.H., 'Solar radiation and its role'. Meteorology, Chap.III,79. Nat. Res.Council Bull., Washington, Nat. Acad. Sci.

38. Moon, P., 'Proposed standard solar radiation curves for engineering use'. J.Franklin Institute, Philadelphia, USA, 230, p.583-617, 1940.

37. Threlkeld, J.L.and Jordan, R.C., 'Direct solar radiation available on clear days'. Heating piping and air-conditioning, ASHVE, Journal section, New York, 33 (12), p.139-149, 1957.

29. Desikan, V. et al, 'Diffuse solar (sky) radiation measurement over India'. Indian J. of Met. Geop. 20 (4), p.389-394, 1969.

30. Mie, G., Ann. Physik, 25, p.377, 1908.

30. Dolmendjian, D. and Sekera, Z., J. Opt. Soc. Am., 48, p.666, 1960; Arch. Meteorol. Geophys. Bioklimatol. Ser. B., 6, p.452, 1955; Ann. Geophys., 13, p.236, 1957; 16, p.318, 1959.

31. Sekera, Z. and Ashburn, E.V., 'Tables relating to Rayleigh scattering of light in the atmosphere, U.S. Naval-Ordinance test station, China Lake, Calif., Naval-Ordinance test station, China Report, No.2061.

32. Albrecht, F., Arch. Meteorol. Geophys. Bioklimatol. Ser. B, 3, p.329, 1951.

33. Ramdas, L.A. and Yoganarayanan, G., 'Solar energy in India'. Wind and solar energy, proceedings of the New Delhi Symposium, UNESCO, p.183, 1956.

34. Angstrom, A., 'Solar and terrestial radiation'. Quart. J. of Royal Met. Soc., 50, p.121, 1924.

35. Mooley, D.A. and Bedekar, V.C., and Raghavan, S. 'Relation between the incident solar radiation and the duration of bright sunshine at Madras'. Indian J. of Met. & Geop., 3, p.510, 1962.

33. Lof, G.O.G., Duffie, J.A. and Smith, C.O., 'World distribution of solar radiation'. Solar energy, 10, p.27, 1963.

37. Hottel, H.C. and Whillier, A., 'Evaluation of flat-plate solar collector performance'. Trans. of the Conf. on the use of solar energy, the scientific basis, Tucson, Arizona, p.74, 1958.

38. Liu, Y.H. and Jordan, R.C., ' A rational procedure for predicting the long term average performance of flat-plate solar energy collectors'. Solar energy, 7, p.53, 1963.

39. Anna Mani and Commen Chacko, 'Measurement of diffuse solar radiation at Delhi and Poona'. Indian J. of Met. and Geop., 14, p.416, 1963.

40. Berg, H., Geophis, Pure Appl. 13, p.167, 1949.

41. Monteith, J.L., 'Local differences in the attenuation of Solar radiation over Britain' Quart. J. of Royal Met. Soc., 92 (392), p.264, 1966.

42. Liu, Y.H. and Jordan, R.C., 'Availability of solar energy for flat-plate solar heat collectors'. Low temperature engineering applications of solar energy, New York, ASHRAE Inc. 1967.

43. Page, J.K., ' The estimation of monthly mean values of daily total short wave-radiation on vertical and inclined surfaces from sunshine records for latitudes $40^{o}N-40^{o}S$. New Sources of Energy, Proc. Conf., Rome, Aug. 21-31, V.4, p.378, 1961.

44. Stranton, J.V., 'Hot water from the sun'. CSIR Rep. D-9, Pretoria, South Africa, 1961.

45. Morco, R.N. and Cournoshi, J.T., 'Plant-photo absorbers: The effect of incident radiation of inclination and orientation', CSIRO, Melbourne, Australia Engrs. Sc., Rep. E.D.6, 1969.

46. Kondratyev, K.Ya, and Manolova, M.P., 'Solar energy 4 (1), p.14, 1960.

47. Moon, P. and Spencer, D.E., Trans. Illum.Eng. Soc. 37 (4), p.707, 1942.

48. Heywood, H., 'A general equation for calculating total radiation on inclined surfaces'. 1970 International solar energy society conference, Melbourne, Australia, 2nd-6th March, 1970.

49. Pasquale, G.V., 'Irradiation of Vertical and horizontal surfaces by diffuse solar radiation from cloudless skies'. Heat. piping Air Cond., 26 (8), p.129-37, 1954.

50. Handbook-Meteorology instruments, part I (HMSO, London), Chapter 8, p.330, 1956.

51. Van Deventer, E.N., Dold, T.B., 'Some initial studies on diffuse sky and ground reflected solar radiation on Vertical surfaces'. Biometeorology II. Proceedings of the third International Biometeorological Congress held at Pau, S. France, 1-7 Sept. 1953.

52. Spencer, J.W., 'Estimation of solar radiation in Australian localities on clear days'. D.S.R. Technical paper No.13, C S I R O, Australia, 1966.

CHAPTER-3.

1. Watkins, Dr.Geo.E., Libbey-Owens-Ford Glass Company, personal communication, 1966.

2. Hardy, A.C. and Perrin, F.H., 'The Principles of optics'. Mc.Graw Hill Book company, Inc., New York N.Y., 1932, P. 20.

3. Stokes, G.G., 'On the intensity of the light reflected from transmitted through a pile of plates'. Proc. Roy Soc.(London),11, 1860-1962, p.546-556.

4. Whillier, ' Plastic Covers for solar collectors'. Solar energy, V.7, No.2, 1963.

5. Parmelee, G.V., 'The transmission of solar radiation through flat glass under summer conditions,' Trans. A.S.H.V.E.,V 51, 1945, p.317-344.

6. Zarem, A.M. and Erway D.D., 'Utilization of solar energy'. Mc Graw Hill, 1963.

7. Edlin, F.E. and Willaver, D.E., 'Plastic films for solar energy applications'. Proc.of the Conf. on New sources of energy, Rome 1961, V.4, p.519.

8. Yellot, J., 'Transmission and absorption of solar radiation in glass' Proc. on Solar and Aeolian energy, Greece, 1961, p.363-381.

9. Hottel, H.C.and Woerts, B.B., 'The performance of flat-plate solar heat collectors'. Trans. of the A.S.M.E., Feb. 1942, p.91-104.

10. Mc. Adams, W.H., 'Heat transmission'. Mc.Graw-Hill, 3rd Edison.

11. Fishenden, M. and Saunders, O.A., 'An introduction to heat transfer'. Oxford university press, 1950.

12. Brown, A.I. and Marco, S.M., 'Introduction to heat transfer'. Mc. Graw Hill, 1951.

13. Mikheyev, M., 'Fundamentals of heat transfer'. Peace publications, Moscow.

14. Brunt, D., 'Notes on radiation in the atmosphere'. Quarterly journal of R.Met. Soc., V.63, 1933, p. 389-420.

15. Rao, K.R. and Ballantyne, E.F., 'Some investigations on the Sol-air temperature Concept'. D.R.Technical paper No.27, CSIRO, Australia 1970.

16. Neumann, E.P., 'Direct utilization of solar energy as heat'. Solar energy project internal report M.4, M.I.T., Cambridge, Massachusetts, March 1943.

17. Ettal, H.C., 'Performance of flat-plate solar energy collectors'. Proceedings of Course-symposium on space heating with solar energy'. Aug. 31-26, 1950, p.60-71.

18. Coulta, A.F. and Safvat, M.M., 'Optimum orientations for the double-exposure, flat-plate collector and its reflectors'. Solar energy, V.10, No.4, 1966, p.170.

C H A P T E R-4.

1. Yellot, J.I., and Dobotka, R., 'An investigation of solar water heater performance'. Trans. of ASHRAE, V.70, 1964, p.425.

2. Morse, R.N., 'Solar energy research & Development & Industrial application in Australia'. 1970 International solar energy society conference, Melbourne, Australia.

3. ~~Tenishita, I.~~ Damey, E.T., 'Solar water heating in Australia' 1970 International solar energy society conference, Melbourne, Australia.

4. Tenishita, I., Present situation of commercial solar water heaters in Japan, 1970 International solar energy society conference, Melbourne, Australia.

5. Richards, S.J. and Chinnergy, D.N.W., ' A solar water heater for low cost housing'. NBRI Bull. 41, CSIR research report 237, South Africa, 1967.

6. Mathur, K.N. and Khanna, M.L. 'Some observations on a domestic solar water heater'. Proceedings of wind & solar energy symposium, New-Delhi, UNESCO publication, 1956, p.202-206.

7. Gupta, C.L., Garg., H.P., and Ganguli, R. 'Solar water heater' Special publication of Central Building Research Institute, Roorkee, 1967.

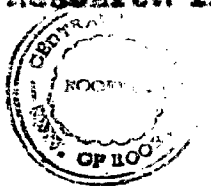

9. Whillier A and Saluja, G.: 'The thermal performance of solar water heaters' Solar energy, V.9, No.1, 1965, p.21.

9. Whillier A. and Richards, G.J.' A standard test for solar water heaters'- U.N.Conf. on new sources of energy, Rome, 1961, p.111.

10. Edvard, D.K., 'Prediction of the onset of natural convection in rectangular honeycomb structures'. Paper No.7/62. 1970 International solar energy society conference, 2-6 March 1970, Melbourne, Australia.

11. Laluda, O.QBuchberg, H., 'Design of honeycomb porous bed solar air heater'. Paper No.7/63. 1970 International solar energy society conference, 2-6th March 1970, Melbourne, Australia.

12. Bottol H.C. and Whillier, A. 'Evaluation of flat-plate solar collector performance'. Trans. of the Conf. on the use of solar energy: The scientific bais, U.2, 1955, p.74.

13. B.Y.H. and Jordan, R.C.'The long term average performance of flat-plate solar energy collectors'. Solar energy, V.7, No.2, 1963, p.53.

14. Anna Mani, C.O. and Venkateswaran, S.P., 'Measurement of the total radiation from sun and sky in India during the I.G.Y., 'Indian J.of Met.& Geop. V 13, No.3, 1962, p.386.

16. Garg, H.P., 'Present status of domestic solar water heater in India'. 1970 International solar energy society conference, Melbourne, Australia, 2-6th March, 1970.

16. Hottel H.C. and Woerts, B.B., ' The performance of flat plate solar heat collectors'. Trans. of Am. Soc, Mech. Engrs. 64, 1942, p.91.

17. Tabor, H. 'Solar energy collector dosing'. Trans. of conference o n the use of solar energy, University of Arizona, Vol 2, 1958, p.1-23.

18. Hottel H.C. and Whiller A. 'Evaluation of flat-plate solar collector performance'. Trans. of conference on the use of solar energy, University of Arizona, U.2, 1959, p.74-104.

19. Liu, B.Y.H. and Jordan, R.C.'The long term average performance of flat-plate solar energy collectors'. Solar energy, Vol 2, 1963, p.62.

20. Donaldson, R.F. ' Prospectus of solar heating in New Zealand'. New Zealand Engineering , 436, 1966.

21. Bliss, R.W., ' The derivation of several plate efficiency factors useful in the design of flat-plate solar heat collectors'. Solar energy, Vol 3, 1959, p.55.

22. Close, D.J., 'The performance of solar water heaters with natural circulation'. Letter to the editor'. Solar energy vol ~~7, 1963, p.80.~~ 6 (1), 33 (1962)

23. Chinnappa, J.C.V., 'Letter to the editor'. Solar energy vol 7, 1963, p.23.

24. De Sa, V.C., ' Solar energy utilization at Jaccob. Solar energy, Vol.6, 1934, p.63.

35. Gupta, C.L. and Garg, H.P., 'System design in solar water heaters with natural circulation'. Solar energy, Vol.12, 1968, p.163-182.

36. Taber, H. ' Selective radiation. I. wavelength discrimination. A new approach to the harnessing of solar energy'. Trans. of the International Conf. on the use of solar energy-the scientific basis, vol 2, part 1, Section A. Tucson, 1963, p.24-33.

37. Dunkle, R.V. and Davey, E.T. ' Flow distribution in solar absorber banks'. Paper No.6/35, Presented in 1970 International solar energy society conference, Melbourne Australia, 2nd-6th March, 1970.

38. Bliss, R.W. 'The derivation of several plate-efficiency factors useful in the design of flat-plate solar heat collectors'. J.Solar energy, Vol.3, No.4, Dec. 1959, p.55-64.

39. Sheridan, N.R., Bullock K.J. and Duffie, J.A. 'Study of solar process with an analog computer'. J. of solar energy, vol 11, No.2, April 1967, p. 69-77.

30. Close, D.J., 'A design approach for solar processes J. of Solar energy, vol 11, No.2, April 1967, p. 112-122.

31. Chinnery, D.N.W., ' Solar water heating in south Africa,'. N.B.R.I-Bulletin 44, CSIR Research report 269, Pretoria, South African, 1967, pp 1-79.

32. Garg, H.P., 'An automatic control circuit for large size solar water heaters'. Research and Industry, Vol.14, No.3, 1969, p.126-127.

33. Robinson, N and Neeman, E., 'The solar switch-An automatic device for economising auxiliary heating of solar water heaters'. Proc. of New Sources of energy, Rome, Aug. 1961, Vol 5, p.76.

34. Richards, S.J. and Chinnergy, D.N.W., ' A solar water heater for low cost housing'. N.B.R.I. Bulletin 41, CSIR Research report 237, Pretoria, S.African, 1967, pp.1-26.

35. Tanishita, I., ' Recent development of solar water heaters in Japan'. Proc. UNESCO Conf. New sources of energy, Rome, 1961, Vol 5, p.23-101.

36. Lof G.O.G. and Close D.J., ' Solar water heaters'. Low temperature engineering application of solar energy, ASHRAE. Chapter 6, 1967, p.61-78.

37. Bouvarin, J., ' Study of solar water heating in Algeria'. Proc. UNESCO Conf. New sources of energy, Rome, 1961, Vol.6, p.93-101.

38. Chinnappa, J.C.V., and Ganalingam, K., 'Aprogoured solar water heater of the combined collector and storage type'. Trans. of the Institution of engineers, Ceylon, 1968, p.83-90.

39. Chinnappa, J.C.V., ' Design and performance of a pressurised solar water heater of the combined collector and storage type'. Presented at 1970 International solar energy society-conference, 2-6th March 1970, Melbourne, Australia.

40. Garg, H.P., 'Solar water heater'. Building digest No.61, Central Building Research Institute, Roorkee.

C H A P T E R 8-9

1. Whillier, A., 'Performance of black painted solar air heaters of conventional design'. Solar energy, Vol 8, No.1, Jan-March 1964, p.31-37.

2. Hoff, G.O.G., 'Solar energy collectors of over-lapped glass plate type'. Proceedings space heating with solar energy M.I.T., 1950, p.72-86.

3. Bliss, R., 'Multiple gauge flat-plate solar air heaters'. Proceedings world symposium on applied solar energy, Phoenix, 1955, p. 101-158.

4. F.L.Engelow, ' Corrugated solar heat collectors for crop drying'. Sun at work, 4th quarter, 1962, p.8.

5. H.M.Tan and W.J.S.Charters, ' An experimental investigation of forced-convective heat transfer for fully developed turbulent flow in a rectangular duct with asymmetric heating'. Solar energy, Vol 13, No.1, 1970, p.121.

6. Eckert, E.R.G., and Irvine, T.F., ' Pressure drop and heat transfer in a duct of triangular cross section. Trans. A.S.M.E., J. Heat transfer, Vol. 82, 1960, p.125.

7. Mac Adams, W.J., ' Heat transmission', McGraw-Hill Book Co., New York, N.Y., 1954.

8. Mikheyev, M., ' Fundamentals of heat transfer'. Peace publications, Moscow.

9. Goluk, K., ' Thermal and economic analysis of the overlapped-glass plate solar air heater'. Solar energy, Vol.13, No.2, May 1971, p.165-191.

10. J.P.Chiou etal, ' A slit and expanded aluminium foil matrix solar collector'. Solar energy, vol 9, No.2, 1965, p.73-80.

11. Bevill, W.D., and Brandt, H., ' A solar energy collector for heating air'. Solar energy, Vol 12, No.1, Sep. 1968, p.19-31.

12. Buelow, F.H., 'Heating air by solar energy'. Agri. Eng., Vol. 38, No.1, 1957, p.28-30.

13. Close, D.J., ' Solar air heaters for low and moderate temperature applications'. Solar energy, Vol.7, No.3, July, 1963, p.117-124.

14. Garg, H.P., ' Measurement of solar absorptivity of black paints'. J.of Inst. of Engrs.(India), Oct. 1970.

15. Whillier, A and C.J. Richards, ' A standard test for solar water heaters', U.N.Conf.on Res sources of energy, Rome 1961, p.111.

16. Gupta, C.L., and Garg, H.P., ' Performance studies on solar air heaters'. Solar energy, Vol.11, No.1, Jan. 1967., p.25-31.

17. Lewond, T.A., 'Preliminary report on solar air heater tests'. Technical report No.T.3. of Space Research Institute of McGill University, March, 1963.

18. Rao, K.R., ' Electric analogue prediction of periodic heat flow in buildings'. Ph.D.Thesis, University of Roorkee, Roorkee, 1964.

19. ASHRAE Guide and data book, 1961, Fundamentals & equipment, New York, A.S.H.R.A.E., 1961.

20. Alford, J.S., Ryan, J.N. and Urban, F.O., ' Effect of heat storage and variation in outdoor temp. and solar intensity on heat transfer through walls'. ASHVE Trans. Vol.45, 1939, p.369.

21. Rao, K.R. and Ballentype, E.R., ' Some investigations on the sol-air temperature concept'. D.B.R. Technical paper No.27, C.S.I.R.O., Australia, 1970.

22. Bliss, R.W., ' The performance of an experimental system using solar energy for heating, and night radiation for cooling a building'., Proceedings of New sources of energy, Rome, 1961, Vol 5, p. 148-157.

23. Engebretson, C.D., ' The use of solar energy for space heating-M.I.T.solar house IV'. Ibid, p.169-173.

BIBLIOGRAPHY

1. Zrem, A.M. and Erwny, D.J., ' Introduction to the utilisation of solar energy'. McGraw-Hill Book Co., New York, 1963.
2. Daniels, F., ' Direct use of the sun's energy'. Yale University press, London, 1964.
3. Daniels, F. and Duffie, J.A., ' Solar energy research'. The University of Wisconsin, 1955.
4. Robinson, N.,' Solar radiation'. New York and Amsterdam, Elsevier, 1966.
5. 'Hand Book of Metsorological instruments part I'. Her Majesty's stationary office, London, 1956.
6. Croundwater, I.C., 'Solar radiation in airconditioning' Crosby Lockwood and sons Ltd., London, 1967.
7. Mc Adams, W.H., ' Heat transmission'. McGraw-Hill Book Co., New York, 1954.
8. Brown, A.I. and Marco, S.M. 'Introduction to heat transfer'. McGraw-Hill Book Co., New York., 1951.
9. Mikheyev, M., ' Fundamentals of heat transfer'. Peace publishers, Moscow.
10. Fishenden, M. and Saunders, O.A.,'An introduction to heat transfer'. The clarendon press, Oxford, 1950.
11. 'Temperature its measurement and control in science and Industry'. Reinhold publishing corporation, New York, 1
12. Billington, N.C., ' Thermal properties of building' Cleaver-Hume press Ltd., London, 1952.

A C K N O W L E D G E M E N T S

The author wishes to express his deep appreciation to his advisors Dr.K.N.Rao, Scientist in charge, heat transfer section, Central Building Research Institute, Roorkee, Dr. Rajendra Prakash, Professor of the department of Mechanical Engineering, University of Roorkee and Dr.S.K.Joshi, Professor and Head of Physics Department, University of Roorkee for their valuable suggestions and general guidance throughout the work.

He is also indebted to Prof.Dinesh Mohan, Director and Dr.N.K.D.Choudhury, Assistant Director, Central Building Research Institute, Roorkee for the interest shown, encouragement given and facilities provided to carry out this study.

The author also expresses his thanks to Dr. C.L.Gupta, formerly a scientist at C.B.R.I., Roorkee for initiating the work on solar energy at C.B.R.I. and for the sustained interest shown in the present study.

The assistant rendered by the solar energy section staff at C.B.R.I., Roorkee and computer centre staff at U.[illegible].C., Roorkee is gratefully acknowledged.

LIST OF TABLES

LIST OF ILLUSTRATIONS

CHAPTER - 1

SCOPE OF WORK

Until now, all methods of deriving the integral wavelength solar constant and its spectral components have entailed extrapolation of measurements made at the earth's surface under clear sky conditions at different heights and at different solar altitudes.

Direct measurements made by satellites in recent years had produced converging evidence that the Johnson value of the solar constant was too high and the spectral distribution curve required significant revisions. Thekaekara[17] of N.A.S.A. Goddard space flight centre made a close study of the data and proposed a value of solar constant 1.94 cal per cm^2 per minute (1.353.KW/m^2) which is about 3 percent lower than the Johnson value of 2.0 cal per cm^2 per minute. The spectral distribution of extraterrestrial solar radiation, according to Thekaekara, is presented in fig 2.1.

The radiation intensity on horizontal surface (Ioh) outside the earth's atmosphere is a function of sun's zenith angle (θh), and is given as :

$$Ioh = Ion \cos \theta h \qquad \text{----------(2.2)}$$

where Ion = Solar constant

The incident angle, θ h, can be written as :

$$\cos h = \cos L \cos \delta \cos \omega + \sin L \sin \delta \qquad \text{------(2.3)}$$

where L = latitude of the place.

δ = declination of sun

ω = hour angle from solar noon.

The various angles are shown in fig (2.2).

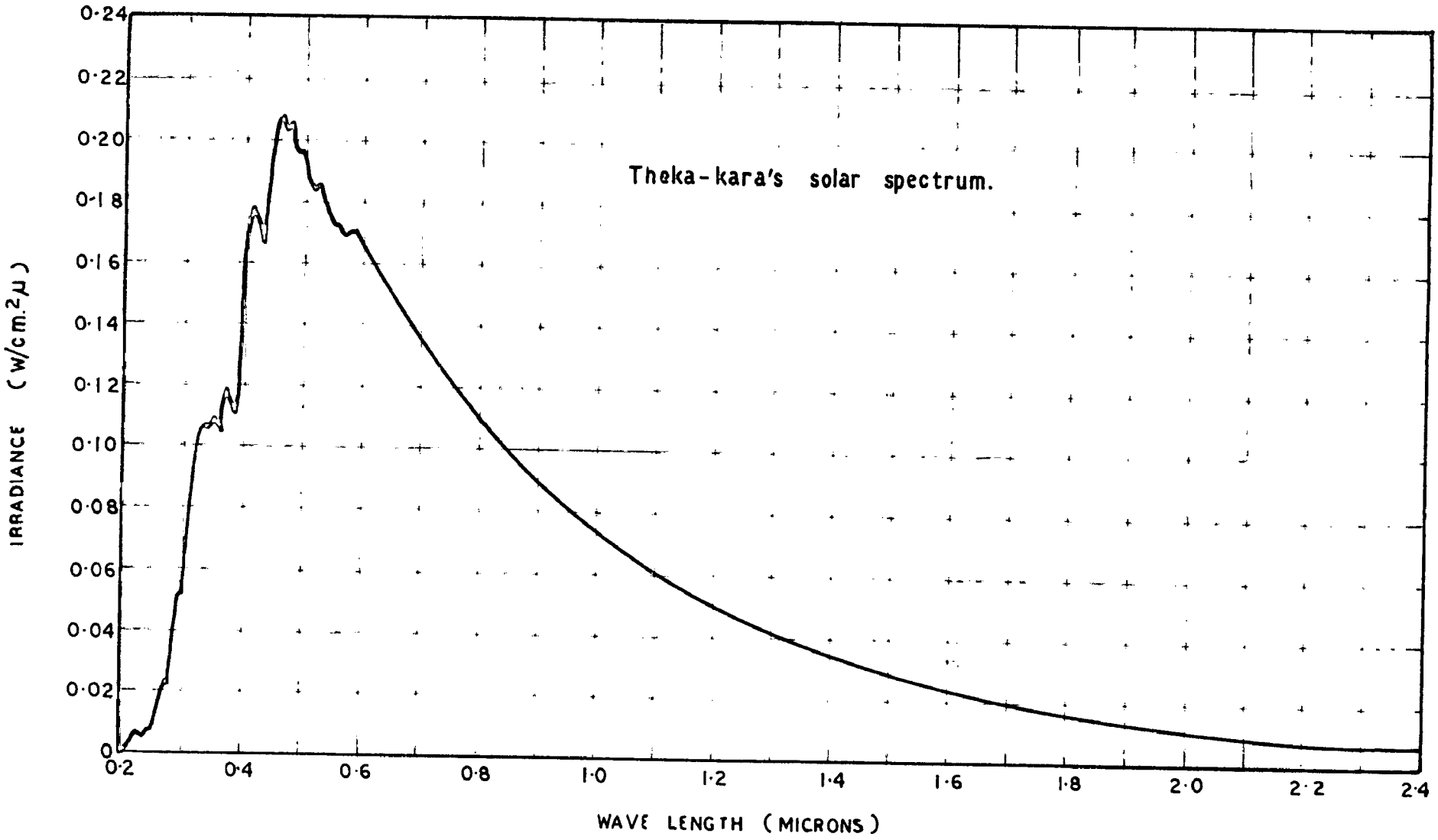

FIG. 2·1 SPECTRAL DISTRIBUTION OF THE EXTRATERRESTRIAL SOLAR RADIATION

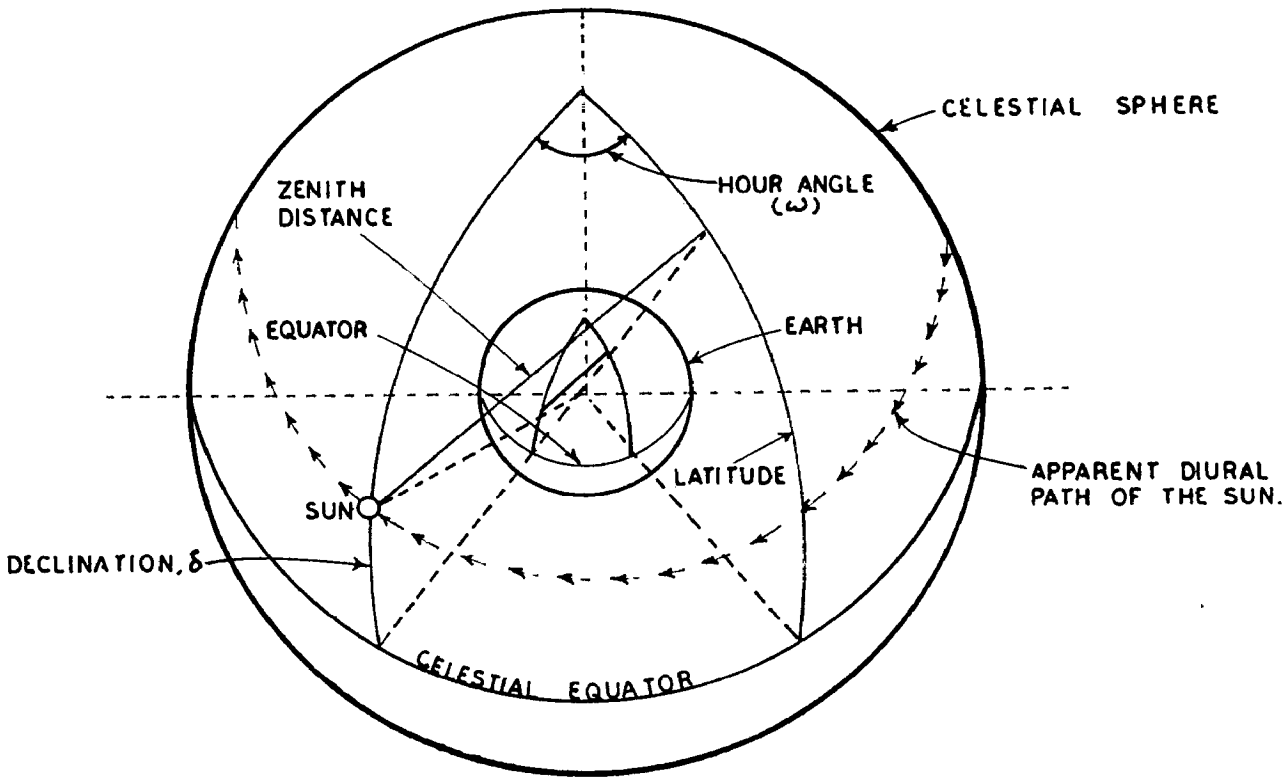

FIG.2·2 RELATIONSHIP OF SOLAR ANGLES

components were present and the overall effect is obtained by superposition.

3.31 Direct Radiation

In United States an analytical approach has been adopted, the effect of each component being considered separately in an attempt to evaluate a comprehensive formula from which the beam radiation or direct radiation at any location may be predicted in the absence of any local radiation measurements. The early work of Kimball[22,23,24,25] has been extended by Moon[26] and more recently by Threlkeld and Jordan[27]. Moon's relation between the monochromatic transmission and the intensities of the various depleting agents may be expressed by the following equations :

$$\log T_\lambda = \log \frac{I_{n\lambda}}{I_{o\lambda}} = m \frac{o_3}{2.5} \log T_{\lambda o_3} + m \frac{p}{760} \log T_{\lambda a} + m \frac{w}{20} \log T_{\lambda wa} + m \frac{w'}{20} \log T_{\lambda wa} + m \frac{d}{250} \log T_{\lambda d} \quad \text{----(2.16)}$$

Here the first term of the right side accounts for absorption by Ozone, the second Rayleigh scattering by clean, dry air, the third and fourth scattering and absorption by water vapour and the last term attenuation by dust. The component transmission factor, T, refer to standard amounts of 2.5 cm Ozone, 760 mm barometric pressure, 20 cm precipitable water vapour and 250 dust

particles per c.c. The assumed standard conditions are different used by different workers as can be seen from table 2.6.

The total effect of each constituent over the whole wavelength range of the solar beam has been computed by Threlkeld and Jordan who presented a series of graphs from which the overall transmission factor may be found. The values of the direct solar radiation normal to the sun's rays (Btu/ft^2hr) for the above assumed conditions are given in table 2.7.

The value of the direct solar radiation measured on horizontal surface is compared with the computed values of the direct solar radiation on horizontal surface as computed by Moon and is shown in fig 2.19.

2.32 Diffused radiation:

As a result of the complex processes of absorption, reflection and multiple scattering of the solar beam by the various constituents of the atmosphere the beam radiation at the ground is reinforced by a second component, the diffused radiation, which approaches the observation point from all parts of the hemispherical sky vault.

For the design of solar energy utilisation devices, the diffused radiation should also be given due weightage. It has been reported by Desikan, Iyer and Mahalkar[29] that at Delhi the diffused radiation on horizontal surface varies from 19 percent (November), to 30 percent (June) of the total solar radiation, on clear days and it varies from 34 percent (November) to 59 percent (July) for all days. It indicates that in tropical regions diffused radiation forms a high percentage and thus plays an important role.

Precise information concerning the intensity of diffused radiation and its variability in different parts of the world is severely limited and any formulae which have been proposed apply only to the particular locations. The scattering functions involved in diffuse radiation are extremely complicated and have only recently been evaluated numerically from Mie's theory[29] using special assumptions about the compositions of the aerosols. The work of Deirmendjain[30] and Sekera and Ashburn[31] has shown that it is possible to estimate the total diffused sky radiation (θ_r) on a horizontal plane with the aid of the following simple formula proposed earlier by Abbrecht[32]

$$\theta_r = \Pi_r \, (I_{o,r} - I_r) \sin r \qquad \text{--------(3.17)}$$

where r is the altitude of the sun and K_r is an empirical coefficient which in the Congo city is given as:

$$K_r = 0.6 \sin r^{1/2} \qquad \text{---------(2.18)}$$

$I_{v,r}$ is the direct solar radiation in the absence of scattering by molecules and dust particles, and I_r is the direct solar radiation when scattering effects are included.

2.4 PROPOSED METHOD FOR THE COMPUTATION OF SOLAR RADIATION:

Total solar radiation on a horizontal surface can be computed with a good degree of accuracy provided climatic conditions such as cloudiness, atmospheric turbidity etc. are known. Unfortunately in tropics not much measured data is available on any of the above factors. Here another line of approach is used for the computation of total solar radiation on horizontal surfaces which is based on actual sunshine hours. There is a large network of stations (80) recording this parameter. Ram Das and Yegnanarayanan[33] have provided data for the monthly mean values of actual sunshine hours, Sa, and possible sunshine hours, Sp, for Indian cities. Following Angstrom's[34] method they have further developed a linear relation between the ratio of daily total solar radiation on a similarly oriented surface on a clear day, H/H_o, and the ratio of sunshine hours stated above,

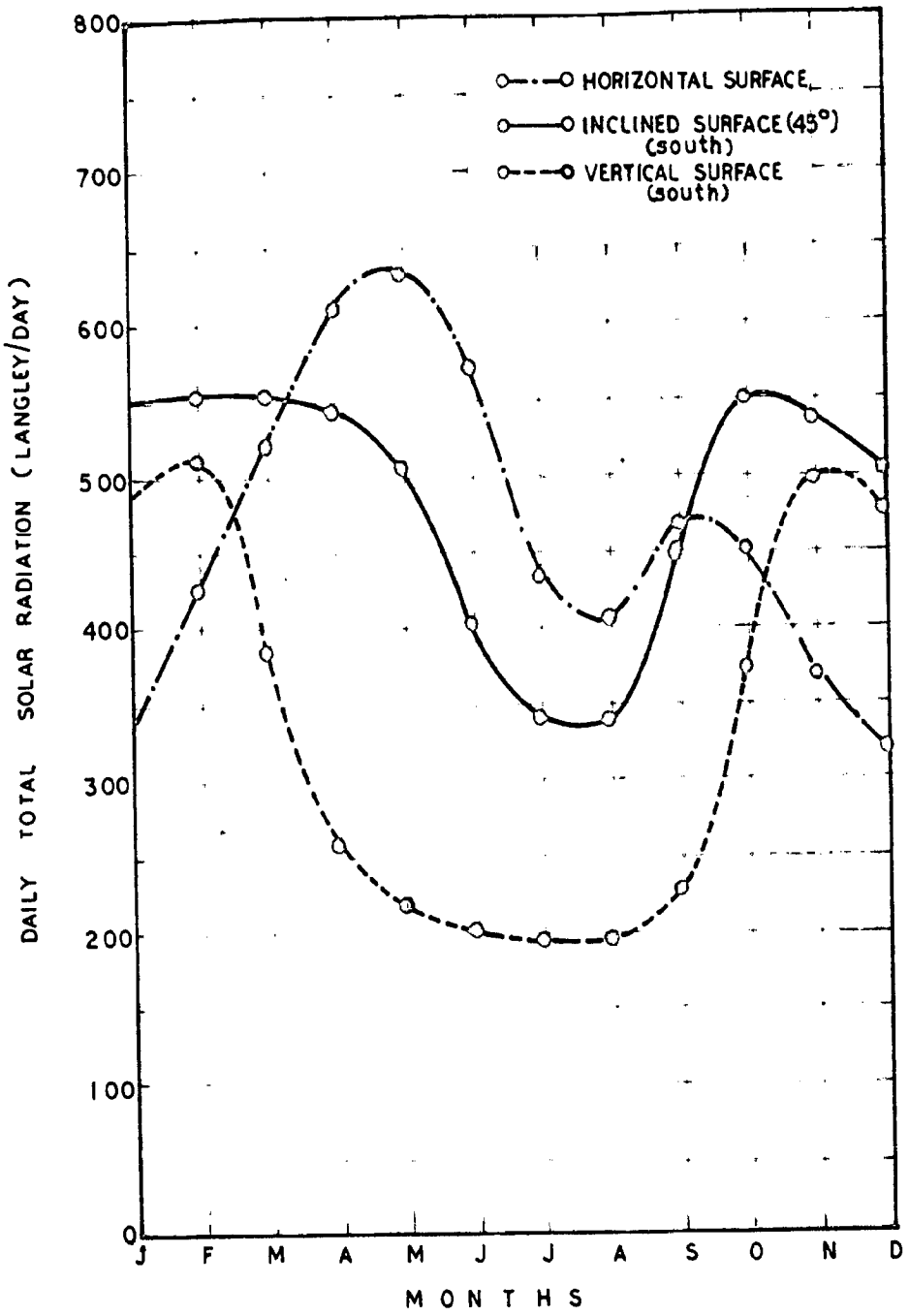

FIG. 2·13 MONTHLY MEAN VALUE OF TOTAL SOLAR RADIATION ON INCLINED SURFACES

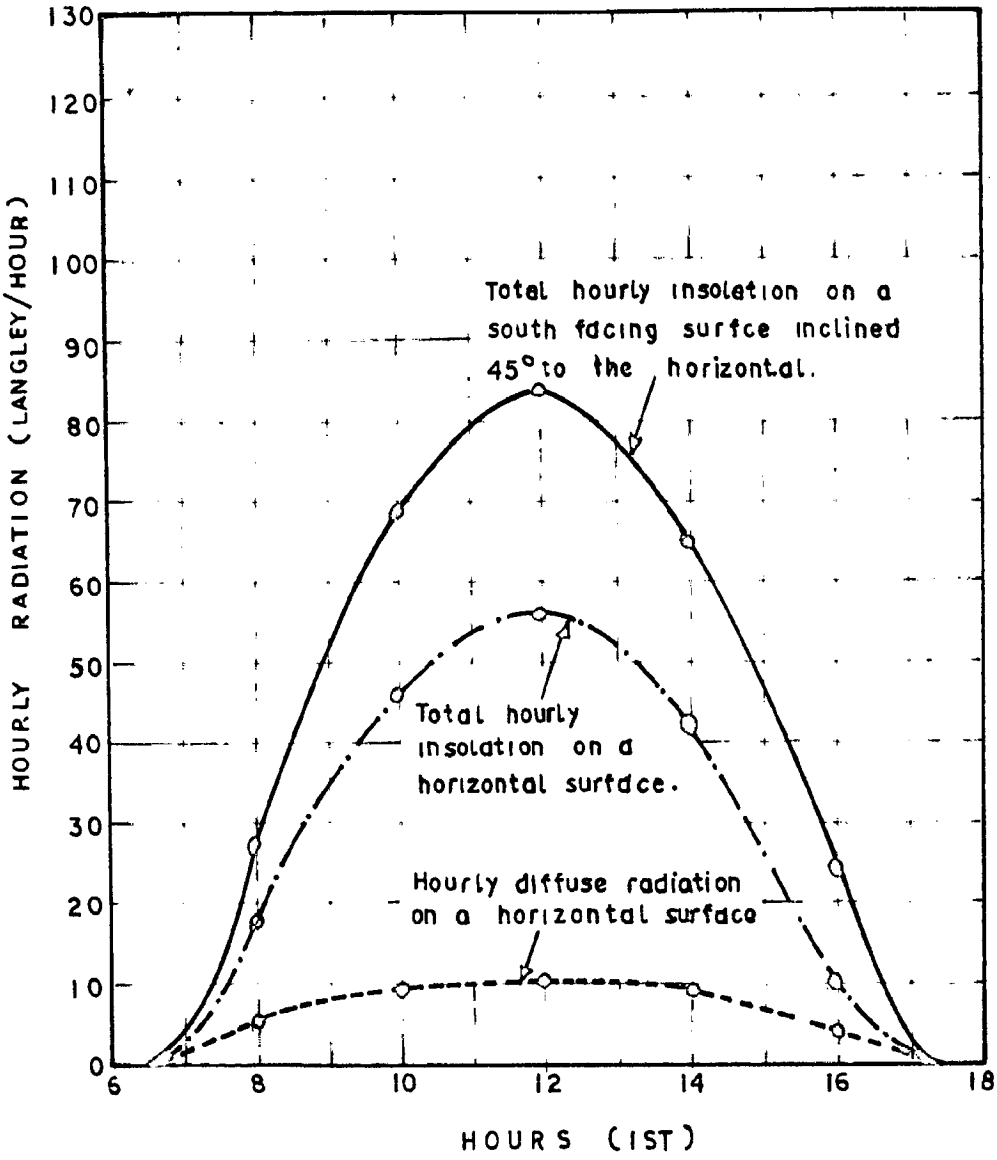

FIG. 2·14 HOURLY SOLAR RADIATION ON A CLEAR WINTER DAY AT ROORKEE

daily average useful collection as a function of the temperature of collection, the number of glass cover plates, flow conditions and for two representative months, January and May, for collectors having angle of outward tilt equal to 0.9 times the latitude in summer and latitude angle plus 10 degrees in winter. The temperature of collection is defined as the difference between the temperature of the fluid stream entering the collector, i.e. the storage temperature and the ambient temperature. Further, the flow conditions are to be maintained such that the solar collection is always positive. This condition is automatically satisfied in natural circulation type solar systems. It is evident from the curves that if the temperature level of the collection is less than 15°C, one glass cover is sufficient. This is in agreement with the experimental findings as discussed earlier.

4.41. APPLICATION OF DESIGN PROCEDURE:

In designing a solar heating installation with insulated thermal storage at any place, following steps are to be undertaken:

1) load calculation: The load is calculated by knowing the required amount of fluid and the design maximum fluid temperature.

Q_L (load) = mass of fluid×specific heat ×(design maximum fluid temperature-morning fluid temp. in storage).

ii) Mean temperature of operation: Since the ambient temperature is continuously varying and so is the storage temperature, the mean temperature level of collection is obtained with the help of the following empirical relations

t_e(mean) = Mean daytime ambient temperature
= 0.7 $t_{max.}$ + 0.3 $t_{min.}$

t_i(mean) = Mean incoming fluid temperature
= 0.5 (Design maximum fluid temp + morning fluid temperature in storage).

Temperature level of operation = Δt = $[t_i(mean) - t_e(mean)]$

Morning fluid temp.(Tap water) = (0.5 $t_{min.}$ + 0.2 t_{max})

iii) Collector design: If the temperature of operation is more than 18°C, two glass covers are required. Depending upon the desired life and cost and the pressure involved, a suitable type of collector is to be chosen on the basis of the configuration which would provide maximum heat exchanger efficiency per unit cost as done earlier.

iv) To compute, F_R, mean flow rate per unit of area, G, should be known. For natural circulation type of heaters, it varies and however may be taken as 40 Kgm/m²hr, for systems employing flat-plate solar collectors which will be confirmed later.

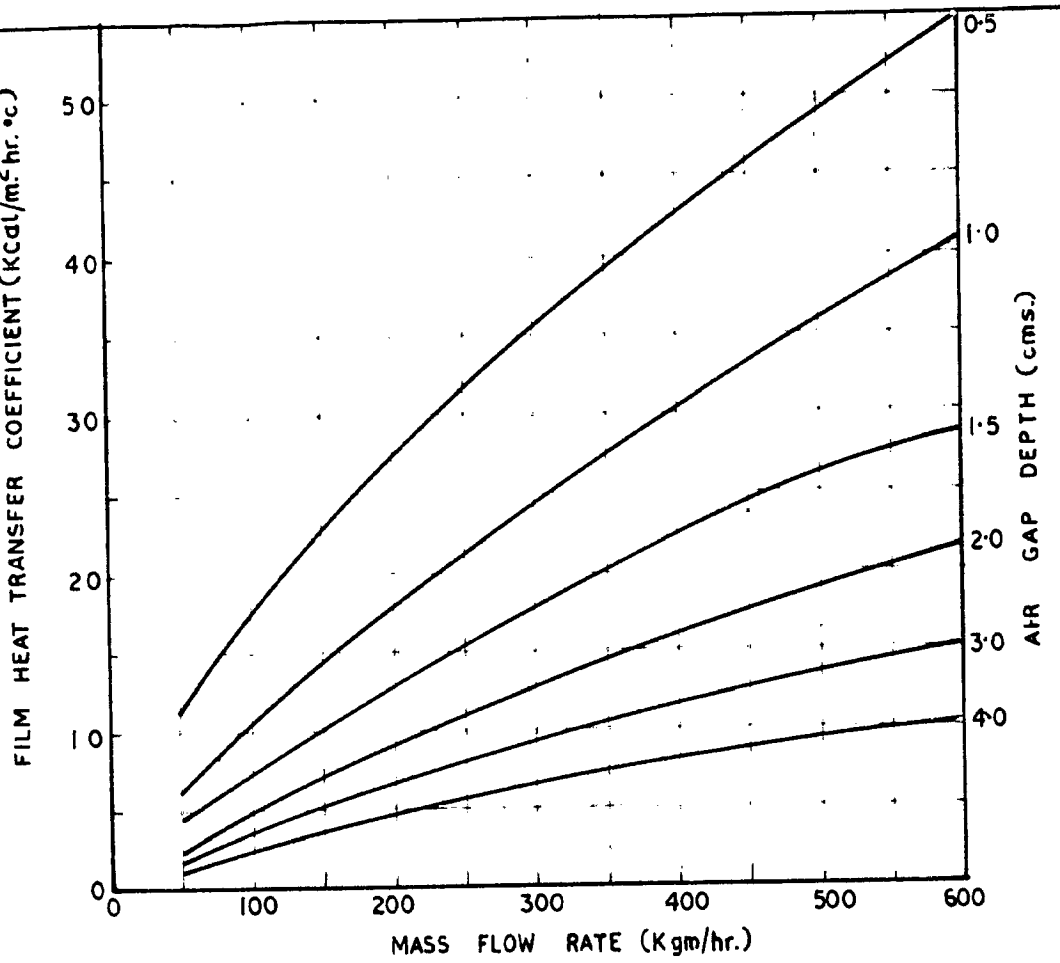

FIG. 5·6 EFFECT OF MASS FLOW RATE ON HEAT TRANSFER COEFFICIENT

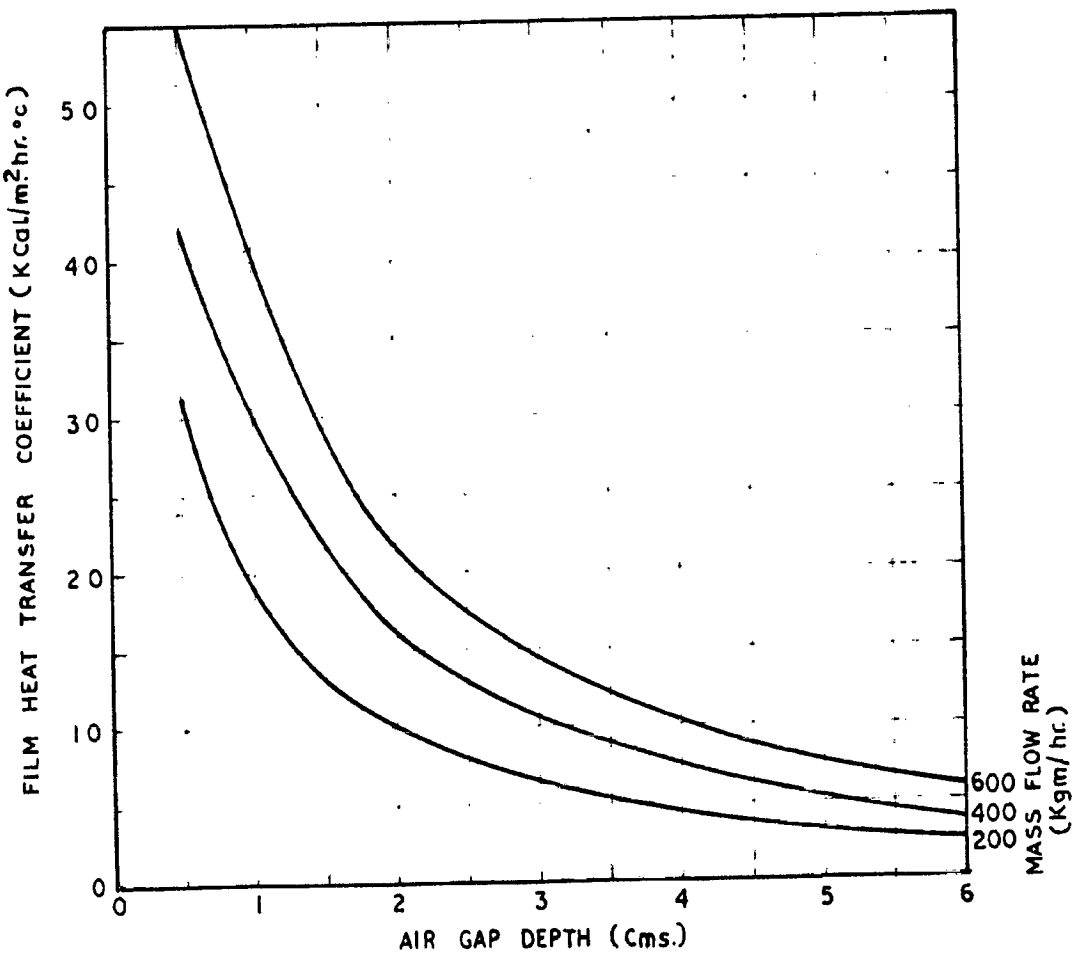

FIG. 5·7 EFFECT OF AIR GAP DEPTH ON HEAT TRANSFER COEFFICIENT

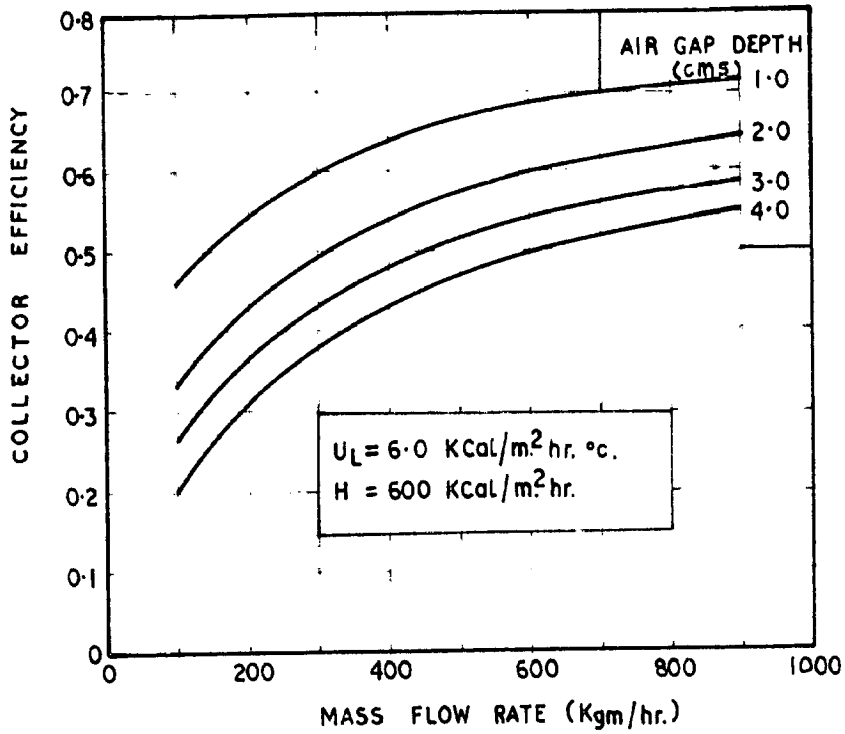

FIG. 5·8 OPTIMIZATION OF MASS FLOW RATE FOR VARIOUS DEPTHS

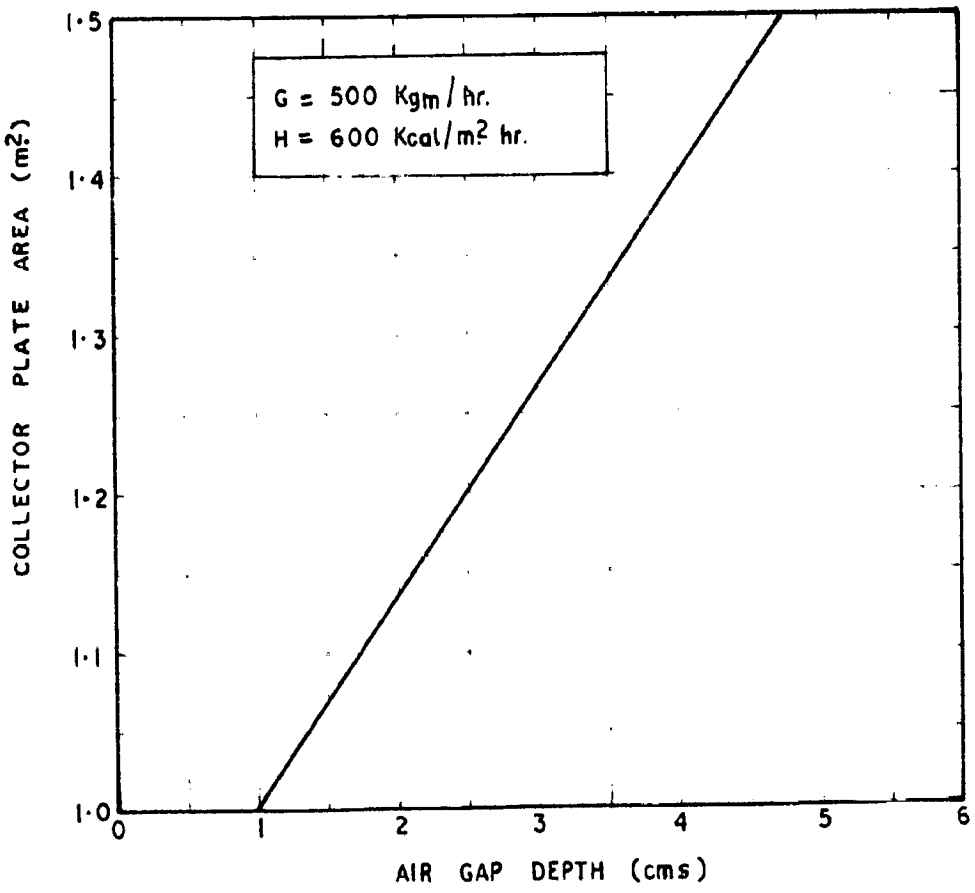

FIG. 5·9 EFFECT OF AIR GAP DEPTH ON THE COLLECTOR PLATE AREA

and P_r = Prandtl number = $\frac{C_p \mu}{K}$

Here

h_c = convective film heat transfer coefficient,

l = length of panel,

K = thermal conductivity of surrounding air,

ρ = density of air,

g = acceleration due to gravity,

$\beta = \frac{1}{T}$

Δt = temperature difference between panel and air,

μ = coefficient of viscosity,

C_p = specific heat of air.

Now consider a panel of standard size say 1m x 1m then l = 1 m^2. The physical properties of air do not change much from 10°C to 80°C. If we assume a mean temperature difference of 30°C, then

$\beta = \frac{1}{303}$ °K.

$\nu = 16 \times 10^{-6}$ m^2/sec.

K = 0.023 Kcal/m hr °C

P_r = 0.701

g = 9.81 m^2/sec.

putting all these values in equation (98), we get

$$N_u = 46.99 \ (\Delta t)^{1/4}$$

But heat loss by convection q_c is given by

$$q_c = h_c \Delta t$$

and by substituting the value of h_c

$$h_c = \frac{N_u . K}{l}$$

we get

$$q_n = 1.08\ (\triangle t)^{5/4} \qquad \ldots(5.29)$$

The heat output by convection for various temperature differences is shown in Fig.(5.18) as computed with the help of equation (5.29).

Radiation Heat Transfer:

The radiation transfer can be evaluated by means of the Stefan and Bottzmann equation,

$$q_r = F_g \epsilon \sigma A_1\ (T_1^4 - T_2^4)$$

where

F_g = configuration factor,

ϵ = emissivity of the surface,

A_1 = area of radiating surface = 1 m^2,

T_1 = absolute temperature of source,

T_2 = absolute temperature of sink,

σ = stefan Boltzmann constant = 4.9×10^{-8} $\frac{Kcal/m^2}{hr\ {}^\circ K^4}$

Hottel[7] has given a combined configuration and emissivity factor for a room in which there is a uniformly heated ceiling, wall and floor with diffusing surfaces. The expressions is given as:

$$F_c = F_g \epsilon = \frac{1}{\frac{1}{F_{1-2}} + \left(\frac{1}{\epsilon_1} - 1\right) + \frac{A_1}{A_2}\left(\frac{1}{\epsilon_2} - 1\right)} \qquad \ldots(5.30)$$

where

ϵ_1 and A_1 = emissivity and area of source,

ϵ_2 and A_2 = emissivity and area of sink,

and F_{1-2} = view factor = 1.0.

A pump of 1/4 H.P. was used for the circulation of water through the absorbers and the storage panels and is controlled by a time switch which keeps the electric circuit on from 9.0 A.M. to 4.0 P.M.

Observations:

Continuous observations of room air temperature with and without heating the room, ambient air temperature and total solar radiation on absorber surface is made for two months i.e. from middle of December 1971 to middle of February 1972. The general feeling of the scientist sitting in the room and of the visitors was also recorded daily. This room which was reported to be the coldest room in the whole of the building was made effectively comfortable ~~comparable~~ through out the winter season. The mean room air temperature measured in the middle of the room for a number of days with and without heating is shown in Table (5.12). It is observed here that when no heating is used the mean room air temperature is about 14.0°C. In the month of January which is the coldest month of the year, it can be expected the mean room air temperature to further drop by 2°C. When solar heating is used was between 19°C to 22°C over a period of one month. It was observed that the diurnal variation of the room air temperature is only of the order of 2°C. Fig. 5.30 shows the hourly variation of room air temperature on a typical day.

TABLE 5.12: Mean room air temperature with and without heating for different days for office room

WITHOUT HEATING		WITH HEATING					
Date	Room Temp. ($^{o}_{C}$)	Date	mean temp. (^{o}C)	Date	mean temp. ($^{o}_{C}$)	Date	mean temp. (^{o}C)
21/12/71	15.0	1/1/72	19.0	11/172	21.5	21/1/72	20.0
22/12/71	14.5	2/1/72	20.0	12/1/72	21.0	22/1/72	20.0
23/12/71	14.5	3/1/72	20.5	13/1/72	20.5	23/1/72	19.5
24/12/71	14.0	4/1/72	20.5	14/1/72	20.0	24/1/72	19.5
25/12/71	14.0	5/1/72	21.0	15/1/72	20.0	25/1/72	19.5
26/12/71	14.0	6/1/72	21.0	16/1/72	20.0	26/1/72	20.0
27/12/71	14.0	7/1/72	21.5	17/1/72	20.5	27/1/72	20.0
28/12/71	14.0	8/1/72	21.5	18/1/72	20.5	28/1/72	20.5
29/12/71	14.0	9/1/72	22.0	19/1/72	20.0	29/1/72	20.5
30/12/71	14.0	10/1/72	22.0	20/1/72	19.5	30/1/72	20.5

TABLE 5.13:

Cost comparison of solar space heating system for insulated and uninsulated construction

	UNINSULATED	INSULATED
1. Walls	1 cm plaster + 22.6 cm Brick + 1 cm plaster	1 cm plaster + 11.25 cm brick +2.5 cm thermocole + 1 cm plaster.
2. Roof	Tarfelt + 6 cm Brickfile + 10 cm mudphuska + 16.5 cm cement Concrete + 1 cm plaster	10 cm dense conc. + 3 cm thermocole.
3. Cooling load (Kcal/day)	23690	9018
4. Collector area required (m^2)	8.4	3.2
5. Panel area required (m^2)	5.3	2.1
6. Number of collectors required (1 collector = 1 m^2)	8	3
7. Number of panels required (1 panel = 2.4 m^2)	3	1
8. Cost of pump & control (Rs)	500	500
9. Cost of collectors @ Rs.150 per m^2	1200	480
10. Cost of panels @ Rs 200 per panel	600	200
11. Total cost (Rs.)	2300	1180